The Effects of Cross Linking on Collagen Type I Nanostructure and Nanostructural Response to Uniaxial Tension

A thesis presented in partial fulfilment of the requirements
for the degree of

Doctor of Philosophy
In
Engineering

at Massey University, Manawatu, New Zealand.

Hanan Kayed
2016

Abstract

Collagen type I, is a fibrillar protein with a complex hierarchical structure, forming the extracellular matrices of an extensive range of organs and tissues. Applications for treated collagen materials vary vastly from commercial uses to the medical field for bioprosthetics and tissue grafts. Glycosaminoglycan (GAG), cross links naturally bridge fibrils, whilst glutaraldehyde is widely used as a synthetic linking agent in medical and other industries. No consensus has been reached regarding what contribution, if any, such cross links have on collagen structure and mechanical responses to applied stresses. This research investigated the role of GAG and glutaraldehyde cross links on the nanostructure and nanostructural response of type I collagen fibrils under uniaxial strain. Bovine pericardium was decellularised, producing native samples, or further treated with glutaraldehyde or chondroitinase ABC to produce glutaraldehyde cross linked or GAG-depleted collagen samples respectively. Synchrotron small angle X-ray scattering (SAXS), and atomic force and polarised light microscopy provided quantitative and qualitative information on collagen nanostructure. Uniaxial tensile experiments in conjunction with SAXS were performed to monitor structural changes with applied strain. Glutaraldehyde cross links constrained fibrils into more networked isotropic structures and demonstrated a mechanical function, recruiting 45% of fibrils into stretching which experienced strains of up to 6.4%. Comparison of native with chondroitinase ABC-treated samples showed GAGs do not constrain fibrils into alignment and have potential fibril lubricating effects; 12% of fibrils in native tissue experienced strains up to 4.1%, and 36% of fibrils experienced strains up to 4.6% in the GAG-depleted tissue. A higher degree of fibril sliding occurs in native tissue. Interestingly, whilst adult pericardia are more cross linked and fibrils of neonatal pericardia are more aligned, both tissues share similar propensities to form more isotropic structures with glutaraldehyde treatment. These findings build a comprehensive picture as to the function cross linking has in collagen structure and mechanical response at the nano-level, where such knowledge may prove useful for the preparation of collagen materials for specific applications.

Acknowledgements

I would like to take this opportunity to acknowledge the many people who have contributed either directly or indirectly to this research project.

Firstly I would like to thank my supervisor, Professor Richard Haverkamp; thank you for your on-going support, scientific writing advice and your enthusiasm. Your passion for your field and research in general never failed to motivate me, and your high standards of work allowed me to strive for quality and to achieve better outcomes.

I would also like to acknowledge the contribution of my co-supervisor, Associate Professor Gillian Norris.

Thank you to my amazing family, Mum, Dad, Abdul, Afnan and Ayah. When interesting findings were made and publications accepted you were there to congratulate and celebrate with me (whether you understood the material or not!), and when the work was challenging you always provided the upmost support and love. Without you the completion of this thesis would not have been possible (or at least very difficult).

I would like to thank my husband, Shadi for being there always. I greatly appreciate your support, love, and belief in me. Thank you for not only listening to my rambling of ideas and my attempts at making sense of results, but also for your attempts to understand my work and provide advice!

Thank you to the Australian Syncrotron SAXS/WAXS beamline team, specifically Nigel Kirby, Adrian Hawley and Stephen Mudie. Your expertise, technical skills and willingness to help allowed for the accommodation of our experimental requirements, made the realisation of ideas possible, and in turn research questions to be answered. The New Zealand Synchrotron Group is acknowledged for providing travel funding.

Thank you to John Shannon and Southern Lights Biomaterials for the supply of pericardium.

Table of Contents

List of Figures

List of Tables

Chapter 1

1. Introduction

1.1 Research Background and Relevance

Collagen comprises a fraction if not the principle component of many materials and products across numerous fields, from joint supplements, upholstery and shoes, to bioprosthetic heart valves and tissue grafts. Collagen constitutes the major component of human and animal organ and tissue extracellular matrices (Exposito et al., 2002). Each natural organ or tissue, industry, or collagen-based product will require the material to have specific properties which enables it to function as intended. Such properties may include high mechanical strength, different degrees of elasticity, high stability, good flexural properties, high compressibility or higher extensibility for example.

Collagen is a complex material with multiple components, each with different structures and compositions assembling in hierarchical levels beginning from the nanoscale and building up to the overall structure at the macroscopic scale. Collagen type I is one of the major collagen types distributed extensively throughout the body and is fibrillar in nature. Briefly, starting from the bottom up, collagen molecules are polypeptide chains with left handed helical twists. Three collagen molecules assemble with a right-handed helical twist to form a triple helix or tropocollagen molecule. Multiples of five tropocollagen molecules adjacent and in register are axially staggered by a defined distance and stabilised by hydrogen and covalent bonding to form collagen fibrils. Design of collagen materials which exhibit the desired bulk properties therefore cannot be achieved without the understanding and consideration of the materials' components and structure, and their responses upon subjection to mechanical forces at these different levels.

Changes in the defining structural characteristics of collagen fibrils have been explored in relation to different stages of mechanical testing and mechanical properties, where studies have indeed shown aspects of collagen nanostructure to relate directly to the material properties (Basil-Jones et al., 2011, Mirnajafi et al., 2005, Fratzl and Weinkamer, 2007). Parameters which can be investigated include the direction and homogeneity of fibril

orientation, both in the natural state and under strain/stress, fibril diameter, and a parameter known as the D-spacing; D-spacing is the characteristic banding pattern of fibrils seen in electron microscopy and atomic force microscopy (AFM) studies, and is the length of repeating overlap and gap regions of the fibrils. However of importance and not to be overlooked are other components of the collagen material such as cross links. Glycosaminoglycans (GAGs) are natural cross links associated with type I collagen fibrils, non-covalently bridging adjacent fibrils regularly at the D-spacing sites (Scott and Orford, 1981, Scott, 1992). Studies into the role of GAG links in the mechanical response and bulk tissue properties of collagen tissues have yielded conflicting results; some report GAGs act as mechanical cross linkers (Liao and Vesely, 2007), whilst others believe GAGs facilitate fibril sliding (Rigozzi et al., 2013), or not to have an active role in the mechanical response at all. Similarly, conflicting suggestions have been made as to the effect of GAGs on the mechanical properties of collagen (Rigozzi et al., 2011, Svensson et al., 2011, Fessel and Snedeker, 2011). Although believed to play a role in the organisation of fibrils during their formation, the influence of GAGs on the nanostructure of mature collagen and the structure of collagen throughout mechanical testing remains unclear.

Common practice is the treatment of collagen materials prior to utilisation, for example to remove cells. Among treatments applied is cross linking of collagen (using chemical agents, enzymes, or physical methods). In the leather industry for example this is in the form of chromium sulfate or tannins (complex phenolic compounds) which are intended to stabilize and strengthen the leather, whilst in the medical field for bioprosthetics and tissue grafts the cross linking agent glutaraldehyde is the most widely used for the stabilisation of the material and reduction in antigenicity (Schoen and Levy, 1999, Jayakrishnan and Jameela, 1996). Glutaraldehyde was previously used as a tanning agent but is now limited to more demanding applications such as car dashboards due to its toxicity. Residual glutaraldehyde can leach from treated tissues causing cytotoxic effects and can induce calcification in tissues. Nevertheless, it is still the most widely used cross linking agent in the medical field due to its availability, low cost, effectiveness in cross linking, and reduction of immunogenicity. Glutaraldehyde is thought to intra and intermolecularly covalently link collagen fibrils through a range of link types (Olde Damink et al., 1995, Cheung and Nimni, 1982, Cheung et al., 1985). As with GAG cross links, the effects of glutaraldehyde cross links on collagen tissue mechanical properties and their function as mechanical linkers is contested, though several investigations report increased strength (Reece et al., 1982, Langdon et al., 1999). Little is known concerning if and how such links alter the collagen nanostructure post treatment and under stress/strain; however understanding such effects may explain any observed changes in mechanical

properties and may aid in the selection of other cross linking agents which cross link efficiently and induce similar structural changes without the negative side effects.

The research presented in this thesis therefore explores the structure of collagen at the nano-level, comparing the effect of natural GAGs and synthetically added glutraraldehyde cross links on fibrillar structure, and monitors the nanostructural changes of the differently cross linked tissue with strain in order to gain an understanding into what contribution such links have on mechanical response and mechanical properties. Bovine pericardium is used as the study collagen material; pericardium is a suitable material due to its availability, low cost, high collagen type I content, and its widespread use in bioprosthetics. Characterisation of collagen nanostructure and changes in nanostructure with strain are based primarily on synchrotron small angle X-ray scattering (SAXS) experiments, and SAXS combined with uniaxial tensile stretching, where SAXS has proven to be an excellent tool for investigating structure of a range in collagen materials (leather, cornea, tendon, cartilage). AFM and collagen staining coupled with cross polarised light microscopy offer qualitative information to support the quantitative SAXS data.

During the maturation of fibrils, levels of glycation cross links and links derived from immature enzyme induced cross links increase in collagen (Bailey, 2001, Haus et al., 2007). Structural differences also exist in collagen between young and old tissue. Utilisation of young pericardium in medical fields is potentially advantageous due to its thinness and superior properties (Sizeland et al., 2014). It is unknown whether glutaraldehyde cross linking of native tissue for use in such applications has different effects on structure between collagen of different ages and if they have the same propensity to be cross linked, and so is investigated here also.

1.2 Research Questions

The overall aim of the research undertaken is to understand if collagen cross linking, both natural GAG cross links and synthetically added glutaraldehyde cross links, influence the nanostructure of collagen type I tissues, and whether they impact the response of collagen to uniaxial tensile forces at the nanostructural level.

The following research questions were established to enable the research aim to be met:

1) Is collagen type I tissue nanostructure influenced by natural GAG cross links (or the removal of these links) or the addition of glutaraldehyde cross links? If so how?

2) Do GAG or glutaraldehyde cross links affect the stress-strain behaviours and mechanical properties of tissues composed of type I collagen? If so how?

3) What changes occur in collagen type I tissues in terms of fibril structure and arrangement at the nano-level when subjected to tensile stretching, and do GAG and glutaraldehyde cross links have a functional role in such responses, mechanical or otherwise?

4) Do the differences in native collagen structure and arrangement, and levels of natural cross linking between native young and old tissues result in different tendencies of the tissues to be cross linked by glutaraldehyde, and does glutaraldehyde treatment have a similar effect on the resulting nanostructures of the old and young tissue?

The thesis aims to address these questions as outlined below:

Chapter 3 of this thesis investigates the role of both naturally occurring glycosaminoglycan and synthetically introduced glutaraldehyde cross links on pericardium collagen structure. More specifically it aims to determine whether GAG or glutaraldehyde cross links affect the fibril orientation using predominantly SAXS. AFM and histology are also used to compliment the SAXS results. The mechanical properties, ultimate tensile stress, stress and failure, and the elastic modulus are obtained from Instron tensile testing and compared between the differently cross linked tissues.

Following on from Chapter 3, Chapter 4 expands on this theme to establish what impact natural and synthetic cross links have on the collagen structural response to subjected stresses. SAXS is used here in conjunction with tensile stretching to relate the stress-strain response of pericardium to nanostructural changes in the collagen tissue, and therefore determine if GAG and glutaraldehyde cross links have a role in response to stress, and if so by what mechanism, mechanical or otherwise. The structural parameters D-spacing, orientation index (OI) and the recruitment of fibrils are investigated here.

Chapter 5 further examines structural changes in the collagen tissue with strain by focusing on changes in fibril diameter. Here, SAXS is used to follow fibril diameter changes with strain, combining it with changes in fibril D-spacing to determine Poisson's Ratio for the differently cross linked pericardium tissues. The aim is to understand if different types of cross links affect individual fibril internal structural responses (in terms of volume change) to stress and strain, and so infer how these cross links affect the way tropocollagens interact under tension.

The effect of bovine pericardium age on native collagen fibril structural rearrangement with glutaraldehyde treatment and the ability of native young verses old collagen to be cross linked by glutaraldehyde is explored in Chapter 6. This chapter aims at determining whether the higher number of natural cross links present in adult bovine pericardium compared to neonatal pericardium, and the higher fibril alignment in neonatal pericardium results in a reduced number of available cross linking sites for glutaraldehyde, consequently affecting the relative changes in fibril structural arrangement (orientation).

Chapter 2

2. Literature Review

2.1 Collagen

Collagen is an extracellular matrix protein with a complex hierarchical structure found extensively in the human body and other mammals (Exposito et al., 2002). It is present in skin tissues, tendons, ligaments, muscle, bone, cartilage, dentin, arteries and organs (Ivanova and Krivchenko, 2012); the structure, type, and mechanical properties varying according to the required function of the specific tissue. It has been reported that 28 types of collagen belonging to different subgroups have been identified. Of particular interest in this thesis are fibrillar collagens, more specifically type I collagen, as it is not only the most abundant type present in tissues and organisms in general (Vincent, 2012), but also in pericardium (Schoen et al., 1986), the tissue used for all sampling in this project. Consequently, collagen type I will be discussed in detail whilst other collagen subgroups will be mentioned briefly.

2.1.1 Collagen Type I

2.1.1.1 Primary structure: The Building Blocks of Collagen

As a protein, collagen is composed of amino acids, molecules containing amide and carboxylic acid functional groups at either end of the molecule. The α carbon is the first C atom in the chain following that attached to the carboxylic acid group and can have a number of different side groups which can differ in size and chemistry, labelled R in Figure 2.1a. The simplest amino acid is glycine, where the R group is a hydrogen atom. Side groups can also be hydrophobic, hydrophilic, neutral, and/or cyclic. Two or more amino acids undergo a condensation reaction (Figure 2.2) forming polymers or polypeptide chains, with peptide

bonds occurring between the carboxyl group of one amino acid and the amide group of another.

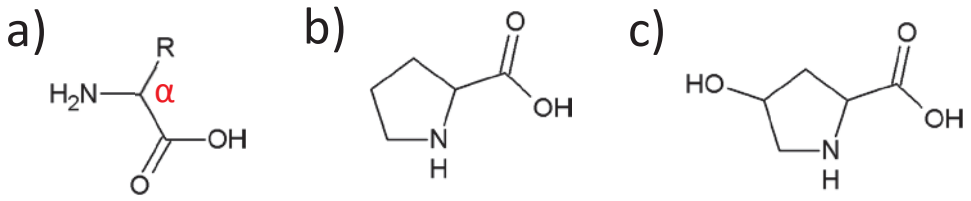

Figure 2.1. The structure of: a) generic amino acid where R is a side group; b) proline; c) hydroxyproline.

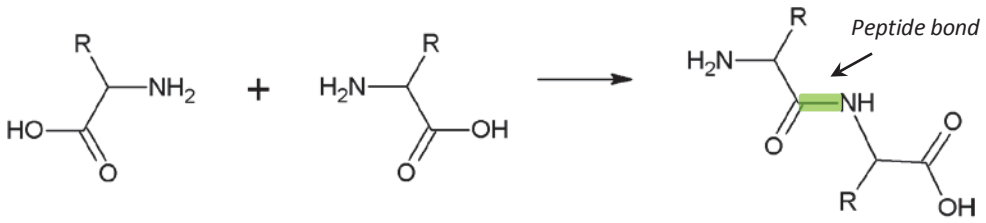

Figure 2.2. Condensation reaction of two amino acids to form a peptide.

In collagen, the polypeptide chains are termed α chains, with the longer central regions containing a repeat unit of three amino acids. The first in the continuous repeat unit is almost always exclusively glycine, giving the unit -(Gly-X-y)$_n$, where n is the number of repeat units, typically 337 to 343 (Fratzl, 2008). The cyclic amino acids proline and hydroxyl proline (Figures 2.1b and c) constitute approximately 20% of total amino acids in fibrillar collagen found in humans, so are often found in the X and Y positions of the repeating unit, with hydroxyproline unique to collagen and collagen-related proteins (Rich and Crick, 1961). Hydroxyproline is not incorporated into the polypeptide chains during chain formation, rather, hydroxylation of proline occurs as a posttranslational modification through the action of prolyl 4-hydroxylase and is most common when proline is located in the y position of the triplet in the helical region (Peterkofsky and Udenfriend, 1963, Kivirikko and Myllylä, 1985). Lysine and hydroxylysine are common amino acids also found in the Y position and are important for stabilisation through cross linking (Fratzl, 2008) as will be discussed later in this section, whilst other common residues include alanine and arginine (Gustavson, 1956). Hydroxylation of lysine residues also occurs as post-translational modification (Ottani et al., 2002). Shorter non-helical termini called teleopeptides are located pre and post central helical regions containing the triplet sequence.

2.1.1.2 Secondary Structure: The Left Handed Helix

Collagen α chains form left handed helices with the small glycine residues located in the core of the helix, leaving the X and Y residues facing the chain surface. There are approximately ten amino acid residues in three turns in a left handed helical polypeptide chain (Bhattacharjee and Bansal, 2005), however the number of residues per turn is variable and dependent on the exact amino acid triplet sequence, so that a single chain may display multiple symmetries along its length.

A number of factors regulate the stability of the α chains, principally hydrogen bonding between the oxygen in the C=O of one peptide link and the nitrogen in either the second, third or fourth successive peptide bond (Vincent, 2012). Stability of the chain will generally increase with the length of the helical region owing to the increase in the possible number of hydrogen bonds that can form (Vincent, 2012). The presence of proline and hydroxyproline also supply stability, firstly by their rigidity, restricting rotation and flexibility around the peptide bond, and secondly the hydroxyl group of hydroxyproline provides further opportunity for hydrogen bond formation (Mayne and Burgesson, 1987, Némethy and Scheraga, 1986).

2.1.1.3 Tertiary Structure: The Collagen Triple Helix

The tertiary structure of collagen involves the assembly of three collagen polypeptide chains to form a tropocollagen molecule with a right- handed triple helical structure, also known as a coiled coil. These three chains can be identical (homotrimeric) or, one of the three or even all three chains can be different (heterotrimeric) (Fratzl, 2008). The nomenclature attributed to a single collagen chain is αn(N), with n denoting the number of the α chain and N being the collagen type in Roman numerals. Collagen type I is heterotypic with two identical chains, therefore collagen type I would be $[\alpha1(I)]_2$ α2(I) (Piez et al., 1963). Tropocollagens are generally 1-2 nm in diameter, have lengths of approximately 300 nm (Ivanova and Krivchenko, 2012, Rice et al., 1964), with each turn of the helix comprising 30 residues per turn (Bhattacharjee and Bansal, 2005).

With the small glycine residues located at every third position and being incorporated in the centre of the helices (Van der Rest and Garrone, 1991), the helices of the other collagen polypeptide chains are able to come into closer proximity around a common axis (Gelse et al., 2003) and form further hydrogen bonding, this time between the three α chains and perpendicular to the helix (Mayne and Burgesson, 1987). Hydrogen bonding is vital in the formation and stability of the triple helix. It was postulated that at least one hydrogen bond

must exist between the three α chains to hold the strands together and later confirmed that a single interstrand hydrogen bond exists between the NH group of glycine and C=O group of the X position amino acid in an adjacent strand per repeat unit (Rich and Crick, 1961, Bella et al., 1994). Brodsky and Ramshaw (1997) discuss the founding theories, experimental studies and analyses leading to the understanding of the role of hydrogen bonding in the triple helix, the major points of note being that not only is there direct hydrogen bonding between amino acid residues in neighbouring polypeptide chains, but water bridges between amino acid polar residues are significant also; the NH groups integrated into the ring structure of proline and hydroxyproline are not available for bonding with the free C=O groups of glycine and hydroxyproline, or the hydroxyproline OH group, due the distances with it being exposed to the triple helix surface. In the absence of these cyclic amino acids, the NH groups of other X and Y position amino acids are available for hydrogen bonding but are hindered by distance from any C=O groups. Due to these circumstances, water molecules contribute to stabilisation by intramolecularly linking C=O or OH groups within the same α chain or intermolecularly between chains with a range in the number of water molecules in the chain bridge (Fraser et al., 1979, Bella et al., 1994). Typically the glycine C=O group hydrogen bonds to one water molecule, whilst there are two available water hydrogen bonding sites for hydroxyproline (C=O and OH groups). Therefore the collagen triple helix is stabilised by an extensive water network.

2.1.1.4 Quaternary Structure: Collagen Fibrils

The interaction of these tropocollagen molecules with one another leads to a higher level of collagen structure, the quarter-staggered array. The quaternary structure of fibrillar type collagens is referred to as collagen fibrils, long cylinder like structures.

Characteristic banding patterns on collagen are readily seen when viewed using microscopy techniques such as atomic force microscopy and staining coupled with electron microscopy. There are several names associated with these banding patterns including cross-striation, axial periodicity and D-spacing (or D), the latter which will be used throughout this thesis. These banding patterns were originally measured to be about 60-70nm long repeats across the length of the collagen fibril. Schmitt (1956) proposed this pattern was a result of tropocollagens aggregating in a parallel fashion, quarter-staggered with respect to each other so that the length of a tropocollagen molecule is equivalent to 4 units of D. This idea of tropocollagen stagger was later confirmed experimentally (Hodge and Schmitt, 1960). The more accurate and now accepted length of a tropocollagen molecule was determined to be 4.4 D (Petruska and Hodge, 1964), where D-spacing includes smaller overlap regions between

parallel tropocollagen molecules in register, and larger gap regions between the ends of tropocollagen molecules as seen in Figure 2.3 (reflected as lighter less dense, and darker more dense zones respectively when negatively stained).

Fibrils form when five tropocollagen molecules come together in this way. Any multiples of these sets of five tropocollagens parallel to one another can constitute a collagen fibril (Gelse et al., 2003), whereas sets of five tropocollagen molecules adjacent to one another is sometimes referred to as a microfibril.

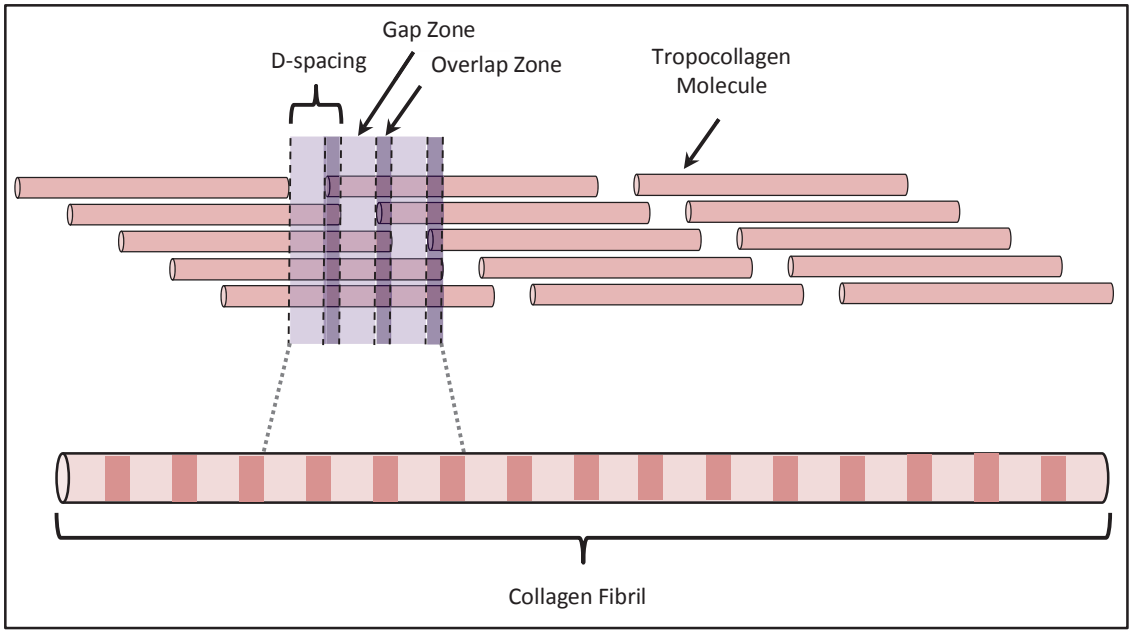

Figure 2.3. The quarter staggered array arrangement of five tropocollagen molecules parallel and in register to from a collagen fibril with regular gap and overlap zones which together comprise the D-spacing.

The D-spacing of collagen is generally reported as being 67nm, though for different tissues this value can vary. D-spacing for a range of tissues in different states has been elucidated, for example, the D-spacing of processed leather originating from different animals has been found to range from 0.628-0.653 nm (Sizeland et al., 2013).

In addition to the triple helices assembling into a quarter staggered array, collagen fibrils in many tissues exhibit crimp, otherwise known as molecular kinking or tilt. In microscopy, the crimp is manifested as a wavy structure, so that each tropocollagen within the set of five has several kinks or tilts along its length with alternating azimuthal orientation in the gap and overlap regions but of similar magnitudes (Orgel et al., 2006, Fraser et al., 1983). The wave

inflections occur in the short telopeptide regions where enzymatic cross links are found (Orgel et al., 2006). Fratzl (2008) summarises literature on a range of tissues which all report tilts of 18° such as skin, cornea and blood vessels. As a result of 18° tilt geometry, the D-spacing decreases from 67 nm to 65 nm, though different crimp magnitudes exist in other tissues. The function of tissues exhibiting fibril crimp is suggested as being the resistance of stresses, the straightening of which correlates to the toe region of the typical collagen stress-strain curves (Fraser et al., 1983).

Hydrogen bonding in the collagen quaternary structure is a contributing factor to fibril stabilisation. Interactions between tropocollagen molecules are strengthened by the presence of hydroxyproline which forms hydrogen bonds (Némethy and Scheraga, 1986). Hydrogen bonding involving water molecules also occurs; Bella et al (1994) found hydration cylinders envelop tropocollagen molecules within collagen fibrils, with which hydroxyproline residues interact to further enhance hydrogen bonding.

2.1.2 Collagen Cross Linking In the Quaternary Collagen Structure

Cross linking within collagen fibrils (between collagen molecules and tropocollagen molecules) and between fibrils is an integral part of fibril formation and stabilisation. Cross linking can be formed enzymatically or non-enzymatically, occur at different sites and bridge different distances. Intermolecular enzyme catalysed site-specific cross links form first, joining tropocollagens end to end, followed by non-enzymatic reactions involving glucose, forming intermolecular cross links with arginine and lysine (Fratzl, 2008). The following sections discuss such cross linking.

2.1.2.1 Enzymatic Cross Linking

Post fibril formation, the enzyme lysyl oxidase acts on the ε-amino groups of lysine and hydroxylysine, oxidatively deaminating such groups resulting in lysine-aldehydes which further react with adjacent ε-amino hydroxylysine residues (Fratzl, 2008). Lysyl oxidase does not target singular tropocollagens, but binds to a helical cross linking region characterised by the amino acid sequence (Hyl-Gly-His-Arg) in tropocollagens opposite the amino and carboxy terminals of adjacent staggered tropocollagens to form lysine-aldehydes (Bailey et al., 1998). These lysine-aldehydes further react with opposing lysine or hydroxylysine residues in the conserved (Hyl-Gly-His-Arg) sequence to form Schiff base intermolecular cross links. Four cross linking sites have been reported, one at each the carboxy and amino termini and two in the triple helical regions (Eyre et al., 1984). The carboxyl terminus of an α2(I) chain cannot undergo enzymatic

cross linking by lysyl oxidase due to the lack of hydroxylysine in its carboxy telopeptide end (Yamada et al., 1983). The nature of the cross links formed can vary depending predominantly on the extent hydroxylation of lysine located in both the telopeptide and triple helical regions, ranging from what are called aldimine cross links to keto-amine cross links when there are low and high levels of lysine hydroxylation respectively (Bailey, 2001, Bailey et al., 1998).

These cross links are known as immature links, they are reducible and divalent, that is they link two tropocollagen molecules in the quarter-staggered arrangement. In older tissues, mature cross links derived from the immature cross links are said to form, whereby these divalent cross links react further with lysine or hydroxylysine-aldehydes on parallel aligned tropocollagens producing trivalent cross links (Gelse et al., 2003). A range of mature cross links are also possible, with the Schiff base cross links alternatively reacting with other amino acids such as histidine for example. Eyre (1984), Bailey et al (1998), Bailey (2001), and Fratzl (2008) can be referred to for more detail about both immature and mature cross links.

2.1.2.2 Non-enzymatic Cross Linking

Non-enzymatic cross linking is referred to as glycation, involving the reaction of mainly lysine ε-amino groups and arginine with glucose (Baynes, 2003). Lysine ε-amino groups react with the aldehyde functional group of glucose in its open chain form by what is known as a Maillard reaction to give a Schiff base intermediate, a glucosyl-lysine (Robins and Bailey, 1972). This intermediate spontaneously rearranges (Amadori rearrangement) to form keto-amines prior to consequent oxidation reactions of the modified lysine residues to form what are called advanced glycation end –products (AGE). AGE is the term given to the end products following the Maillard and Amadori arragements that are protein bound and can result in intermolecular cross links (Bailey et al., 1998). Some AGE include, pentosidine and glucosepane which form cross links between lysine and arginine residues on adjacent molecules, or MOLD, GOLD and vesperlysine cross links resulting from reactions between two lysine residues (Bailey, 2001, Fratzl, 2008).

Glycation cross links can form intra, or inter-fibrillarly, though the exact locations of the cross links are not yet known (Fratzl, 2008). It is believed however, the glycation cross links occur in the helical regions as experiments have shown increases in denaturation temperature and decreases in enzyme susceptibility post glycation which thought to be related to helical-helical cross linking (Bailey et al., 1998).

2.2.3 Other Collagen Types

Collagen type I is only one of over 28 known vertebrate collagens and can be sorted into subgroups based on their structure or molecular organisations, function and collagenous/non-collagenous domains (Ivanova and Krivchenko, 2012, Kadler et al., 2007). Table 2.1 summarises the different collagen types.

Table 2.1. Summary of the different collagen types, features and distribution in the body and tissues based on information from Mayne and Burgeson (1987), and (Fratzl, 2008).

Collagen Type	Subgroup/ Classification	Location	Description
I	Classic fibrillar collagen	Non-cartilaginous tissues, e.g. tendon, bone, lung, skin, ligament, vasculature & cornea.	Triple helical regions with short non-helical telopeptide regions on either end.
II	Classic fibrillar collagen	Specifically cartilage.	Triple helical regions with short non-helical telopeptide regions on either end.
III	Classic fibrillar collagen	Found with type I in somewhat elastic tissues such as lung, blood vessels & embryonic skin.	Triple helical regions with short non-helical telopeptide regions on either end.
V	Fibrillar collagen	Associated with type I in minor quantities, for example in cornea and embryonic tissue.	
XI	Fibrillar collagen	Associated with type II in cartilage in minor quantities.	
XXIV &	Fibrillar collagen	Selective expression in bone & cornea development.	Shorter triple helical region with 1-2 short interruptions.
XXVII	Fibrillar collagen	Developing dermis, cornea, embryonic cartilage, major heart arteries, & retina membrane.	Shorter triple helical region with 1-2 short interruptions.
IX	FACITs & related collagens	Covalently cross linked to type II & XI cartilage fibrils.	Has 3 short interrupted collagenous regions & 4 non-collagenous regions. Sometimes acts as a PG as can attach chondroitin or dermochondan sulfate GAG.
XII, XIV	FACITs & related collagens	XII associates with type I fibril surface in ligaments, skin, tendons & cornea.	
XVI, XIX, XXII	FACITs & related	Localised in specific areas in tissues though not directly associated with	Three or more collagenous domains

	collagens	collagen fibrils, e.g. hair follicle-dermis &cartilage-synovial fluid.	
XX, XXI	FACITs & related collagens	Widespread, predominantly found in epithelium.	
VI	Beaded filament	Various locations, particularly in muscle.	Triple helical region approximately 1/3 fibrillar collagen. Forms beaded filaments with disulfide cross links stabilising tetramers which form beaded microfibrils.
IV	Basement membrane & associated collagens	Tissue boundaries: underlying epithelial, endothelial, nerve & fat cells in cornea, gut, skin, lung & blood vessels for example. Also acts as a macromolecule selective barrier/filtration in kidneys & placenta for example.	Longer than fibrillar collagens with several interruptions. Forms open meshwork structure with 40-50 nm thin sheets.
VII	Basement membrane & associated collagens	Basement membrane at dermal-epidermal junction.	Of the vertebrate collagens, has the longest triple helical region. Forms anchoring filaments.
XV, XVIII	Basement membrane & associated collagens	Associate with basement membranes.	Referred to as multiple triple helices with interruptions. Contain several collagenours domains and carry GAG chains
VIII	Short chain collagens	Underlies endothelial cells, Descemet's membrane of the cornea.	Approximately ½ length of fibrillar collagen triple helix region with numerous interruptions. Forms hexagonal supramolecular networks.
X	Short chain collagens	Restricted to zone of cartilage separating hyaline cartilage from the subchondral bone.	Approximately ½ length of fibrillar collagen triple helix region with numerous interruptions. Thought to form networks similar to VIII.
XIII, XVII, XXIII & XXV	Transmembrane collagen	Occur on many cell types including malignant cell.	Have long interrupted triple helical domains. Various functions in cell signalling and adhesion.
XXVI &XXVIII	Other collagens		

2.2 Proteoglycan Cross Links

As stated earlier, collagen comprises a large fraction of the extracellular matrix of tissues. Another important component of such tissues are carbohydrate macromolecules, known as glycosaminoglycans (GAGs), which, when combined with core proteins form what are known as proteoglycans (PGs). GAGs form connections or interfibrillar bridges between fibrils so are a kind of cross link; in this thesis these links are referred to as natural cross links or GAG cross links. Understanding the role of GAGs on collagen nanostructure and nanostructural changes in response to uniaxial tension is one of the major aims of this thesis. This section of the literature review will cover the basics of different GAGs and PGs, their interactions with collagen and each other to form these natural cross links, and the removal of GAG cross links using the enzyme chondroitinase ABC.

2.2.1 Glycosaminoglycans

GAGs are a type of macromolecular carbohydrate consisting of two or more different sugars, with repeating disaccharide units. One of the monosaccharides has nitrogen present and the other an acid, and form long polysaccharide chains with alternation of the two types of monosaccharides (Kiernan, 2010, Kjellen and Lindahl, 1991). The first monosaccharide is a hexoamine (either D-gluscosamine or D-galactosamine), and the second either hexuronic acid (D-glucuronic acid or L-iduronic acid), or galactose units, where the two units form long unbranched polysaccharides with sulfate substitutions (half-sulfate ester groups) in various locations (Kjellen and Lindahl, 1991). Due to the range in possible sulfate positions on the sugar units, over 16 types of disaccharides can exist (Scott, 2003). The carbohydrate units are joined by a covalent glycosidic bond, a bond between a hemiacetal or hemiketal group of one carbohydrate to a hydroxyl group of another to form an O-glycosidic bond. When the oxygen in the glycosidic bond is replaced with nitrogen this is termed an N-glycosidic bond.

Common GAGs include dermochondan sulfate, chondroitin sulfate, hyaluronan, heparin, heparan sulfate, and keratan sulfate. Of these GAGs, hyaluronan is the only one with no sulfate group and does not bind to a core protein to form PGs (Kjellen and Lindahl, 1991, Lovekamp et al., 2006). Both dermochondan sulfate and heparan sulfate GAGs can have D-glucuronic acid and L-iduronic acid as the hexuronic acid component in the repeat unit, whilst the hexuronic acid constituent in chondroitin sulfate can only be D-glucuronic acid. Keratan sulfate contains galactose units in place of hexuronic acid (Kjellen and Lindahl, 1991).

GAG chains are highly charged, that is anionic and hydrophilic, due to the presence of charged sulfate groups and the carboxylate functional groups and are capable of absorbing water (Hardingham and Fosang, 1992).

2.2.2 Proteoglycans

A core protein linked to one or more GAG chains is called a proteoglycan. There are various types of PGs which differ in the size of the core protein, the nature of association of the protein with GAG chains, and the types of GAG chains attached. Some PGs include aggrecan, syndecan, betaglycan, decoran, biglycan, fibromodulin, versican and thrombomodulin (Kjellen and Lindahl, 1991, Hardingham and Fosang, 1992). The names given to PGs often relate to functional and structural characteristics of the protein-GAG complex, and these PGs can be loosely classified under 3 different families: 1) large-molecular PGs, 2) small PGs, and 3) basement membrane/extracellular matrix heparan sulfate PGs (Kjellen and Lindahl, 1991). There are many types of PGs, of which only a few will be covered in more detail in this section. Small PGs directly bind to collagen, of which decoran is one PG commonly associated with collagen type I in tissues such as tendons and ligaments, for this reason it is more widely and specifically referred to in the literature regarding PGs.

2.2.2.1 A Large PG: Aggrecan

Aggrecan is considered a large PG (225-250 kDa) and is distributed in tissues such as cartilage, developing bone, embryonic skeletal muscle and the aorta (Hardingham and Fosang, 1992, Kjellen and Lindahl, 1991). Keratan sulfate, N and O-linked oligosaccharides, but mostly chondroitin sulfate, together make up approximately 90% of aggrecan. Structurally, aggrecan is a very large aggregate of many PG monomers which are non-covalently linked to the GAG hyaluronan (Hardingham and Fosang, 1992).

2.2.2.2 Small PGs: Decorin, Biglycan and Fibromodulin

Decoran, biglycan and fibromodulin all have small core proteins (approximately 40 kDa) rich in the amino acids leucine and cysteine; leucine is located in the protein core, whilst the end domains are rich in cysteine (Lujan et al., 2007, Hardingham and Fosang, 1992). Examples of the distribution of these PGs in mammals include connective tissues, cornea and cartilage.

Decoran is known to be present in regions rich in type I collagen, binding to collagen fibrils and is thought to have roles in the development and organisation of the extracellular matrix, maintaining fibril orientation and interfibrillar space (Scott and Thomlinson, 1998, Scott, 1992,

Hardingham and Fosang, 1992). One or two dermochondan sulfate or chondroitin sulfate GAG chains are attached at the amino terminus of the core protein via a serine linked oligosaccharide.

Biglycan is found at the surface of cells, does not bind to collagen, can have two chondroitin or dermochondan sulfate chains and is O-linked at the amino terminus of the protein core.

Fibromodulin, like decoran, can bind to collagen fibrils (types I and II), though the associated GAGs are that of keratan sulfate, which are N-linked to the leucine rich central region of the protein core. Some of these leucine binding sites have short oligosaccharides, so keratan sulfate chains and oligosaccharides can be present in this central region (Hardingham and Fosang, 1992).

2.2.3 Interactions of Proteoglycans with Collagen

PGs can be stained (either positively or negatively) to increase their contrast in comparison to the surrounding environment. Combining PG staining with electron microscopy has revealed small PGs to associate with collagen in the D-spacing of the fibrils, more specifically in the gap region of the D-spacing (Scott, 1980, Scott and Orford, 1981). Polar and non-polar regions exist on the surface of collagen fibrils due to the sequences of amino acids which make up the collagen α chain backbone (and so tropocollagens and fibrils). Staining fibrils with UO_2^{2+} reveals these regions as bands of varying thickness and darkness (Mayne and Burgesson, 1987). Five bands labelled a to e exist within the collagen D-spacing, of which four of these bands per collagen fibril D-spacing can act as PG binding sites; decoran PGs bind at the d and e sites (so chondroitin and dermochondan sulfate GAGs) whilst PGs containing keratan sulfate are located at the a and c bands (Scott, 1988). The core protein of a common collagen type I assoicated PG, decoran, has been modelled and visualised by microscopy to be horseshoe shaped (Orgel et al., 2009). The concave face is thought to bind to the gap zone in the D-spacing of a single tropocollagen in a collagen fibril rather than interacting directly in the triple helix interior (Figure 2.4), and so the association is inter not intra-fibrillar (Lujan et al., 2007, Scott, 1996, Scott, 1988). The association of the protein core with the collagen fibril is non-covalent in nature (Scott, 2003). Shorter range non-electrostatic binding is thought to occur in the d-band of the D-spacing where PGs such as decoran are located as this region is non-cationic (Scott and Orford, 1981).

The anionic GAGs which are covalently linked to the protein core extend away from this core and the collagen fibril surface. Two or more GAG chains from different protein cores attached to adjacent parallel collagen fibrils, aggregate to form a cross link. The protein-GAG complexes form mainly orthogonal regularly spaced bridges or cross links between collagen fibrils in register at the D-spacing gap zones in mature tissues, whilst it has been observed that a small amount PG links can occur axially in immature tissues (Scott, 1980, Scott and Orford, 1981, Cribb and Scott, 1995). The length of these GAG cross links varies between tissues, i.e. some fibrils are more tightly packed and require shorter GAG cross links, (Scott and Thomlinson, 1998). It is proposed that dermochondan and chondroitin sulfate GAGs associate in an antiparallel fashion to form a 'duplex' GAG bridge between neighbouring fibrils as seen in Figure 2.4, with keratan sulfate bridges also possible (Scott, 1992).

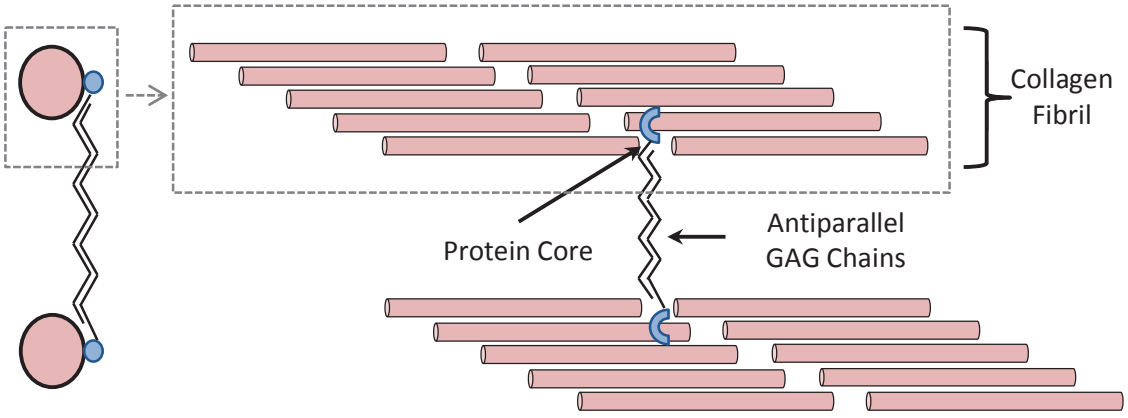

Figure 2.4. Association of PG core proteins with collagen fibrils in the gap region of the D-spacing, and antiparallel arrangement of GAG chains with one another to bridge fibrils: the left image shows the end-on view of fibrils, and the right image depicts the association of a PG-GAG complex with individual tropocollagen molecules in a fibril.

The GAGs chondroitin and keratan sulfate form a two-fold helix in aqueous solutions (as does hyaluronan) where hydrophobic regions are alternated on either side of the polymer chains, located in similar positions (Scott, 1992, Scott, 2003, Scott and Thomlinson, 1998) which encourage the aggregation of GAG chains through hydrophobic bonding. Regions of hydrophobicity also exist in the dermochondan sulfate GAG chains leading to similar aggregation. However hydrophobic bonding alone does not stabilise the GAG cross links, van der Waals forces and hydrogen bonding are also involved and overcome the mutual repulsion forces of the anionic functional groups between duplexed GAGs (Scott and Thomlinson, 1998).

It has been suggested that the absence of non-covalent bonding between GAG chains may allow the GAG chains to disassociate and possibly re-associate under tension or compression, enabling relative sliding of adjacent collagen fibrils (Scott, 1992, Scott, 2003).

2.2.4 Removal of GAG Cross Links

The enzymes papain and chondroitinase ABC are examples of common enzymatic methods for the removal or disruption of GAG cross links. The enzyme chondroitinase ABC is used in this thesis for the purpose of GAG removal to allow comparison of structures and response to mechanical stresses of collagen with and without GAGs, thereby gaining an understanding of their role in the extracellular matrix of bovine pericardium.

2.2.5 The Chondroitinase ABC Enzyme

Chondroitinase is an enzyme originating from Proteus Vulgaris with a molecular mass of 120 kDa and is used in tissue engineering for the removal GAGs in collagen. Chondroitinase ABC removes cross links by attacking the GAG side chains of a PG rather than the core protein. More specifically, it cleaves the glycosidic bonds between the polysaccharide units. Chondroitinase ABC can act on chondroitin sulfate cross links (chondroitin-4-sulfate and chondroitin 6-sulfate) and dermochondan sulfates at high rates, while slowly degrading hyaluronate (Hamai et al., 1997).

Activation of the chondroitinase ABC enzyme can be achieved using 0.05M acetate. A range of treatment temperatures have been used, among which are 37 °C, 20 °C, 25 °C, and room temperature (Saito et al., 1968, Al Jamal et al., 2001, Lujan et al., 2009, Schmidt et al., 1990).

A range of GAG removal efficiencies have also been reported in literature for chondroitinase ABC and may in part be due to the concentrations, physical and chemical conditions used as well as the nature of the tissues being degraded. Examples of the extent of GAG removal achieved using chondroitinase ABC are:

- 54%, 47% and 44% decreases in GAG content in the middle, proximal and distal regions of Achilles tendon respectively (Rigozzi et al., 2009).
- 60% (Rigozzi et al., 2013).
- 90% removal of sulfated GAGs (Lujan et al., 2009).
- 37 ± 8% removal of sulfated GAGs(Al Jamal et al., 2001).
- 85% removal of chondroitin and dermochondan sulfate (Schmidt et al., 1990).

2.3 Synthetic Cross Links

There are a number of fixatives or cross linking agents used in the medical industry and commercially to treat biological tissues. The chemical glutaraldehyde is one of the most common cross liking agents utilised, from tanning of leather, fixing biological tissue specimens in preparation for electron microscopy to treatment of biological graft materials , artificial skin, tendon xenografts and prosthetic valves in heart valve replacement surgeries (Jayakrishnan and Jameela, 1996, Schoen and Levy, 1999, Jastrzebska et al., 2003). Glutaraldehyde is the chemical agent used in this thesis to introduce synthetic cross linking and will therefore be discussed in detail in this section. Other cross linking agents and techniques used and/or investigated elsewhere will be mentioned briefly also.

2.3.1 Glutaraldehyde

Glutaraldehyde (pentane-1,5-dial) is an organic compound belonging to the aldehyde family with a five carbon long chain and two aldehyde functional groups on either end of the molecule giving the molecular formula $OCH(CH_2)_3CHO$, (Figure 2.5).

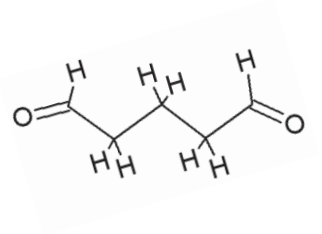

Figure 2.5. Skeletal diagram of a glutaraldehyde molecule.

Glutaraldehyde is miscible in water and is available in aqueous solutions of varying concentrations.

2.3.2 Cross Linking Collagen with Glutaraldehyde

The mechanism by which glutaraldehyde forms cross links and the types of cross links formed is complex and not universally agreed upon. However it is widely accepted that the initial reaction step involves the reaction of an aldehyde functional group from glutaraldehyde with the ε-amine groups of lysine and hydroxylysine residues from collagen to form what is known as a Schiff base intermediate, alternatively referred to as imines. A Schiff base contains a functional group consisting of a carbon-nitrogen double bond to which either an alkene or aryl group is attached to the nitrogen atom. There is debate as to the stability of this Schiff base and the subsequent reaction pathways leading to different cross link formation (Olde Damink et al., 1995).

Suggested reactions pathways include further interactions with glutaraldehyde molecules via aldol condensation reactions forming glutaraldehyde polymers of varying lengths. Schiff base intermediates can react with a collagen amine group via Michael addition to form cross links. Evidence suggests Schiff base intermediates undergo Mannich-type reactions to form secondary amines which eventually lead to pyridinium-type cross links (Olde Damink et al., 1995, Jastrzebska et al., 2003). Olde Damink et al (1995) can be referred to for more details regarding the proposed mechanisms and types of glutaraldehyde cross links discussed in the literature.

Both intra and intermolecular cross linking of collagen are thought to be possible, that is, cross linking of lysyl and hydroxylysl residues from different α chains of a single tropocollagen molecule, and cross linking of lysyl and hydroxylysl residues of different tropocollagen molecules respectively (Cheung and Nimni, 1982, Cheung et al., 1985). Factors such as the type of collagen material (collagen in solution, reconstituted collagen or collagen tissues), which dictates the distance between available ε-amino residues, and concentration of the glutaraldehyde solution used, affect the type and nature of cross links present in collagen tissues (Cheung and Nimni, 1982, Cheung et al., 1985, Olde Damink et al., 1995).

Glutaraldehyde concentration is reported by some not to significantly affect the number of ε-amino groups involved in cross linking, however can influence time of fixation and the types of cross links formed. Experiments conducted by Cheung and Nimni (1982) and Cheung et al (Cheung et al., 1985) found that in reconstituted collagen and collagen tissues, higher glutaraldehyde concentration results in rapid glutaraldehyde polymerisation with cross linking initially localised to the fiber surface, depleting the free glutaraldehyde molecules. Therefore large complicated intermolecular glutaraldehyde polymer links are formed between collagen molecules or fibers bridging a range of distances. The size of these links and competition for the free available glutaraldehyde between the polymer nucleation sites and unreacted lysyl and hydroxylysyl groups may result in steric hindrance and uneven glutaraldehyde penetration and fixation through the tissue depth.

In contrast to these findings, others have presented evidence against the formation of such glutaraldehyde polymer networks. Olde Damink et al (1995) conclude that despite the formation of numerous types of cross links by glutaraldehyde, polymeric network formation is not the main mechanism of cross linking as for every reacted ε-amine group there is an average uptake of only three glutaraldehyde molecules. In these investigations it was found that the Schiff base intermediate is stabilised within 24 h, after which cross linking of the tissue

occurs. Of these links, polymers are possible; very low portions are aldol polymers resulting from fast stabilising reactions post aldol condensation. A low portion of high molecular cross links with large repeat sequences, or a larger fraction of high molecular cross links with low repeat sequences are also possible.

Direct comparison of results of cross linking experiments for the determination of final cross linking products and cross linking mechanisms is not straightforward, where the use of impure glutaraldehyde solutions could lead to different outcomes; glutaraldehyde solutions can be mixtures of free aldehydes, monomeric glutaraldehyde, monomeric and polymeric cyclic hemiacetals and unsaturated polymers (Jastrzebska et al., 2003, Jayakrishnan and Jameela, 1996).

2.3.4 Glutaraldehyde Cross Linking of Collagen Tissues for Bioprosthetic Heart Valves

All animal tissue derived heart valves are chemically treated or cross linked prior to use so as to introduce stability, longer shelf life and sometimes for enhanced mechanical properties. Consequent to the establishment that stabilisation of collagenous materials can be achieved with glutaraldehyde cross linking, it was first introduced into bioprostheses such as replacement heart valves and grafts in the late 1960s (Schmidt and Baier, 2000). Glutaraldehyde is the most widely utilised cross linking agent in the medical industry for this purpose, with vascular grafts and a range of commercial bioprosthetic valves currently using glutaraldehyde as a fixative (Singhal et al., 2013).

Examples of commercially available glutaraldehyde-treated bioprosthetic heart valves (aortic and pericardial) still in use include:

- Carpentier Edwards Perimount
- Carpentier-Edwards Standard
- Carpentier-Edwards Supraannular
- Mitroflow model 12
- Hancock II
- Medtronic Mosaic
- Medtronic Freestyle
- SJM Quattro

(Singhal et al., 2013, Schoen and Levy, 1999, Reece et al., 1982).

A variety of glutaraldehyde concentrations are used in these commercial valves and in the literature for the cross linking of collagen based tissues, ranging from 0.2 % to 0.6 %. Although a number of factors (treatment time and temperature for example) regulate the extent of cross linking within the tissue and properties, higher concentrations of glutaraldehyde are reported to increase tissue stiffening whilst lower concentrations result in less effective sterilisation (Jayakrishnan and Jameela, 1996).

2.3.5 Advantages of Glutaraldehyde Collagen Cross Linking

Cross linking in general can provide major benefits to bioprostheses, among which are the following:

- Higher material stability and therefore increased shelf-life; tissues can be pre-treated ahead of time and be available for use at any time.
- Reduces though not completely eliminates antigenicity/immunogenicity; antigens are masked by the cross links.
- Maintains thromboresistance and antimicrobial sterility.
- Increases resistance to degradation by enzymes or chemicals.
- Sterilises biological tissue.
- Anticoagulation therapy is not required post introduction into the body.

(Jayakrishnan and Jameela, 1996, Schmidt and Baier, 2000, Schoen and Levy, 1999, Singhal et al., 2013).

Advantages more specific to glutaraldehyde include its effectiveness as a cross linking agent, with a higher degree of cross linking achieved compared to other chemical cross linking agents, and the ability to fix tissues at low temperatures such a room temperature or as low as 4°C (Shi, 2006).

2.3.6 Disadvantages of Glutaraldehyde Collagen Cross Linking

Whilst there are a number of positive consequences to cross linking of collagenous bioprotheses, cross linking in general can also lead to a number of problems, including:

- Rendering of cells as non-viable so that required proteins cannot be produced.
- The alteration of the micro and nanostructure of the tissue so that it's fixed, limiting nanostructural rearrangements and often best suited to a specific phase in the cardiac cycle.

- Different mechanical properties to natural aortic valves (this could be considered an advantage or disadvantage depending on the required end function).

(Schoen and Levy, 1999, Reece et al., 1982)

It is reported that glutaraldehyde specifically can leach slowly from tissue-derived bioprosthetics to produce cytotoxic effects (Jayakrishnan and Jameela, 1996, Schmidt and Baier, 2000). Breakdown of unstable Schiff bases formed upon the reaction of glutaraldehyde with collagen free amine groups of lysine and hydroxylysine residues is suggested as being responsible.

Calcification of tissues cross linked with agents such as glutaraldehyde is the primary stimulant for premature failure of bioprostheses (Schmidt and Baier, 2000, Jayakrishnan and Jameela, 1996). Calcification describes the formation of deposits of calcium derived minerals and occurs in two phases, nucleation and mineral deposit propagation. In the nucleation phase, calcium balance is disrupted due to the damage of the non-viable cell membranes induced by glutaraldehyde cross linking, and high concentrations of calcium in the cells and surrounding fluid react with phosphorus from membrane phospholipids and nucleus to initiate crystals (Schoen and Levy, 1999, Singhal et al., 2013). The propagation phase involves the perpetuation of the crystals, the degree of which is governed by factors such as calcium and phosphorus concentrations. Alteration of collagen groups is stated as a requirement for calcification on collagen (Schoen and Levy, 1999), whilst other aspects including unreacted glutaraldehyde groups, degree of cross linking, and mechanical stresses are also thought to affect or instigate calcification (Schmidt and Baier, 2000).

Despite these disadvantages which can lead to failure and toxicity to surrounding cells, glutaraldehyde remains the dominant cross linking agent or fixative of biological tissues for applications such as heart valve replacements. In the recent years much research has been directed at mitigating glutaraldehyde cytotoxicity and calcification. Methods include but are not limited to, the use of sodium dodecyl sulfate for the removal of lipids before cross linking, treatment with alkaline inhibitors, use of low pH L-glutamic acid for the neutralisation and extraction of aldehyde groups, prevention of calcium permeation using trivalent cations, addition of PGs or GAGs post cross linking, and ethanol treatment (Schmidt and Baier, 2000, Schoen and Levy, 1999).

2.3.7 Other Cross Linking Methods

A variety of other cross linking methods have been used previously or are being investigated, these include other chemical cross linking agents, enzyme induced cross linking, and physical cross linking techniques. Examples of such cross linking techniques will be mentioned here briefly.

2.3.7.1 Chemical Cross Linking Methods

The amide, carboxyl, and hydroxyl groups of amino acids such as lysine, hydroxylysine, aspartic acid and glutarmic acid in collagen are often target points for chemical cross linkers, where the cross linking agents typically have two functional groups which can react with collagen at two locations (Suh et al., 1999).

Formaldehyde is another aldehyde cross linking agent which like glutaraldehyde reacts with the amino groups of lysine and hydroxylysine to form a Schiff base or imine intermediate. The intermediate further reacts with asparagine or glutamine amide groups to form cross links. Disadvantages of formaldehyde for cross linking have been reported to include less stable cross links leading to early failure, brittleness, decreases in tensile strength and potential toxicity (Friess, 1998, Schoen and Levy, 1999).

In addition to aldehydes, other common chemical cross linking agents include epoxy compounds and polyepoxy compounds, carbodiimides and acyl azides.

Polyepoxy cross linking agents are based on glycerol and are bi or tri-functional glycidyl ethers (Shi, 2006). The reaction of epoxy compounds with collagen amino acid groups is pH dependent; for pH < 6, ester bonds form between the carboxyl groups of aspartic and glutamic aicds and the expoxide, whilst for pH > 8, the epoxide reacts with lysine and hydroxylysine amine groups (Shi, 2006). Examples of polyepoxy compounds are ethylene glycol diglycidyl ether, glycerol polyglycidyl ether and methylglycidyl ether (Friess, 1998, Schmidt and Baier, 2000).

Carbodiimides and acyl azides are agents which mediate cross linking between carboxyl and amide groups of amino acids whilst not being integrated into the final cross links themselves. A common carbodiimide is 1-ethyl-3-(3-dimethylaminopropyl) carbodiimide (EDC) which is water soluble. EDC activates aspartic or glutamic acid carboxyl groups resulting in the formation of O-isoacylurea structures which form amide cross links following the nucleophilic attack of lysine or hydroxylysine amino groups (Olde Damink et al., 1996, Shi, 2006). The

nucleophilic attack liberates the isoureaderivative of the carbodiimide, which can be removed by rinsing. Acyl azides likewise form amide cross links by methylation and conversion of carboxyl groups to hydrazides consequent to further reactions forming intermediates with azide functionalities. These intermediates interact with collagen amino groups to form cross links and are not incorporated into these links (Friess, 1998).

The cross linking agents described are a few of many investigated or being investigated for the fixation and cross linking of collagen based materials, others include carboxylic acids such as citric acid, sodium metaphosphate, epichlorohydrin, and genipin (Sung et al., 1999, Reddy et al., 2015).

The paper by Jang et al (2012) describes a range of different cross linking agents and the effects of these cross linkers after single or double cross linking treatment on mechanical properties and toxicity. They found that none of the combinations improved mechanical performance, cytotoxicity or cross linking properties when compared to glutaraldehyde or genipin treatment.

2.3.7.2 Biological Cross Linking Methods

The introduction of enzymes such as transglutaminase to collagen can also lead to formation of cross links. Transglutaminase catalyses the formation of inter or intramolecular ε-(ɣ-glutamyl)lysine links between the amino acids lysine and glutamic acid, and has an advantage of being non-cytotoxic (Chen et al., 2005).

2.3.7.3 Physical Cross Linking Methods

Irradiating collagen with X-rays, ɣ-rays or UV light are all physical methods which may be used to introduce cross links in collagen. In the case of X-ray or ɣ-ray radiation, the collagen must be in a hydrated state to form thermally stable cross links as peptide bond degradation can occur if collagen is dry (Fratzl, 2008). It is presumed that the formation of free radicals in the water post irradiation induces random cross links, though the exact mechanism of formation is unknown (Fratzl, 2008).

Introduction of UV light is thought to produce di-tyrosine and 3,4-dihydroxyphenylalanine (DOPA) cross links (Kato et al., 1995), however a significant amount of collagen degradation can be incurred, the level of which is dependent upon factors such as collagen type, the UV wavelength used, pH and the levels of oxygen (Fratzl, 2008).

Another physical cross linking method which does not involve radiation is dehydrothermal treatment. This treatment method significantly dehydrates collagen under a vacuum for a number of days with temperatures reaching up to 110 °C (Weadock et al., 1996). This results in condensation or β-elimination of collagen amino and carboxylic groups, more specifically thought to be alanine, which then reacts to lysine residues to form inter-chain amide cross links (Shi, 2006, Fratzl, 2008).

These physical cross linking methods are beneficial in that no toxic or harmful chemicals are utilised, however major disadvantages include possibilities of significant collagen degradation and lower degrees of cross linking achieved when compared to chemical methods (Shi, 2006).

2.4 Pericardium

The naturally produced collagen material used in this thesis to investigate the effects of cross linking of collagen nanostructure and nanostructural response to uniaxial tension is bovine pericardium. Bovine pericardium was chosen for this purpose as it is a widely available low cost material (Yang et al., 2009). It is also used extensively in the medical field for bioprosthetic heart valves and skin grafts. Pericardium is commonly fixed with glutaraldehyde, the synthetic cross linking agent investigated in this thesis, prior to use in such bioprostheses. Although the actual design and mechanics heart valves is outside the scope of this work, it is hoped the research presented here will not only prove to be insightful in terms of the science and understanding of GAG and glutaraldehyde cross links on collagen structure and mechanics, but may provide useful information to those in the field of bioprosthetic design and implementation.

Other advantages of bovine pericardium include its biocompatibility (it is a biological material which when glutaraldehyde cross linked, reduces antigenicity), where its compliance is said to be greater than other materials for bioprostheses and similar to native arteries (Li et al., 2011), high collagen content (compared to porcine aortic valves for example), symmetrical opening design in prosthetic valves result in enhanced hemodynamics (compared to aortic valves sourced from other animals), and compared to aortic derived prosthesis, larger tissue sizes can be selected to compensate for future shrinkages (Aslam et al., 2007).

This section of the literature review will cover the structure of pericardium and briefly summarise the heart, natural heart valves and bioprosthetic heart valves.

2.4.1 Pericardium: Structure and Function

Pericardium is often described as a double-walled conical sac which contains the heart and the great blood vessels. Figure 2.6 shows the pericardium sac in relation to the heart and pericardial regions/features. It functions to anchor the heart, protect it from infections and provide lubrication. A closer look at the pericardium cross-section reveals multiple layers of tissue, membranes and cavities which comprise the overall sac.

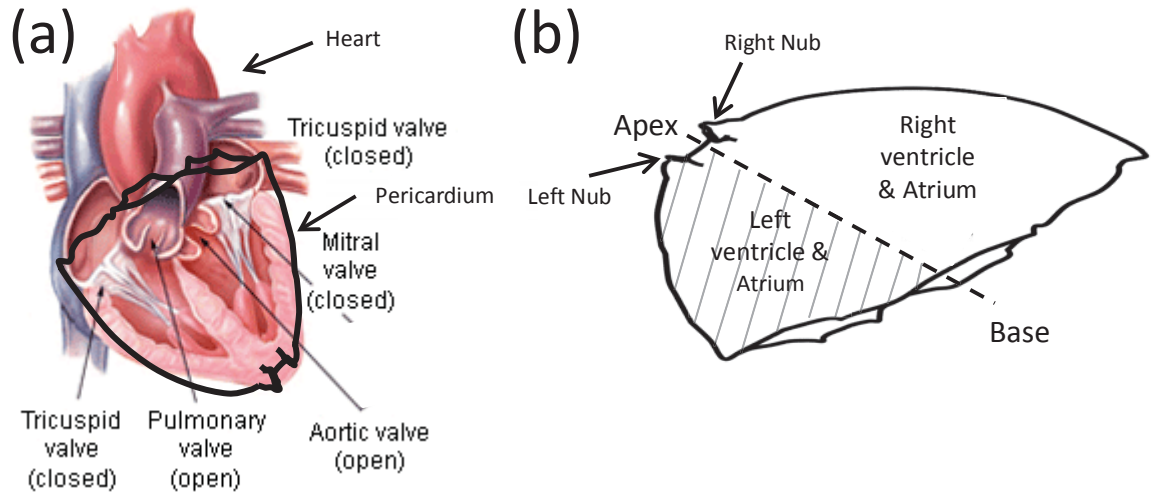

Figure 2.6. Pericardium: a) positon of a pericardial sac in relation to the heart, where the heart image is adapted from http://www.yourheartvalve.com/heartbasics/pages/heartvalves.aspx; b) regions and features of pericardium sac on the ventricular side.

The outermost layer of the pericardium is termed the fibrous layer, a tougher layer rich in connective tissue; randomly orientated crimped collagen fibrils and elastic fibers are present in the fibrous layer (Ishihara et al., 1981). The fibrous pericardium anchors the heart to the diaphragm and the back of the breastbone whilst loosely enveloping the heart itself. The fibrous pericardium prevents the overfilling of the heart with blood. Adhered and inseparable to the fibrous pericardium is the parietal pericardium, a thin serous membrane lining the inner surface of the fibrous layer. A cavity referred to as a potential or pericardial cavity separates the parietal pericardium from a second thin serous membrane called the visceral pericardium. This cavity is filled with serous/pericardial fluid which protects the heart from shock. The visceral pericardium more tightly encloses the heart, extending to the start of the hearts great blood vessels thus providing protection. The point of contact or where the visceral pericardium is continuous with the outer fibrous layer of the heart and the blood vessels is referred to as the epicardium. Collectively, the parietal and visceral pericardia and the pericardial cavity are

termed the serous pericardium. Both the serous membranes, the parietal and the visceral, enable pericardial fluid excretion into the pericardial cavity. A thin wall of this fluid (10-15 ml) lies within the cavity. It provides a lubricated surface which minimises friction of both heart activity/contractions and the movement of the diaphragm and lungs due to the ways in which the two surrounding membranes attach to the heart and these surrounding body structures.

2.4.2 Pericardium: Nanostructure

Pericardium, as a connective tissue is rich collagen and associated GAGs, as well as containing glycoproteins (Athar et al., 2014). Of the proteins in the extracellular matrix of pericardium, collagen constitutes 90%, type I being the predominant collagen (Schoen et al., 1986). Dermochondan sulfate is the major GAG present in bovine pericardium, to which the associated protein core is of similar size to that found in tendon (40 kDa) and the GAG chain itself smaller, associating as in other collagenous tissue at the d and e bands of the collagen fibril D-spacing (Simionescu et al., 1989).

Collagen fibrils can be orientated in any direction within collagenous tissues. Often fibrils adopt preferred orientations depending on the required specific function of the tissue in different areas of the body. They can be randomly aligned with respect to one another (isotropic), highly aligned so they are parallel to one another in one or more directions (anisotropic), or any variation in between. Pericardial sacs show differences in fibril alignment and direction of fibril alignment at different locations (Hiester and Sacks, 1998a). Three main fibril layers with preferred orientation 60° to one another have been reported by some, whilst the results of other experiments suggest similar fibril orientation directions between layers (Hiester and Sacks, 1998b).

It has also been reported that pericardium thickness varies with age as well as animal type and species; young neonatal pericardium is thinner than that of adult pericardium (Sacks et al., 1994) which can lead to differences in mechanical properties. For example it was found that neonatal pericardium is stronger than adult pericardium and correlates to fibril orientation in the edge-on plane of bovine pericardium (Sizeland et al., 2014). Variation in pericardium thickness not only exists between animals, species and age of species, but also within each pericardial sac itself. Mapping of thickness over entire pericardium sacs has repeatedly shown regional variations in thickness (Hiester and Sacks, 1998a). Different areas of a pericardium sac attach to different sites and will experience different external forces, so regional inconsistencies in thickness, and fibril alignment and orientation direction of the sac would be expected.

2.4.3 Pericardium: Sample Selection

In terms of valve leaflets, the ideal selection area would have thickness uniformity and consistent fibril alignment (high or low) and direction (Hiester and Sacks, 1998a). In this thesis it is primarily the structure of samples having undergone different treatments that is investigated, therefore it would also be ideal to choose regions of consistent fibril alignment in order to ensure differences are due to the type of treatment rather than sampling position. Careful selection of tissue sampling areas or tissue selection sites for grafts and prostheses is therefore required to ensure consistency and homogeneity of sample/prostheses nanostructure and mechanical properties.

It has been suggested there may exist specific regions which meet these requirements. Regions near the left ventricle and apex have been reported as ideal tissue selection sites (Hiester and Sacks, 1998a, Sacks et al., 1994, Simionescu et al., 1993). However the exact location of these so called ideal sites, sizes of these sites and fibril orientations have been stated to vary between different sacs of the same species and age. Therefore selection of ideal tissue sampling sites based on specific areas of the pericardium may not be possible or sufficient (Hiester and Sacks, 1998a, Hiester and Sacks, 1998b). It has been proposed that presortment methods be developed and employed which detect fibril orientation and direction should structural homogeneity be of significance (Hiester and Sacks, 1998b).

2.4.4 Pericardium: Processing

Prior to the implantations of pericardium as grafts and bioprostheses, it is fixed to reduce antigenicity and stabilise the tissue. Glutaraldehyde is the most extensively used fixative or cross linking agent for this purpose (see section 2.3.4).

Another important aspect of the preparation of pericardium is decellularisation as cells are a major trigger for an immunoreaction (Gilbert et al., 2006). Decellularisation is beneficial in multiple ways; it can remove antigens associated with cells in addition to remnants which promote calcification (Mendoza-Novelo et al., 2011). Enzymatic, physical, and chemical methods, or a combination of the three, are able to be used to destroy cellular membranes and remove cells. Methods used to decellularise collagen tissues include, but are not limited to, those listed in Table 2.2.

Table 2.2. Physical, enzymatic and chemical methods for the decellularisation of collagen.

	Decellularisation Method	References
Physical	Snap freezing Mechanical Agitation Mechanical force Sonication	(Schenke-Layland et al., 2003, Roberts et al., 1991, Freytes et al., 2004, Jackson et al., 1988, Gilbert et al., 2006)
Enzymatic	Can be based on nucleases, calcium chelating agents and protease digestion. Trypsin (main enzyme used)	(Bader et al., 1998, Gamba et al., 2002, McFetridge et al., 2004, Teebken et al., 2000, Gilbert et al., 2006)
Chemical	Alkaline and acid treatment Sodium dodecyl sulfate (anionic detergent) Sodium deoxycholate (ionic) Triton X-200 (ionic) Alkylphenol ethoxylate/Triton X-100 (non-ionic) Tridecyl alcohol ethoxylate (non-phenolic) Zwitterioinc detergents	(Mendoza-Novelo et al., 2011, Yang et al., 2009, Rieder et al., 2004, Grauss et al., 2003, Dahl et al., 2003)

Although most of these methods are effective in cell removal, many result in undesirable side effects. For example, treatment with sodium dodecyl sulfate, a common ionic detergent, has resulted in decreases in the collagen denaturation temperature, irreversible swelling and changes in mechanical properties such as significant decreases in tensile strength and changes to collagen network (Liao et al., 2008, García Páez et al., 2000). Ideally, decellularisation methods/agents would preserve the collagen network structure, removing cellular material and leaving the collagen fibril nanostructure intact, including the quantity and localisation of the GAGs. However this is not always the case, with some decellularisation methods better in this regard than others; the enzyme Trypsin and a combination of Triton X-100 and sodium-deoxycholate do not preserve the native collagen structure as well as that of Triton X-100 alone (Yang et al., 2009).

In this thesis, all the collagen type I rich bovine pericardium samples were washed with the non-ionic detergent Triton X-100 before experiments and analyses were conducted. Triton X-100 is a commonly employed decellularisation agent that has been proven efficient in cell

removal with many researchers using it as a control to compare cell removal efficiencies with new or alternative decellularisation methods (Liao et al., 2008, Gilbert et al., 2006). Of differing opinion however is the effect Triton X-100 has on the GAG content and collagen network preservation. It has been demonstrated by some that Triton X does not disrupt GAG cross links in collagen, therefore it does not interfere with the native collagen structure (Scott and Thomlinson, 1998, Courtman et al., 1994), whilst others argue the opposite, suggesting it lowers GAG content and/or can effect collagen microstructure (Mendoza-Novelo et al., 2011, Liao et al., 2008); although it is suggested the overall collagen architecture incurs little changes, it has been reported Triton X-100 may remove crimp (Liao et al., 2008).

2.4.5 The Heart and Heart Valves

The heart is one organ and is often described as having a left and right side, each containing two chambers, an atrium and a ventricle. The left and right atriums are chambers which receive blood flowing back to the heart, whilst the left and right ventricles are what pump the blood out of the heart and around the body.

To regulate the blood flow within the heart, there exists four valves; these are the tricuspid valve, the pulmonary valve, the mitral valve and the aortic valve, as shown in Figure 2.7. The general function of all these valves is the permission of blood flow in one direction and preventing backflow in the opposite direction by undergoing a cycle of ventricular systole (opening) and diastole (closing). They open and close due to a combination of muscles and pressure differences within the heart, during which the valve leaflets or cusps experience loads causing significant dimensional and shape deformations, reportedly up to 50% (Schoen and Levy, 1999). A correctly functioning valve will:

- Be flexible
- Open completely, allowing free blood flow in a single direction
- Close completely and tightly, preventing backflow of blood into the heart chambers

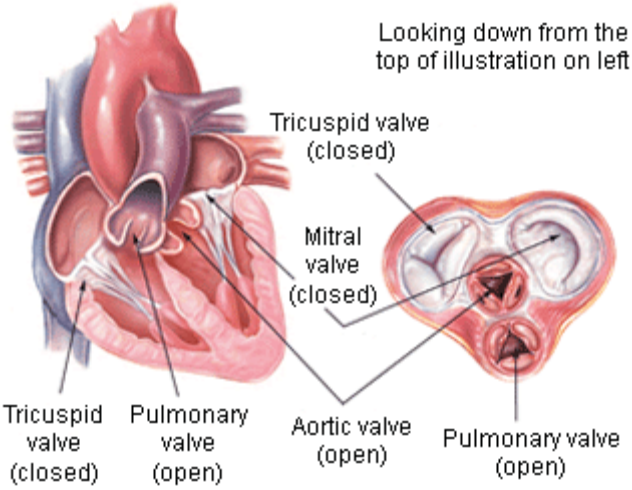

Figure 2.7. Illustration of the heart showing the major valves: tricuspid valve, pulmonary valve, aortic valve and the mitral valve, sourced from: http://www.yourheartvalve.com/heartbasics/pages/heartvalves.aspx

The tricuspid valve is composed of three leaflets and allows blood to flow from the right atrium to the right ventricle, and prevents backflow of blood back into the right atrium. The pulmonary valve then opens, permitting blood from the right ventricle to be pumped through the pulmonary artery to the lungs in order to receive the oxygen the blood needs to carry around the body. The oxygenated blood then collects in the left atrium, where the bicuspid mitral valve opens to permit the flow of blood to the left ventricle. The oxygenated blood then leaves the left ventricle through the aortic valve where it is distributed around the body. The pulmonary and aortic valves, like the tricuspid valve, consist of three leaflets, however are described as semilunar in shape.

Of the four heart valves, the aortic valve is the most highly diseased and is widely studied and replaced, providing a useful example of the importance of the valve structure and collagen nanostructure in the functioning of the valve tissues (Schoen and Levy, 1999). Natural aortic valves consist of three layers, with differing structures, including collagen, leading to high anisotropy (Langdon et al., 1999, Schoen and Levy, 1999). Table 2.3 shows the different layers, composition and nanostructure of a natural aortic valve.

Table 2.3. The different layers of a natural aortic valve, their composition, nanostructure and collagen arrangement (Schoen and Levy, 1999, Liao et al., 2008).

Layer	Description	Content	Collagen Packing	Alignment
Fibrosa	Below outflow surface, facing aorta with corrugations on the surface	Mostly crimped type I collagen	Densely packed	Circumferentially aligned, parallel to free cuspal edges
Spongiosa	Middle layer	Collagen, many GAGs and water	Loosely packed	Loosely arranged
Ventricularis	Below inflow surface, facing left ventricle	Elastin and collagen		Radially aligned elastic fibers

A combination of the fibrosa corrugations, the collagen crimp and alignment, in conjunction with the elastin fibers and the hydrophilic GAGs, allows the valves to expand, undergo significant deformations and transfer and diminish stresses through actions such as uncrimping, collagen and elastic fiber stretching, and swelling and gel formation in the central GAG rich layer (Schoen and Levy, 1999, Langdon et al., 1999, Lovekamp et al., 2006, Mavrilas et al., 2005).

Common problems with heart valves which require prosthetic valve replacement to mitigate the effects are valve regurgitation, where the valve is dysfunctional and will permit blood flow in the opposite direction than that required, and valve stenosis, narrowing of the valve due to thickening. Heart valve diseases can be congenital, that is an anomaly present from birth, or acquired. Valve regurgitation is an example of a congenital disease, whilst acquired diseases can be due to bacterial or non-bacterial infections which may lead to inflammation for example. The fusing of two leaflets or cusps during the development of an embryo to produce a bicuspid rather than a tricuspid valve is one of the most common congenital heart defects. Another known problem is mitral valve prolapse which is a result of weakening of the mitral valve connective tissue.

2.4.6 Prosthetic Heart Valves

Prosthetic heart valves can be categorised under two major classes, mechanical prosthetic valves or tissue derived bioprosthetic valves. Both classes share a common group of disadvantages, whilst individually have different advantages and disadvantages.

Mechanical prosthetic heart valves are manufactured from synthetic non-biological materials. Mechanical valves may be constructed entirely or partially from materials such as polymers (e.g. polyester), titanium, teflon, tungsten or carbon (Schoen and Levy, 1999, Aslam et al., 2007). A range of mechanical prosthetic valve designs exist, amongst which are ball-cage valves, disk valves, tilting disk valves and Medtronic Hall valves. The most extensively used mechanical valve design is the bileaflet valve, more specifically the St. Jude Medical valve, where two semicircular leaflets are combined with a unique hinge system (Aslam et al., 2007). Aslam et al (2007) can be referred to for more information regarding mechanical valve design and properties.

Unlike mechanical valves, bioprosthetic valves may be entirely biological, or can be made from a combination of biological and non-biological materials. Most tissue derived valves are constructed with some degree of synthetic material, typically Dacron (Aslam et al., 2007). Bioprosthetic heart valves used in the medical industry can be classified under three main groups: 1) Porcine xenograft (porcine aortic), 2) Bovine pericardial, and 3) homograft or allograft (Vesely, 2005). Of these, porcine aortic and bovine pericardial materials are the most commonly used (Singhal et al., 2013, Li et al., 2011, Mirnajafi et al., 2005). The terms homograft and autograft refer to valves sourced from humans, the first from a different human, whilst the latter involves the removal and implantation of a patient's own valve from one site to another (Singhal et al., 2013). Xenografts involve the grafts from one species implanted into another. As stated earlier, higher collagen content, freedom of design using the tissue, and larger material sizes are all attributes which make bovine pericardium an attractive tissue source for valve replacements.

Bioprosthetic valves can be unstented or stented, that is mounted on a support of usually three struts encompassed by a sewing cuff base. Stented bioprosthetic valves are more common and are advantageous in that surgical implantation is easier and can be done at a number of different valve sites (Schoen and Levy, 1999). As with the mechanical valves, a range of tissue valve designs exist and are available commercially, some of which include Carpentier Edwards Perimount bovine pericardial, Carbomedics Mitroflow Synergy Stented bovine pericardial, Hancock stented porcine, Mosaic Aortic and Mitral Porcine Bioprosthesis, Biocor Stentless and Toronto Stentless (Aslam et al., 2007).

Both mechanical and biological valves can incur a number of problems/disadvantages such as infection of the valves, thromboembolism, thrombosis and hemorrhaging related to anticoagulation, non-structural issues (paravalvular leakage and overgrowth of tissue for

example), and structural issues (Schoen and Levy, 1999). Table 2.4 lists some of the advantages and disadvantages correlating specifically with both mechanical and tissue derived prosthetic valves. The major disadvantage of tissue valves is calcification (see section 2.3.6) and their premature failure, with the maximum lifetime being approximately 20 years and often requiring reoperation in patients. Despite this, it is believed the risk of reoperation is lower than the risk of thromboembolism in mechanical valves (Vesely, 2005).

Table 2.4. Advantages and disadvantages of mechanical and biological based prosthetic heart valves.

Valve Type	Advantages	Disadvantages
Mechanical	• Structurally reliable • Higher durability	• Substantial risk of thromboembolism • Chronic anticoagulation therapy required
Tissue	• Rates of thromboembolism are lower • Anticoagulation therapy not required • Similar patterns of flow to natural valves	• Pressure changes and abrasion can lead to cusp tearing • Calcification • Patients often require reoperation due to premature failure

2.5 Collagen Mechanics and Mechanical Properties

The mechanical response of collagen materials to subjected forces and their mechanical properties have been the subject of many investigations. This section of the literature will cover some basic mechanical terms and properties, the stress-strain curve as it relates to collagen, and summarises the results of investigations into the effects of cross linking, both GAGs and glutaraldehyde cross links, on collagen mechanics.

2.5.1 Mechanical Parameters

2.5.1.1 Strain

The work presented in this thesis explores collagen nanostructural response to applied tensile forces. A tensile force can be thought of as a pulling force. Application of tensile forces on a specimen will most often result in its elongation along the force direction. The mechanical parameter, strain, is used to describe the relative elongation and is defined in Equation 2.1,

where strain (ε) is reported as a fraction or as a percentage. L_i is the length of the sample at any given point in time, and L_0 is the initial sample length.

$$\varepsilon = \frac{(L_i - L_0)}{L_0} \qquad \text{Equation 2.1}$$

2.5.1.2 Stress

Stress is defined as force per unit area, where area refers to the original cross-sectional area, experienced by the specimen subjected to external forces (tensile or compression) and is denoted σ. A number of different units can be used to report stress, common units being Pascals (Pa) and Newtons per unit area (N/mm^2 for example).

2.5.1.3 Poisson Ratio

A sample subjected to tensile forces will experience elongation in the direction of the tensile forces and contraction in the transverse direction (normal to the direction of applied force). The negative of the ratio of the transverse or lateral strain to the longitudinal or axial strain is known as the Poisson or Poisson's ratio. For isotropic materials the reported Poisson ratio is limited to the range -1 to 0.5. However, anisotropic materials have been found to have values exceeding 0.5 (Vader et al., 2009, Persson et al., 2010, Wells et al., 2015c), where the material experiences volume decreases.

2.5.2 The Stress-Strain Curve of Collagen

Collagen materials under tensile forces often produce non-linear stress-strain curves; an example of a typical stress-strain curve is depicted in Figure 2.8. Such stress-strain curves are divided into three regions, the foot, heel, and linear regions, each of which are a result of different structural changes or mechanisms by which collagen responds to strain at the different hierarchical levels. A number of mechanical properties can be extracted from such curves, including ultimate tensile stress, strain at failure and the elastic modulus of the tissue. The ultimate tensile stress is the maximum stress the tissue experiences prior to failure. A material with a high ultimate tensile stress is said to be strong and can withstand high forces before failure/breaking (Fratzl, 2008). The maximum strain or strain at failure is an indication of the level of deformation/elongation that the material can experience before failing. The elastic modulus is the ratio of stress to strain, and is measured in the linear portion of the stress-strain curve. The elastic modulus is basically a measure of the sample stiffness, and so

describes the level of resistance the sample has against deformations at any given stress (Fratzl, 2008).

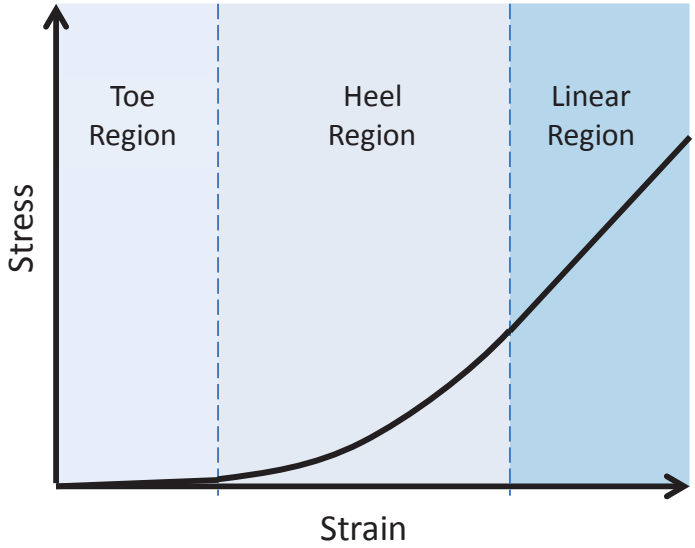

Figure 2.8. A typical collagen material stress-strain curve showing the toe, heel and linear regions.

The toe region of the stress-strain curve is where deformations begin with no to little stress uptake by the tissue. Removal of collagen fibril macroscopic crimp and the beginning of fibril realignment are associated with the toe region (Fratzl et al., 1997). In the heel region, straightening of the kinks in the gap regions of the D-spacing where there is lower packing density and greater collagen molecule flexibility is said to occur and collagen fibrils continue to rearrange so that they become aligned in the load direction (Fratzl et al., 1997, Basil-Jones et al., 2012). Beyond the heel region, most of the fibrils have orientated to the strain direction and it has been shown that collagen fibrils uptake the forces and experience elongation (Basil-Jones et al., 2012). Such elongation may be a result of tropocollagen elongation and/or the relative sliding of tropocollagens so that the length of gap and overlap regions change (Mosler et al., 1985, Folkhard et al., 1987).

2.5.3 Cross Linking and Collagen Mechanics

Attention has been directed at determining if and how cross linking alters the mechanical properties of collagen tissues. Here, only natural GAG cross links and added glutaraldehyde cross links will be discussed in relation to collagen mechanics as these are the focus of research undertaken.

Very different views exist as to actual role GAG cross links play in the response of collagen and its components to imposed strains and stresses. Some believe GAGs not to contribute to some

or any mechanical behaviours and properties (Lujan et al., 2007) whilst others suggest their contribution is significant and should not be ignored (Mavrilas et al., 2005). Of those reports that claim GAGs do impact on collagen mechanics, the exact mechanisms of how are debated. Some reports have concluded GAGs have an active mechanical role, transmitting forces directly to collagen fibrils through the non-covalent the PG-GAG links which bridge adjacent fibrils (Liao and Vesely, 2007, Cribb and Scott, 1995). However there are those that propose that GAGs facilitate fibril sliding rather than acting as mechanical linkers (Rigozzi et al., 2013). Ways in which forces could be transferred to fibrils via GAG connections has also been modelled by several groups (Redaelli et al., 2003, Chan et al., 2009, Puxkandl et al., 2002, Cranford and Buehler, 2013, Fessel and Snedeker, 2011).

The impact of the presence or absence of GAGs on collagen tissue properties is likewise contested. Experiments have been conducted to study the role of GAGs on collagen mechanical properties in which native material is compared with chondroitinase ABC-treated material to lower the GAG content. Some work has found there is no influence by GAGs on viscoelastic behaviour and properties such as ultimate tensile stress, strain at failure and elastic modulus (Lujan et al., 2009, Fessel and Snedeker, 2011, Fessel and Snedeker, 2009, Svensson et al., 2011). Other work has shown elastic modulus decreases upon chondroitinase ABC treatment (Mavrilas et al., 2005).

Cross links can also be introduced into the collagen network by treating with glutaraldehyde, a common collagen fixative which forms covalent cross links both within and between fibrils as discussed in section 2.3.2. These links are different in nature to GAG cross links, however as with GAGs, the resulting mechanical properties of glutaraldehyde-treated tissue remains under debate and the mechanisms by which these links function with collagen fibrils to respond to strains and stresses is unknown. Tensile testing of glutaraldehyde-treated tissue has been reported to increase ultimate tensile stress (Hansen et al., 2009), decrease stiffness/elastic modulus (Langdon et al., 1999), reduce extensibility (Reece et al., 1982), not to change ultimate tensile strength (Olde Damink et al., 1995, Chachra et al., 1996), increase elastic modulus (Mirnajafi et al., 2005) and increase extensibility (Sung et al., 1999, Olde Damink et al., 1995, Chachra et al., 1996).

2.6 Small Angle X-ray Scattering

Small angle X-ray Scattering, otherwise known as SAXS, is a powerful technique based on X-ray diffraction and is commonly used for investigating the nanostructure of matter, including

metals and alloys, crystals both single and poly, synthetic and biological polymers and macromolecules, and amorphous liquids and solids (Feigin and Svergun, 1987). Study of such matter can be done under a range of conditions, for example at specific humidity levels, temperatures, and hydration states, and can be studied in real time under different stresses or to analyse the response to biological and chemical additives for example (Blanchet and Svergun, 2013). Much information can be obtained from SAXS data of such samples, for example pore sizes, structural defects in diamonds, characterisation of catalysts, lattice dimensions and surface to volume ratios (Boldon et al., 2015, Pauw, 2013) Therefore SAXS can be of high value in the branches of pure scientific knowledge in addition to providing significant information related to specific applications.

The determination and characterisation of collagen structural parameters such as D-spacing, fibril orientation, fibril recruitment into stretching, and fibril diameter are based primarily on the results of SAXS in this research project. SAXS experiments were all conducted at the Australian Synchrotron facility in Melbourne, Victoria Australia.

This section of the literature review will cover the basic aspects of SAXS and synchrotron radiation. Scattering and diffraction are used interchangeably here to describe the interaction of the X-rays with the sample.

2.6.1 SAXS: Basic Principles and Theory

Simply stating the SAXS technique, the structure of matter at the nanometre scale is obtained from the interaction of a radiation beam with the study specimen and the resulting scattering pattern analysed. X-rays are electromagnetic radiation, travelling as waves with wavelengths and amplitudes (Jacques and Trewhella, 2010). The wavelength of the X-ray beam is generally in the order of magnitude of several angstroms, corresponding with the interatomic distances of the sample, hence the resulting scattering pattern falls in what is known as the small-angle region (Feigin and Svergun, 1987).

Depending on the source of radiation, the X-ray beams can have a broad spectral range, in which case it is necessary to isolate the wavelength required using a monochromator. The monochromatic X-rays are directed at the sample of interest, where the incident rays will interact with the electrons/atoms in the sample consequent to being scattered or diffracted. SAXS involves the elastic scattering of radiation (Blanchet and Svergun, 2013). A number of factors influence the scattering of the X-rays such as the degree of order in the sample, the composition of the sample, and the incident angle of the beam. The electrons in the sample

which have interacted with the beam generate secondary wavelets of coherent scattering (Blanchet and Svergun, 2013, Jacques and Trewhella, 2010), where if the sample is an ordered crystal lattice or molecular structure, destructive and constructive interference can occur between these scattered waves and are recorded using a detector. Figure 2.9 depicts a basic SAXS experiment setup.

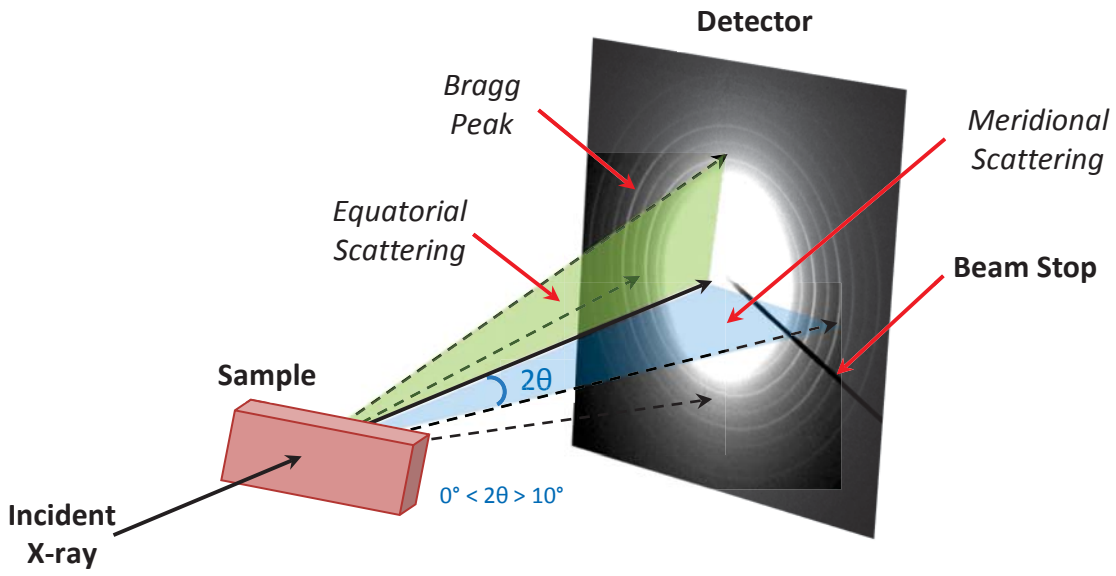

Figure 2.9. Basic SAXS setup showing the incident x-ray beams and the scattered rays which interfere to give a scattering pattern recorded by a detector.

In such SAXS experiments, it is the intensity of the scatter that is of interest at different scattering angles. However, what is known as a scattering vector or momentum transfer, q, is used in the analysis of SAXS diffraction patterns for mathematical convenience (Jacques and Trewhella, 2010, Boldon et al., 2015). The scattering vector is usually reported in $Å^{-1}$ and is given by Equation 2.2. Of interest is the lower values of q, smaller than the interatomic distance or D-spacing (Feigin and Svergun, 1987).

$$q = \frac{4\pi(sin\theta)}{\lambda} \qquad \text{Equation 2.2}$$

Where: θ = half scattering angle (half the angle between the scattered and incident beams)

λ = wavelength of the incident X-rays

The regions on the scattering pattern showing high intensity are where constructive interference occurs between scattered rays and are termed Bragg peaks (Figure 2.9). Bragg's Law defines the conditions under which constructive interference occurs and can be used to determine the distances between atoms/planes/ordered macromolecules in a regular ordered structure from the positions of these Bragg peaks. Bragg's Law is shown in Equation 2.3:

$$n\,\lambda = 2d(\sin\theta) \quad \text{Equation 2.3}$$

Where n = an integer multiple of the radiation wavelength, also known as peak order

λ= the wavelength of the incident radiation (Å or nm)

d = the distance or spacing between planes/atoms/molecules (Å or nm)

θ = half the angle between the scattering plane and incident radiation beam (°)

Figure 2.10 shows how this law is derived from the scattering of two X-rays of the same wavelength off different atoms in a crystalline structure located on two planes separated by a distance, d. For waves to produce maximum constructive interference they must be in phase, hence the path length between two waves interfering must be an integer multiple of the X-ray wavelength, which is equivalent to 2d(sinθ).

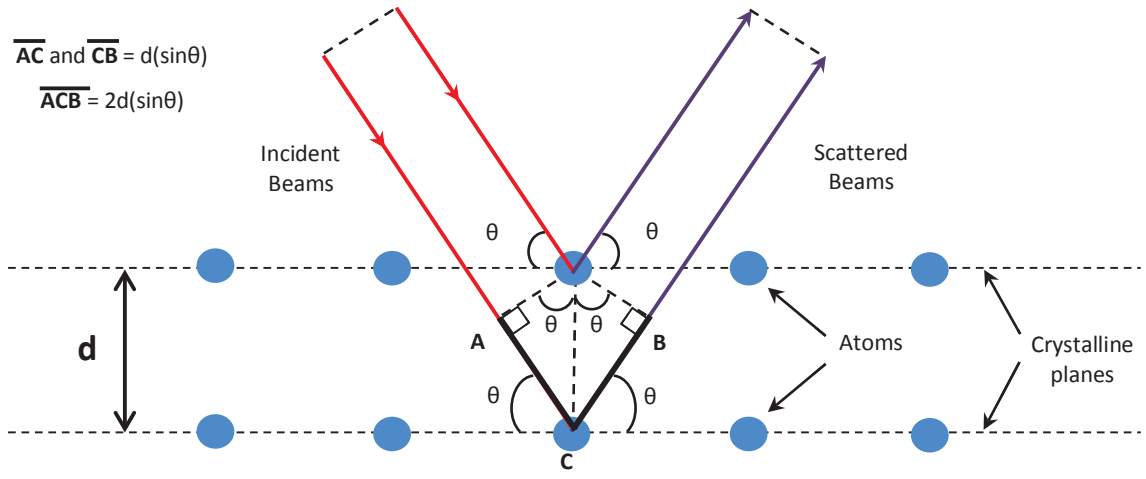

Figure 2.10. Visual representation of Bragg's law showing incidence X-ray beams of the same wavelength and the scattered rays from a crystalline structure, where one ray must travel and extra distance equivalent to an integer multiple of 2d(sinθ) to interfere constructively.

2.6.2 SAXS: Fibrillar Structures

SAXS is an ideal technique for the study of fibrillar structures such as collagen at these very small scales. Collagen materials show diffraction patterns with many reflection or diffraction orders corresponding with larger separation distances (approximately 64-700 nm) which is suggestive of long range ordering (Feigin and Svergun, 1987). As explained in the collagen section of the literature review, collagen tropocollagen molecules are staggered axially with respect to adjacent tropocollagen molecules in resister by a specific distance dependent on the collagen material. Such a structure results in areas of higher and lower electron density, this is apparent from scattering patterns of collagen; the d from the scattering patterns is much smaller than that of the tropocollagen molecule length (approximately 300 nm) and so the values would appear discordant. However the discrepancy can be accounted for by factoring in the regular shifting of the tropocollagens. Here the d is called the D-spacing and is consists of both overlap and gap regions.

D-spacing can be determined from the SAXS data collected using the equations of the scattering vector and Bragg's Law (Equations 2.2 and 2.3 and respectively). Rearranging Equation 2.2 to make the wavelength the parameter of interest gives Equation 2.4:

$$\lambda = \frac{4\pi(sin\theta)}{q} \quad \text{Equation 2.4}$$

Substituting Equation 2.4 into Bragg's Law (Equation 2.3) gives Equation 2.5

$$n\left(\frac{4\pi(sin\theta)}{q}\right) = 2d(\sin\theta) \quad \text{Equation 2.5}$$

Simplifying this equation and rearranging for d gives the final Equation 2.6 for D-spacing:

$$d = \frac{2\pi n}{q} \quad \text{Equation 2.6}$$

The D-spacing is inversely proportional to the distance from the centre of the scattering pattern to the meridional scattering or Bragg peaks (Figure 2.11a). Thus, the locations of the meridional scattering peaks provide information about the structure of collagen fibrils along the fibril axis.

SAXS can also provide information about the orientation of collagen fibrils. If the collagen fibrils were randomly orientated with respect to one another, scattering from the D-spacing of the fibrils along their axis would occur at any number of azimuthal angles with similar intensities. Therefore the result would be more uniform scattering around the entire azimuthal angle range for a given diffraction peak, appearing as full circles of diffraction (Figure 2.11a). Should the fibrils have a preferred orientation, the scattering along the fibril axis would be confined to smaller azimuthal angle ranges, seen as diffraction peaks with high intensity arcs extending only partially around the scattering pattern in the direction of the preferred or average orientation (Figure 2.11b).

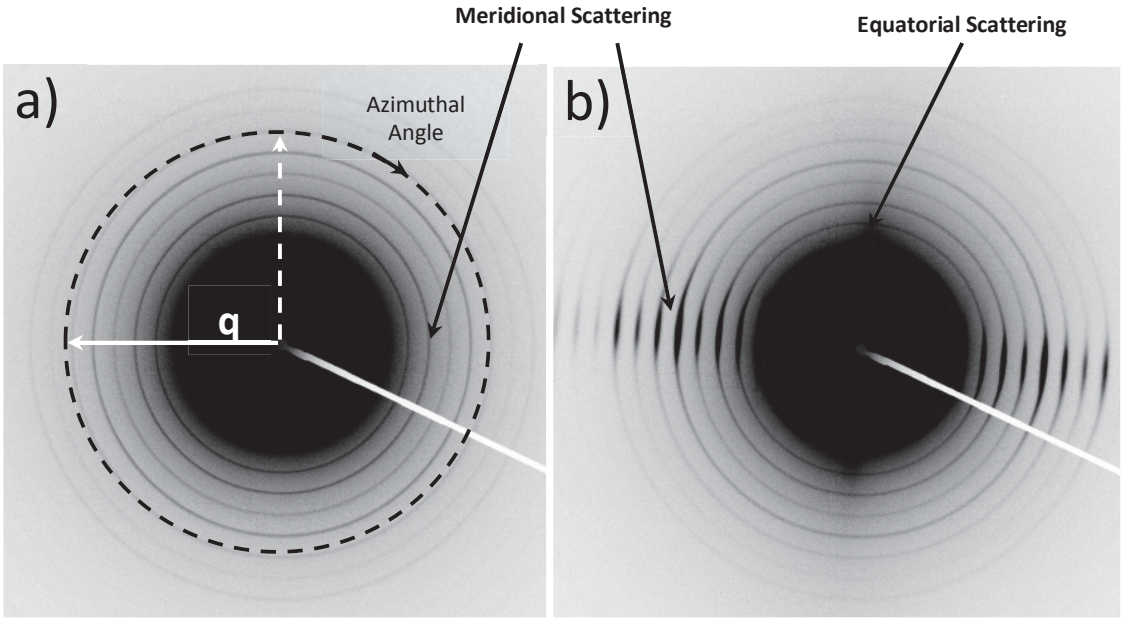

Figure 2.11. Representative scattering patterns of a collagenous biomaterial, a) scattering pattern demonstrating isotropic fibril arrangement; b) scattering pattern showing more anisotropic fibril alignment.

Integration of the scattering intensity across the q range gives the plot in Figure 2.12. The D-spacing can be determined from the position of these peaks whilst the orientation of the fibrils is obtained from looking at the intensity distribution of a given diffraction peak order across the entire azimuthal angle range; the breadth of the peak is suggestive of the orientation, a wider peak suggests a more isotropic fibril arrangement whilst a narrower peak is indicative of more anisotropic fibril alignment.

Orientated biological polymers such as collagen fibrils are approximately cylindrical, showing ordering not only along the fibril axis, but also orthogonally in the way they pack together. Equatorial scattering such as that observed in Figure 2.11b, is a result of scattering from the fibril diameter which occurs 90° from the scattering along the fibril axis. For collagen, fibril diameters are of similar magnitude to the D-spacing, therefore the diameters can be extracted using the same q-range as that of D-spacing (Figure 2.12).

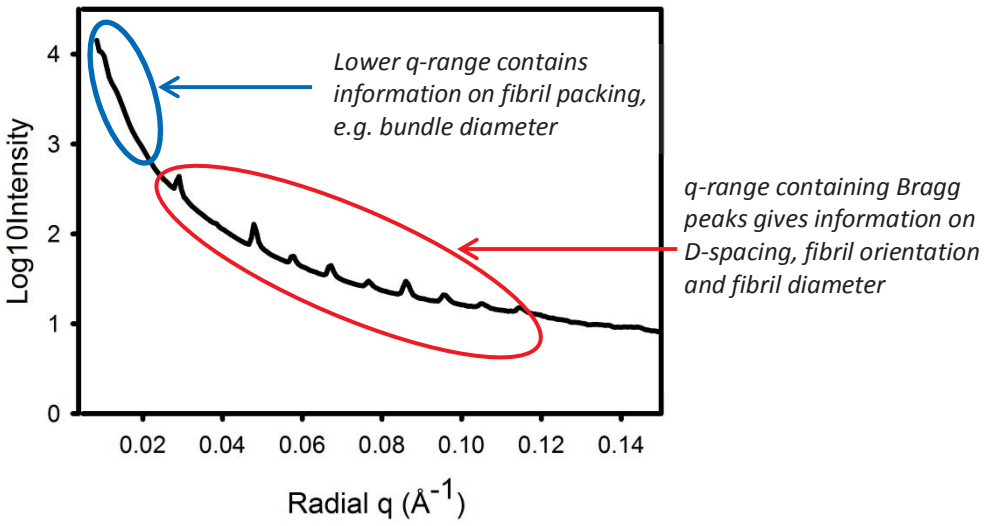

Figure 2.12. Average integrated scattering pattern of a collagen material.

2.6.3 Synchrotron Radiation and SAXS

A basic SAXS setup will have the following instrumentation/components:

- A radiation source, usually either laboratory type X-ray tubes, synchrotron radiation or neutron beams (Feigin and Svergun, 1987)
- A collimator
- Specimen block
- Detector

Synchrotrons are large circular machines that are used to generate high intensity light beams through the circular motion of electrons before selecting the appropriate wavelengths for the experiment/technique required, e.g. from wavelengths correlating to X-rays in the electromagnetic wavelength spectrum to infrared wavelengths.

The radiation sources are very different for conventional laboratory type SAXS and synchrotron SAXS. High vacuum sealed X-ray tubes are used in conventional SAXS, where metallic atoms in various metallic anodes are excited by electrons. Therefore for each setup the resulting X-rays generally have high beam divergence and a single wavelength (Feigin and Svergun, 1987, Chu and Hsiao, 2001). In comparison, synchrotron radiation involves the generation of electrons which are accelerated before being forced into circular motion by magnetic fields, causing the emission of electromagnetic radiation upon directional change (Feigin and Svergun, 1987). Radiation from synchrotron sources are advantageous due to their smaller beam divergence and high power densities or brilliance (Chu and Hsiao, 2001).

Figure 2.13 shows the setup and main components of the Australian Synchrotron used in the work presented in the subsequent chapters. To expand on the generation of synchrotron light, the electrons produced by the electron gun are accelerated in a linear accelerator before moving into the booster ring and then the outer storage ring.

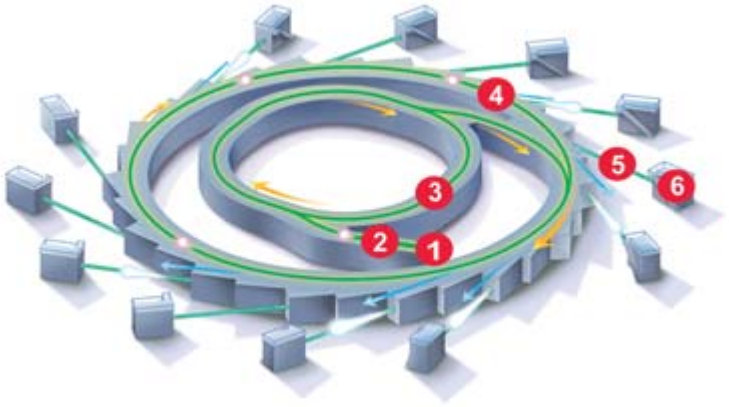

Figure 2.13. The Australian Synchrotron facility showing setup, beamlines and main components: 1) electron gun; 2) linac linear accelerator; 3) booster ring; 4) storage ring; 5) example of a beamline; 6) end station. Image sourced from: http://www.synchrotron.org.au/synchrotron-science/how-is-synchrotron-light-created.

Bending magnets and straight tunnel sections are located around the storage ring sequentially. When electrons encounter such bending magnets, the magnetic fields deflect their motion and light beams are emitted (Figure 2.14a). Insertion devices such as undulators and wigglers introduced into the straight tunnel sections provide radiation of brilliance several magnitudes or orders larger than the use of bending magnets alone (Chu and Hsiao, 2001).

Multipole wigglers consist of a series of magnets with alternating poles that cause the lateral deflection of electrons so that they oscillate, resulting in the emission of a broad spectrum of radiation in cones tangential to the travel direction (Figure 2.14b). These cones of light overlap to increase the light intensity obtained.

Undulators work on a similar principle, where dipole magnets of lower power are used to cause electron oscillation of lower amplitudes and wavelengths depending on the distance between magnets (Figure 2.14c). Superimposition of the light cones is smaller to enhance chosen light wavelengths, where the radiation produced has a narrower spectrum.

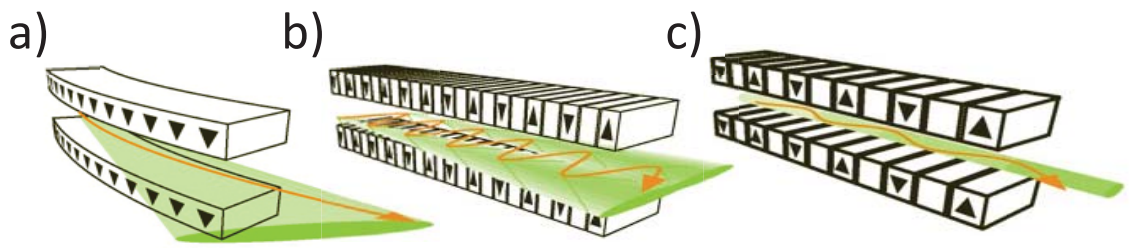

Figure 2.14. Magnetic components in synchrotron storage rings: a) bending magnet; b) wiggler insertion device; c) undulator insertion device. Images sourced from: http://www.synchrotron.org.au/synchrotron-science/how-is-synchrotron-light-created.

The synchrotron radiation is focused and wavelengths selected at each beamline. Reflections from single crystal faces, e.g. Ge(111) and Si(220), can be used to monochromatise the broad spectral range. Properties of synchrotron radiation that make it ideal include:

- High intensity light
- Broad continuous spectral range which covers a range of techniques (from SAXS to infrared)
- Small angular divergence
- Small focal size

(Feigin and Svergun, 1987)

2.7 Histology

Histology is a general term describing the study of biological materials such as plants, animals, tissues and cells at the microscopic level. Staining is generally involved to better visualise

samples. The nature of stains used today vary significantly, ranging from simple dyes, dyes with special chemical functional groups and fluorescent tags, to biologically added substrates enabling researchers to target very specific structures or chemical groups and perform qualitative and/or quantitative analyses (Kiernan, 2010, Alturkistani et al., 2015). In Chapter 3 of this thesis, the picrosirius red stain is used to stain collagen rich pericardium, with qualitative analysis of the collagen fibrils achieved using cross polarised light microscopy. This section will therefore present some background into the basic theory of the microscopy technique and stain, as well as briefly summarising literature which has utilised this type of histology.

2.7.1 Birefringency

This section combines information on the theory and background of birefringency sourced from Murphy et al. (2012) and Robinson and Davidson (2000).

Collagen tissues such as pericardium are optically anisotropic, that is, the optical properties of such materials are spatially non-uniform due to structural differences across the material axes so that the properties vary depending upon the orientation of the sample and incident light. Anisotropic materials can be birefringent, a phenomenon where incident light passing through an anisotropic material is separated into two ray components with mutually perpendicular vibrational directions, experiencing different refractive indices, so travel at different velocities through the material.

The optic axis (OA) of a birefringent material is the direction at which light propagates through the material without experiencing birefringence. Anisotropic birefringent materials can be uniaxial or biaxial, that is they can have one or two optical axes. Light which enters parallel to the OA will not experience any consequences to its vibrational directions/oscillations and will travel through at the same velocity as in isotropic materials. In instances where the light rays travel perpendicular to the optical axis, birefringence will be observed and the light will separate into two components. One of the rays refracts following the normal laws of refraction, becoming polarised perpendicular to the material OA, this is called the ordinary ray. The other ray, termed the extraordinary ray, does not behave according to the normal laws of refraction and is polarised parallel to the OA. Light entering at angle to the OA will also result in birefringence with the ordinary ray polarised perpendicular to the OA, as in the case of light travelling at right angles to the OA, with the extraordinary ray vibrations orthogonal to the ordinary rays but in a plane that is at an angle compared to the OA.

2.7.2 Polarised Light Microscopy

This section combines information on the theory and background of polarised light and polarised light microscopy sourced from Murphy et al. (2012) and Robinson and Davidson (2000).

Polarised microscopy is often used when investigating birefringent materials as it enhances the contrast between the sample image and background compared to basic brightfield microscopy.

Light waves oscillate or vibrate perpendicular to the direction of light propagation. Supposing the light is non-polarised, these vibrations can occur in any direction within the perpendicular plane with equal probability. A single vibrational direction can be selected by using polarising filters which have a specific vibration azimuth, linearly polarising the light so only light polarised in this specific direction is permitted through. When utilising polarised light microscopy for looking at birefringent samples, two polarising filters are used with a light microscope, a polarising filter located between the light source and sample, and an analyser positioned after the sample. The filters are orientated such that their vibration azimuths are at right angles. At this crossed position, no light passes through the analyser and a dark background is observed.

The polarised light enters the anisotropic sample and is refracted as described above into two orthogonal components which travel through the sample with different velocities and exit the sample with different phases and vibration directions. Only those components traveling in the same direction pass through and are recombined by the analyser. The two rays interfere constructively and destructively due to phase differences if they have identical vibration directions through the analyser resulting in a spectrum of polarisation colours.

Should the polariser axis be orientated parallel to the sample optical axis, the incident light will enter the sample polarised parallel to the optical axis and emerge as a single ray with wave vibrations parallel to the polariser and perpendicular to the analyser, subsequently there is no vibration in an orientation that can exit the analysing filter to produce interference and a dark image is observed. If the sample optical axis is placed at an angle to the polariser, the polarised incident light will be diffracted into ordinary and extraordinary rays upon entering the sample and emerge with different phases, a portion of which will exit the analyser. The emerging light rays can constructively or destructively interfere with one another producing colour. Maximum brightness or intensity can be achieved by placing the sample at a 45 degree angle to both

polarising filters. So as the sample is rotated relative to the filters, cyclic variations in the intensity of polarisation colours are observed.

2.7.3 Picrosirius Red Stain Coupled with Cross Polarised Light Microscopy

In this thesis (Chapter 3), histology using picrosirius red (PR) staining and polarised light microscopy is used principally to qualitatively asses differences in collagen crimp between treatment types, however more information regarding the structure and organisation of fibrils can be yielded by comparison of polarisation colours.

2.7.3.1 Picrosirius Red: Collagen Staining Mechanism and Polarisation Colours

PR is a dye used to stain collagen and enhances the intensity of normal birefringence of collagen by binding in such a way that the axes of the dye and collagen fibrils are parallel (Constantine and Mowry, 1968, Junqueira et al., 1979). PR binds to collagen via the reaction of its sulfonic groups with the basic amino groups on collagen fibrils (Junqueira et al., 1979, Nielson et al., 1998), with experiments involving the deamination or blocking of basic amino groups on collagen fibrils showing decreases in PR staining (Junqueira et al., 1979).

PR is not a collagen specific dye despite initial belief, and can stain non-collagenous structures containing basic amino acids (Nielson et al., 1998, Junqueira et al., 1979). However, staining of such structures does not result in birefringence if they do not display this phenomenon to begin with (Junqueira et al., 1979, Constantine and Mowry, 1968). Collagen appears pink-red on a pale yellow background under brightfield microscopy and displays different colours ranging from green to red under polarised light microscopy, which initially was believed to be related to collagen type. The differences in colour were then attributed to collagen thickness, with the thinner fibrils generally appearing green to yellow, and the thicker fibrils more of an orange to red colour (Junqueira et al., 1978). These colours do not necessarily correlate to collagen type; collagen type I is generally thicker than type III, however thickness may be a result of differences in fibril maturity for example (Rich and Whittaker, 2005).

However it was later discovered that thickness does not account for all colour observations. Fibrils of different thicknesses can show similar birefringence colours under polarised light microscopy (Dayan et al., 1989); fibril packing and possibly alignment are major factors in the resultant colour observations. Consequently green-yellow colours can be a result of thinner fibrils, immature fibrils, procollagens, and/or less well packed and aligned fibrils, whilst the orange-red colours may suggest thicker fibrils and/or better packed more aligned fibrils (Dayan et al., 1989, Wågsäter et al., 2013, Hirshberg et al., 1999).

2.7.3.2 Picrosirius Red: Factors in Staining Uptake and Collagen Birefringency

PR stains collagen though the interaction of its sulfonic groups with the basic amino groups on collagen fibrils, therefore availability of these groups affects dye binding capacity.

Glutaraldehyde like PR, reacts with basic free amino groups on collagen, more specifically lysine and hydroxylysine, thus preventing the dye from binding. A 39% decrease in bound dye to glutaraldehyde-treated tissues has been reported (Junqueira et al., 1979).

Experiments conducted by Junqueria et al (Junqueira et al., 1980) also show the removal of PG by digestion with the enzyme papain to affect PR binding capacity and increase birefringency. Reduction in PG bound to collagen resulted in increased PR uptake by the tissue samples which the authors attribute to 'unmasking' of the basic amino groups by papain.

Chapter 3

3. Collagen Cross Linking and Fibril Alignment in Pericardium[1]

Abstract

The influence of natural cross linking by glycosaminoglycans (GAGs) on the structure of collagen in animal tissue is not well understood. Neither is the effect of synthetic cross linking on collagen structure well understood in glutaraldehyde-treated collagenous tissue for medical implants and commercial leather. Bovine pericardium was treated with chondroitinase ABC to remove natural cross links or treated with glutaraldehyde to form synthetic cross links. The collagen fibril alignment was measured using synchrotron based small angle X-ray scattering (SAXS) and supported by atomic force microscopy (AFM) and histology. The alignment of the collagen fibrils is affected by the treatment. Untreated pericardium has an orientation index (OI) of 0.19 (0.06); the chondroitinase ABC-treated material is similar with an OI of 0.21 (0.08); and the glutaraldehyde-treated material is less aligned with an OI of 0.12 (0.05). This difference in alignment is also qualitatively observed in atomic force microscopy images. Crimp is not noticeably affected by treatment. It is proposed that glutaraldehyde cross linking functions to bind the collagen fibrils in a network of mixed orientation tending towards isotropic, whereas natural GAG cross links do not constrain the structure to quite such an extent.

[1] Chapter 3 is based on the following published paper however the experimental methods section has been expanded upon to include more detail regarding setups and data analysis: Kayed, H.R., Sizeland, K.H., Kirby, N., Hawley, A., Mudie, S., Haverkamp, R.G. (2015). Collagen cross linking and fibril alignment in pericardium. *RSC Advances, 5, 3611-3618*. This article can be found in section 8.1.3 of the Appendix.

3.1 Introduction

The Collagen I molecule is prevalent as the basis of many structural components in animals. It assembles with a complex hierarchical structure. This extracellular matrix forms resilient materials which are mechanically very tough (Stamov and Pompe, 2012). This toughness is due in part to the highly fibrillar nature of collagen. Polypeptide molecules twist in left handed α-helical chains, and three of these in turn assemble with a right handed twist to form tropocollagens. Collagen fibrils are multiples of five tropocollagen strands thick and of extended length. The fibrils in turn may be assembled into larger fibers and a variety of structural motifs. There is great inherent strength and elasticity in each individual fibril. It is believed that the structure of materials composed of collagen I also require cross linking of the fibrils. This mechanically couples the fibrils restricting them from sliding past each other in order to achieve high strength (Picu, 2011).

In nature, these cross links between collagen fibrils are provided by proteoglycan bridges, predominantly decoran, forming shape modules (Scott and Stockwell, 2006, Cribb and Scott, 1995). These proteoglycan bridges are elastic containing the glycosaminoglycan dermochondan sulfate (Scott, 2003, Haverkamp et al., 2005). The way in which these connections might transmit force between fibrils to resist sliding forces has been modelled (Chan et al., 2009, Puxkandl et al., 2002, Cranford and Buehler, 2013, Fessel and Snedeker, 2011, Redaelli et al., 2003). The energy absorbed by enthalpic transformations in the dermochondan can be significant (Haverkamp et al., 2007, Haverkamp et al., 2005).

It has been found that the tensile elastic modulus of mouse tendon was reduced over much of the stress-strain curve when the natural glycosaminoglycan (GAG) content was lowered by the application of chondroitinase ABC while the ultimate tensile force and ultimate stress were relatively unchanged (Rigozzi et al., 2011). However, this is not universally agreed as other work has found no altered mechanical properties in tendon from the removal of GAGs (Fessel and Snedeker, 2009, Svensson et al., 2011).

The GAG cross links associate with the collagen fibril at several different sites but are believed to always be associated with the Gly-Asp-Arg amino acid sequence (Scott, 1995). Natural cross linking of collagen also increases with age due to glycation and has been shown to increase stiffness in connective tissues (Bailey, 2001) and collagen gels (Francis-Sedlak et al., 2009) and increase brittleness in bones (Leeming et al., 2009).

Methods of cross linking other than that found in nature can be used to modify the properties of collagen materials. Cross linking of bovine pericardium with glutaraldehyde either under strain or with no tension has been reported to result in a less extensible and stiffer material which is stronger than the untreated material (Reece et al., 1982, Langdon et al., 1999). However, there is still much to learn about cross linking of collagen and the contribution these cross links make to the structure and mechanical properties of collagen tissues.

The arrangement of collagen fibrils, particularly the extent of alignment or anisotropy, is an important contributor to the strength of collagen materials. The structure-function relationship between collagen alignment and mechanical properties has been elucidated for a range of tissue types (Kamma-Lorger et al., 2010, Sellaro et al., 2007, Liao et al., 2007, Gilbert et al., 2008, Purslow et al., 1998). The orientation of collagen measured edge-on (alignment in-plane) has been shown in a range of mammal skins processed to leather to be correlated with strength (Sizeland et al., 2013, Basil-Jones et al., 2011).

Small angle X-ray scattering (SAXS) is a powerful method for measuring the orientation of collagen fibrils in tissue (Basil-Jones et al., 2012, Purslow et al., 1998, Liao et al., 2005). Other methods may also be used such as small angle light scattering (Billiar and Sacks, 1997), confocal laser scattering (Jor et al., 2011), reflection anisotropy (Schofield et al., 2011), and atomic force microscopy (Friedrichs et al., 2007).

Bovine pericardium is a suitable material to use as a model in investigating the effect of cross linking, both natural and synthetic, on mechanical properties. Bovine pericardium has an established use for heart valve leaflet replacement (Nwaejike and Ascione, 2011, Paez et al., 2006). The material requires high mechanical strength and a long performance life (Mirnajafi et al., 2010). The orientation of collagen in pericardium heterograft materials for heart valve leaflets has been shown to affect the stiffness during flexing (Mirnajafi et al., 2005).

We investigate here the hypothesis that cross links, both natural (GAGs) and synthetic (glutaraldehyde), may constrain the alignment of the collagen fibrils to result in different extents of orientation in collagen tissues which in turn may partially explain the different physical properties of the materials.

3.2 Experimental Methods

3.2.1 Native Pericardium Sampling and Treatment

Fresh bovine pericardium was obtained from John Shannon and from Southern Lights Biomaterials and stored in phosphate buffered saline (PBS) solution, pH = 6.90 ± 0.10 (Lorne Laboratories Ltd). The tissue was rinsed briefly in PBS solution before being cut using a sharp scalpel into rectangular samples of approximate dimensions 40-45 mm x 10 mm from across the left and right ventricle and atrium regions of the ventricular side of the pericardium, as shown in Figure 3.1, with the long axis taken from the long axis of the heart, that is, the long axis of the samples aligns with the base to apex direction of the pericardium. The samples were decellularised using a method based on Yang et al (2009). The pericardium was washed for 24 h in a 1% octylphenol ethylene oxide condensate (Triton X-100, Sigma), 0.02% EDTA solution made up in PBS. This washing step was conducted under constant agitation at 4 °C. The samples were then rinsed in PBS buffer and stored in PBS. These are referred to as "native" samples. Subsequent processing of this material produced glutaraldehyde-treated or chondroitinase ABC-treated material.

As mentioned in 2.4.3 of the literature review, there have been some attempts to locate ideal sampling sites where there are higher levels of homogeneity in terms of collagen fibril alignment and alignment direction; it has been reported ideal selection sites are located near the left ventricle close to the apex (Hiester and Sacks, 1998a, Sacks et al., 1997). However the same authors also reflect on the fact these 'ideal sites' differ in terms of area size, exact location and fibril orientation between sacs from the same species and age, therefore the selection of these sites based on the criteria of homogeneity may not be sufficient. Due to the requirement for multiple sample selection from a single pericardia to allow direct structural comparisons between treatment types, these regional structural differences, and to mitigate any bias, all samples in the in this and following experiments were taken from the same region on the pericardia (Figure 3.1b) and randomly assigned to the required treatment type. Here, all samples were taken from one pericardium and randomly assigned to each treatment method.

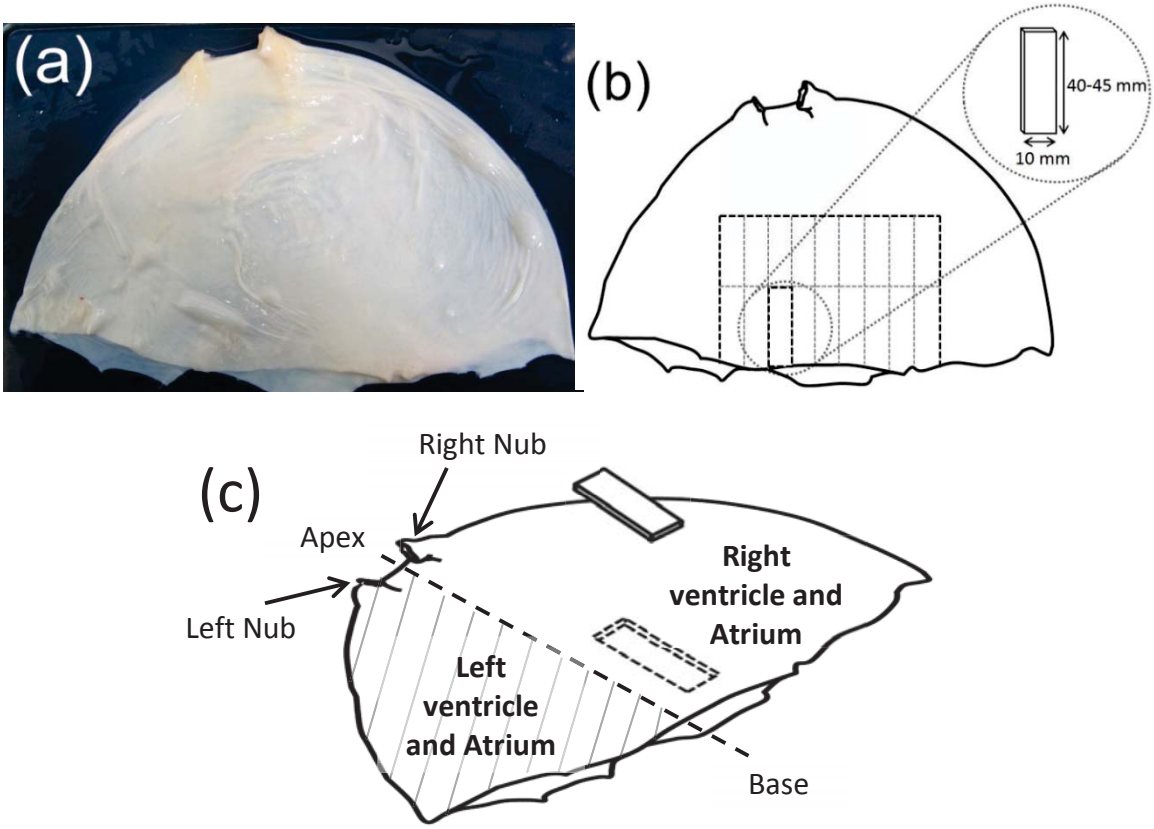

Figure 3.1. Pericardium a) ventricular side ready to be cut for samples; b) showing sampling area used and sample size; c) the different regions and axis of the pericardium. Adapted from (Kayed et al., 2015b) with permission of The Royal Society of Chemistry.

3.2.2 Glutaraldehyde Treatment

The Triton treated pericardium was incubated in a 0.6% glutaraldehyde solution made up in PBS buffer, at 4 °C for 24 h with constant agitation (Umashankar et al., 2011). It was then stored in a sealed container in a solution of the same composition until SAXS measurements were performed. The total time in storage was 3-5 days.

3.2.3 Chondroitinase ABC Treatment

Removal of GAG cross links was based on the method described by Schmidt et al. (1990). The Triton treated pericardium was incubated in 0.125 units of chondroitinase ABC per ml of buffer solution comprising of 0.05 M tris-HCl, 0.06 M sodium acetate and EDTA-free protease inhibitors (complete, EDTA-free protease inhibitor tablets, Roche Diagnostics, Mannheim, Germany), pH 6.5, at approximately 27 °C for 24 h before rinsing and storing in 0.05 M tris-HCl and 0.06 M sodium acetate buffer in a sealed container at 4 °C.

Care was taken with all handling, cutting and treatment of the samples not to stretch the material as this might cause fibril alignment to change. The data presented here represents a duplication of this experiment with additional care taken in sample selection and handling in the second set of samples and SAXS analysis informed by the experience from the initial experiments.

3.2.4 GAG Assay Procedure and Quantification

The extraction and quantification of sulfated GAGs (sGAG) was performed to assess the effectiveness of the chondroitinase ABC GAG removal method and to ensure the glutaraldehyde cross linking method used throughout the project did not result in any unwanted or unintentional removal of GAGs by comparison to the native pericardium samples.

Extraction and quantification of sGAGs for the pericardium samples was based on the Blyscan Sulfated Glyscosaminoglycan Assay protocol (Bicolor, Carrickfergus, UK). This protocol is suitable as it detects sGAGs extracted both as a proteoglycan core and GAG unit, or as free GAGs, including 4- and 6-sulfated chondroitin sulfates, dermochondan sulfate, keratan sulfates and heparan sulfates. This assay works on the basic principle of sGAG or sGAG-PG complex extraction into a liquid phase using the enzyme papain, precipitation of the extracted GAGs using 1, 9-dimethylmethylene blue which binds specifically to the sGAG component, and dissociation of the GAG-dye complex under conditions which improves the free dye absorption.

Samples of each fresh, glutaraldehyde and chondroitinase ABC-treated pericardium were analysed for sGAG content. Excess water was removed from sections of fresh, chondroitinase ABC and glutaraldehyde pericardium samples by patting briefly with tissue paper. 1 ml of an extraction agent comprising of a 0.2 M sodium phosphate buffer, pH 6.4, containing 8, 4, 0.8 and 0.1 mg/ml buffer of sodium acetate, EDTA, cysteine HCl and papain enzyme (from Carica papaya, Sigma, Biochemika, Enzyme no. 3.4.22.2) was added to each sample respectively and incubated at 65 ^{o}C for 26 hours. Subsequently, the samples were centrifuged at 10,000 r.p.m for 10 minutes and the supernatant containing the extracted sGAGs decanted and collected.

Duplicate 0, 1, 2, 3, 4 and 5 µg sGAG standards were prepared by dilution of the reference standard to volumes of 100 µl using deionised water. Similarly, test samples were prepared in triplicate; glutaraldehyde and fresh samples were prepared using 20 µl aliquots of the supernatant containing the extracted sGAGs and chondroitinase samples prepared using 40 µl aliquots of the chondroitinase supernatant , and made up to 100 µl. A lower quantity of GAGs

was expected in the chondroitinase ABC supernatant due to the prior treatment of the tissue with the chondroitinase ABC enzyme, hence, a larger aliquot was selected to ensure there were enough GAGs present to produce an absorbance reading that would fall on the standard curve. 1 ml dye reagent was then added to each 100 µl sample and mechanically inverted for 30 minutes. Samples were centrifuged for 10-20 minutes at 14,000 r.p.m and the unbound dye drained off. 1 ml of Blyscan dissociation reagent was added to the precipitate, left to dissolve for approximately 10 minutes, and centrifuged briefly. Absorbance of 1 ml of each sample was measured at a wavelength of 656 nm against water in triplicate using a spectrophotometer. A sGAG standard curve relating absorbance to the known standard concentrations was produced and sGAG amino content of the pericardium samples calculated from the standard curve, expressed as µg sGAG per mg wet tissue.

The absorbance readings of the standards were averaged and plotted against their respective known GAG concentrations and a linear regression line fitted. Using the average absorbance readings and the equation from the standard curve linear fit, the sGAG content in the sample aliquots were determined (µg sGAG). GAG concentration as sGAG/mg tissue was then calculated by determining first the total extracted sGAGs using Equation 3.1, then dividing this by the original sample weight.

$$Total\ sGAG = \left(\frac{aliquot\ sGAG\ content}{volume\ aliquot\ used}\right) \times total\ volume\ supernatant \qquad \text{Equation 3.1}$$

$$= \left(\frac{\mu g\ sGAG}{ml}\right) \times ml$$

3.2.5 SAXS Setup and Analysis

All SAXS experiments presented in this thesis were conducted at the Australian Synchrotron SAXS/WAXS beamline located in Melbourne, Victoria, Australia.

In preparation for SAXS analysis, the pericardium was removed from the glutaraldehyde and tris-HCl, sodium acetate buffer solutions in which they had been stored. After soaking for at least 1 h in buffered saline solution, pH = 6.90 ± 0.1 (Lorne Laboratories Ltd), pericardium strips were mounted on a stainless steel metal plate containing 10 mm diameter holes (Figure 3.2a) and diffraction patterns recorded while the pericardium was wet. All diffraction patterns were recorded at room temperature. Throughout the data collection, care was taken to ensure the pericardium remained wet by sealing off the samples in the sample holder using Kapton tape which does not interfere with the SAXS data collection or resulting patterns, preventing

moisture loss and holding the samples in place without tension (Figure 3.2 a and c). The metal plate contains numerous holes in a grid allowing the mounting of multiple samples for SAXS at once and minimising setup time.

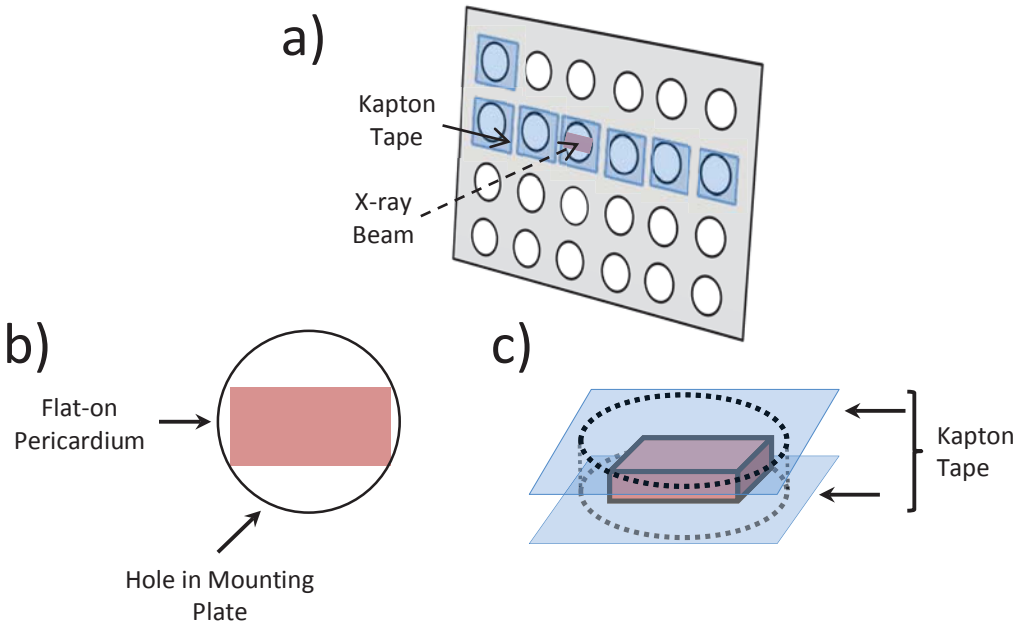

Figure 3.2. Mounting of pericardium samples in preparation for SAXS data collection: a) mounting plate with Kapton tape, showing direction of the X-ray beam relative to the plate and sample; b) in-plane view of the pericardium sample to be measured normal to the surface; c) side-on view illustrating the sealing of the sample holder to maintain moisture.

The mounting plate was subsequently introduced into the beamline setup in the SAXS/WAXS beamline hutch by attachment to a stage which can be controlled remotely in the control room. All SAXS measurements were taken normal to the sample surface (flat on).

Four samples were prepared of native material, three with treatment by chondroitinase ABC for 24 h and three with treatment by glutaraldehyde. For each sample one diffraction pattern was recorded at each of nine positions in a grid, therefore nine diffraction patterns were collected for each sample. Visualisation of the samples and mapping of the grids was made possible by the use of a camera setup in the control room (Figure 3.3), allowing accurate selection of data points and maintenance of the beam on the sample, whilst ensuring regions of the pericardium were not re-exposed to the X-ray beams.

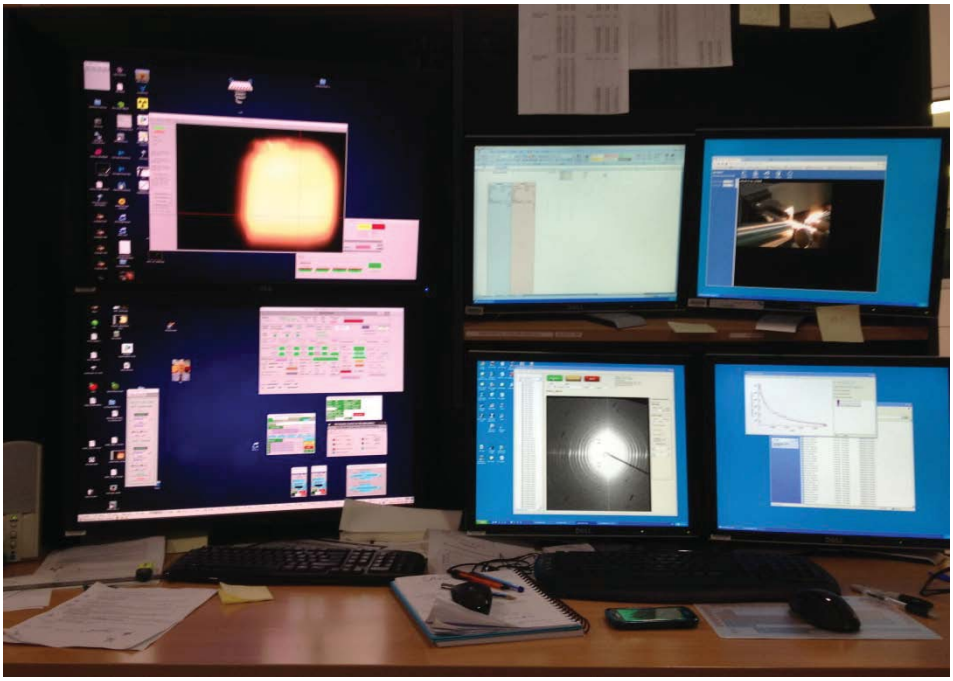

Figure 3.3. Control room setup with monitors displaying the camera output, SAXS patterns recorded and parameter controls

Diffraction patterns were recorded utilizing a high-intensity undulator source. Energy resolution of 10^{-4} (e.g. 1 x 10^{-4} Å for 1 Å radiation) was obtained from a cryo-cooled Si(111) double-crystal monochromator and the beam size (FWHM focused at the sample) was 250 x 80 µm, with a total photon flux of about 2 x 10^{12} ph.s^{-1}. All diffraction patterns were recorded with an X-ray energy of 12 keV using a Pilatus 1M detector with an active area of 170 x 170 mm and a sample–to-detector distance of 3371 mm. Exposure time for diffraction patterns was 1 s.

The orientation index (OI) is used to give a measure of the spread of fibril orientation (an OI of 1 indicates the fibrils are parallel to each other; an OI of 0 indicates the fibrils are randomly oriented). OI is defined by Equation 3.2, where OA is the minimum azimuthal angle range that contains 50% of the fibrils, based on the method of Sacks for light scattering (Sacks et al., 1997) but converted to an index (Basil-Jones et al., 2011), using the spread in azimuthal angle of one or more D-spacing diffraction peaks. Here the 5th collagen diffraction peak is used.

$$OI = \frac{90\,° - OA}{90\,°} \qquad \text{Equation 3.2}$$

To determine OA and OI the software scatterBrainAnalysis V2.30 (Cookson et al., 2006) was used in combination with Microsoft Excel. Firstly, the SAXS data collected was opened in scatterBrainAnalysis and the raw scattering patterns (Figure 3.4 a) integrated at each q around the entire azimuthal angle range in azimuthal angle increments of 5 °. This data was then saved as ASCII files and opened in a customised Excel spreadsheet for the processing of SAXS data. Taking the logarithm of the intensities and plotting against q gives an integrated scattering pattern showing the Bragg diffraction peaks at each azimuthal angle (Figure 3.4b). As the SAXS measurements were done in air, air scattering patterns were collected, where the scattering intensity of air was found to be negligible (not shown here); hence there is no sizeable contribution of background scatter to the integrated scattering patterns. The logarithm of the q values were then taken and plotted against the log of the intensity values at each given azimuthal angle before selecting the q-range containing the 5th order collagen diffraction peak (around 0.05 $Å^{-1}$) (Figure 3.4c). The peak area (intensity) was then measured above a logarithmic baseline fitted over this q-range (Figure 3.4d). The azimuthal angles and the corresponding peak intensities were then plotted to give azimuthal intensity variation plots for the diffraction peak (Figure 3.4e).

To calculate OA the first step was to sum the intensities 90 ° either side of the azimuthal intensity variation plot peak maximum (so summing the intensities across a 180° azimuthal angle range centred on the peak maximum). Subsequently, the intensities were incrementally summed either side of the peak maximum and divided by the intensity sum in the 180 ° azimuthal angle range. This was repeated until the value reached 0.5 which is equivalent to the angle range containing 50% of the collagen fibrils. Equation 3.2 was then used to determine OI.

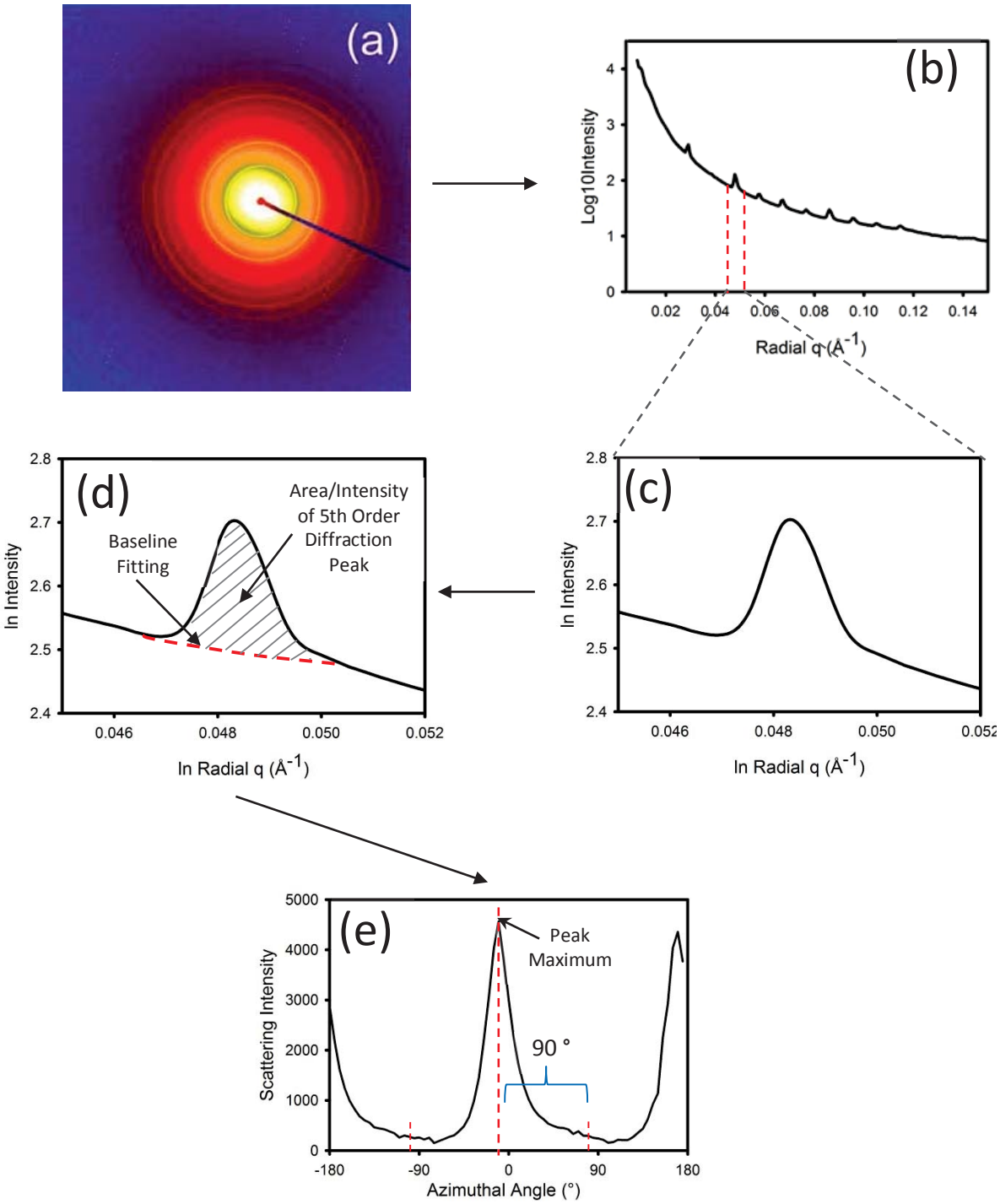

Figure 3.4. Visual representation of conversion of scattering patterns to OI value: a) representative raw scattering pattern of collagen; b) representative integrated scattering pattern of pericardium, the sharp peaks are due to diffraction from the D-spacing (at different orders); c) selection of the 5th order diffraction peak; d) baseline fitting to diffraction peak and resulting peak area/intensity; (e) representative azimuthal intensity variation plot for pericardium 5th collagen diffraction peak.

3.2.6 Atomic Force Microscopy

Small square sections were cut from the native, chondroitinase ABC and glutaraldehyde-treated pericardium samples and mounted onto 12 mm diameter magnetic metal discs with double sided tape. The samples were left to air dry for a few h before being imaged. A Nanoscope E (Veeco) atomic force microscope with a JV scanner was used with x-y calibration to ±3% completed just prior to imaging. CSG01 cantilevers (NT-MDT, Russia) with a force constant of about 0.05 N/m were used for contact mode imaging.

3.2.7 Histology

The native, chondroitinase ABC and glutaraldehyde-treated pericardium samples were rinsed then soaked in PBS for at least 1 hour in preparation for staining. Small sections of pericardium were cut and frozen flat in a Leica CM1850 UV cryogenic microtome at -30^{o}C before being mounted on microtome disks using embedding medium for frozen tissue specimens. 10 µm thick cross-sections and flat sections were cut using the microtome and transferred to glass microscope slides.

The pericardium was stained as per the protocols of the Picrosirius Red Stain Kit (Polysciences, Inc.). The microscope slides containing the pericardium sections were rinsed in distilled water, placed in picrosirius red stain solution A for 2 minutes, rinsed in distilled water, placed in picrosirius red F3A solution B for 1 hour, placed in 1 N hydrochloride acid solution C for 2 minutes before being placed in 70% ethanol for 45 seconds and left to air dry for several hours.

A Nikon Eclipse TE2000-U microscope fitted with a Nikon Digital Sight DS-Fi2 camera and cross-polarising filters, T-P2 DIC rotating DIC polariser HT and T-A2 rotating DIC analyser HT above and below the condenser and objective lenses respectively, was used to image the pericardium sections.

3.2.8 Tensile Properties

Post treatment to produce native, chondroitinase ABC-treated and glutaraldehyde-treated pericardium samples, the tissues were cut using a standard press knife as per the International Standard ISO 3376:2011. Thickness was measured in duplicate or triplicate along the sample length using an anvil and pressure foot thickness gauge as specified in BS EN ISO 2589:2002, however with the weight removed so as to decrease the load on the tissue, preventing tissue damage and compression. The press knife width was taken to be the width of the sample.

An INSTRON 4467 mechanical testing machine with the clamps mounted vertically was used to uniaxially stretch the samples at a rate of 100 mm/min until failure. Samples were mounted in accordance with International Standard 3376:2011. Force and time data were collected.

Stress was calculated using Equation 3.3:

$$\sigma = \frac{F}{wT} \qquad \text{Equation 3.3}$$

Where σ = stress in N/mm2

F = force (N)

w = width (mm)

T = average sample thickness (mm)

Strain was calculated using Equation 3.4

$$\varepsilon = \frac{L_t - L_0}{L_0} \qquad \text{Equation 3.4}$$

Where ε = strain as a fraction

L_t = sample length at a given point in time

L_0 = original sample length

L_t-L_0 is equivalent to the time (min) x stretching rate (mm/min). Failure was taken to be at the point where the stress decreased. The slope of a linear regression of the straight portion of the stress-strain curve gives the tissue elastic modulus.

3.2.9 Statistical Analysis

Statistically significant differences between treatment mean OI values, GAG content and tensile properties were tested for using One Way ANOVA implemented in SigmaPlot 12.0 with a significance level, alpha, of 0.05. If statistical differences were found ($P \leq 0.05$), pairwise multiple comparisons were performed using the Holm-Sidak method in SigmaPlot 12.0 where

the overall significance level used was 0.05. Pairwise comparisons with P-values less than 0.05 were considered to be significantly different.

3.3 Results

3.3.1 Chondroitinase ABC GAG Removal

The GAG assay found that approximately 81% of GAGs were removed with chondroitinase ABC treatment (Figure. 3.5), which can be considered a success. It would appear the protease inhibitors used do not affect the ability of chondroitinase ABC to remove GAGs as evidenced by percentage of GAG removal which is on level with, or in some cases, higher than values reported in the literature (see section 2.2.5). As expected, glutaraldehyde treatment did not remove the GAGs, showing similar GAG content to the native material. Therefore the chondroitinase treated samples do represent pericardium with most of the GAGs removed.

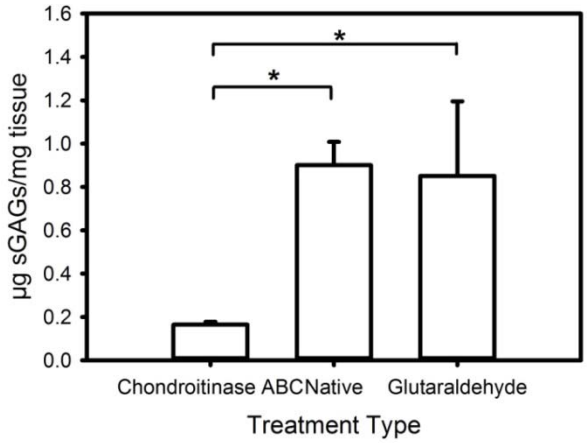

Figure 3.5. GAG assay for pericardium for triplicate samples (error bars for 95% confidence intervals). Pairs that are significantly different ($P<0.05$ for $\alpha = 0.05$) are shown by a *. Reproduced by permission of The Royal Society of Chemistry (Kayed et al., 2015b).

3.3.2 Histology

The picrosirius red stained sections of each of the treated samples show a similar level of crimp in each sample type (Figure 3.6). Crimp is the wavy structure of collagen fibrils which is typically seen in tendon and pericardium (with a period of 25-45 µm in pericardium (Sellaro et al., 2007)) but not as prominently in skin. The chondroitinase ABC-treated sample and native sample are the most similar. The glutaraldehyde-treated pericardium has the appearance of a more open structure (which may be because it did not microtome as well) and it has some variation in colour. While picrosirius red is intended as a specific stain for collagen with type I collagen showing as red, other factors can affect birefringence and the resulting colour under

cross-polarised filters, such as fibril thickness and organisation, and the availability of free basic amino acid binding sites (see sections 2.7.3.1 and 2.7.3.2 of the literature review). The sulfonic acid groups of the picrosirius red dye molecule bind to the free amino acid residues on collagen, as do the aldehyde groups of glutaraldehyde; therefore binding of glutaraldehyde to these sites will inhibit dye binding and may result in decreased birefringence. The presence of colours other than red in the glutaraldehyde-treated samples does not therefore indicate other types of collagen present, but rather, modification to the type I collagen (Nielsen et al., 1998, Junqueira et al., 1982, Dayan et al., 1989).

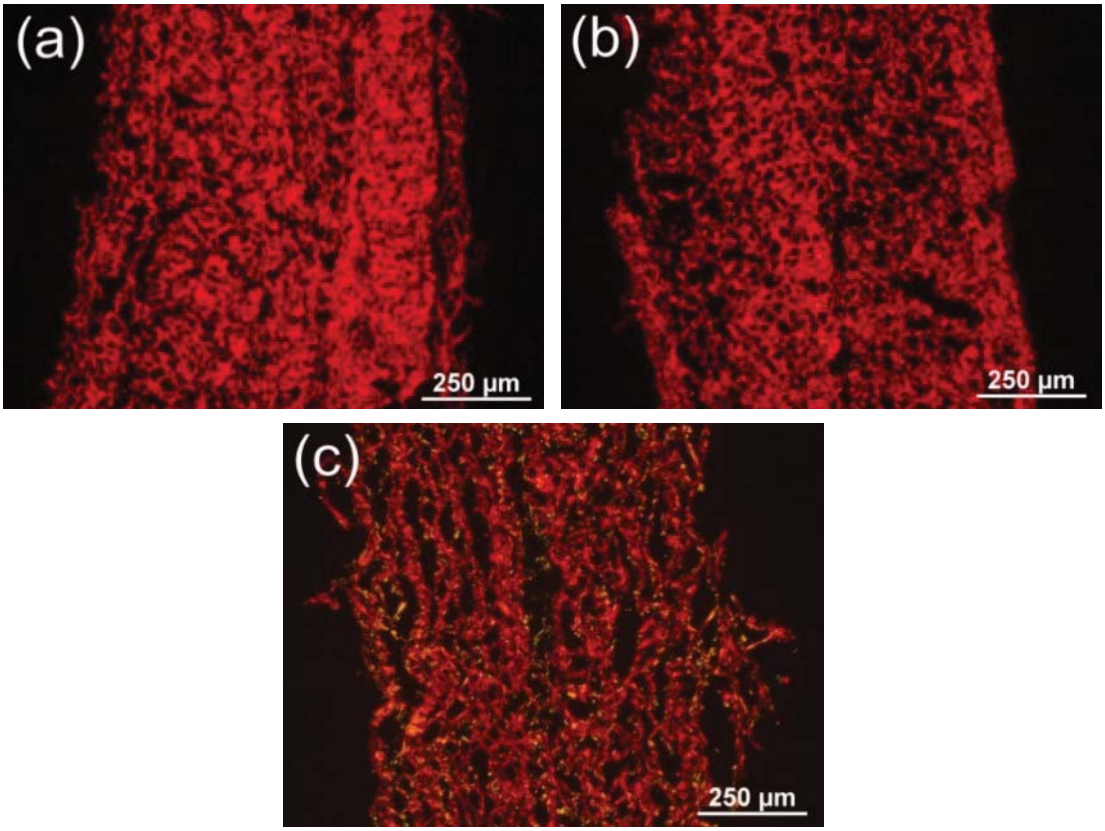

Figure 3.6. Picrosirius stained sections of pericardium treated with a) chondroitinase ABC; b) native; c) glutaraldehyde. Reproduced by permission of The Royal Society of Chemistry (Kayed et al., 2015b).

3.3.2 Tensile Properties

The tensile properties of the pericardia samples had a high variability (Figure. 3.7, Table 3.1). There is a foot region of variable length followed by an approximately linear region until the material reached its ultimate tensile stress and broke (the failure region is not shown). The chondroitinase treatment perhaps increases the elastic modulus, in agreement with other studies (Bailey, 2001), however with the small sample size this difference cannot be considered

statistically significant (P = 0.097, F = 2.8, for α = 0.05). The stress at failure may be higher for glutaraldehyde, also in keeping with other studies (Langdon et al., 1999, Reece et al., 1982), but this also cannot be considered statistically significant (P = 0.052, F = 3.7, for α = 0.05). The only statistically significant difference between the mechanical properties of the treatment types is the strain at failure, which is higher for the glutaraldehyde-treated material (P = 0.013 F = 6.1 for α = 0.05 from the ANOVA test. For the Holm-Sidak pairwise comparisons: P = 0.029, t = 3.0 for α = 0.05 for glutaraldehyde vs. chondroitinase ABC; P = 0.022, t = 3.0 for α = 0.05 for glutaraldehyde vs. native; P = 0.948, t = 0.1 for α = 0.05 for native vs. chondroitinase ABC).

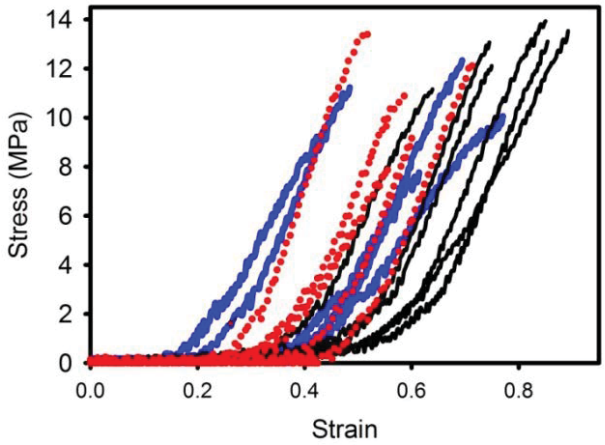

Figure 3.7. Stress-strain curves for native pericardium (blue thick lines); chondroitinase ABC-treated pericardium (red dotted lines); glutaraldehyde-treated pericardium (black thin lines). Reproduced by permission of The Royal Society of Chemistry (Kayed et al., 2015b).

Table 3.1. Tensile properties of pericardium (with 95% confidence intervals).

Sample	Elastic Modulus in Linear Region (MPa)	Stress at Failure (MPa)	Strain at Failure (%)
Native	40 ± 12	10.2 ± 2.2	60 ± 17
Chondroitinase ABC	52 ± 13	10.8 ± 2.7	60 ± 9
Glutaraldehyde	50 ± 6	12.8 ± 1.1	79 ± 10

3.3.3 SAXS

The pericardium gives good scattering patterns with clearly defined diffraction rings due to the D-spacing periodicity (Figure 3.4a). The integrated intensity plots show well defined peaks corresponding to the collagen D-period (Figure 3.4b). The odd numbered peaks have a much

higher intensity than the even numbered peaks, a characteristic attributed to a fully hydrated sample (Stinson and Sweeny, 1980). This provides some reassurance that the samples are maintained in the hydrated state during collection of the diffraction patterns, as intended.

3.3.4 OI

The distribution of orientation of the fibrils can be seen with a plot of the intensity (peak area) of any of the collagen diffraction peaks (Figure 3.8). A narrow peak in this plot is indicative of more highly aligned collagen fibrils, as seen for the native and chondroitinase treated tissue, whereas broader peaks such as that for glutaraldehyde indicate a more isotropic arrangement. This can be quantified as an orientation index, OI. The orientation angle (OA) is calculated first, which is defined as the minimum angle which contains 50% of the fibrils (Basil-Jones et al., 2010). From this the OI is calculated as (90° – OA)/90°.

The OI calculated for the three treatments provide different average OI values (Table 3.2, Figure 3.9). There is a statistically significant difference in the OI between the glutaraldehyde-treated material and the other two materials but the difference in the OI between the native and chondroitinase treated pericardium does not pass the significance test. Previously chondroitinase ABC treatment for 48 h and 24 h with diffraction patterns recorded and analysed were compared, however the OI obtained from the 48 h treated samples was not significantly different from that obtained after 24 h, probably indicating that most of the GAGs were removed already by 24 h of treatment (not shown here).

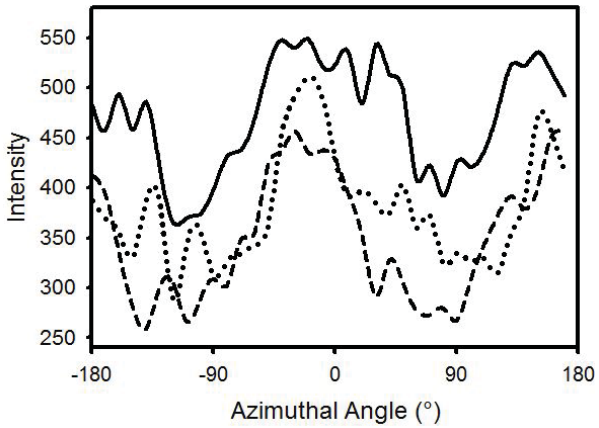

Figure 3.8. Representative azimuthal intensity variation plots of the fifth collagen D-period diffraction peak for pericardium. The width of the central peak represents the spread in fibril orientation. Solid line, glutaraldehyde; dotted line, native; dashed line, chondroitinase ABC. Reproduced by permission of The Royal Society of Chemistry (Kayed et al., 2015b).

Table 3.2. Orientation Index obtained for pericardium samples.

Sample	Number of diffraction peaks analysed (N)	Mean OI	95% confidence interval
Chondroitinase ABC	27	0.208	0.032
Native	36	0.192	0.021
Glutaraldehyde	27	0.117	0.021

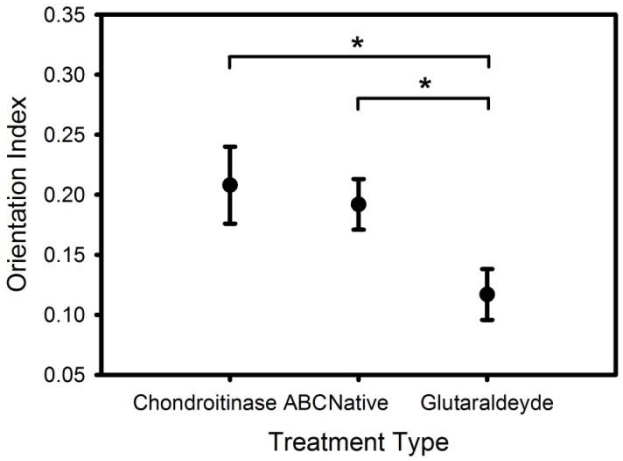

Figure 3.9. Orientation index for each of the three levels of cross linking (error bars for 95% confidence intervals). Pairs that are significantly different ($P<0.05$ for $\alpha = 0.05$) are shown by a *. Reproduced by permission of The Royal Society of Chemistry (Kayed et al., 2015b).

3.3.5 Atomic Force Microscopy

Atomic force microscopy provided clear images of collagen fibrils on the fibrous (outer) surface of the pericardium (Figure 3.10). AFM provides small area images of a diverse surface so that unbiased selection of images can be difficult. One image of each material was selected that is generally representative of that sample. The glutaraldehyde-treated sample clearly had more of a collagen fibril network with fibrils not so often seen in parallel. In contrast the native material and the pericardium treated with chondroitinase ABC contained many aligned collagen fibrils.

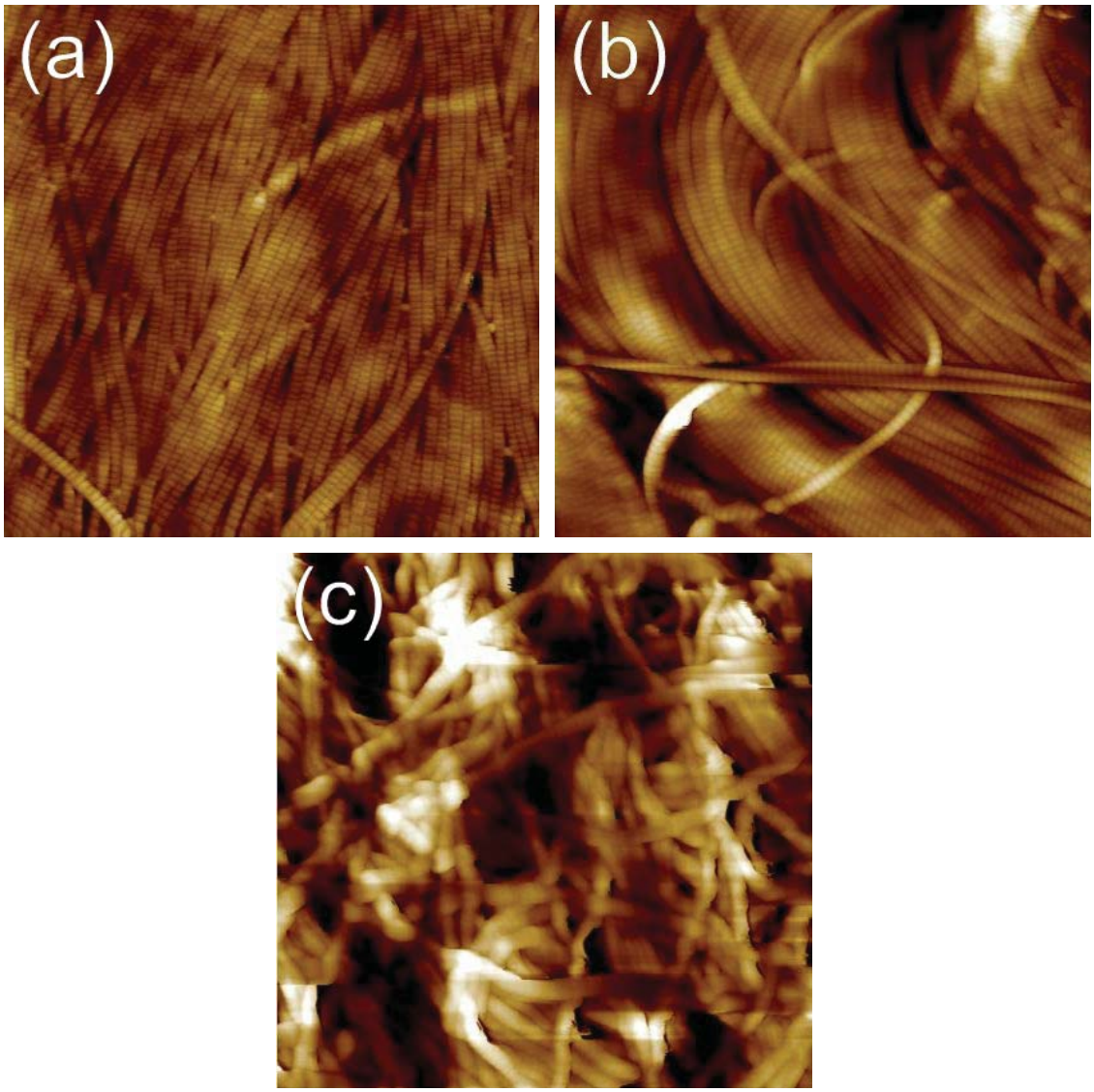

Figure 3.10. Atomic force microscopy height images for a) native bovine pericardium b) chondroitinase ABC-treated pericardium c) glutaraldehyde-treated pericardium. Images are 5 µm square. Reproduced by permission of The Royal Society of Chemistry (Kayed et al., 2015b).

3.4 Discussion

It was found cross linking has an effect on collagen fibril alignment. Native tissue containing GAG cross links has a moderate degree of fibril alignment. When these cross links are removed by treatment with the enzyme chondroitinase ABC the alignment of the fibrils does not show a significant change. When cross links are added, in the form of glutaraldehyde, the alignment of the fibrils decreases, becoming more isotropic with a network like structure forming. These changes do not appear to be associated with a change in crimp. Glutaraldehyde cross links therefore appear to have a direct effect on the arrangement of the collagen fibrils whereas

native GAG cross links do not have a statistically significant effect on alignment for tissue that is not under any mechanical load.

Glutaraldehyde has long been used as a cross linking agent for collagen, reacting primarily with ε-amino groups of lysine and hydroxylysine located on the outer surface of the triple helix region. Such links have been reported to occur both intramolecularly and intermolecularly depending on the treatment conditions and may involve some polymerisation of the glutaraldehyde to link greater distances (Olde Damink et al., 1995, Cheung and Nimni, 1982, Cheung et al., 1985). Here it is shown that this network structure means not just a cross linked network of collagen but that the collagen fibrils also rearrange into a less aligned, more isotropic network structure under the action of glutaraldehyde cross linking without the application of external force. This chemically induced restructuring results in a decrease in the OI.

Heterogeneity with depth was not specifically investigated, however the treatment time was ample to enable glutaraldehyde to penetrate the tissue fully (Cheung et al., 1985). In other work on glutaraldehyde treatment of pericardium, the variation of OI with depth through the glutaraldehyde-treated pericardium tissue has been investigated and the OI did not vary greatly throughout the thickness, although a comparison has not been made with untreated pericardium (Sizeland et al., 2014).

In contrast to glutaraldehyde cross links, proteoglycan (containing GAG) cross links are reported to occur solely on the outer surface of collagen fibrils, forming both axially and orthogonally with the majority located orthogonally between adjacent fibrils by the interaction of GAG side chains localised on the surface of collagen fibrils in mature tissues (Scott, 1980, Scott and Orford, 1981). More specifically, it is believed proteoglycan cross links are associated with the gap region of the collagen D-spacing, binding to a single tropocollagen molecule (Scott, 1980, Scott and Orford, 1981). Here, it is proposed that these GAG bridges do not constrain the fibrils in a somewhat unaligned network structure in a higher energy state; these links appear only to form between adjacent fibrils at specific locations. Removal of these links therefore does not result in relaxation of some kind and fibrils do not spontaneously realign into a lower energy state and adopt some sort of preferred alignment. However, we suggest that the removal of the GAG links by chondroitinase ABC may give the potential for fibrils in the treated pericardium to become more easily aligned under tension.

This understanding of structural changes with treatment also has consequences for the preparation of materials for medical applications such as the treatment of bovine pericardium for heart valve repair, or ovine forestomach extracellular matrix material for surgical scaffolds (Floden et al., 2010). The modifications imposed on the native tissue due to the processing of the material, sometimes including glutaraldehyde cross linking, may be better understood in terms of the structural changes that lead to altered physical properties. A careful balance of cross linking is then is required to achieve the properties required for in-service applications.

3.5 Conclusions

It was found that the extent and nature of cross linking present in pericardium has an impact on the collagen fibril orientation. When additional cross links with glutaraldehyde are added the fibrils form more of a network structure. It is suggested that formation of cross links via glutaraldehyde addition progressively constrains the fibrils into a random network. The relationship between cross linking and fibril alignment provides a perspective on the importance of cross links in determining the structure of tissues. This could have relevance both in the preparation of new biomaterials and in the understanding and treatment of ageing and disorders in human tissues.

Chapter 4

4. Collagen Fibril Strain, Recruitment and Orientation for Pericardium under Tension and the Effect of Cross Links[2]

Abstract

The structural response of collagen fibrils in pericardium and other tissues when subjected to strain and the effect of cross linking on those structural changes are not well understood. Specifically, there is uncertainty about whether natural cross links of glycosaminoglycan (GAG) and synthetic cross links of glutaraldehyde have a mechanical function. Bovine pericardium was treated either with chondroitinase ABC to remove natural cross links or with glutaraldehyde to form synthetic cross links. The collagen fibril orientation index (OI) and D-spacing was measured on pericardium subjected to strain using synchrotron-based small angle X-ray scattering (SAXS). Under strain the collagen fibrils become much more oriented in the direction of the strain, with OI increasing from 0.25 to 0.89 in chondroitinase ABC-treated material, 0.22 to 0.93 in native material, and 0.22 to 0.77 in the glutaraldehyde-treated material. The proportion of fibrils that are recruited during stress varies from 36% in chondroitinase ABC-treated material, 12% in native material, to 45% in the glutaraldehyde-treated material. The increase in D-spacing shows the individual fibrils are strained in chondroitinase ABC-treated material by 2.4% on average or 4.6% for those in the direction of applied strain, in native material, 2.7% and 4.1%, respectively, and in the glutaraldehyde-treated material, 3.2% and 6.4%, respectively. Glutaraldehyde cross links are, therefore, shown to constrain the collagen fibrils and link them together mechanically. GAGs do not have such a

[2] Chapter 4 is based on the following published paper however the experimental methods section has been expanded upon to include more detail regarding setups and data analysis: Kayed, H.R., Kirby, N., Hawely, A., Mudie, S.T., Haverkamp, R.G. (2015). Collagen fibril strain, recruitment and orientation for pericardium under tension and the effect of cross links. *RSC Advances, 5, 103703-103712*. This article can be found in section 8.1.3 of the Appendix.

marked mechanical effect; contrarily, the nature of internal structural responses to strain suggests that GAGs may have a lubricating rather than a binding effect.

4.1 Introduction

The collagen I molecule assembles with a complex hierarchical structure and is a major extracellular matrix component in a multitude of animal structural tissues including pericardium, tendon, cornea, lung and skin. The responses to stresses imposed on collagen materials has been widely studied with the aim of understanding what and how components of collagen play a role in its mechanical properties, both at the macroscopic and microscopic levels.

Collagen materials can be stiff, flexible or extensible, depending on the required function in the body. For example, tendons and ligaments are crucial to joint movement, enabling force transmission and are therefore required to be flexible and have high tensile strength. The mechanical properties of collagen are due in part to its highly fibrillar nature (Meyers et al., 2013, Wells et al., 2015c) and its ability to respond to stresses (Yang et al., 2015). However, it has also been suggested that the cross links between collagen fibrils contribute to the mechanical properties of collagen materials.

Proteoglycan bridges are considered to form shape modules, and are found in the gap regions of collagen fibril D-spacing, linking fibrils together in natural tissue (Scott and Stockwell, 2006, Cribb and Scott, 1995, Scott and Orford, 1981, Scott, 1980). These proteoglycan bridges are elastic and predominantly of decoran, containing the glycosaminoglycan (GAG) dermochondan sulfate (Scott, 2003, Haverkamp et al., 2005).

The role of GAGs in the mechanical response of collagen tissues to stress is contested. Among those who consider the role of GAGs to be significant, there are divided opinions on how these cross links function under tension. Some believe GAGs act as force-sharing elements, transferring shear forces via their connections to the collagen fibrils, allowing fibril stretching and restricting sliding (Liao and Vesely, 2007), whilst others propose the hydrophilic nature of GAGs facilitates fibril sliding (Rigozzi et al., 2013). How GAGs might transmit forces between fibrils so that the fibrils resist the sliding forces has been modelled (Chan et al., 2009, Puxkandl et al., 2002, Cranford and Buehler, 2013, Fessel and Snedeker, 2011, Redaelli et al., 2003). The energy absorbed by enthalpic transformations in specific GAGs such as dermochondan sulfate can be significant (Haverkamp et al., 2007, Haverkamp et al., 2005).

Experimental studies of the changes in collagen's mechanical properties resulting from the depletion of the natural GAG content by the application of chondroitinase ABC have highlighted the differences in results and opinions. On one hand the tensile elastic modulus of mouse tendon was found to be reduced over much of the stress–strain curve when GAG content was lowered, while the ultimate tensile force and ultimate stress for the tendon were relatively unchanged (Rigozzi et al., 2011, Rigozzi et al., 2013). However, other work has found no altered mechanical properties in tendon resulting from the removal of GAGs (Fessel and Snedeker, 2009, Svensson et al., 2011, Fessel and Snedeker, 2011). Natural cross linking of collagen in connective tissues increases with age due to glycation and older tissues have been shown to have higher stiffness; therefore, a causal link has been proposed between cross links and stiffness (Bailey, 2001).

Synthetic cross links can also be introduced; glutaraldehyde is commonly used as a cross-linking agent, particularly in materials for biological heart valve replacements, forming both inter- and intramolecular cross links between collagen fibrils (Cheung and Nimni, 1982, Cheung et al., 1985, Olde Damink et al., 1995). As with GAG cross links, there is debate as to the resulting mechanical properties of collagen tissue treated with glutaraldehyde. Such treatment of bovine pericardium has been reported to result in a less extensible and stiffer material which is stronger than the untreated material (Reece et al., 1982, Langdon et al., 1999). Contrary to these findings, others have observed an increase in extensibility upon glutaraldehyde treatment (Olde Damink et al., 1995, Sung et al., 1999), reduced ultimate tensile strength (Sung et al., 1999), no changes to ultimate tensile strength (Olde Damink et al., 1995).

Cross linking of collagen may affect the arrangement of the collagen fibrils. Glutaraldehyde treatment has been shown to result in a less highly oriented material whereas the removal of GAGs does not have a significant modifying effect (Kayed et al., 2015b). The arrangement of collagen fibrils, particularly the extent to which the fibrils are well oriented, is an important determinant of the strength of collagen materials. The structure–function relationship between collagen orientation and its mechanical properties has been determined for a range of tissue types (Purslow et al., 1998, Liao et al., 2005, Gilbert et al., 2008). The orientation of collagen measured in-plane has been shown in a range of mammal skins processed to leather to be correlated with strength (Basil-Jones et al., 2011, Sizeland et al., 2013). A useful method of quantitatively measuring this structural arrangement of collage*n* fibrils is small angle X-ray

scattering (SAXS) (Basil-Jones et al., 2012, Purslow et al., 1998, Liao et al., 2005, Wells et al., 2015a).

Here, the structural response of collagen cross linked by glutaraldehyde or GAGs to applied strain and stress is investigated to add to the understanding of the mechanical function, or lack of mechanical function, of these cross links. Bovine pericardium is used as a suitable model material for this study. Bovine pericardium has an established use for heart valve leaflet replacement (Nwaejike and Ascione, 2011) and the effect on the mechanical properties of this material by the removal of GAGs has been investigated (Mavrilas et al., 2005, Kayed et al., 2015b).

4.2 Methods

4.2.1 Native Pericardium Samples

Fresh bovine pericardium was obtained from Southern Lights Biomaterials and stored in phosphate-buffered saline (PBS) solution, pH = 6.90 ± 0.10 (Lorne Laboratories Ltd). The tissue was rinsed briefly in PBS solution, and then cut into rectangles approximately 45–50 x 15 mm, with the long axis taken from the long axis of the heart (further details regarding pericardium sampling can be found in section 3.2.1 of Chapter 3). The pericardium was washed for 24 h in a 1% octylphenol ethylene oxide condensate (Triton X-100, Sigma), 0.02% EDTA solution made up in PBS. This washing step was conducted under constant agitation at 4 °C. The samples were then rinsed in PBS buffer and stored in PBS. Samples in this state are referred to as “native”. Subsequent processing of this material produced glutaraldehyde-treated or chondroitinase ABC-treated material. All samples were taken from one pericardium and randomly assigned to each treatment method.

4.2.2 Glutaraldehyde Treatment

The native pericardium was incubated in a 0.6% glutaraldehyde solution made up in PBS buffer, at 4 °C for 24 h with constant agitation (Umashankar et al., 2011). It was then stored in a sealed container in a solution of the same composition for 12 days, before being rinsed and stored in PBS until SAXS measurements were performed. The total time in storage was approximately 18 days.

4.2.3 Chondroitinase ABC Treatment

Removal of GAG cross links was based on the method described by Schmidt et al. (1990). The native pericardium was incubated in 0.125 units of chondroitinase ABC per ml of buffer solution comprising of 0.05 M tris-HCl, 0.06 M sodium acetate and EDTA-free protease inhibitors (complete, EDTA-free protease inhibitor tablets, Roche Diagnostics, Mannheim, Germany), pH 6.5, at approximately 27 °C for 24 h before rinsing and storing in 0.05 M tris-HCl and 0.06 M sodium acetate buffer in a sealed container at 4 °C for 12 days. The samples were then rinsed and stored in PBS, pH = 6.90 ±0.1, at 4°C until SAXS measurements were performed. The total time in storage was approximately 18 days.

Care was taken with all handling, cutting and treatment of the samples not to stretch the material as this might cause fibril alignment to change. The data here represents a duplication of this experiment (on a different pericardium) with additional care taken in sample selection and handling in the second set of samples and SAXS analysis informed by the experience from the initial experiments. However, one portion of the initial data, that for fibril recruitment, is included (in section 3.5).

4.2.4 GAG Assay

An assay for sulfated GAGs was performed in triplicate for each of the sample treatments. GAGs were extracted with 1 ml extraction reagent consisting of a 0.2 M sodium phosphate buffer at pH 6.4, containing 8 mg/ml sodium acetate, 4 mg/ml EDTA, 0.8 mg/ml cysteine HCl and 0.1 mg/ml papain enzyme (Carica papaya, Sigma, Biochemika, Enzyme no. 3.4.22.2). Each pericardium sample was incubated at 65 °C for 26 h. These samples were centrifuged and the supernatant containing the extracted GAGs collected. The concentration of GAGs in solution was determined with a Blyscan Sulfated Glyscosaminoglycan Assay kit (Bicolor, Carrickfergus, UK). GAGs were precipitated with 1 ml of dye reagent to 20 or 40 µl of supernatant diluted to 100 µl, mechanically inverted for 30 minutes, and then centrifuged. The unbound dye was drained off and 1 ml of Blyscan dissociation reagent was added to the precipitate, left to dissolve for approximately 10 minutes, and centrifuged. Absorbance was measured at a wavelength of 656 nm and compared with a standard curve of Chondroitin 4-sulfate GAG reference standard (Biocolor, UK).

4.2.5 SAXS Uniaxial Stretching Setup and Data Processing

Prior to the recording of SAXS patterns and uniaxial stretching, the pericardium samples were removed from the PBS solutions in which they were stored and mounted between clamps of a

custom built stretching device compatible with the Australian Synchrotron SAXS/WAXS beamline setup as described by Basil-Jones et al (2012).

The stretching device consists of a frame to which a L6D Aluminium Alloy OIML single-point load cell (Hangzhou Wanto Precision Technology Co., Zhejang, China) is attached on one end and a linear motor (Linmot PS01-48x240/3x180-C, NTI AG, Switzerland) is attached to the other. Two clamps designed in such a way so as to not introduce sharp point loads to the sample and cause sample tearing or failure in the clamping regions, are attached to the slider of the linear motor on one side and to the single-point load cell on the other side (Figure 4.1a). The apparatus is connected to the sample stage allowing for direct or remote control of the setup so that the sample can be adjusted relative to the X-ray beam. The clamps can also be set a defined distance apart or moved to account for different sample lengths.

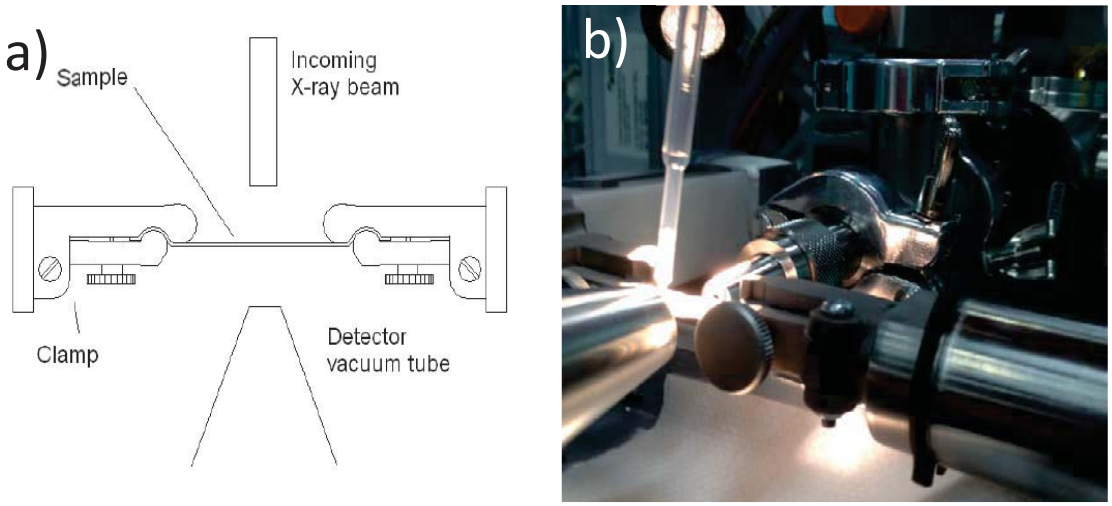

Figure 4.1. Experimental setup of pericardium samples in custom built stretching machine: a) representation of clamp-sample set up in alignment with the SAXS beamline (Basil-Jones et al., 2012); b) photo of pericardium sample mounted between stretching apparatus clamps being wetted.

Load cell calibration was done by the successive addition of weights to the load cell and recording of the resulting load cell voltages. The cumulative masses (g) were plotted against the voltage readings and a linear regression fitted to obtain a relationship between the two.

Vernier callipers were used to measure the thickness and width of the pericardium samples prior to mounting using a consistent light force. Thickness measurements were taken in triplicate across the sample length to account for regional variations and averaged for the use in stress calculations. The rectangular samples were then mounted horizontally between the

clamps away from the X-ray beam and setup under no tension (some slackness across the sample was visible) and wetted across the length to ensure sufficient collagen hydration. The stage was then lifted so as to align the samples in the direction of the X-ray beam (this can be checked via camera output in the control room).

To obtain SAXS measurements under no tension and have them set for further stretching and SAXS measurements, the samples must be taut enough to be flat and straight, however loose enough so as not to register a force by the load cell. To achieve this, the samples were stretched in 1 mm increments remotely until the load cell registered a force reading. Retracting the clamp/slider back 1 mm removed the tension. The actuator position was recorded and length of the sample measured using Vernier callipers, allowing a relationship between the two to be established for the determination of exact sample lengths. SAXS scattering patterns were then recorded; this is the data at no strain and stress.

Subsequently, samples were stretched uniaxially in 1-2 mm increments, where the load cell readings were left to stabilise prior to recording of the cell voltage and actuator position and taking of SAXS measurements. The incremental stretching procedure was repeated until sample failure occurred, that is, the voltage reading decreased or pericardium tearing was observed (from camera output). Samples were wetted every two stretches to maintain hydration throughout the stretching process.

Strain (ε) was calculated using equation 4.1:

$$\varepsilon = \frac{(L - L_0)}{L_0} \qquad \text{Equation 4.1}$$

Where L = sample length at given point (determined from the actuator position)

L_0 = the original sample length under no tension

Stress is defined as force over an area. Stress in N/mm^2 was determined by conversion of the recorded voltage readings to mass (g) using the calibration data, divided by 1000 to convert to kg, multiplied by the acceleration due to gravity (9.81 ms^{-2}) to convert to N, before dividing by the pericardium cross-section area (average width x average thickness).

Diffraction patterns were recorded on the Australian Synchrotron SAXS/WAXS beamline, utilizing a high-intensity undulator source. Energy resolution of 10^{-4} (e.g. 1 x 10^{-4} Å for 1 Å radiation) was obtained from a cryo-cooled Si(111) double-crystal monochromator and the

beam size (FWHM focused at the sample) was 250 x 80 µm, with a total photon flux of about 2 x 10^{12} ph/s. All diffraction patterns were recorded with an X-ray energy of 12 keV using a Pilatus 1M detector with an active area of 170 x 170 mm and a sample-to-detector distance of 3371 mm. Exposure time for diffraction patterns was 1 s and data processing was carried out using the software scatterBrainAnalysis V2.71 (Cookson et al., 2006).

One chondroitinase ABC-treated sample and two of each native and glutaraldehyde-treated samples were tested. One of each sample type are discussed in detail, whilst data from both native and glutaraldehyde repeats are used to determine average fibril recruitment. Six diffraction patterns were recorded at different positions across the samples (in a grid) following every stretch at room temperature. From each scattering pattern the OI and D-spacing were calculated from the azimuthal spread of the 5th and 9th order collagen diffraction peaks (at around 0.05 $Å^{-1}$ and 0.09 $Å^{-1}$, respectively) and averaged where there were single diffraction peaks.

Orientation index (OI) is used to give a measure of the uniformity of fibril orientation (an OI of 1 indicates the fibrils are parallel to each other; an OI of 0 indicates the fibrils are randomly oriented). OI is defined as (90° – OA)/90°, where OA is the minimum azimuthal angle range that contains 50% of the fibrils, based on the method of Sacks for light scattering (Sacks et al., 1997) but converted to an index (Basil-Jones et al., 2011), using the spread in azimuthal angle of one or more D-spacing diffraction peaks. The peak area is measured, above a fitted baseline, at each azimuthal angle. Details pertaining to the SAXS processing procedure for OI determination can be found in section 3.2.5 of Chapter 3.

D-spacing is the characteristic banding pattern of collagen fibrils as seen in electron microscopy and AFM and measures the overlap and gap regions between adjacent axially staggered tropocollagen molecules in register within a collagen fibril. An equation for D-spacing can be derived by combining that of the scattering vector q, and Bragg's law (see section 2.6.2 of Chapter 2) to yield:

$$d = \frac{2\pi n}{q} \qquad \text{Equation 4.2}$$

Where d = D-spacing (Å)

n = Bragg peak order

q = selected Bragg peak position as a scattering vector ($Å^{-1}$).

D-spacing is determined from the SAXS data by first integrating the raw scattering patterns in scatterBrainAnalysis V2.71 (Cookson et al., 2006) and exporting the resulting data as ACSII files to Microsoft Excel, plotting q vs. the logarithm of the intensity for each azimuthal angle, selecting the collagen diffraction peak of interest, and subtracting a fitted logarithmic baseline at each azimuthal angle as described in the method section 3.2.5 of Chapter 3. An in-built macro function discerns the peak position in terms of q and calculates D-spacing as per the above equation, dividing the value by 10 to convert to nm. This is done for the selected Bragg peaks at every azimuthal angle and averaged to give the D-spacing for a scattering pattern, which correlates to one SAXS measurement on the sample.

For those diffraction patterns displaying peak splitting and/or double peaks (at higher strains and stresses), the 9th order diffraction peak was used to calculate OI and D-spacing. For some of the glutaraldehyde-treated samples, the 9th order peak became very complex at higher strains and background intensity could not be identified and subtracted; in such instances, the 5th order diffraction peak was used to determine OI and D-spacing. In the case of peak splitting, two values of both OI and D-spacing were extracted from either the 5th or 9th order diffraction peaks, which involves dealing with the diffraction peak as two peaks; a shifted peak whose maximum is positioned at lower q values correlating to the more highly stretched fibrils ($q \alpha$ D-spacing), and a peak positioned at a higher q value.

Here the intensity of the chosen diffraction peak required for OI determination was found by providing initial fitting parameter estimates for two Gaussian curves covering the split peaks at each azimuthal angle: mean, probability, and standard deviation, so peak position, peak height, and width respectively. An in-built macro then fitted the two peaks more accurately and calculated the intensities for each peak as an area above a fitted logarithmic baseline before returning the OI of the shifted peak in the same way OI was calculated for a single peak (section 3.2.5 of Chapter 3). The OA used in the calculation of OI for the second peak was based on the same peak position as that of the shifted peak maximum position (azimuthal angle) in the azimuthal intensity variation plot. Similarly, two D-spacing values in nm were obtained from the chosen diffraction peak at every azimuthal angle from the positons of both peaks (in terms of q), using the equation given above and dividing the result by 10. The maximum D-spacing for the shifted peak was returned and the D-spacing of the second peak reported at the same azimuthal angle of the shifted peak.

The shifted peak represents the portion of fibrils experiencing higher stresses (larger D-spacing), whose associated nanostructural parameters are referred to as the recruited fibril OI and D-spacing. Those parameters related to the second less shifted peak are referred to as the non-recruited OI and D-spacing. The portion of recruited fibrils was determined using the intensities of these split/double diffraction peaks as intensity is proportional to the quantity of collagen fibrils involved in diffraction (the sum of the recruited fibril peak intensities across all azimuthal angles, divided by the total sum of both recruited and non-recruitment diffraction peak intensities across all azimuthal angles).

Three different OI and D-spacing values are reported throughout this chapter, that is the recruited and non-recruited OI and D-spacing values described above (these are given as averages of the six positions measured per stretch), and the weighted sum OI and D-spacing. The weighted sum OI and D-spacing are the averages of recruited and non-recruited fibril OI and D-spacing values taking into account the proportion of fibrils involved in each. Weighted sum OI and D-spacing are calculated according to Equation 4.3. The recruited and non-recruited fibril portion values used are the average values per stretch (form the six diffraction patterns).

$$Weighted\ Sum\ OI/D = \left[OI/D(RF) \times \left(\frac{RF(\%)}{100}\right)\right] + \left[OI/D\ (NRF) \times \left(\frac{NRF\ (\%)}{100}\right)\right] \quad \text{Equation 4.3}$$

Where RF = recruited fibril

NRF = non-recruited fibril

D = D-spacing

4.3 Results

4.3.1 GAG removal by Chondroitinase ABC Treatment

Chondroitinase ABC treatment removed 81% of GAGs initially present in native pericardium (from 0.90 μg GAGs/mg tissue to 0.17 μg/mg). Pericardium treated with glutaraldehyde had a similar GAG content to the native material (0.85 μg/mg). The GAG content of the chondroitinase ABC-treated material was statistically significantly lower than the other two materials (Figure 4.2).

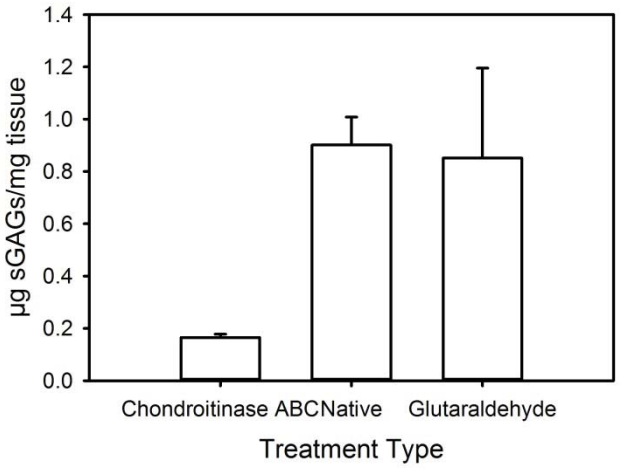

Figure 4.2. Assay results for the GAG content of the three differently treated pericardium samples. Reproduced by permission of The Royal Society of Chemistry (Kayed et al., 2015a).

4.3.2 Tensile Properties

Stress–strain curves were recorded on the samples being progressively strained during the SAXS measurements (Figure 4.3). The stress-strain curves obtained are typical for collagen, showing a foot region and linear region (Reece et al., 1982). While the stress–strain curves are on small samples, and may therefore not give a representative measure of the mechanical properties to be expected of bulk samples of these materials, these curves are important in the context of the structural analysis during strain of these tissues presented in the body of this work. However, in a previous report we found the ultimate tensile stress was highest for glutaraldehyde-treated pericardium (Kayed et al., 2015b). Other studies of glutaraldehyde treatment of bovine pericardium have reported that this material is stronger than the untreated Material (Reece et al., 1982, Langdon et al., 1999) although there is a wide variety of opinions regarding changes to other mechanical properties with glutaraldehyde treatment, (Olde Damink et al., 1995, Sung et al., 1999, Mirnajafi et al., 2005).

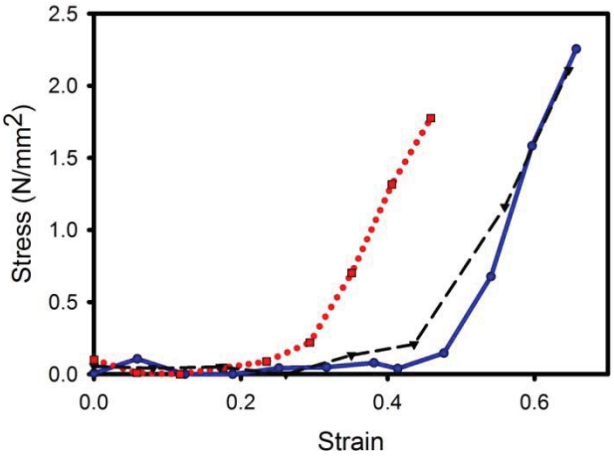

Figure 4.3. Stress–strain curves for the pericardium after three different treatments, while under increasing tension during the SAXS measurements: (●, _____, blue) chondroitinase ABC-treated; (▼, – – –, black) native; (■, ·····, red) glutaraldehyde-treated. Reproduced by permission of The Royal Society of Chemistry (Kayed et al., 2015a).

4.3.3 SAXS

The pericardium scattering patterns had clearly defined diffraction rings due to the D-spacing periodicity (Figure 4.4). When the tissue was not under strain, these rings were of almost uniform intensity around the circle (Figure 4.4a), but as the samples were subjected to more strain, the rings subtended a smaller azimuthal angle (Figure 4.4b and c). This was a result of the fibrils aligning in the direction of strain. Also, the central region of the pattern elongated at 90° to the direction of the diffraction rings. (This central region is the low q part of the pattern and represents scattering from the collagen fibril diameter, which is at right angles to the D-banding.) Another feature of the scattering patterns of pericardium under strain was the shifting of the D-spacing scattering angle, particularly of those fibrils aligned in the direction of the strain. This shift is seen as a protuberance on the inside of the diffraction ring but is more readily seen on the integrated intensity plots (Figure 4.5). In these, the splitting of the D-spacing into multiple peaks or a broad peak is more apparent at higher diffraction orders. The odd-numbered peaks have a much higher intensity than the even-numbered peaks, a characteristic attributed to a fully hydrated sample (Stinson and Sweeny, 1980).

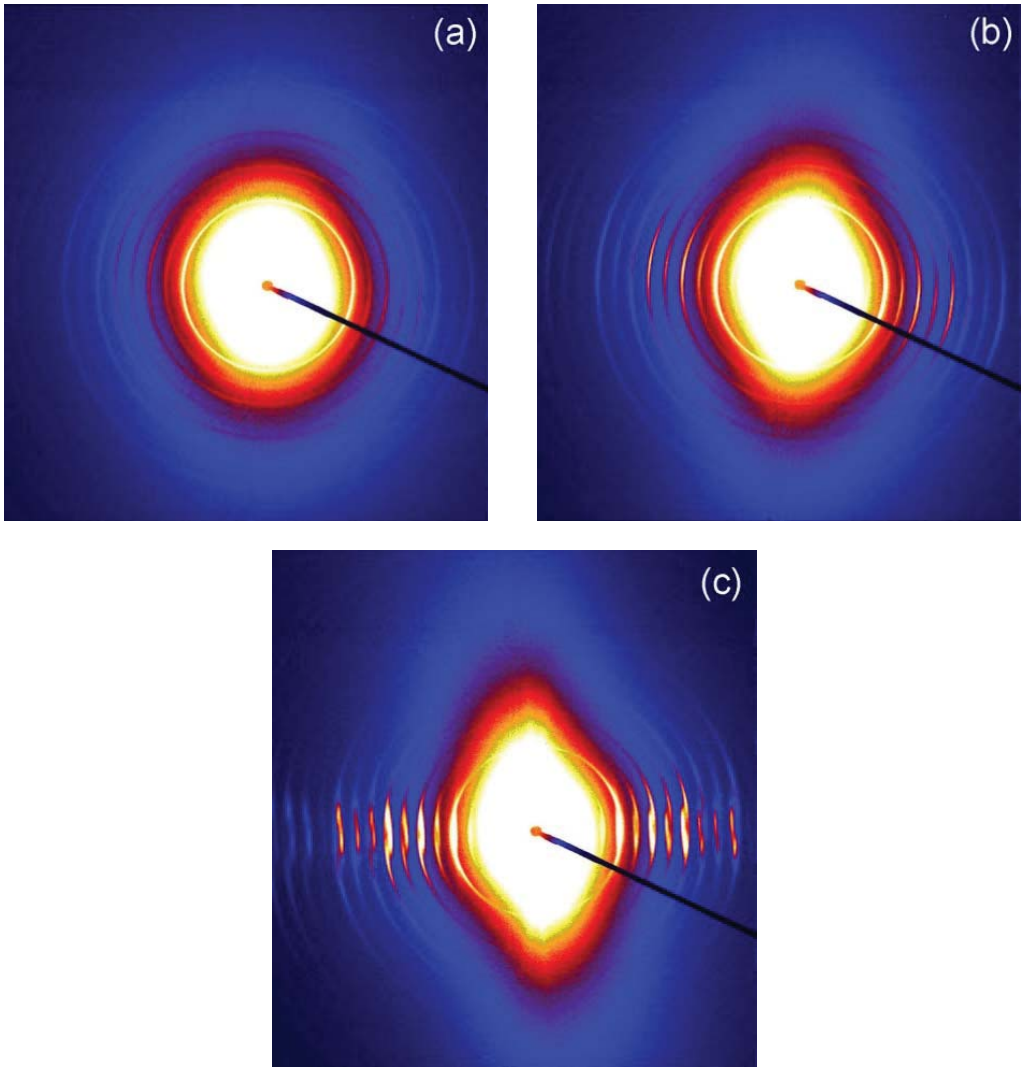

Figure 4.4. A series of typical scattering patterns of native pericardium subjected to a) no strain; b) strain of 0.18; c) strain of 0.45. Reproduced by permission of The Royal Society of Chemistry (Kayed et al., 2015a).

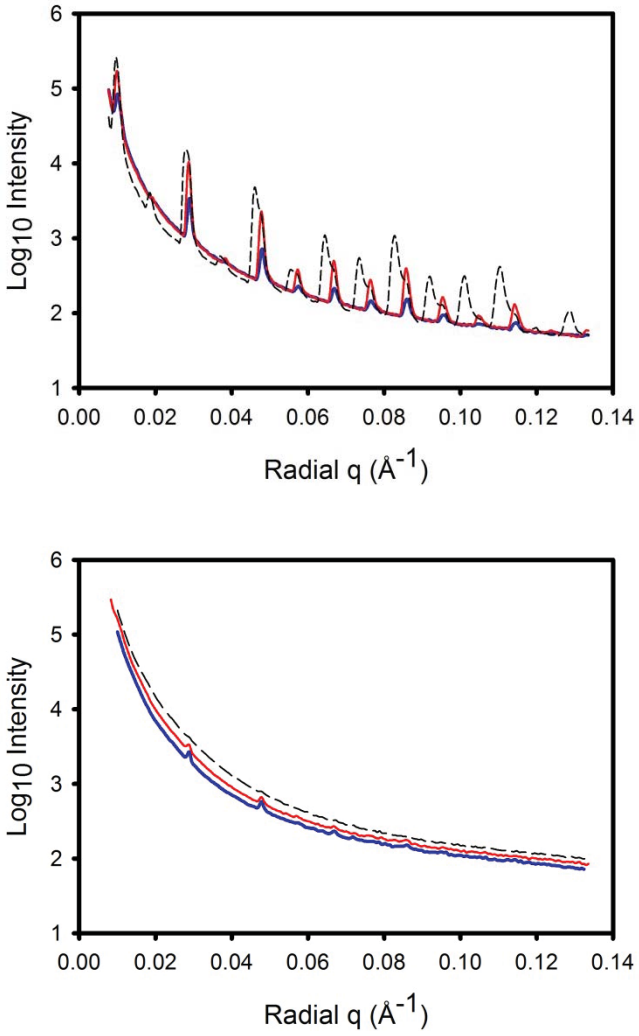

Figure 4.5. Representative integrated scattering patterns of pericardium subjected to varying levels of strain: no strain (_____, blue); 18% strain (_____, red); 45% strain (– – –, black). The sharp peaks are due to diffraction of the D-spacing (at different orders) and the peaks split at higher strain. The top image is for a 5° azimuthal angle segment in the direction of strain, the bottom image if for a 5° azimuthal angle segment normal to the direction of strain. Reproduced by permission of The Royal Society of Chemistry (Kayed et al., 2015a).

4.3.4 OI

The distribution of fibril orientation is measured from a plot of the intensity (peak area used) of any of the collagen diffraction peaks (Figure 4.6). A narrow peak in this plot is indicative of more highly aligned collagen fibrils whereas a broader peak indicates a more isotropic arrangement. This can be quantified as the orientation index, OI.

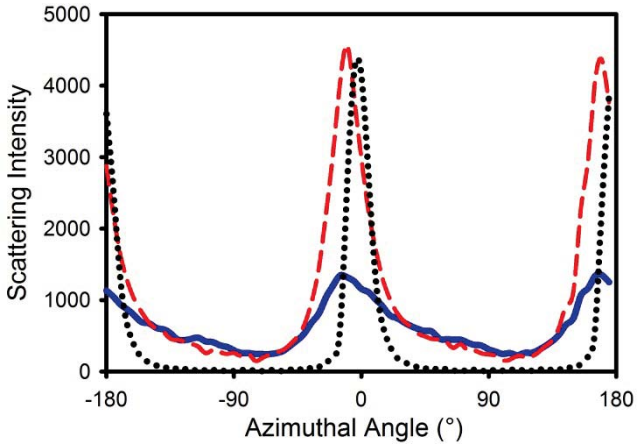

Figure 4.6. Representative integrated scattering intensity at the 5th order D-spacing diffraction peak verses azimuthal angle for pericardium subjected to: no strain (_____, blue); 18% strain (– – –, red); 45% strain (·····, black). Reproduced by permission of The Royal Society of Chemistry (Kayed et al., 2015a).

Both the OI and the D-spacing can be visualized in a three-dimensional plot (Figure 4.7), where the D-spacing of fibrils in a given direction can be seen more clearly.

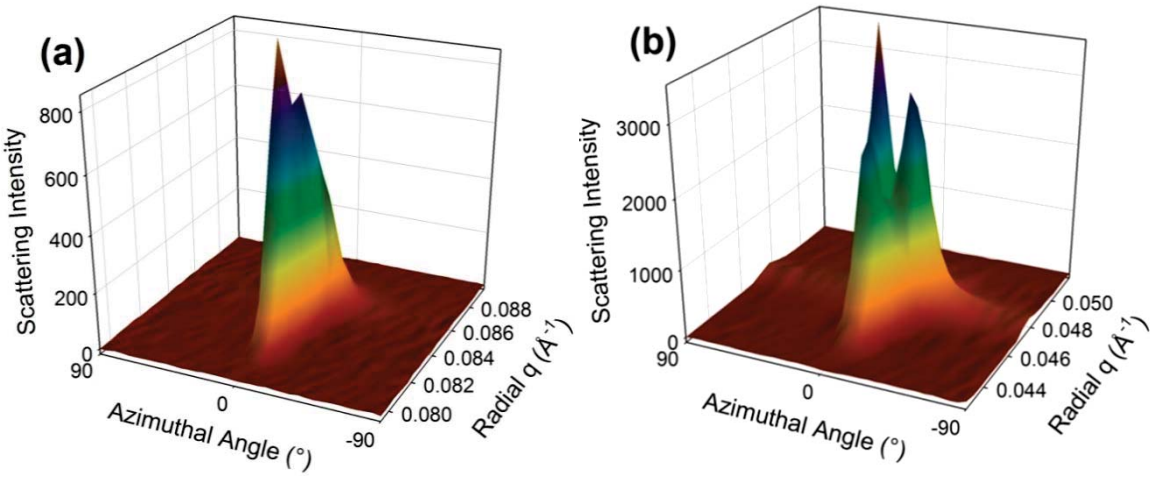

Figure 4.7. Three-dimensional representation of an example scattering pattern of a) native pericardium at a strain of 0.45; b) chondroitinase ABC-treated pericardium at a strain of 0.69, where both the fibril orientation (from the azimuthal angle axis) and the D-spacing shift (from the radial q axis) can be visualized. Only the azimuthal range –90° to 90° is represented as the remaining range is a duplication of this information and only a small portion of the radial angle is displayed representing one D-spacing diffraction peak. Reproduced by permission of The Royal Society of Chemistry (Kayed et al., 2015a).

4.3.5 Changes to Structure during Strain

Initially, the pericardium exhibited little physical resistance to the strain (the stress was low), and there was little change in the D-spacing (Figure 4.8). During this period, however, there was a large change in the OI. The change in OI at this stage of the tensile testing can be attributed to a combination of crimp straightening and re-orientation of the collagen fibrils towards the direction of strain. The D-spacing increase represents the stress on individual fibrils and this increased in tandem with the increasing stress on the whole tissue. (Note that the increase in D-spacing can arise either from the direct stretching of the collagen molecules in a fibril, so that the relative lengths of the overlap and gap regions remain constant, or from the sliding of the collagen molecules past one another, so that the relative length of the gap and overlap regions change. Or the increase can arise from a combination of the two. The mechanism of D-spacing change was not measured here, so D-spacing in this work includes the possibilities of both mechanisms.) Not all fibrils experienced the same stress: the fibrils in line with the direction of applied strain experienced greater stress and underwent a greater change in D-spacing until there were two distinct diffraction peaks for D-spacing at different angles. At the point when these two distinct D-spacings could be identified, the split diffraction peaks were fitted individually to obtain both OI and D-spacing, and were plotted in Figure 4.8 in the high-strain portion of the plot.

While the behaviour for all three sample types was broadly similar there were some differences. All three materials have a portion of fibrils that are highly strained and highly oriented. In the glutaraldehyde-treated material, this portion (which can be called “recruited fibrils”, i.e. fibrils that participate in absorbing the stresses) was higher (Table 4.1) and the stress experienced by these fibrils was greater (evidenced in the D-spacing in Figure 4.8), followed by chondroitinase ABC-treated material and finally native material.

4.3.6 Comparison of OI between Treatments with Increasing Strain

As the pericardium was strained, the fibrils reoriented to line up in the direction of strain, as reflected in the lowering of the OI. However, changes in sample OI varied among the treatments (Figure 4.9), with the maximum OI achieved being highest for native pericardium, slightly less for the GAG-depleted pericardium and lowest for the glutaraldehyde-cross linked pericardium. The recruited fibrils were all highly oriented as expected (Yang et al., 2015) whilst the remaining non-recruited fibrils in the collagen matrix were less aligned in the glutaraldehyde-treated pericardium than in the native or chondroitinase ABC-treated tissue (Figure 4.9b and 4.9c, respectively).

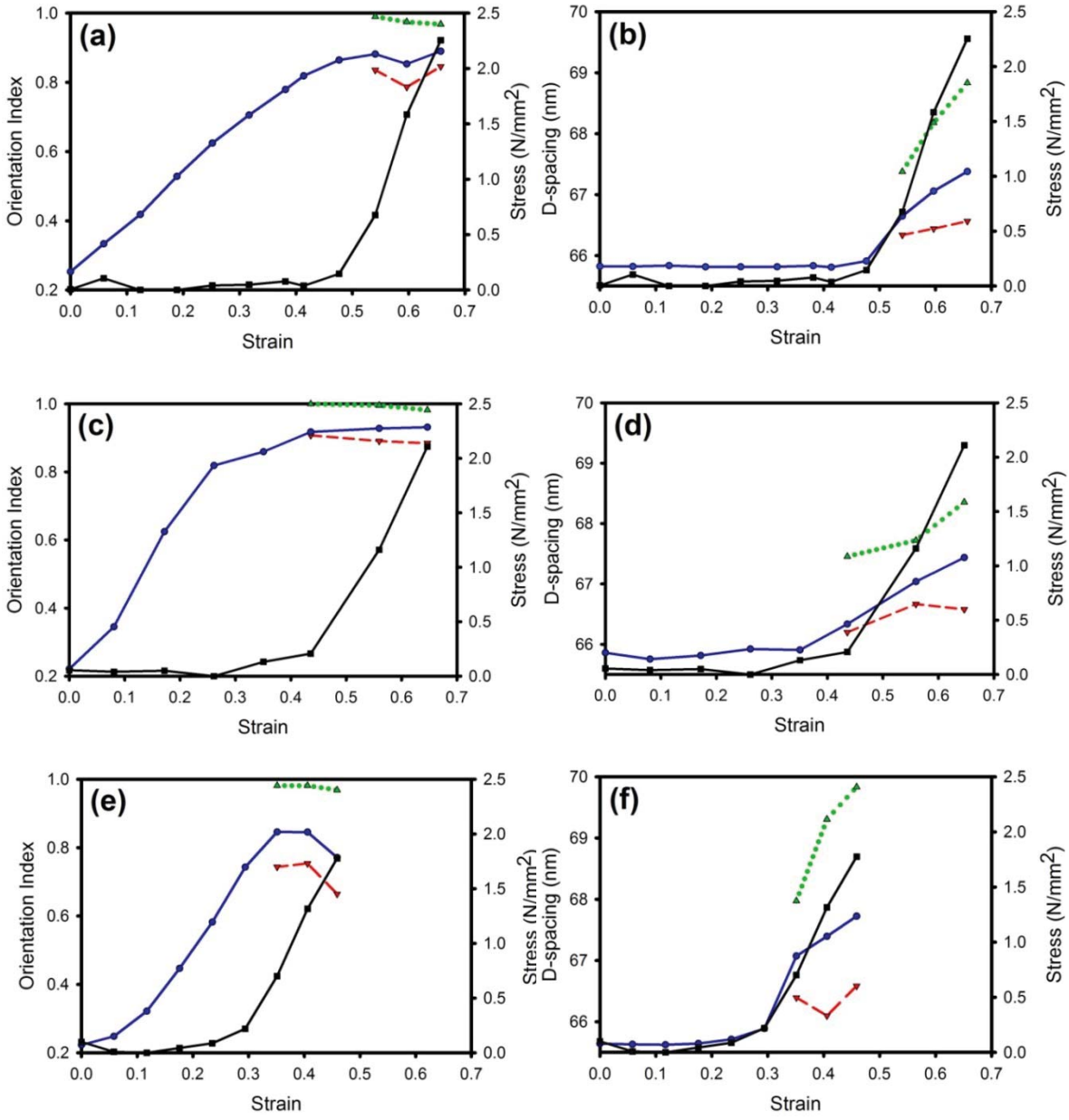

Figure 4.8. Changes in OI and D-spacing as pericardium was subjected to increasing strain for each of the treatment types: (a and b) chondroitinase ABC-treated; (c and d) native; (e and f) glutaraldehyde-treated, where stress (■, _____, black); weighted sum OI or D-spacing (●, _____, blue); non-recruited fibril OI or D-spacing (▼, – – –, red); recruited fibril OI or D-spacing (▲,·····, green), Reproduced by permission of The Royal Society of Chemistry (Kayed et al., 2015a).

Table 4.1. Recruitment of fibrils during stretching.

	% Fibrils Recruited to Stretching		
Pericardium Treatment	(Duplicate pericardium measurements)	(from Fig. 4.7)	Average
Glutaraldehyde	37.9	52.1	45.0
Native	13.1	10.9	12.0
Chondroitinase ABC	37.4	33.7	35.6

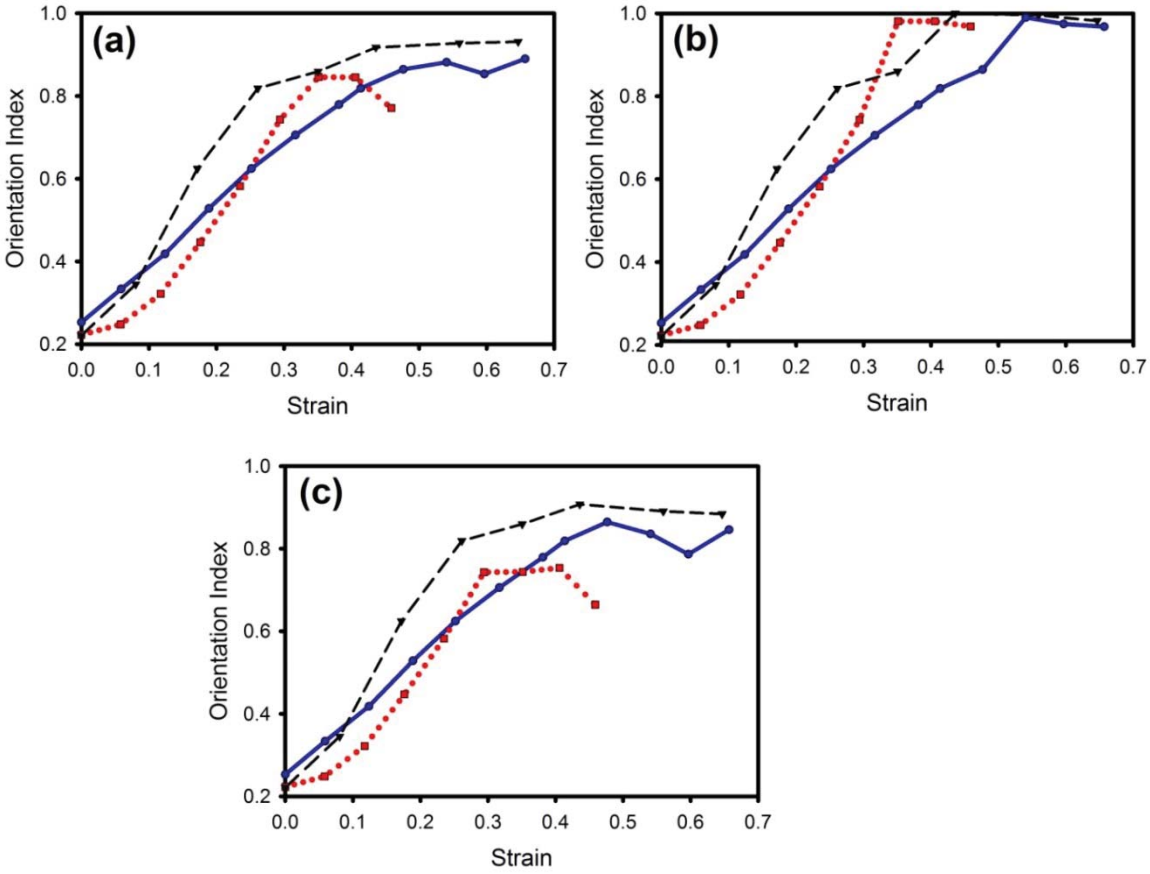

Figure 4.9. Comparison of change in OI with increasing strain for the three treatments: a) average of all fibrils; b) recruited fibrils; c) non-recruited fibrils. Chondroitinase ABC-treated pericardium (●, _____, blue); native pericardium (▼, – – –, black); glutaraldehyde-treated pericardium (■, ·····, red). Reproduced by permission of The Royal Society of Chemistry (Kayed et al., 2015a).

4.3.7 Comparison of Fibril Strain with Stress

As stress is applied to pericardium, this stress is transmitted to the individual collagen fibrils. This results in an extension of length of the fibrils which can be directly measured by the D-spacing change. The D-spacing change, therefore, acts as an internal strain gauge (Wells et al.,

2015c, Haverkamp, 2013). There was a significant variation in the internal strain placed on the collagen fibrils between treatments. Collagen fibrils in the glutaraldehyde-treated materials experienced the greatest strain for a given sample stress, with the chondroitinase ABC-treated material experiencing the least, and native pericardium intermediate between these for the analysis of all the fibrils (Figure 4.10). Of those fibrils recruited into stretching, those of native and chondroitinase ABC-treated pericardium experienced similar strains (slightly higher in the latter) whilst those in the glutaraldehyde-treated pericardium experienced significantly higher strains (Figure 4.10b).

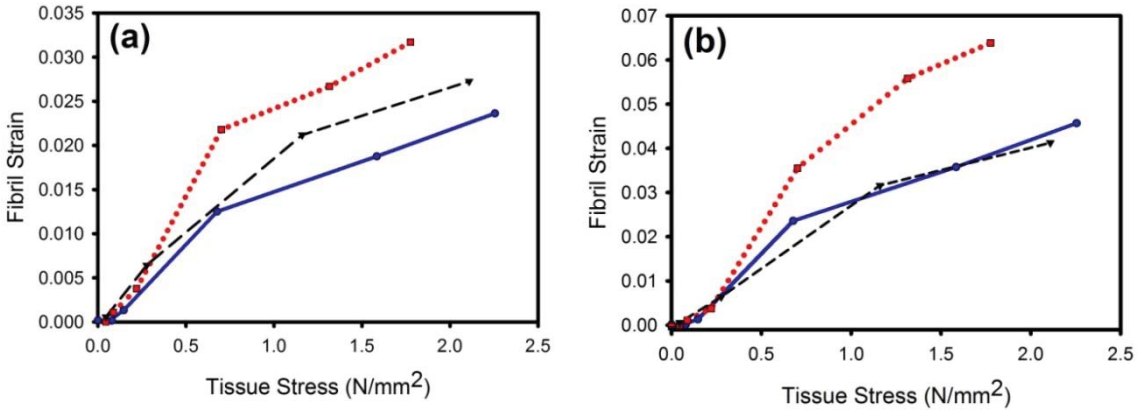

Figure 4.10. Comparison of D-spacing change (indicating fibril strain) with increasing sample stress for the three treatments: chondroitinase ABC-treated (●, _____, blue); native (▼, – – –, black); glutaraldehyde-treated (■, ·····, red). a) Average of all fibrils; b) recruited fibrils only. Reproduced by permission of The Royal Society of Chemistry (Kayed et al., 2015a).

4.3.8 Fibril Strain and Tissue Strain

The ratios of fibril strain (measured by D-spacing increase) to tissue strain (measured by the extension of the pericardium sample; calculated from data in Figure 4.8b, d and f) were the following for the overall tissue for each treatment type: chondroitinase ABC-treated samples 0.12; native 0.12; glutaraldehyde-treated samples 0.16. These ratios are similar to that reported elsewhere of 0.18 for a different sample of native pericardium (Wells et al., 2015c). Of those fibrils taking up the stress, the ratio of fibril strain to tissue strain was 0.24, 0.2 and 0.37 for chondroitinase ABC-treated, native and glutaraldehyde-treated pericardium, respectively.

4.4 Discussion

The internal structural response and stresses on pericardium collagen fibrils subjected to strain can be interpreted in terms of the contribution that the GAG or glutaraldehyde cross linking has on the rearrangement and stress on the individual collagen fibrils.

It is proposed that there are three ways in which this tissue can accommodate the strain and the stresses: 1. By removal of crimp and re-orienting of fibrils (manifested as an OI increase); 2. by stretching of fibrils (D-spacing increase); 3. by sliding of the fibrils (not directly measured here).

The data, and the analysis of it, yields information about the nanostructural behaviours of pericardium tissue being stretched. In turn, these behaviours – strain-induced recruitment of fibrils; strain-induced changes in OI (from crimp removal and rearrangement); and a D-spacing increase from fibril stress – can provide insights into the mechanical structure of the tissue.

4.4.1 Recruitment

Recruitment is one aspect of re-orientation, and is a measure of the proportion of collagen fibrils that take up the stress that the tissue experiences (Table 4.1). Fewer fibrils were recruited in the native pericardium (12%) than in the glutaraldehyde-treated (45%) or the chondroitinase ABC-treated pericardium (36%). This suggests that the collagen fibrils in glutaraldehyde-treated tissue are mechanically locked together by cross links and, therefore, when collagen fibrils in one direction are subjected to strain, other fibrils also take part in this strain. In native tissue, the minimal recruitment suggests that GAGs do not provided a strong mechanical connection between collagen fibrils. However, if this were so, one would expect the chondroitinase ABC-treated pericardium to behave similarly to the native pericardium, which it does not. So, the evidence from recruitment does not provide evidence for a mechanical cross linking effect of GAGs in tissue.

4.4.2 Reorientation with Strain

The amount of strain that a tissue must undergo before reaching maximum OI was similar for native pericardium (0.35) and glutaraldehyde-treated pericardium (0.35) but higher for chondroitinase ABC-treated (GAG depleted) pericardium (0.5). This suggests that in chondroitinase ABC-treated pericardium, mechanical cross links have been removed, allowing more sliding of the collagen fibrils to occur compared with native and glutaraldehyde-treated pericardium. This is consistent with GAGs having a mechanical cross linking action. However, it is noted the variability in the length of the toe region of the stress–strain curves within

treatment groups (Kayed et al., 2015b) could have been influenced by the initial placement of the samples.

4.4.3 Ratio of Fibril Strain (Stress) to Tissue Strain

For all three treatment types, the macroscopic tissue strain was larger than the fibril strain, even after the OI reached a plateau, showing that either strain was taken up by other tissue components or that the fibrils had slid axially relative to one another as well as stretching. Therefore, a ratio of fibril strain to tissue strain may indicate the level of fibril sliding.

For the overall tissue, that ratio of fibril strain to tissue strain was highest in glutaraldehyde-treated pericardium (0.16), with ratios for native tissue and GAG-depleted tissue being the same (0.12). Of the fibrils experiencing the most stress, glutaraldehyde-treated pericardium again had the highest ratio (0.37), whilst native had the lowest (0.20) and chondroitinase ABC-treated material intermediate (0.24). These findings suggest that in glutaraldehyde-treated pericardium the collagen fibrils are held in place, and less able to slide past each other, by the more highly networked structure resulting from the action of cross links. That the ratio of recruited fibril strain to tissue strain for chondroitinase ABC-treated pericardium was slightly higher than that of native pericardium implies that the presence of GAGs encourages more fibril sliding. This strain ratio data, therefore, does not support the theory of GAGs as mechanical cross linkers.

4.4.4 Ratio of Fibril Stress to Tissue Stress

For a given tissue stress, the individual collagen fibrils in glutaraldehyde-cross linked tissue experienced more stress (reflected by the D-spacing increase) than did the native tissue (Figure 4.10). The collagen fibrils in GAG-depleted (chondroitinase ABC-treated) tissue experienced less stress than did the native or glutaraldehyde-treated tissue when considering the behaviour of all fibrils. This could be interpreted to mean that in the glutaraldehyde-treated and native pericardia, there are mechanical cross links that hold the fibrils together so that when the tissue is stressed, this stress is transmitted to a greater proportion of the collagen fibrils in the material. In light of this interpretation, the ratio of fibril stress to tissue stress supports a mechanical action of GAGs. However, for those fibrils aligned in the direction of stress, the fibril strain at a given stress was highest for glutaraldehyde-linked pericardium, but was slightly lower for native than for chondroitinase ABC-treated pericardium. From the behaviour of these fibrils, it appears that GAGs do not transmit stresses to individual fibrils.

4.4.5 Alternative Explanations

The above interpretations of the analyses of fibril stress and orientation change data can be explained by the mechanical action of glutaraldehyde but do not all support GAGs as mechanical cross linking agents. A radically alternative explanation is that GAGs promote fibril sliding perhaps by acting as lubricants to the collagen fibrils. The sliding forces in fibrous protein systems are typically rather large (Ward et al., 2015). Lubrication to reduce these forces does not mean weaker material, and it is well known in the leather industry that lubricating processed leather with oil components is necessary to achieve high strength in leather (Sizeland et al., 2015). Such a role for GAGs acting as lubricants and glutaraldehyde acting as a mechanical cross link are consistent with almost all observations in this work.

The lower fibril recruitment in native material compared to that in chondroitinase ABC-treated material, the ratio of fibril strain to tissue strain (particularly the ratio of the portion of fibrils that take up the most stress), and the ratio of recruited fibril strain/stress to tissue stress are all consistent with GAGs acting as lubricants in the native material, such that the fibrils slide past each other rather than co-opting other fibrils into taking up the applied stress. Unlike glutaraldehyde cross links, which covalently bond to amino acid sidechains on the collagen fibril, GAGs are thought to aggregate through hydrophobic and hydrophilic interactions which can dissociate and reform (Scott and Thomlinson, 1998, Scott, 1992); GAG bridges may, therefore, not be as strong as glutaraldehyde cross links, and rather than pulling fibrils into stretch or directly transferring forces, these GAG bridges may skew, dissociate and possibly re-associate as fibrils slide past one another. There is only one set of observations that is not compatible with GAGs acting as lubricants: the reorientation of fibrils with strain (OI change, maximum) although the differences are small.

4.5 Conclusions

An investigation into the mechanical nature of glycosaminoglycans present in collagen tissue by comparing native pericardium, GAG-depleted pericardium (using chondroitinase ABC) and robustly cross linked pericardium (using glutaraldehyde) identified significant differences in the nanostructural behaviour of the different tissues during mechanical loading. The evidence suggests both GAG and glutaraldehyde cross links have a role in response to applied tension forces, however, the mechanisms by which they respond vary vastly; glutaraldehyde had a clear role in producing a constrained network structure, involving more fibrils in the mechanical response and experiencing higher fibril strains. In contrast, fewer fibrils in native

tissue partake in stretching with the fibrils experiencing lower strains. It is proposed GAGs may act as a lubricant, resulting in more fibril sliding relative to fibril stretching.

Chapter 5

5. The Role of Cross Linking on Collagen Fibril Diameter and Poisson Ratio for Fibrils under Uniaxial Tension

Abstract

The Poisson ratio of many materials both biological and non-biological has been elucidated, including that of collagen fibrils. The effect of cross linking, both natural and synthetic on the Poisson ratio of collagen fibrils has not previously been investigated. Treatment of collagen materials by cross linking is common practice in areas such as the medical field; understanding the nanostructural response of collagen and collagen fibrils to applied forces is therefore important for the purpose of modelling and preparation of tissues to meet specific requirements. This work explores the role of glycosaminoglycan (GAG) and glutaraldehyde cross links on the Poisson ratio of bovine pericardium collagen fibrils by conducting uniaxial tensile experiments in conjunction with, and simultaneous to synchrotron small angle x-ray scattering (SAXS). The longitudinal and transverse fibril strains (from D-spacing and fibril diameters respectively) were determined from the recorded SAXS patterns. Chondroitinase ABC-treated (GAG deficient) pericardium exhibited the largest Poisson ratio range (2.26-3.61), glutaraldehyde lower ranges (1.47-1.80), and native demonstrated Poisson ratios in the range of both glutaraldehyde and chondroitinase ABC-treated samples (0.83-2.47). It is proposed that glutaraldehyde cross links limit the extent of fibril diameter decrease possible due to steric hindrance, directional constraint of the fibrils, and prevention of water molecule expulsion from with the triple helices and fibril structure. Chondroitinase ABC samples are free of the constraints imposed by glutaraldehyde cross links, and less energy is directed to fibril sliding than in the native tissue, allowing for higher volume decreases. The degree of fibril sliding due to lubricating GAGs may result in the lower ratios whilst the lack of covalent glutaraldehyde-like links could allow for larger volume changes in the native tissue.

5.1 Introduction

Collagen type I comprises a large fraction of the extracellular matrices of human and animal skin, organs, muscle, and cartilage. Collagen based biomaterials are also widely encountered in everyday life, where applications of such materials are diverse, ranging from commercial uses as leather in seating, cars, and shoes, to being a significant component in bioprosthetic heart valves and skin/tissue grafts for surgical applications (Floden et al., 2010).

Each application will require the collagen material to have specific mechanical properties to enable it to function as intended. The mechanical properties of bulk collagen tissue, such as tensile strength, tear strength, elasticity and flexural properties have all been investigated, and their correlations between collagen structural parameters such as fibril orientation, fibril D-spacing and fibril diameter attempted (Basil-Jones et al., 2011, Sizeland et al., 2014, Mirnajafi et al., 2005, Fratzl and Weinkamer, 2007). Higher fibril orientation in collagen cross-sections is a determining factor in the strength of collagen tissues such as leathers from a range of animals (Sizeland et al., 2013). There have been suggestions that strength may also be related to fibril diameter for some collagen tissues (Wells et al., 2013, Parry et al., 1978).

The Poisson ratio of a material (ν) is defined as the negative of the ratio of the transverse strain to the longitudinal or axial strain and provides information regarding the material's behaviour to applied forces. For collagen, ν corresponds to the lateral strains from fibril diameter relative to the fibril strain along the axis from D-spacing. Isotropic materials are said to have Poisson ratio values between -1 and 0.5 (as determined by energy arguments). Deformations under tensile forces are positive, and deformation due to compression considered negative for normal materials (due to the minus sign)(Prawoto, 2012). Materials displaying negative ν values are called auxetic and undergo lateral expansion when stretched axially (Prawoto, 2012). Poisson ratios greater than 0.5 are possible for anisotropic materials such as collagen, and are indicative of volume decreases. Tensile and compression tests on a variety of bulk collagen materials have revealed ratios ≥ 0.5. For example, collagen gels under tension $\nu \approx 3$ (Vader et al., 2009), $\nu = 2.2$ and $\nu = 0.6$ for surface zone and mid zones of human articular cartilage under uniaxial tension (Elliot et al., 1999), $\nu \approx 0.5\text{-}1.6$ for bovine dura mater depending if the sample was taken in the circumferential or longitudinal direction (Persson et al., 2010), $\nu = 0.8$ for tendon under compression (Cheng and Screen, 2007), and $\nu = 0.1$ and 0.5 for cartilage chondron superficial and middle zones, and deep zones respectively under compression (Choi et al., 2006).

Less explored is the Poisson ratio of collagen at the nano-level, that is, the Poisson ratio of individual collagen fibrils. A previous SAXS study of native pericardium found the fibrils to experience volume decreases with a Poisson ratio of 2.1 ± 0.7 (Wells et al., 2015c). Evidence suggests that small differences in the collagen matrix can alter the Poisson ratio of collagen materials (Kiviranta et al., 2006). Structural differences do exist among different collagen materials and even between different pericardia. The orientation of fibrils and extent and nature of cross links present affects the structural response of collagen to tensile forces (Kayed et al., 2015a). Tissue regions dense in collagen with higher levels of fibril alignment have demonstrated larger Poisson ratio values (Elliot et al., 1999, Kiviranta et al., 2006).

This chapter is concerned with the effects of natural GAG links and added glutaraldehyde cross links on the Poisson ratio of collagen fibrils under uniaxial tension. GAG cross links are located on the surface of collagen fibrils in the gap regions of the D-spacing, orthogonally bridging neighbouring fibrils through hydrophobic and hydrophilic interactions of at least two GAG chains (Scott, 1992, Scott and Orford, 1981). In contrast, glutaraldehyde cross links may be intra or intermolecular with a range of cross links possible covalently linking fibrils (Cheung and Nimni, 1982, Cheung et al., 1985, Olde Damink et al., 1995). It is thought that the differences in the nature of these links and different collagen structure networks as a result (Kayed et al., 2015b) may influence the Poisson ratio of collagen. Bovine pericardium is used as the study collagen material.

5.2 Methods

5.2.1 Native Pericardium Sampling and Treatment

Fresh bovine pericardium was obtained from Southern Lights Biomaterials and stored in phosphate-buffered saline (PBS) solution, pH = 6.90 ± 0.1 (Lorne Laboratories Ltd). Prior to sample selection, the tissue was rinsed briefly in fresh PBS solution before being cut into rectangles measuring approximately 45–50 x 15 mm from the ventricular side of the pericardium, with the long axis taken from the long axis of the heart (more details regarding the exact sampling locations are given in section 3.2.1 of Chapter 3). The pericardium was washed for 24 h in 1% octylphenol ethylene oxide condensate (Triton X-100, Sigma), 0.02% EDTA solution made up in PBS to decellularise the samples (Yang et al., 2009). This washing step was conducted under constant agitation at 4 °C. The samples were then rinsed in PBS buffer and stored in PBS. These decellularised samples are referred to as “native” pericardium. Subsequent processing of this material produced glutaraldehyde-treated or chondroitinase

ABC-treated material. All samples were taken from one pericardium and as with all experiments presented in this thesis, randomly assigned to each treatment method.

5.2.3 Glutaraldehyde Treatment

The native pericardium sections were incubated in a 0.6% glutaraldehyde solution made up in PBS buffer, at 4 °C for 24 h with constant agitation (Umashankar et al., 2011). It was then stored in a sealed container in a solution of the same composition for 12 days, before being rinsed and stored in PBS until SAXS measurements were performed. The total time in storage was approximately 18 days.

5.2.4 Chondroitinase ABC Treatment

Removal of GAG cross links was based on the method described by Schmidt et al. (1990). The native pericardium was incubated in 0.125 units of chondroitinase ABC per ml of buffer solution comprising of 0.05 M tris-HCl, 0.06 M sodium acetate and EDTA-free protease inhibitors (complete, EDTA free protease inhibitor tablets, Roche Diagnostics, Mannheim, Germany), pH 6.5, at approximately 27 °C for 24 h before rinsing and storing in 0.05 M tris-HCl and 0.06 M sodium acetate buffer in a sealed container at 4 °C for 12 days. The samples were then rinsed and stored in PBS, pH = 6.90 ± 0.1, at 4°C until SAXS measurements were performed. The total time in storage was approximately 18 days. Care was taken with all handling, cutting and treatment of the samples not to stretch the material as this might cause fibril alignment to change.

5.2.5 SAXS Experimental and Data Processing

The pericardium samples were removed from their PBS storage solutions and sample width and thickness measurements were taken in triplicate. The pericardium strips were mounted horizontally between two clamps of a customised stretching apparatus comprising of a linear motor and single point load cell whilst wet in such a way that the pericardium surface was aligned normal to the X-ray beam, therefore SAXS measurements were taken flat-on. The data required for stress-strain measurements and SAXS patterns were recorded at zero strain and following 1-2 mm incremental uniaxial stretches until the sample failed according to the procedure described in section 4.2.5 of Chapter 4.

All diffraction patterns were recorded at room temperature. Diffraction patterns were recorded on the Australian Synchrotron SAXS/WAXS beamline, utilizing a high-intensity undulator source. Energy resolution of 10-4 (e.g. 1 x 10^{-4} Å for 1 Å radiation) was obtained from a cryo-cooled Si(111) double crystal monochromator and the beam size (FWHM focused

at the sample) was 250 x 80 µm, with a total photon flux of about 2 x 1012 ph/s. All diffraction patterns were recorded with an X-ray energy of 12 keV using a Pilatus 1M detector with an active area of 170 x 170 mm and a sample-to-detector distance of 3371 mm. Exposure time for diffraction patterns was 1 s and data processing was carried out using the software scatterBrainAnalysis V2.71 (Cookson et al., 2006). One chondroitinase ABC-treated sample and one of each native and glutaraldehyde-treated samples were tested. Six diffraction patterns were recorded at different positions across the samples following every stretch.

The orientation of the collagen fibrils throughout the uniaxial stretching is quantified using an orientation index (OI). The OI is a measure which describes the uniformity of collagen fibril orientations within the tissue, where it can have minimum and maximum values of 0 and 1 respectively; an OI of 0 suggests the fibrils are orientated completely randomly with respect to each other, whilst an OI of 1 is indicative of highly aligned fibrils (basically parallel to one another). OI is defined as (90° – OA)/90°, where OA is the minimum azimuthal angle range that contains 50% of the fibrils, based on the method of Sacks for light scattering (Sacks et al., 1997) but converted to an index (Basil-Jones et al., 2011) using the spread in azimuthal angle of one or more D-spacing diffraction peaks. The peak area is measured, above a logarithmic fitted baseline at each azimuthal angle. For details on the OI calculation procedure for a single peak refer to section 3.2.5 of chapter 3).

From each scattering pattern, D-spacing was determined from the wave vector position (q) of the 5^{th} and 9^{th} order diffraction peak maxima, whilst OI was calculated from the azimuthal angle spread of the 5^{th} and 9^{th} order collagen diffraction peaks (at around 0.05 $Å^{-1}$ and 0.09 $Å^{-1}$ respectively) and averaged where there were single diffraction peaks. For those diffraction patterns displaying peak splitting and/or double peaks, the 9^{th} order diffraction peak was used to calculate OI and D-spacing where two individual peaks were fitted to account for the portion of fibrils experiencing higher stresses, otherwise referred to as recruited fibrils (larger D), and non-recruited fibrils, which appear at the selected wave vector; therefore two OI and D-spacing values are reported for each scattering pattern (see section 4.2.5 of Chapter 4 for more information regarding the details of these calculations). For some of the glutaraldehyde-treated samples, the 9^{th} order peak became very complex at higher strains and background intensity could not be identified and subtracted; in such cases, the 5^{th} order diffraction peak was used to determine OI and D-spacing. The portion of recruited fibrils was determined using the intensities of these split/double diffraction peaks as intensity is proportional to the quantity of collagen fibrils involved in diffraction.

The D-spacing reported at higher strains where peak splitting occurred was calculated as a weighted average of the recruited and non-recruited fibril D-spacing values at a single azimuthal angle segment (a single segment represents a 5° interval in azimuthal angle); the azimuthal angle chosen is where the highest value of D-spacing is observed, which is approximately at a 90° angle to the fibril diameter. The weighted average of the D-spacing was calculated using Equation 5.1, where D = D-spacing, I = Intensity, RF = recruited fibril, and NRF = non-recruited fibril, for each of the six scattering patterns per stretch of the uniaxial tension tests. The averages of the D-spacing weighted averages are plotted in this chapter, whilst the set of six values were used to determine the 95% confidence intervals at each particular strain.

$$Weighted\ Average\ D-spacing = \frac{[(D(RF)\times I(RF))+([D(NRF)\times I(NRF)])]}{[I(RF)+I(NRF)]} \qquad \text{Equation 5.1}$$

The D-spacing at a single azimuthal angle segment is used as the software package employed to determine fibril diameter only uses diffraction peak intensities at one specific azimuthal angle (or increment of the azimuthal angle); the Poisson ratio includes both D-spacing and fibril diameter, and so to get a more accurate meaningful value, the azimuthal angle range used to obtain the different parameters must be consistent.

The recruited and non-recruited fibril OI values were determined from each of the six scattering patterns recorded per stretch, before calculating the OI as a weighted sum according to Equation 5.2. The averages of the weighted sum OI values are plotted in this chapter, whilst the set of six values were used to determine the 95% confidence intervals at each particular strain.

$$Weighted\ Sum\ OI = \left[OI(RF)\times\left(\frac{RF(\%)}{100}\right)\right]+\left[OI\ (NRF)\times\left(\frac{NRF\ (\%)}{100}\right)\right] \qquad \text{Equation 5.2}$$

Collagen fibril diameters were determined from each SAXS scattering pattern using the Irena software package (Ilavsky and Jemian, 2009) running within Igor Pro. The q range fitted was from 0.009438 to 0.039754 $Å^{-1}$, so approximately 0.01 to 0.04 $Å^{-1}$, at an azimuthal angle 90° relative to the majority of the collagen fibril long axes. This angle was selected by determining the average orientation of the collagen fibrils from the azimuthal angle for the maximum intensity of the D-spacing diffraction peaks. The 'cylinerAR' shape model was used in order to determine fibril diameter, with minimum and maximum diameters set as 300 nm and 3000 nm respectively and an aspect ratio of 30. However the aspect ratio may exceed 30 for some fibrils at different stages of uniaxial tension. The averages of the six fibril diameters

determined per stretch are plotted in this chapter and the set of diameter values at each strain were used to determine the 95% confidence intervals.

The Poisson ratio was calculated over the linear portion of the stress –strain curves for each of the three treatment types using Equation 5.3 (Wells et al., 2015c), where $\emptyset_0$ = fibril diameter at the start of the linear portion of the stress-strain curve, $\emptyset_i$ = fibril diameter at the end of the linear portion of the stress-strain curve, D_0 = fibril D-spacing at the start of the linear region of the stress-strain curve, and D_i = fibril D-spacing at the end of the linear region of the stress-strain curve:

$$Poisson\ ratio = -1\left(\frac{\sqrt{\pi}}{2}\right)\left[\left(\frac{(\emptyset_i - \emptyset_0)}{\emptyset_0}\right)/\left(\frac{(D_i - D_0)}{D_0}\right)\right] \qquad \text{Equation 5.3}$$

A factor of √π/2 was introduced to the Poisson ratio to account for the cylindrical/rod shape of collagen molecules (Wells et al., 2015c). Three different Poisson ratios are discussed in this section: the first is the average Poisson ratio which is calculated based on the average D-spacing and fibril diameters from the set of six points taken at every strain, the second is the Poisson ratio using the -95% confidence interval of D-spacing and fibril diameters (so the start and end D-spacing and diameters were determined by subtracting the 95% confidence interval of the averages from the average D-spacing and diameter values), and the last is the Poisson ratio using the +95% confidence interval of D-spacing and fibril diameters (so the start and end D-spacing and diameters were determined by adding the 95% confidence interval of the averages from the average D-spacing and diameter values). These give the Poisson ratio range by taking into account the variation of diameters across the sample.

5.3 Results

5.3.1 SAXS

The SAXS patterns given in Figure 5.1 show well defined Bragg peaks (rings) which at 0% strain appear as a full circle of relatively uniform intensity, consistent with fibril scattering occurring equally at all angles and therefore random fibril alignment (Figure 5.1a). As the pericardium is stretched (Figure 5.1b and c) two points of interest can be noted about the SAXS patterns: the first is the higher intensity of scatter concentrated over small azimuthal angle ranges in one direction which is suggestive of successive fibril alignment (meridional scattering), the second is the scattering intensity occurring at 90 ° from the scatter associated with the fibril D-spacing

(equatorial scattering) and is attributed to that from the fibril diameter. At higher strains both scattering intensities increase with strain (Figures 5.1 and 5.2), with Bragg peak shifting and peak splitting occurring (Figure 5.2b), and elongation of the scatter due to fibril diameter; this is indicative of an increase in the number of fibrils aligning in the direction of strain and stretching of these fibrils. The higher fibril alignment is also apparent in the integrated scattering patterns for the equatorial scattering, where at higher strains the Bragg peaks become no longer visible in the azimuthal angle range 90° from the loading direction (Figure 5.2a and b).

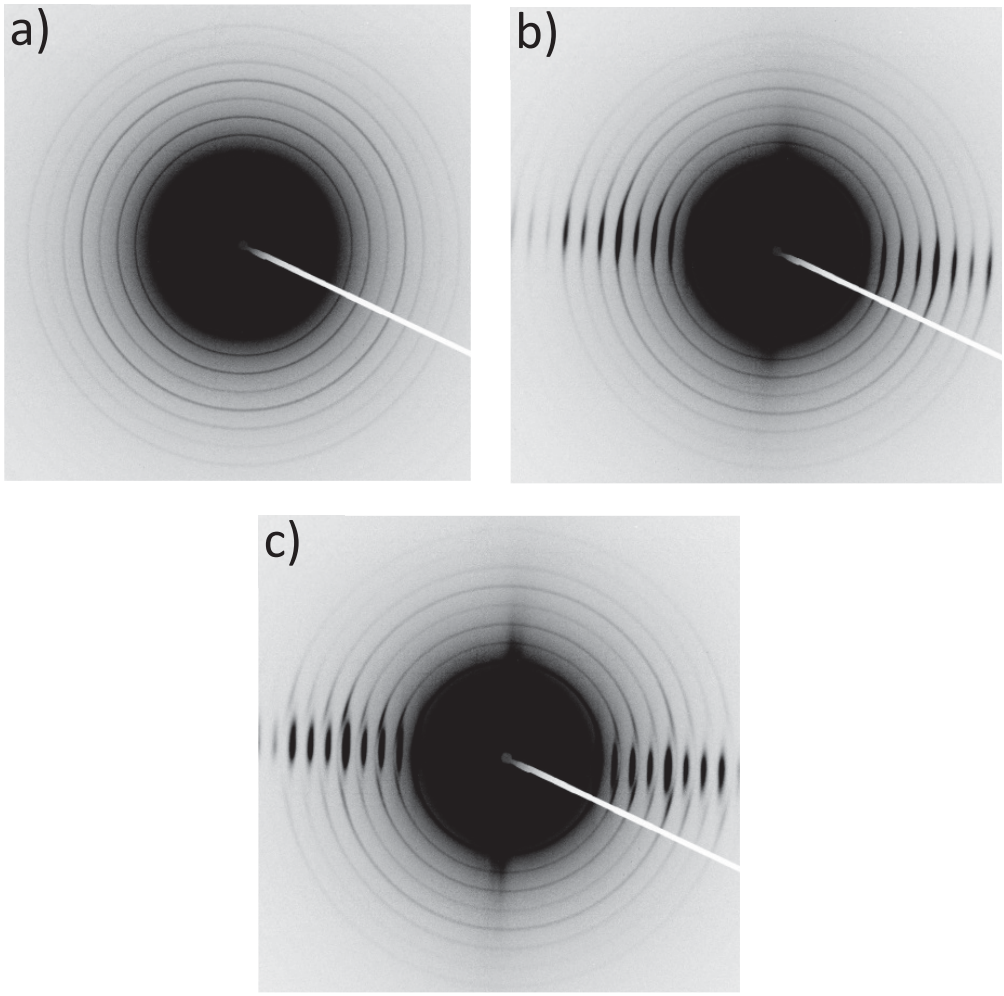

Figure 5.1. Representative SAXS scattering patterns of pericardium at different stages of uniaxial stretching: a) 0 % tissue strain; b) 20% tissue strain; c) 30% tissue strain.

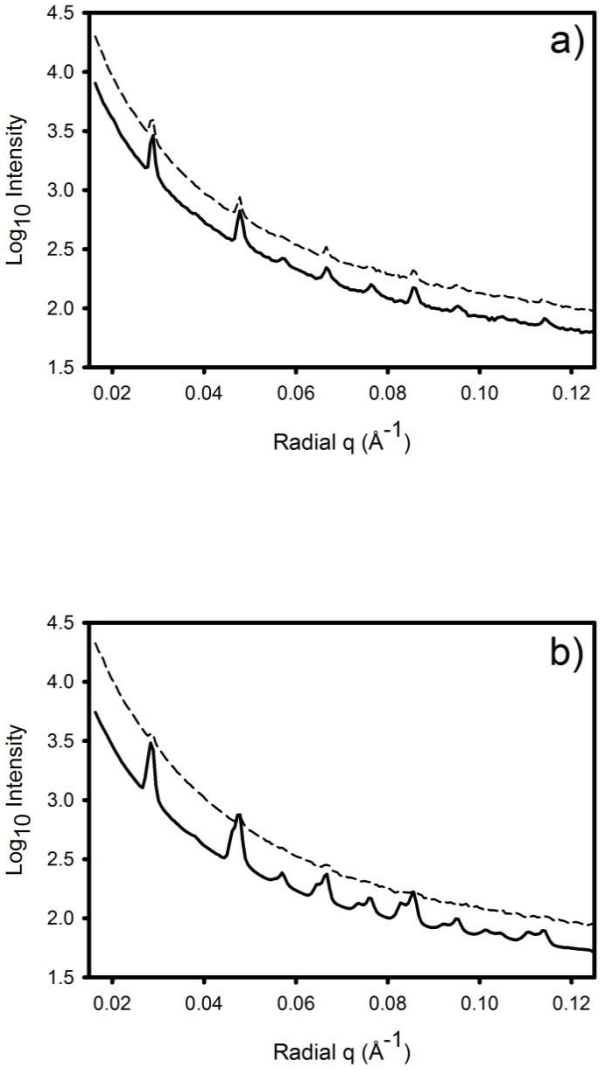

Figure 5.2. Representative integrated scattering patterns for pericardium showing scattering from different collagen structural features: meridional scattering from D-spacing (_____); equatorial scattering from fibril diameter (- - - -). a) Integrated scattering patterns for pericardium at 0% strain; b) integrated scattering patterns for pericardium at 60% tissue strain.

The D-spacing of glutaraldehyde-treated pericardium was found to be statistically significantly different (using one way ANOVA, $\alpha = 0.05$) to that of native and chondroitinase ABC-treated pericardium under no tension (Table 5.1, Figure 5.3). However the difference between the native and chondroitinase ABC-treated tissue D-spacing means does not pass the significance test. This is in agreement with the results of another set of experiments (not shown here) which found glutaraldehyde treatment to significantly decrease D-spacing compared to the

other two treatment types. Such an observation has been reported previously (Meek, 1981), where possible mechanisms may include tightening of collagen crimp (Chachra et al., 1996), contraction of the collagen network by intramolecular cross links (Sung et al., 1999) or changes to the hydration network within the fibril.

Table 5.1. D-spacing values for differently cross linked pericardium under no tension.

Sample	Number diffraction peaks analysed (N)	Mean D-spacing (nm)	95% confidence interval
Chondroitinase ABC	6	65.82	0.036
Native	8	65.75	0.096
Glutaraldehyde	11	65.55	0.086

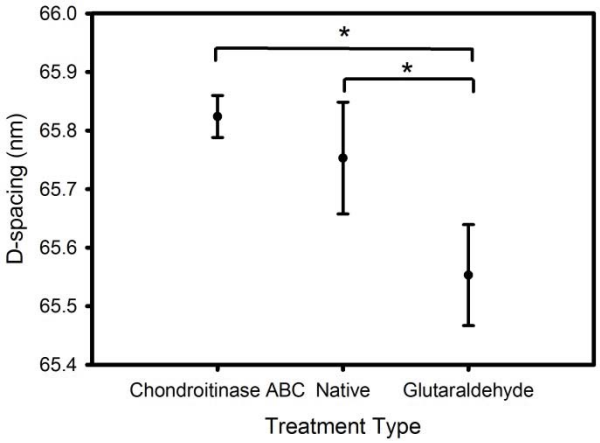

Figure 5.3. D-spacing for each of the three types of cross linking (error bars for 95% confidence intervals). Pairs that are significantly different ($P<0.05$ for $\alpha = 0.05$) are shown by a *.

5.3.2 OI, D-spacing and Fibril Diameter Changes with Strain

Examples of the fibril diameter fitting from an integrated SAXS pattern in the Irena software are provided in Figure 5.4. Under no strain a single distinct peak of fibril distributions is observed correlating to single point of SAXS measurements (Figure 5.4a), whilst a bimodal fibril distribution appears at higher strains, suggesting two sets of fibrils experiencing different forces or fibril diameter changes (Figure 5.4b).

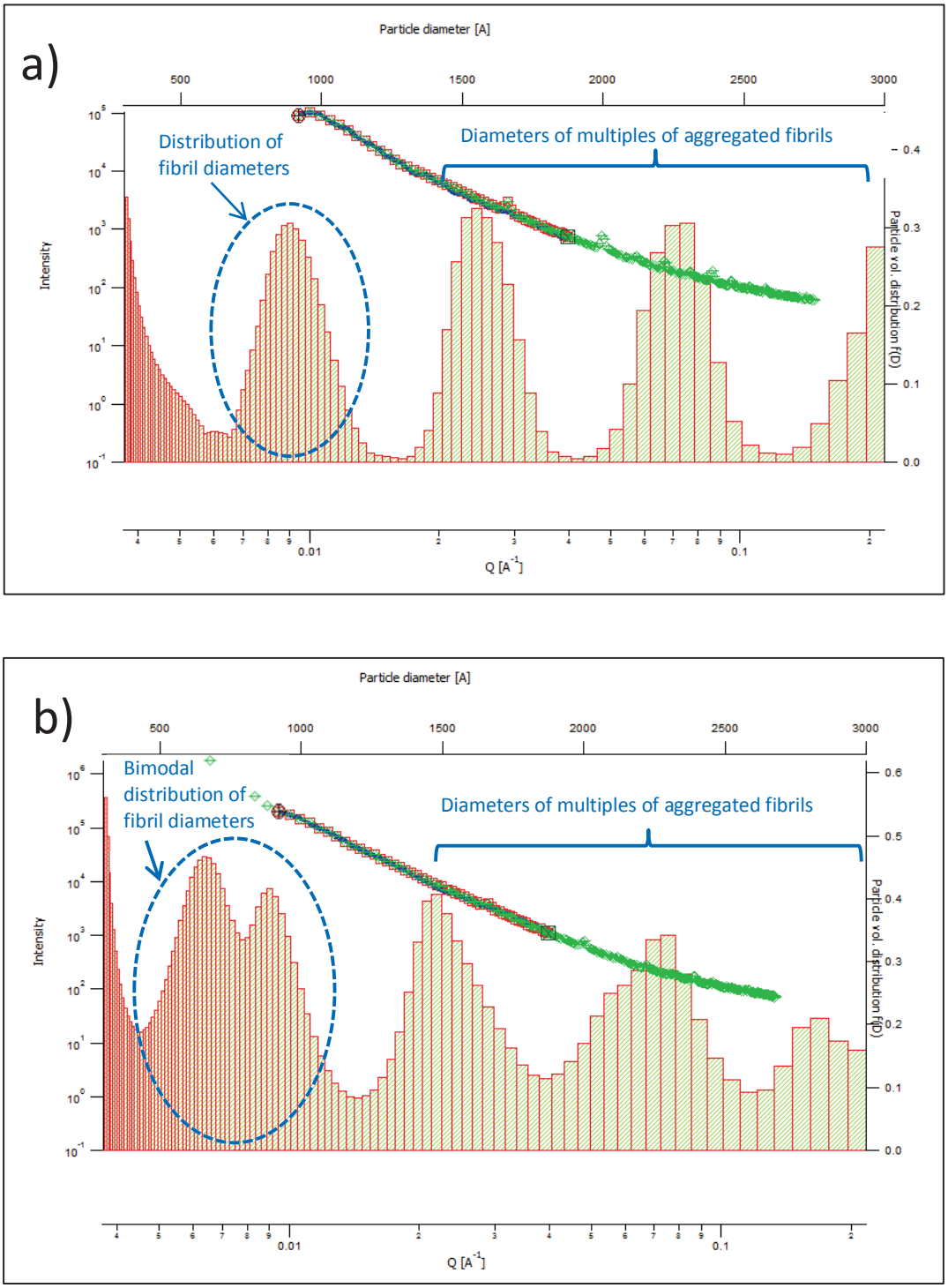

Figure 5.4. Fibril diameter fitting using the Irena software package showing fibril diameter distributions for: a) pericardium at 0% strain with a single peak of fibril diameter distributions; b) pericardium at 30% strain with a bimodal fibril diameter distribution.

Figure 5.5 follows the average fibril diameters and weighted sum OI and D-spacing with increasing strain for each of the three treatment types. The response of collagen fibrils to strain here are consistent with the responses observed in Chapter 4; initially there is little to no uptake of stress by the fibrils which exhibit no change in D-spacing, instead the forces are involved in crimp straightening and fibril realignment. However, at higher strains stress is transmitted to the individual fibrils in the pericardium causing fibril elongation as evidenced by the significant increases in D-spacing, either by extension of the tropocollagen molecule lengths, or relative sliding of tropocollagens within the molecule.

The average fibril diameter increases with strain initially before decreasing in the linear region of the stress-strain curve for both native and chondroitinase-treated samples. Glutaraldehyde-treated material also shows an initial increase though over a shorter strain range before declining. All samples show large fibril diameter 95 % confidence intervals, particularly in the lower regions of strain. These 95% confidence bars shown in Figure 5.5 are not due to errors in the measurement of fibril diameter; rather, they represent regional variation of diameters across the pericardium samples. The distribution of diameters across the glutaraldehyde-treated pericardium sample decreases with larger strains, whilst there remains a large variation of diameters across the native samples. The sample treated with chondroitinase ABC shows a change in regional variation of fibril diameters in between the other two treatments, that is, there is more regional variation in diameter than the glutaraldehyde-treated sample and less variation than the native sample.

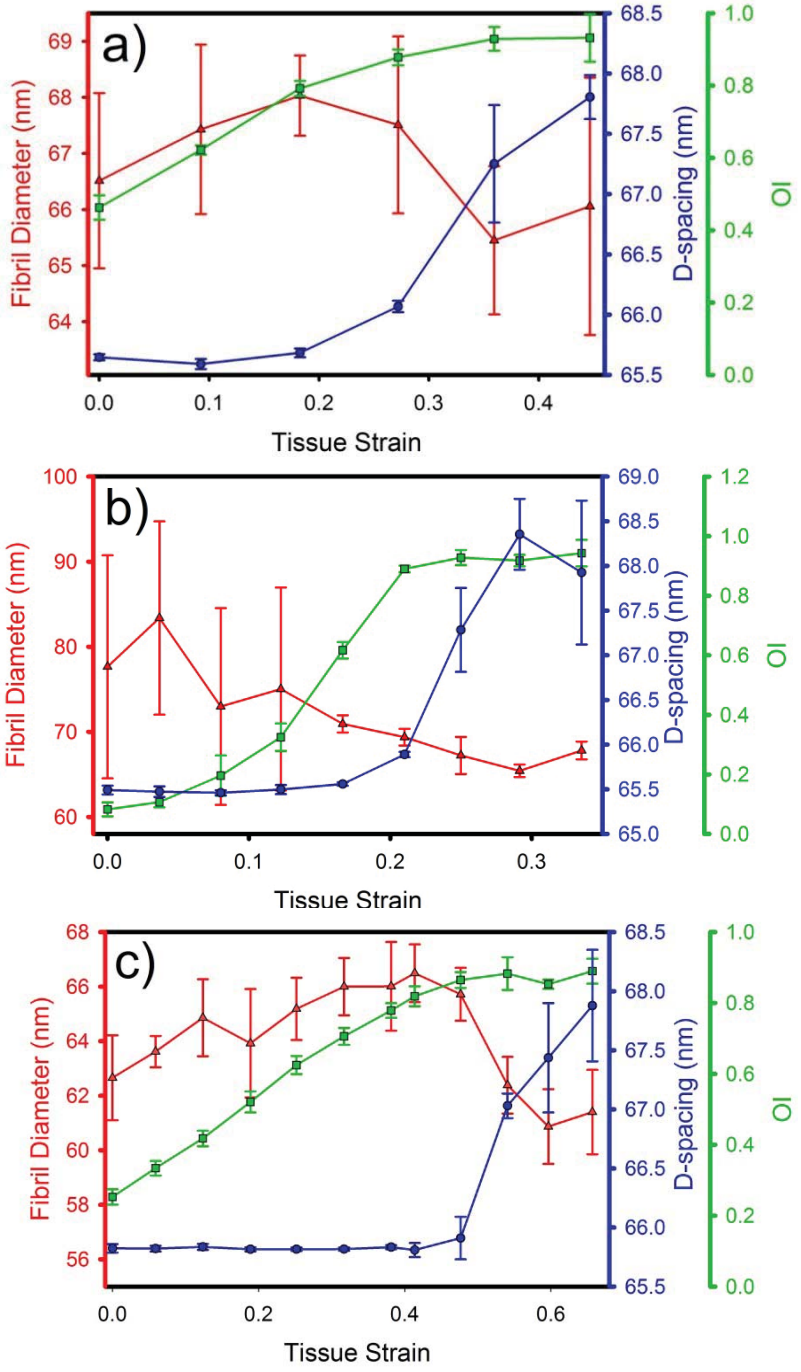

Figure 5.5. Changes in fibril diameter (nm), D-spacing (nm) and OI as pericardium was subjected to strain for each of the treatment types: a) native; b) glutaraldehyde-treated; c) chondroitinase ABC-treated, where (▲, ___, red): fibril diameter; (■, ___ , blue): D-spacing ; and (●, ___, green): OI. The 95% confidence intervals of the six measurements at each strain are represented here.

5.3.3 Poisson Ratio

Pericardium treated with chondroitinase ABC demonstrated the highest average fibril Poisson ratio at 3.03 over the linear region of the stress-strain curves when the fibrils begin to uptake the stresses (the strain and stress region where the D-spacing shows marked increases), whilst that of glutaraldehyde and native samples were much lower at 1.62 and 1.41 respectively (Table 5.2). The Poisson ratio was also determined using the upper and lower limits of the D-spacing and fibril diameters values calculated using the 95% confidence intervals, as the average Poisson ratio values alone are not sufficient for describing the behaviour across the entire samples; there are D-spacing and fibril diameter variations across the sample areas suggestive of range of nanostructural responses to strain. Taking into account the distribution of fibril diameters and D-spacing in a sample at any given strain, the range in Poisson ratio for the native sample becomes 0.83 to 2.47, for the glutaraldehyde-treated sample the range is 1.47 to 1.80, and the range is 2.26-3.61 for the chondroitinase-treated sample.

Table 5.2. Average Poisson Ratio and Poisson ratio calculated using the 95% confidence intervals of fibril diameter and D-spacing for each treatment type: native, glutaraldehyde-treated, and chondroitinase ABC-treated pericardium.

	Poisson Ratio		
Sample	Average	-95% CI	+95% CI
Native	1.4	2.5	0.8
Glutaraldehyde	1.6	1.8	1.5
Chondroitinase ABC	3.0	3.6	2.3

5.4 Discussion

In Chapter 4, it was established that cross linking, particularly the nature of cross links have different roles in the nanostructural response of pericardium collagen fibrils to uniaxial stresses. However all samples, native, glutaraldehyde, and chondroitinase ABC-treated pericardium samples showed general trends in collagen fibril orientation and D-spacing with increasing strain, which are also observed here. At the lower strains (corresponding to the 'foot' and 'heel' regions of collagen stress-strain curves) fibrils orientate in the direction of applied tension and lose their characteristic crimp, whilst no elongation occurs as seen by the relatively constant D-spacing. It might therefore be expected that the fibril dimensions in the transverse direction, so fibril diameter, would also remain constant in this strain range. It would appear however that this is not the case, with all three samples showing initial increases

in the diameters, most evident for the chondroitinase and native samples (Figure 5.5a and c). Fibril diameters obtained from SAXS data are the true diameters, where the angle of fibrils to the X-ray beam and degree of fibril bending bear no consequence to the resulting diameters. Why the fibril diameter should increase in the low strain regions is unknown. Repeat experiments would reveal if collagen diameters always experience initial increases before fibril stretching occurs, or if this is a one off observation. At higher strains, a portion of the stress introduced is transferred to the collagen fibrils, causing elongation either by stretching of the tropocollagen molecules, or sliding of these tropocollagens so that the relative length of the gap and overlap regions of the D-spacing between tropocollagen molecules in register changes, or a mixture of both.

The Poisson ratio is basically a measure of the transverse strain relative to the longitudinal strain of a material. In this research, the Poisson ratio was investigated at the level of individual collagen fibrils rather than the bulk collagen tissue. Therefore the ratio equates to the change in fibril diameter relative to the change in D-spacing over the linear region of the stress-strain curves (this linear region is where the D-spacing begins to increase with strain). Isotropic materials have Poisson ratio upper bounds of 0.5, as it is expected tensile forces will not cause volume shrinkage (Fratzl, 2008), and lower bounds of -1. However for anisotropic materials the Poisson ratio may exceed this range; values of the ratio above 0.5 suggest decreases in volume.

Collagen fibrils have a structure that is very much anisotropic, consisting of any number of repeats of five tropocollagen molecules in register axially staggered by a defined distance, where each tropocollagen molecule consists of three left handed helical collagen polypeptide molecules which come together to form a right handed alpha helix (Fratzl, 2008, Petruska and Hodge, 1964). Poisson ratios above 0.5 have been reported previously for collagen under tension (Elliot et al., 1999, Vader et al., 2009). These preliminary experiments investigating the Poisson ratio of collagen fibrils have shown all samples, irrespective of the quantity or nature of cross links present, to have Poisson rations greater than 0.5, with all average ratios greater than 1. This signifies substantial decreases in volume of the collagen fibril. Since the fibril is composed of multiple repeats of five axially staggered adjacent and in register tropocollagen molecules, a decrease in the diameter will involve some sort of contraction of these repeat units.

The mechanism of diameter contraction was not explored here and little is found in the literature regarding real time studies or modelling of the response of the components of collagen fibrils (such as tropocollagen or collagen molecules, and changes in the bonding both covalent and non-covalent) to tension (Buehler and Wong, 2007). There have been attempts at modelling or simulating collagen mechanics and deformation mechanics (Tang et al., 2010, Buehler, 2008, Buehler and Wong, 2007), however this involves many assumptions and limitations, where modelling is difficult due to the interconnection of multiple levels of collagen structure and the chemistries involved. Some suggested micromechanical deformation mechanisms include tropocollagen extension and relative slippage, uncoiling and breaking of cross links (Tang et al., 2010). Possible ways in which the diameter specifically may decrease to cause decreases in volume are proposed here.

Uniaxial stretching of the collagen may extend the tropocollagen molecules so that the opposite twists of the individual molecules and three together prevent the triple helix from untwisting and allow the collagen molecules to come into closer proximity, also increasing D-spacing. Tightening of the individual tropocollagen molecules within a fibril could cause overall contraction of the fibril diameter. Mechanisms of tropocollagen molecule diameter decrease may include shortening of direct interstrand hydrogen bonding or shortening of interstrand water mediated hydrogen bonding to stabilise the triple helical structure (the amine groups of glycine on one collagen molecule hydrogen bond with the carboxyl groups of a neighbouring polypeptide chain). A range in number of water molecules also bridge the carboxyl groups of glycine with the amine groups of other amino acids in the X or Y positions of neighbouring polypeptide repeat units through hydrogen bonding, which would otherwise be hindered by distance (section of 2.1.1.3 of Chapter 2 discusses hydrogen bonding in the triple helix in more detail). These bonds are not covalent and may shorten to allow the three collagen molecule strands to come together more tightly. Tensile stretching experiments conducted in conjunction with, and simultaneous to infrared experiments may reveal if indeed changes in hydrogen bonding take place as the vibrational frequencies would be expected to change.

Fluid exchange from a materials inner structure has been proposed by some as a mechanism which may permit the decrease in volume of materials under tension (Elliot et al., 1999), so water exclusion may be another method for fibril volume shrinkage. The interstrand water mediated hydrogen bonding bridges could not only shorten, but potentially one or all of the water molecules could be expelled from the inner helix. Hydrogen bonding through water molecules also occurs within fibrils in addition to covalent bonding for stabilisation of the

quaternary structure, therefore there is potential for water exclusion from within the fibrils also.

Sliding of tropocollagen molecules within a collagen fibril is another mechanism which does not involve the shrinking of tropocollagen diameter by which collagen fibril diameter might decrease. (This would involve the alteration of enzyme induced covalent cross links between tropocollagens in a fibril via lysine and hydroxylysine residues and glycation links by either changing bond lengths or breaking these bonds, so more likely at higher strains were the fibrils experience higher stresses).

Having discerned that all three differently treated pericardium samples exhibit collagen fibril volume decreases, as evidenced by the high Poisson ratios, the average and range of these ratios must now be compared to establish if and how cross linking influences collagen fibril nanostructural response to tension in terms of diameter. Chondroitinase had the highest average and range of Poisson ratios (2.3-3.6) of the three treatment types; glutaraldehyde had a lower Poisson ratio range (1.5-1.8), whilst the native sample exhibited a range of Poisson ratio values extending to values lower than glutaraldehyde and in the range of chondroitinase ABC (0.8-2.5). By considering the results and conclusions of Chapter 4 and combining them with the results of the experiments conducted here, possible explanations for these observed results can be suggested.

The collagen fibrils in samples of chondroitinase ABC were shown in Chapter 4 to undergo a mixture of sliding and stretching when subjected to uniaxial tensile forces, where less fibril sliding occurs relative to native fibrils and less stress uptake and elongation occurring than in glutaraldehyde samples. Of those fibrils partaking in stretching, there is nothing to prevent longitudinal elongation and transverse contraction of the fibrils, hence significant volume decreases can arise. Glutaraldehyde collagen fibrils were found to experience the highest level of stress uptake of the three treatment types with more fibrils involved in stretching and demonstrating the most fibril elongation (highest fibril strains). It might therefore be expected fibrils of the glutaraldehyde-treated sample would also show large diameter decreases and overall fibril volume decreases, though the opposite was found; glutaraldehyde is believed to covalently cross link fibrils through lysine and hydroxyl lysine residues both intra and intermolecularly, with a variety of different types of links and lengths possible. Such links may prevent the tropocollagens from tightening or the five tropocollagen molecule units from coming together. For example, cross links between different fibrils may assert pulling forces on the tropocollagen molecules in the opposing direction to diameter contraction or prevent such

contractions as they are stronger than the hydrogen bonds that shorten. Intramolecular links may also sterically hinder the closer approach of the triple helices and restrict the amount of water exclusion possible.

Of the three treatment types, less collagen fibrils are recruited into stretch in native pericardium, with the GAG links present possibly providing lubrication which encourages fibril sliding. As more energy is directed to fibril sliding, some fibrils experience much lower stretching and diameter decrease which would result in Poisson ratios lower than that of glutaraldehyde and chondroitinase ABC. However, as in the case of chondroitinase ABC, for those fibrils to which stresses are transferred, there are none of the bulky and strong covalent cross links found in the glutaraldehyde samples to prevent tropocollagen volume decreases, hence native samples can incur Poisson ratio values higher than glutaraldehyde and in the range of chondroitinase-treated samples. It should be noted that this analysis is based on a single sample of each native, chondroitinase ABC-treated, and glutaraldehyde-treated pericardium. Three distinct behaviours are revealed by these samples which provide potentially promising and interesting results, though to instil higher levels of confidence in the results and make final conclusions, more repeats would be required to ensure reproducibility.

Examination of the 95% confidence intervals which represent the range in fibril diameters across the area of each sample also yields valuable information which supports the above theories. In the lower strain regions of the stress-strain curves there were significant variations in the fibril diameters over the sample area for all three treatment types due to the distribution of diameters across the sample (seen as large 95% confidence intervals in Figure 5.5). These regional variations substantially decreased with increasing strain for the glutaraldehyde-treated sample, suggesting that diameter decreased throughout the sample, though likely to only or mostly be the larger diameters; if all diameters large and small across the sample were to decrease, the result would still be a large range of fibril diameters. It could be that the fibril volumes are able to decrease to a certain extent before the glutaraldehyde cross links interfere and prevent further volume decreases, hence the diameters across the sample are of a similar magnitude at the higher strains which is reflected in the small range in Poisson ratio upper and lower limits for glutaraldehyde sample of 0.3.

At higher strains, the native sample still demonstrated large regional fibril diameter variations. This could be attributed to the range of fibril diameter magnitudes present decreasing with increasing strain as there is nothing to prevent this, whilst those fibrils experiencing sliding don’t decrease much at all, this is reflected in the largest difference in the Poisson ratio range

of the three samples (1.7). Like the native sample, chondroitinase ABC-treated pericardium also showed significant fibril diameter distributions across the sample area at higher strains, though less than that in the native sample. Again both the larger and smaller diameters may decrease with increasing strain, with more fibrils experiencing stress than those of the native sample, resulting in a Poisson ratio range in between that of native and glutaraldehyde-treated samples (1.4).

It is also worth noting that at any specific point on a sample, there was some distribution of fibril diameters (Figure 5.4a), though these distributions were not quantified here. It would seem that like OI and D-spacing, the fibril diameters begin to split into two more distinct bimodal distributions at higher strains, corresponding to recruited and non-recruited fibrils (Figure 5.4b). Therefore determination of recruited fibril and non-recruited fibril diameter may be distinguished and followed throughout the uniaxial stretching experiments. Further investigations exploring and quantifying the different distributions of fibril diameter from low to high strains, and comparing the shifts in diameter for recruited and non-recruited fibrils within a sample and between differently treated samples, could add further insight into the nanostructural response of fibrils to tension and build on the theories proposed in this work.

5.5 Conclusion

A study into the role of cross linking on the nanostructural response of pericardium collagen fibrils in terms of fibril diameter changes and Poisson ratios has revealed cross links may play an important role in how individual fibrils respond to uniaxial tension. The findings show collagen fibrils in general experience significant volume decreases under strain whilst evidence suggests the presence of glutaraldehyde cross links and the presence or lack of presence of GAGs lead to three distinct mechanisms of nanostructural response to strain; glutaraldehyde-treated tissue exhibited the lowest volume change, possibly attributed to the hindrance of overall fibril diameter decrease via tropocoallgen molecule volume decrease or restriction of water expulsion, by intra and intermolecular covalent glutaraldehyde cross links. Chondroitinase ABC exhibited the largest fibril volume decreases and a larger range in Poisson ratio, suggesting a lack of mechanical cross links and lubricating cross links confers freedom to more fibrils of different diameters to experience both longitudinal elongation and/or transverse contraction. Interestingly native pericardium was found to have a Poisson ratio range (from the 95% confidence intervals of D-spacing and fibril diameter across the sample) that extends into the range of both glutaraldehyde and chondroitinase ABC-treated pericardium. This may be due to a combination of both small changes in diameter for fibrils

undergoing sliding, and larger decreases for those fibrils partaking in stretching. Repeats of the experiments conducted are required to ensure reproducibility and enable definitive conclusions to be drawn. Further investigations including both experimental and modelling into possible mechanisms for fibril diameter decrease and quantifying and comparing single and bimodal fibril distributions with increasing strain would build on the theories established in this work and provide valuable insight into the overall behaviour of collagen fibrils to stress at the nanoscale.

Chapter 6

6. Age Differences with Glutaraldehyde Treatment in Collagen Fibril Orientation of Bovine Pericardium[3]

Abstract

Glutaraldehyde treatment of bovine pericardium produces a more isotropic structure with less oriented collagen fibrils. Skin from old animals has more natural cross linking than skin from young animals and structural differences exist between old and young tissue. However, it was not known whether structural changes resulting from glutaraldehyde treatment (considered to be cross linking) are affected by tissue age. Bovine neonatal and adult pericardia were treated with glutaraldehyde and the collagen fibril orientation measured for both using synchrotron based small angle X-ray scattering (SAXS). Neonatal pericardium is more oriented than adult with a higher orientation index (OI) of 0.40 compared to an OI of 0.19 for adult pericardium (with X-rays normal to the surface). With glutaraldehyde treatment the OI decreased for both tissue types by similar amounts to give an OI of 0.23 for neonatal and 0.12 for adult pericardium, so a 41% and 39% decrease for neonatal and adult pericardium respectively. While there are differences in structure of bovine pericardium with age, the age of the pericardium does not alter relative structural changes that take place on glutaraldehyde treatment. Therefore, the propensity to develop more isotropic structures by glutaraldehyde cross linking is similar for neonatal and adult tissue.

[3] Chapter 6 is based on the following published paper: Kayed, H.R., Sizeland, K.H., Wells, H.C., Kirby, N., Hawely, A., Mudie, S.T., Haverkamp, R.G. (2016). Age differences with glutaraldehyde treatment in collagen fibril orientation of bovine pericardium. *Journal of Biomaterials and Tissue Engineering, 6, 992-997*. This article can be found in section 8.1.3 of the Appendix.

6.1 Introduction

Bovine pericardium is a useful established material for heart valve leaflet replacement (Nwaejike and Ascione, 2011, Paez et al., 2006, Cribier et al., 2003). This material is normally used after treatment with glutaraldehyde and there are several devices in the market using this material. Although glutaraldehyde treatment is not commonly used for other types of tissue heterografts, in heart valve technology it is believed to stabilise and impart superior mechanical properties on the valve leaflets (Cheung and Nimni, 1982). Glutaraldehyde was previously in widespread use as a tanning agent although now this is restricted to only very demanding applications of leather such as car dashboards.

It has been shown that glutaraldehyde-treated bovine pericardium from neonatal animals has a higher strength than pericardium from adult animals and this has been ascribed to the greater degree of orientation of the collagen fibrils in the neonatal material (Sizeland et al., 2014). It has also been shown that glutaraldehyde treatment of pericardium causes a more networked structure to form, thereby reducing the degree of orientation of collagen fibrils (Kayed et al., 2015b). It has not been previously determined whether the young and old native bovine pericardia have the same relationship of more oriented collagen fibrils in the young material than the old as is seen in the glutaraldehyde-treated material.

It could be expected that the amount of cross linking that can occur between collagen in young and old pericardium tissue with glutaraldehyde treatment would be different. It has been observed that skin from old animals has more natural cross linking than skin from young animals (Bailey, 2001, Haus et al., 2007, Couppe et al., 2009). Ageing of collagen tissues with increased cross linking results in differences in physical properties. The differences in thermal stability of tendon collagen of steers aged 24-30 months and bulls aged 5 years old have been attributed to increased level of maturity and thermally stable cross links (Willett et al., 2010). Glycation of collagen increases with age and has been shown to increase stiffness in connective tissues (Bailey, 2001) and collagen gels (Francis-Sedlak et al., 2009), and increase brittleness in bones (Leeming et al., 2009). The cross links are in the form of histidino-hydroxlysinonorleucine or hexosyl-lysine links in young tissue but then with increasing glycation cross links as the tissue ages (Bailey, 2001). Glutaraldehyde forms linkages between collagen fibrils by a variety of routes beginning with the reaction of lysine or hydroxylysine amino acid residues of the polypeptide chains to form Schiff base intermediates (Olde Damink et al., 1995). Both natural and glutaraldehyde cross links target lysine or hydroxylysine residues. Therefore if neonatal or adult pericardia have a different propensity to form cross

linkages with glutaraldehyde, it might be expected that the amount of structural change in these two tissues upon treatment might be different. To reverse the perspective, a study of the differences in the structural changes in pericardium post glutaraldehyde treatment may be indicative of differences in the cross linking behaviour of pericardium.

Pericardium is a fibrous collagen extracellular matrix material with structural similarities to dermis. Small angle X-ray scattering can be applied to provide quantitative measures of collagen fibril orientation and fibril D-spacing (Liao et al., 2005, Purslow et al., 1998, Basil-Jones et al., 2010). There is a function-structure relationship between collagen alignment and mechanical strength (Fratzl and Weinkamer, 2007). The orientation of collagen measured edge-on (alignment in-plane) has been shown in skin across a range of mammal species to be correlated with strength (Sizeland et al., 2013, Basil-Jones et al., 2011, Basil-Jones et al., 2012).

The primary focus of the work presented here is to understand the differences in the effect on the collagen structural arrangement of young and old bovine pericardium tissues when treated with glutaraldehyde for medical applications of these materials. The secondary interest is to learn more about the ability of collagen in pericardium to cross link and the consequences of cross linking with age in general.

6.2 Materials and Methods

6.2.1 Native Pericardia Samples

Fresh adult and neonatal bovine pericardia were obtained from Southern Lights Biomaterials and stored in phosphate-buffered saline (PBS) solution, pH = 6.90 ± 0.1 (Lorne Laboratories Ltd). The pericardia were rinsed in PBS solution, and rectangular samples of approximate dimensions 45-50 x 15 mm were cut from regions containing both the right and left ventricle and atrium of the ventricular side of the pericardium with the long axis taken from the long axis of the heart (base to apex direction) as shown in Figure 6.1. The pericardia were then decellularised for 24 h at 4 °C in a 1% octylphenol ethylene oxide condensate (Triton X-100, Sigma), 0.02% EDTA solution made up in PBS. The samples were then rinsed in PBS buffer and stored in PBS. Samples in this state are referred to as “native”. All samples were taken from one pericardium (either the adult or neonatal) and randomly assigned to either native treatment or glutaraldehyde treatment with the exception of the adult edge-on samples, originating from a second adult pericardium. Section 3.2.1 of Chapter 3 can be referred to for more details regarding sampling rationale.

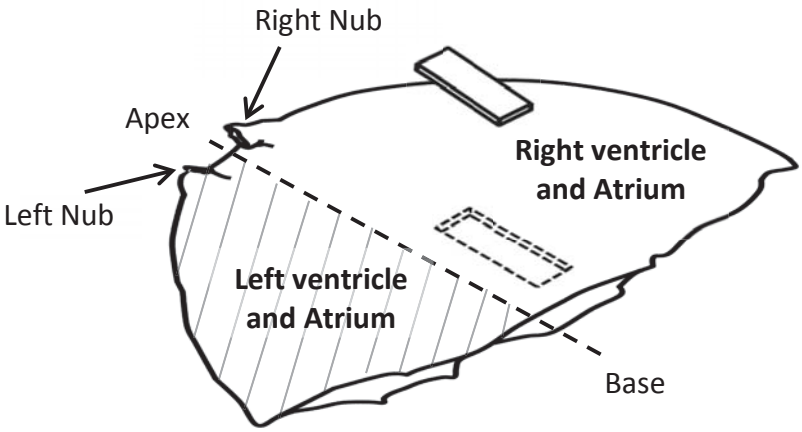

Figure 6.1. Ventricular side of pericardium showing sample selection area (Kayed et al., 2016).

6.2.2 Glutaraldehyde Treatment

The adult and neonatal native pericardia were incubated in a 0.6% glutaraldehyde solution made up in PBS buffer, at 4 °C for 24 h with constant agitation (Umashankar et al., 2011). They were then stored in a sealed container in a solution of the same composition for 12 days, before being rinsed and stored in PBS at 4°C until SAXS measurements were performed. The total time in storage was approximately 18 days.

6.2.3 SAXS Analysis

The native and glutaraldehyde adult and neonatal pericardia samples were removed from the PBS solutions, mounted on a metal plate (Figure 6.2a) and diffraction patterns recorded while the samples were wet. Care was taken to ensure the pericardium stayed wet (free water) throughout the diffraction pattern collection by sealing the samples with Kapton tape (Kapton tape doesn't interfere with the diffraction pattern). The samples were mounted either flat-on (Figure 6.2b), or edge-on (Figure 6.2c). Because the pericardium is thin (approximately 0.5 mm), the samples to be measured edge-on were mounted between two rigid polymer strips to ensure the X-ray beam penetrated edge on through the sample parallel to the pericardium surface.

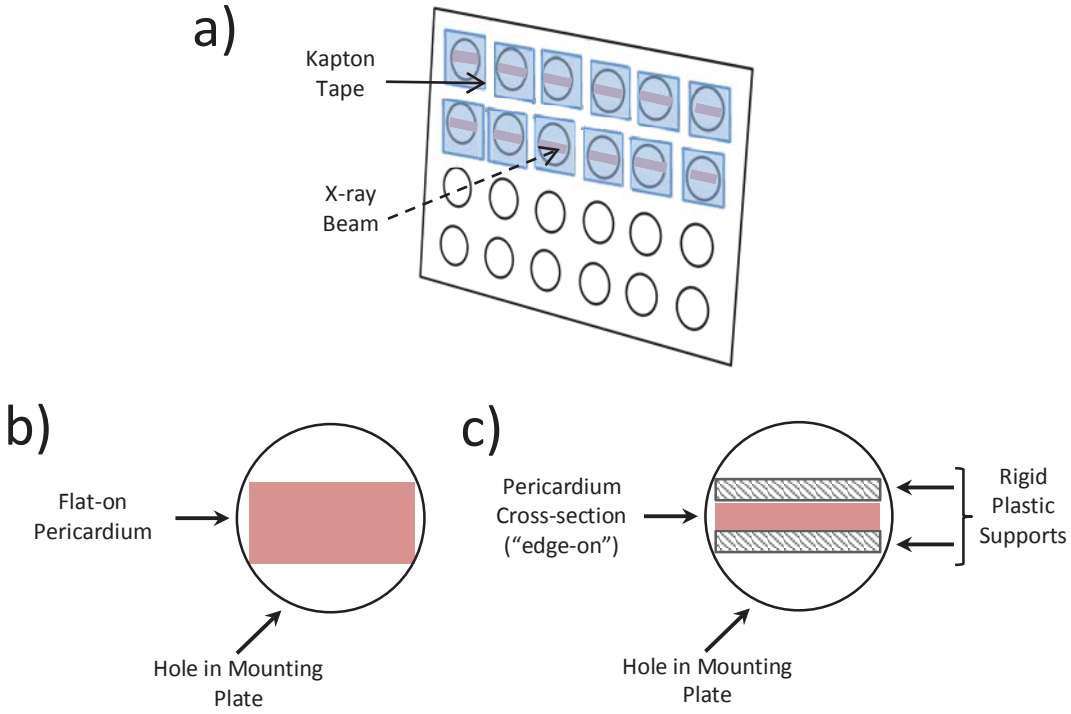

Figure 6.2. Mounting of the pericardium samples: a) metal mounting plate showing holes for the samples and direction of the X-ray beam relative to the mounting plate; b) mounting of flat-on pericardium samples; c) mounting of the edge-on pericardium samples between rigid plastic supports in the metal plate (Kayed et al., 2016).

The diffraction patterns were recorded on the Australian Synchrotron SAXS/WAXS beamline, utilizing a high-intensity undulator source. Energy resolution of 10^{-4} (i.e.. 1 x 10^{-4} Å for 1 Å radiation) was obtained from a cryo-cooled Si(111) double-crystal monochromator and the beam size (FWHM focused at the sample) was 250 x 130 µm, with a total photon flux of about 2 x 10^{12} ph/s. All diffraction patterns were recorded with an X-ray energy of 12 keV using a Pilatus 1M detector with an active area of 170 x 170 mm and a sample-to-detector distance of 3371 mm. Exposure times for diffraction patterns were around 1 s. Diffraction patterns were recorded with the X-rays two different directions relative to the sample – normal to the surface of the pericardium and edge-on to the surface (Figure 6.3). A grid of approximately nine points (nine scattering patterns) were collected for each of the flat-on samples, whilst three lines each consisting of approximately six points (six scattering patterns) were collected along the cross-section for each edge-on sample, so total sample exposure times did not exceed 9 s and 18 s for the flat and edge-on samples respectively. Mapping of the grids was made possible by the use of a camera setup in the control room, allowing accurate selection of

data points and maintenance of the beam on the sample, whilst ensuring regions of the pericardium were not re-exposed to the X-ray beams. No beam damage was detected at this exposure time (in separate repeated exposure tests).

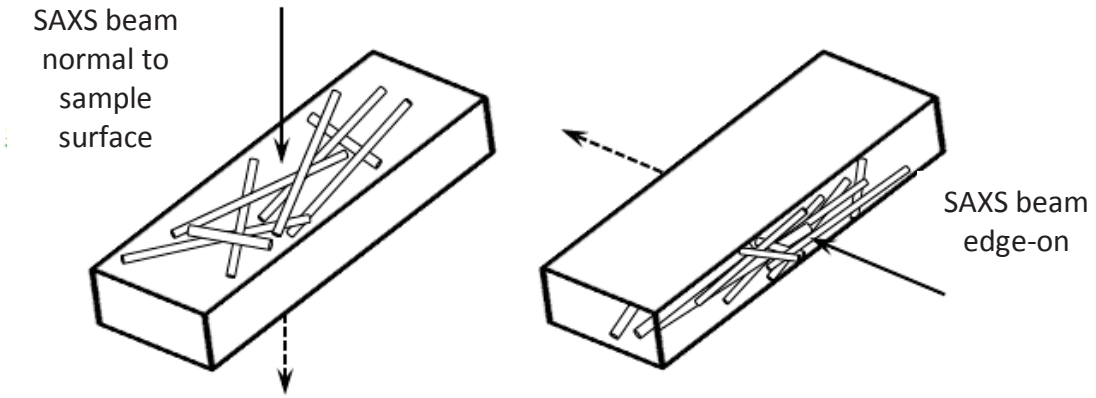

Figure 6.3. Experimental setup: a) measurement with X-rays normal to the surface which provides information on the collagen fibril orientation in the plane of the tissue; b) measurement with X-rays edge-on to the sample which provides information on the layering of collagen fibrils in the tissue (Kayed et al., 2016).

Data processing was carried out using the software scatterBrainAnalysis V2.71 (Cookson et al., 2006). The spread in collagen fibril orientation was quantified using an OI, where an OI of 1 indicates the fibrils are similarly oriented (parallel), and an OI of 0 indicates the fibrils are isotropically orientated. OI is defined as (90° – OA)/90°, where OA is the minimum azimuthal angle range that contains 50% of the fibrils, based on the method of Sacks for light scattering (Sacks et al., 1997) but converted to an index (Basil-Jones et al., 2011), using the spread in azimuthal angle of one or more D-spacing diffraction peaks. From each scattering pattern the OI was calculated from the azimuthal spread of the 5th order collagen diffraction peak at around 0.048 $Å^{-1}$. This provides an OI that represents the spread of collagen fibrils as viewed on a surface (normal X-ray measurement) and an OI that represents the extent to which the fibrils are stacked in layers (the edge-on measurement). Background subtraction for the peak used a logarithmic background over the small q range of the peak at each azimuthal angle. Details regarding OI calculation are provided in section 3.2.5 of Chapter 3.

Two native and two glutaraldehyde-treated neonatal samples, and four native and three glutaraldehyde-treated adult samples were analysed normal to the sample surface. For the edge-on OI measurements, one native neonatal and two of each native adult, glutaraldehyde-treated neonatal and glutaraldehyde-treated adult samples were analysed.

6.3 Results

The pericardium gave clear scattering patterns with well-defined diffraction peaks due to the collagen D-spacing (Figure 6.4a and b). From the variation of intensity with azimuthal angle (Figure 4d) the orientation index was calculated (Table 6.1).

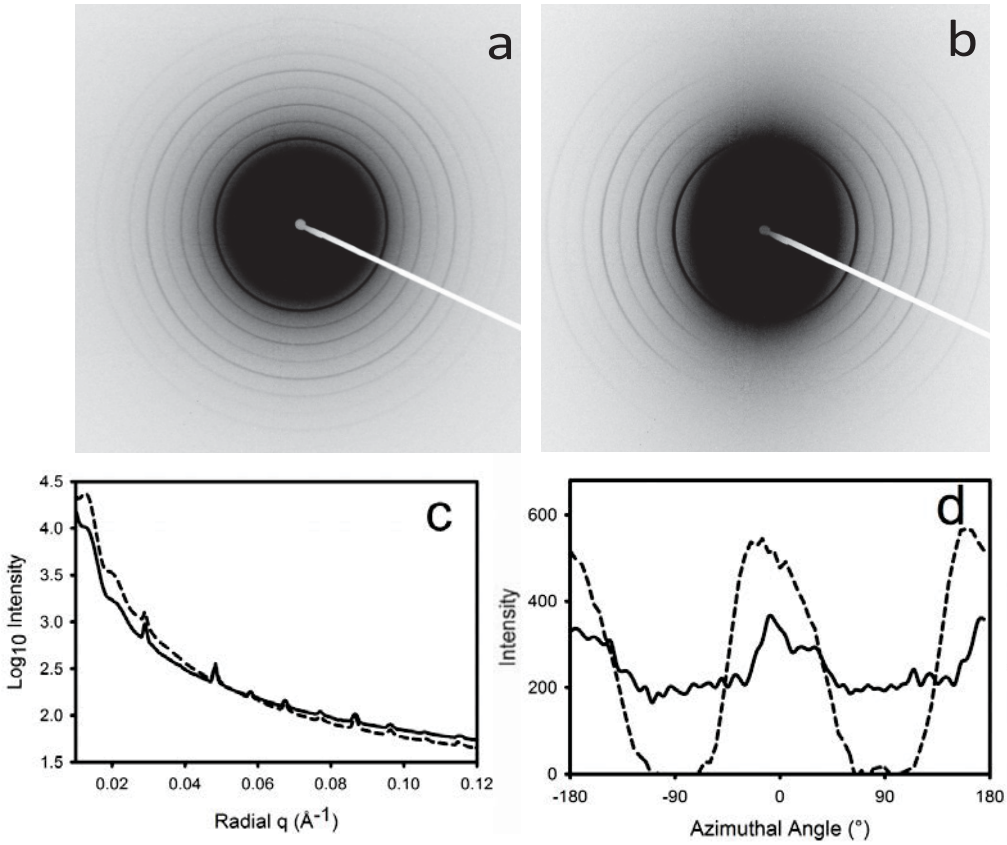

Figure 6.4. a) Representative normal to the sample surface scattering pattern of pericardium; b) representative edge-on scattering pattern of pericardium; c) integrated intensity of the scattering pattern: —, normal to the sample surface; - - - -, edge-on; d) scattering intensity with azimuthal angle for the 5th order collagen diffraction peak at 0.048 A^{-1}: —, normal to the sample surface; - - - -, edge-on (Kayed et al., 2016).

The adult pericardium in its native state has a lower OI than the neonatal pericardium for both normal to the surface and edge-on measurements, in line with previous studies (Kayed et al., 2015b) (Table 6.1). After glutaraldehyde treatment this relationship is maintained so that the adult pericardium has a lower OI than neonatal pericardium in the cross linked glutaraldehyde-treated material. These differences are statistically significant (Table 6.2). There is a change in OI for both adult and neonatal pericardium on glutaraldehyde treatment, with a more isotropic structure developing with treatment (with the exception of the neonatal edge on measurements where the difference is not statistically significant, possibly due to the small

sample size for this comparison). This change in OI is a decrease of 39 % for the adult pericardium and a decrease of 41 % for the neonatal pericardium (with X-rays normal to the surface) or 30% for adult pericardium with X-rays edge-on.

Table 6.1. Orientation indices for the native and glutaraldehyde-treated neonatal and adult pericardia samples measured with X-rays both normal to the pericardium face and edge-on.

SAXS Measurement type	Sample age and treatment type	Number of diffraction patterns analysed (N)	Mean OI	95% Confidence interval
Normal to Surface	Adult native	36	0.19	0.02
	Adult glutaraldehyde-treated	27	0.12	0.02
	Neonatal native	17	0.40	0.06
	Neonatal glutaraldehyde-treated	17	0.24	0.04
Edge-on	Adult native	10	0.47	0.04
	Adult glutaraldehyde-treated	13	0.33	0.03
	Neonatal native	7	0.61	0.07
	Neonatal glutaraldehyde-treated	4	0.56	0.04

Table 6.2. t-test with α=0.05 for differences in orientation indices between native and glutaraldehyde-treated samples for neonatal and adult tissues, and both normal to the pericardium face and edge-on.

SAXS Measurement type	Samples compared	Mean OI	t-value	Two tailed P-value	Different
Normal to Surface	Adult native vs. glutaraldehyde-treated	0.19;0.12	0.19	<0.001	Yes
	Neonatal native vs. glutaraldehyde-treated	0.40;0.24	5.07	<0.001	Yes
Edge-on	Adult native vs. glutaraldehyde-treated	0.47;0.33	5.31	<0.001	Yes
	Neonatal native vs. glutaraldehyde-treated	0.61;0.56	2.03	0.07	No
Normal to Surface	Neonatal native vs. adult native	0.40;0.19	8.84	<0.001	Yes
	Neonatal glutaraldehyde-treated vs. adult glutaraldehyde-treated	0.24;0.12	6.03	<0.001	Yes
Edge-on	Neonatal native vs. adult native	0.61;0.47	3.93	=0.001	Yes
	Neonatal glutaraldehyde-treated vs. adult glutaraldehyde-treated	0.56;0.33	10.44	<0.001	Yes

6.4 Discussion

It is apparent that the young pericardium has a more aligned structure than the older pericardium, as has been seen previously (Sizeland et al., 2014). These differences apply both with the edge-on X-ray measurements and with the measurements taken normal to the surface. The edge-on measurements represent the extent to which the fibrils are stacked in layers, with the neonatal pericardium having a more layered structure with less crossover between the layers. This has been shown to result in greater strength for pericardium (Sizeland et al., 2014) but also for a range of leathers made from dermal material (Sizeland et al., 2013) and acellular dermal materials for medical scaffolds made from a range of animals including human skin (Wells et al., 2015a). However, when this structure is too layered with insufficient connection between the layers, in leather this results in a defect known as looseness where failure occurs between the layers (Wells et al., 2015b). While such an effect has not been reported in other materials than leather, it is apparent that some connection is necessary between layers of any tissue in order to maintain structural integrity.

The effect of glutaraldehyde cross linking on the collagen structure in both neonatal and adult bovine pericardia is very similar. In both materials the collagen develops a more isotropic arrangement with glutaraldehyde treatment. It has previously been proposed that a decrease in OI from glutaraldehyde cross linking is the result of the formation of more of a networked structure where the formation of cross links via glutaraldehyde addition progressively constrains the fibrils into a random network (Kayed et al., 2015b). However now two further inferences can be drawn from the comparison of young and old pericardium, native and cross linked.

It can be inferred that a comparison of the relative OI values in glutaraldehyde-treated materials will reflect the relative OI values in the native materials. Previously, a relationship had been established between the OI measured edge-on and the strength of the material for glutaraldehyde-treated pericardium (Sizeland et al., 2014, Kayed et al., 2015a) and for tanned leather (Sizeland et al., 2013, Basil-Jones et al., 2011). However, it had not been determined whether this structure-strength relationship also applied to the untreated materials. However, here it has been shown that the relative degree of orientation is preserved after cross linking even while there is a significant change in structure. Therefore, it is likely that the relationships between orientation and strength applies to native materials or materials that have not been cross linked, such as many other heterograft materials (Wells et al., 2015a).

It may also be inferred that the capacity of pericardium to be cross linked by glutaraldehyde may be similar in both neonatal and adult pericardium. It can be speculated, based on the observation that the amount of structural change is similar, that the number of sites available for glutaraldehyde cross linking may be similar in neonatal and adult pericardium. This may also apply to other tissues. This is despite probable initial differences in the amount of natural cross links present. Although the actual amount of cross linking by glutaraldehyde has not been determined directly here, the consequences of the cross linking on the structure, making it more isotropic, has been determined. This is perhaps more important than a knowledge of the number of cross links as the structure is closely related to the mechanical properties of the materials (Wells et al., 2015a).

It should be noted that even though the change in OI of the collagen in the pericardium as a result of glutaraldehyde treatment is not dependent on the age of the animal from which the pericardium came, the structural arrangement of collagen fibrils in young and old pericardium is quite different. The young material has a higher OI. As described previously, this difference in the edge-on measured OI is responsible for the higher thickness normalised strength of the neonatal material (Kayed et al., 2015b , Sizeland et al., 2013).

The discovery that the relative structural differences between neonatal and adult pericardium are maintained after glutaraldehyde treatment means that it is possible to assess the differences in structure of native tissues and from these structures to predict the structures of the glutaraldehyde-treated processed materials for medical applications.

6.5 Conclusions

The structural arrangement of collagen in bovine pericardium from neonatal and adult animals was analysed by SAXS before and after treatment with glutaraldehyde. Neonatal pericardium had a more aligned structure than adult pericardium. This relationship was true for both untreated and glutaraldehyde-treated material. Glutaraldehyde treatment resulted in a change in the structure to a more isotropic arrangement of the collagen fibrils. The extent of this change is similar in both neonatal and adult pericardium. We speculate that the number of sites available for glutaraldehyde cross linking may be similar in both neonatal and adult pericardium and by implication in other tissues, despite probable initial differences in the amount of natural cross linking present. For the application of pericardium as a medical biomaterial we have shown that both young and old sourced pericardium undergo similar changes on glutaraldehyde treatment, maintaining relative differences between the starting materials.

Chapter 7

7. Concluding Remarks

7.1 Research Conclusions

This research endeavoured to investigate natural glycosaminoglycan (GAG) cross linking and synthetic glutaraldehyde cross linking effects on bovine pericardium collagen nanostructure and structure-function relationships between the links, the collagen fibril nanostructural organisation, and fibril behaviour under uniaxial tension. No consensus exists as to the role both cross links play in collagen type I structure and mechanics. Studies into the fine structures of collagen were made possible by the powerful technique of small angle X-ray scattering (SAXS).

The discovery that both GAGs and glutaraldehyde cross links influence the ways in which the pericardial collagen fibrils respond to strains and stress however by very different mechanisms is of the most significant in the work presented in this thesis.

It was shown that glutaraldehyde alone under no external forces substantially altered the orientation of collagen fibrils in the plane of the pericardium surface to result in more tangled isotropic fibril network structures, and decreased fibril D-spacing, perhaps due to slightly tightened crimp. The ability of glutaraldehyde to form covalent links with amino residues of collagen both inter and intramolecularly of different lengths and chemical compositions is likely to enable such changes in fibril conformations. Such a finding is of importance in the preparation of collagen materials for specific applications; it is important to understand and consider the nature of the cross links formed upon treatment with a fixing agent rather than focusing entirely on the quantity of links present. The type of cross links formed influences the structural modifications of the tissue and subsequently the final tissue properties.

This was indeed found to be the case, where pericardium treated with glutaraldehyde experienced higher strains than native tissue at failure as a bulk collagen material, whilst at a nano-level, a higher portion of fibrils (45%) were involved in direct stress uptake following fibril reorientation to the direction of applied strain, individually experiencing the highest stresses of up to 6.4%. This leads to the conclusion the cross links formed upon glutaraldehyde treatment

function as mechanical cross links, pulling fibrils into stretch and transferring applied stresses to these fibrils, more than would otherwise occur in the absence of such links.

Native pericardium rich in GAGs was compared with pericardium treated with chondroitinase ABC, which removes GAG cross links from the collagen network, so as to establish the role of GAG links. Unlike glutaraldehyde cross links, the GAG content does not correlate with fibril restructuring in the mature tissue; GAGs do not appear to be fibril constraining, hence their removal does not result in spontaneous fibril realignment to preferred orientation states of lower energy without external forces.

The importance of the nature of cross linking on tissue structural response to applied strains was again manifested in investigations comparing native and chondroitinase ABC-treated pericardium structure under tension. Unlike glutaraldehyde cross links, GAGs do not covalently link fibrils, they bridge fibrils orthogonally at the D-spacing sites through hydrophobic and hydrophilic interactions. Such associations were found to encourage more fibril sliding in native tissue than the other treated tissues, where only 12% of fibrils experience maximum strains of 4.1%. GAG links may therefore be lubricating, and their ability to dissociate and reform might enable relative fibril sliding in addition to the elongation of the recruited fibrils. In comparison, GAG depleted pericardium demonstrated fibril recruitment levels in between native and chondroitinase ABC (36%) with these fibrils experiencing strains up to 4.6%.

Fibril volume decreases were observed during uniaxial tensile stretching following fibril reorientation and simultaneous to fibril elongation (and/or fibril sliding) in all tissues despite the quantities and types of cross links present. The exact mechanism by which the diameter of a fibril decreases is unknown, however decreases due to changes in the bond lengths of the extensive hydrogen bonding network within and surrounding the tropocollagen molecules, and water expulsion are suggested as possible mechanisms.

Glutaraldehyde treatment was found to have the same effect on collagen fibril orientation in neonatal bovine pericardium tissue as adult tissue, that is, fibril orientation decreased significantly. The orientation index (OI) of both young and old tissue decreased similarly by approximately 40% in the pericardium plane, despite neonatal pericardium having higher OI values initially, and the higher levels of natural covalent cross linking present in adult collagen tissue; it would seem that a similar number of available cross linking sites exist for glutaraldehyde in both tissues even though glutaraldehyde reacts with the same groups as the natural cross links. This finding that cross linking effectiveness and relative structural

modification is maintained in nenonatal pericardium is of relevance in the medical field as neonatal pericardium has reported advantages due its thinness, higher ultimate tensile stress, and higher elastic modulus, therefore it could be considered as a substitute for adult pericardium in bioprosthetics.

This work has made significant advances in the building of a comprehensive picture relating cross linking nature to collagen structure and the roles of different cross links in the internal structural responses to strain at the nano-level.

7.2 Future Research Directions

Whilst the research conducted has met the overall aim, there are some aspects of the research which require further work or could be expanded upon to grow the founding ideas and theories established from the work presented.

The research question put forward regarding the determination of mechanical properties of collagen type I tissue in the native, glutaraldehyde-treated, and GAG-depleted states has yet to be fully realised. Although stress-strain data was generated during SAXS experiments, not enough repeats were measured to enable real comparisons, and there was much variability among results of the Instron tensile tests. Pericardium is a thin, stretchy material where small changes in set up during tensile tests (clamp pressure, angle loaded at, introduction of strains whilst loading), and variability within and between samples could affect the results. Therefore bigger sampling sets are required to get a better representation of the effect of cross links on the mechanical properties and to allow definitive conclusions to be drawn. This information would provide value to the theories established in this work as the tissue properties can be compared with the treatment type, and the observed structural changes under tension used to explain differences if any exist. This further aids in the understanding of the effects of different treatments on collagen which can be used for the preparation of these materials with specific properties for various applications.

The preliminary work on Poisson ratios for differently cross linked pericardium tissues in Chapter 5 yielded potentially interesting results; it appears larger fibril volume decreases occur in chondroitinase ABC-treated tissue, smaller fibril volume decreases are experienced in glutaraldehyde-treated tissue, whilst native tissue seems to have higher variability, where some fibrils experience higher volume decreases and others much lower. It was suggested this is due to the extent of fibril sliding and the presence or lack of stronger covalent cross links, where the cross links of glutaraldehyde may limit the extent of fibril diameter contraction by

physical constraints; they couple fibrils together and can be large and bulky. In the case of fibril sliding, more energy is dissipated through fibril sliding rather than decreasing the volume of the fibril. These results were based on a single sample of each treatment type, hence further repeats of this experiment would allow the ratios or range of ratios to be statistically compared for differences.

Branching from the work on Poisson ratios, experiments could be conducted, and/or computer and physical models generated to explore ways in which the fibril diameter could decrease, and as a consequence, the fibril volume. Infrared experiments could reveal if hydrogen bond lengths change and/or if water expulsion both within and around tropocollagen molecules are mechanisms by which such decreases occur. It is also worth investigating the distribution of diameters at a single point of SAXS measurement with strain, and any changes from single to bimodal diameter distributions in addition to relative shifts or changes in these distributions. This would show if fibril diameters behave similarly to OI and D-spacing where there are two distinctly different behaviours associated with recruited and non-recruited fibrils. Such knowledge would add to the overall understanding of nanostructural changes to strain at the nano-level and the roles cross links play in these changes.

Another potentially useful avenue that could be explored is the quantification and perhaps characterisation of glutaraldehyde cross links. This would confirm the existence of cross links formed whether they be more complex, larger glutaraldehyde cross links or otherwise, and determine the extent of cross linking achieved. Experiments could be performed to determine if lower concentrations of glutaraldehyde could be as effective as that used here (0.6%). Quantifying glutaraldehyde cross links could also substantiate the speculation that similar levels of glutaraldehyde cross linking occur in neonatal and adult pericardial tissues to result in similar decreases in OI.

Chapter 8

8. Appendices

Outputs based both entirely or partially on the work presented in this thesis including journal publications, poster presentations and conference presentations are provided in these Appendices.

8.1 Appendix A: Journal Publications

8.1.1 List of Journal Publications

1. **Kayed, H. R.,** Sizeland, K. H., Kirby, N., Hawley, A., Mudie, S. T., & Haverkamp, R. G. (2015). Collagen cross linking and fibril alignment in pericardium. *RSC Advances, 5*, 3611-3618.
2. **Kayed, H.R.**, Kirby, N., Hawely, A., Mudie, S.T., & Haverkamp, R.G. (2015). Collagen fibril strain, recruitment and orientation for pericardium under tension and the effect of cross links. *RSC Advances*, 5, 103703-103712
3. Wells, H. C., Sizeland, K. H., **Kayed, H. R.,** Kirby, N., Hawley, A., Mudie, S. T., & Haverkamp, R. G. (2015). Poisson's ratio of collagen fibrils measured by small angle X-ray scattering of strained bovine pericardium. *Journal of Applied Physics*, 117, 044701.
4. **Kayed, H.R.,** Sizeland, K.H., Wells, H.C., Kirby, N., Hawley, A., Mudie, S.T., & Haverkamp, R.G. (2016). Age differences with glutaraldehyde treatment in collagen fibril orientation of bovine pericardium. *Journal of Biomaterials and Tissue Engineering,* 6, 992-997.

8.1.2 Statements of Contributions to Publications

1. Collagen cross linking and fibril alignment in pericardium

DRC 16

MASSEY UNIVERSITY
GRADUATE RESEARCH SCHOOL

STATEMENT OF CONTRIBUTION
TO DOCTORAL THESIS CONTAINING PUBLICATIONS

(To appear at the end of each thesis chapter/section/appendix submitted as an article/paper or collected as an appendix at the end of the thesis)

We, the candidate and the candidate's Principal Supervisor, certify that all co-authors have consented to their work being included in the thesis and they have accepted the candidate's contribution as indicated below in the *Statement of Originality*.

Name of Candidate: Hanan Kayed

Name/Title of Principal Supervisor: Prof. Richard Haverkamp

Name of Published Research Output and full reference:

Kayed, H.R., Sizeland, K.H., Kirby, N., Hawley, A., Mudie, S., Haverkamp, R.G. (2015). Collagen cross linking and fibril alignment in pericardium. RSC Advances. 5, 3611-3618

In which Chapter is the Published Work:

Please indicate either:

- The percentage of the Published Work that was contributed by the candidate: 90%
  and / or
- Describe the contribution that the candidate has made to the Published Work:

Candidate's Signature — 28/04/2016 Date

Principal Supervisor's signature — 28/4/2016 Date

GRS Version 3– 16 September 2011

2. Collagen fibril strain, recruitment and orientation for pericardium under tension and the effect of cross links

DRC 16

MASSEY UNIVERSITY
GRADUATE RESEARCH SCHOOL

STATEMENT OF CONTRIBUTION
TO DOCTORAL THESIS CONTAINING PUBLICATIONS

(To appear at the end of each thesis chapter/section/appendix submitted as an article/paper or collected as an appendix at the end of the thesis)

We, the candidate and the candidate's Principal Supervisor, certify that all co-authors have consented to their work being included in the thesis and they have accepted the candidate's contribution as indicated below in the *Statement of Originality*.

Name of Candidate: Hanan Kayed

Name/Title of Principal Supervisor: Prof. Richard Haverkamp

Name of Published Research Output and full reference:

Kayed, H.R., Kirby, N., Hawley, A., Mudie, S.T., Haverkamp, R.G. (2015). Collagen fibril strain, recruitment and orientation for pericardium under tension and the effect of cross links. RSC Advances. 5, 103703-103712

In which Chapter is the Published Work:

Please indicate either:

- The percentage of the Published Work that was contributed by the candidate: 90%

  and / or
- Describe the contribution that the candidate has made to the Published Work:

Candidate's Signature — Date: 28/04/2016

Principal Supervisor's signature — Date: 28/4/2016

GRS Version 3– 16 September 2011

3. Poisson's ratio of collagen fibrils measured by small angle X-ray scattering of strained bovine pericardium

DRC 16

MASSEY UNIVERSITY
GRADUATE RESEARCH SCHOOL

STATEMENT OF CONTRIBUTION
TO DOCTORAL THESIS CONTAINING PUBLICATIONS

(To appear at the end of each thesis chapter/section/appendix submitted as an article/paper or collected as an appendix at the end of the thesis)

We, the candidate and the candidate's Principal Supervisor, certify that all co-authors have consented to their work being included in the thesis and they have accepted the candidate's contribution as indicated below in the *Statement of Originality*.

Name of Candidate: Hanan Kayed

Name/Title of Principal Supervisor: Prof. Richard Haverkamp

Name of Published Research Output and full reference:

Wells, H.C., Sizeland, K.H., Kayed, H.R., Kirby, N., Hawley, A., Mudie, S.T. & Haverkamp, R.G. (2015). Poisson's ratio of collagen fibrils measured by SAXS of strained bovine pericardium. Journal of Applied Physics, 117, 044701

In which Chapter is the Published Work:

Please indicate either:

- The percentage of the Published Work that was contributed by the candidate:

  and / or

- Describe the contribution that the candidate has made to the Published Work:
  Obtained & prepared/treated pericardium samples, collected SAXS data, did data processing (used for stats: CI & errors), took the electron microscopy images.

Candidate's Signature — 17/05/2016 Date

Principal Supervisor's signature — 18/5/2016 Date

GRS Version 3– 16 September 2011

4. Age Differences with glutaraldehyde treatment in collagen fibril orientation of bovine pericardium

DRC16

MASSEY UNIVERSITY
GRADUATE RESEARCH SCHOOL

STATEMENT OF CONTRIBUTION
TO DOCTORAL THESIS CONTAINING PUBLICATIONS

(To appear at the end of each thesis chapter/section/appendix submitted as an article/paper or collected as an appendix at the end of the thesis)

We, the candidate and the candidate's Principal Supervisor, certify that all co-authors have consented to their work being included in the thesis and they have accepted the candidate's contribution as indicated below in the *Statement of Originality*.

Name of Candidate: Hanan Kayed

Name/Title of Principal Supervisor: Prof. Richard Haverkamp

Name of Published Research Output and full reference:
Kayed, H.R., Sizeland, K.H., Wells, H.C., Kirby, N., Hawley, A., Mudie, S.T., Haverkamp, R.G. (2016). Age differences with glutaraldehyde treatment in collagen fibril orientation of bovine pericardium. Journal of Biomaterials and Tissue Engineering, 6, 992-997.

In which Chapter is the Published Work: 6

Please indicate either:

- The percentage of the Published Work that was contributed by the candidate: 90%.

  and / or
- Describe the contribution that the candidate has made to the Published Work:

Candidate's Signature — Date: 27/11/2016

Principal Supervisor's signature — Date: 2/12/2016

GRS Version 3– 16 September 2011

RSC Advances

PAPER

Cite this: *RSC Adv.*, 2015, **5**, 3611

Collagen cross linking and fibril alignment in pericardium

Hanan R. Kayed,[a] Katie H. Sizeland,[a] Nigel Kirby,[b] Adrian Hawley,[b] Stephen T. Mudie[b] and Richard G. Haverkamp*[a]

The influence of natural cross linking by glycosaminoglycan (GAG) on the structure of collagen in animal tissue is not well understood. Neither is the effect of synthetic cross linking on collagen structure well understood in glutaraldehyde treated collagenous tissue for medical implants and commercial leather. Bovine pericardium was treated with chondroitinase ABC to remove natural cross links or treated with glutaraldehyde to form synthetic cross links. The collagen fibril alignment was measured using synchrotron based small angle X-ray scattering (SAXS) and supported by atomic force microscopy (AFM) and histology. The alignment of the collagen fibrils is affected by the treatment. Untreated pericardium has an orientation index (OI) of 0.19 (0.06); the chondroitinase ABC treated material is similar with an OI of 0.21 (0.08); and the glutaraldehyde treated material is less aligned with an OI of 0.12 (0.05). This difference in alignment is also qualitatively observed in atomic force microscopy images. Crimp is not noticeably affected by treatment. It is proposed that glutaraldehyde cross linking functions to bind the collagen fibrils in a network of mixed orientation tending towards isotropic, whereas natural GAG cross links do not constrain the structure to quite such an extent.

Received 17th September 2014
Accepted 5th December 2014

DOI: 10.1039/c4ra10658j

www.rsc.org/advances

1. Introduction

The collagen I molecule is prevalent as the basis of many structural components in animals. It assembles with a complex hierarchical structure. This extracellular matrix forms resilient materials which are mechanically very tough.[1] This toughness is due in part to the highly fibrillar nature of collagen. Polypeptide molecules twist in left handed α-helical chains, and three of these in turn assemble with a right handed twist to form tropocollagens. Collagen fibrils are multiples of five tropocollagen strands thick and of extended length. The fibrils in turn may be assembled into larger fibres and a variety of structural motifs. There is great inherent strength and elasticity in each individual fibril. It is believed that the structure of materials composed of collagen I also require cross linking of the fibrils. This mechanically couples the fibrils restricting them from sliding past each other in order to achieve high strength.[2]

In nature, these cross links between collagen fibrils are provided by proteoglycan bridges, predominantly decoran, forming shape modules.[3,4] These proteoglycan bridges are elastic containing the glycosaminoglycan dermochondan sulfate.[5,6] The way in which these connections might transmit force between fibrils to resist sliding forces has been modelled.[7–11] The energy absorbed by enthalpic transformations in the dermochondan can be significant.[6,12]

It has been found that the tensile elastic modulus of mouse tendon was reduced over much of the stress–strain curve when the natural glycosaminoglycan (GAG) content was lowered by the application of chondroitinase ABC while the ultimate tensile force and ultimate stress were relatively unchanged.[13] However, this is not universally agreed as other work has found no altered mechanical properties in tendon from the removal of GAGs.[14,15]

The GAG cross links associate with the collagen fibril at several different sites but is believed to always be associated with the Gly-Asp-Arg amino acid sequence.[16]

Natural cross linking of collagen also increases with age due to glycation and has been shown to increase stiffness in connective tissues[17] and collagen gels[18] and increase brittleness in bones.[19]

Methods of cross linking other than that found in nature can be used to modify the properties of collagen materials. Cross linking of bovine pericardium with glutaraldehyde either under strain or with no tension has been reported to result in a less extensible and stiffer material which is stronger than the untreated material.[20,21]

However, there is still much to learn about cross linking of collagen and the contribution these cross links make to the structure and mechanical properties of collagen tissues.

The arrangement of collagen fibrils, particularly the extent of alignment or anisotropy, is an important contributor to the

[a]*School of Engineering and Advanced Technology, Massey University, Private Bag 11222, Palmerston North 4442, New Zealand. E-mail: r.haverkamp@massey.ac.nz*
[b]*Australian Synchrotron, 800 Blackburn Road, Melbourne, Australia*

strength of collagen materials. The structure–function relationship between collagen alignment and mechanical properties has been elucidated for a range of tissue types.[22–26] The orientation of collagen measured edge-on (alignment in-plane) has been shown in a range of mammal skins processed to leather to be correlated with strength.[27,28]

Small angle X-ray scattering (SAXS) is a powerful method for measuring the orientation of collagen fibrils in tissue.[26,29,30] Other methods may also be used such as small angle light scattering,[31] confocal laser scattering,[32] reflection anisotropy,[33] and atomic force microscopy.[34]

Bovine pericardium is a suitable material to use as a model in investigating the effect of cross linking, both natural and synthetic, on mechanical properties. Bovine pericardium has an established use for heart valve leaflet replacement.[35,36] The material requires high mechanical strength and a long performance life.[37] The orientation of collagen in pericardium heterograft materials for heart valve leaflets has been shown to affect the stiffness during flexing.[38]

We investigate here the hypothesis that cross links, both natural (GAGs) and synthetic (glutaraldehyde), may constrain the alignment of the collagen fibrils to result in different extents of orientation in collagen tissues which in turn may partially explain the different physical properties of the materials.

2. Methods

2.1 Fresh pericardium samples

Fresh bovine pericardium was obtained from John Shannon and from Southern Lights Biomaterials and stored in phosphate buffered saline (PBS) solution (Lorne Laboratories Ltd). The tissue was rinsed briefly in PBS solution. The tissue was then cut into rectangles of approximate dimensions 40–45 mm × 10 mm with the long axis taken from the long axis of the heart (as shown in Fig. 1). The method of decellularisation was based on Yang *et al.* (2009).[39] The pericardium was washed for 24 h in a 1% octylphenol ethylene oxide condensate (Triton X-100, Sigma), 0.02% EDTA solution made up in PBS. This washing step was conducted under constant agitation at 4 °C. The samples were then rinsed in PBS buffer and stored in PBS. These are what we refer to as "native". Subsequent processing of this material produced glutaraldehyde treated or chondroitinase ABC treated material. All samples were taken from one pericardium and randomly assigned to each treatment method.

2.2 Glutaraldehyde treatment

The Triton treated pericardium was incubated with a 0.6% glutaraldehyde solution made up in PBS buffer at 4 °C for 24 h with constant agitation.[40] It was then stored in a sealed container in the solution of the same composition until SAXS measurements were performed. The total time in storage was 3–5 days.

2.3 Chondroitinase ABC treatment

Removal of GAG cross links was based on the method described by Schmidt *et al.* (1990).[41] The Triton treated pericardium was incubated in 0.125 units of chondroitinase ABC per mL of buffer solution comprising of 0.05 M Tris–HCl, 0.06 M sodium acetate and EDTA-free protease inhibitors (complete, EDTA-free protease inhibitor tablets, Roche Diagnostics, Mannheim, Germany) at approximately 27 °C for 24 h before rinsing and storing in 0.05 M Tris–HCl and 0.06 M sodium acetate buffer in a sealed container at 4 °C.

Care was taken with all handling, cutting and treatment of the samples to not stretch the material as this might cause fibril alignment to change. The data presented here represents a duplication of this experiment with additional care taken in sample selection and handling in the second set of samples and SAXS analysis informed by the experience from the initial experiments.

2.4 GAG assay

An assay for sulfated GAGs was performed in triplicate for each of the sample treatments. GAGs were extracted with 1 mL extraction reagent consisting of a 0.2 M sodium phosphate buffer at pH 6.4, containing 8 mg mL^{-1} sodium acetate, 4 mg mL^{-1} EDTA, 0.8 mg mL^{-1} cysteine HCl and 0.1 mg mL^{-1} papain enzyme (*Carica papaya*, Sigma, Biochemika, enzyme no. 3.4.22.2). Each pericardium sample was incubated at 65 °C for 26 h. These samples were centrifuged and the supernatant containing the extracted GAGs collected. The concentration of GAGs in solution was determined with a Blyscan Sulfated Glycosaminoglycan Assay kit (Bicolor, Carrickfergus, UK). GAGs were precipitated with 1 mL of dye reagent to 20 or 40 μL of supernatant diluted to 100 μL, mechanically inverted for 30 minutes, and then centrifuged. The unbound dye was drained off and 1 mL of Blyscan dissociation reagent was added to the precipitate, left to dissolve for approximately 10 minutes,

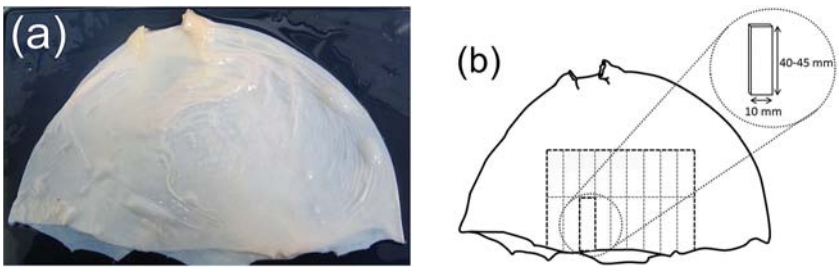

Fig. 1 Pericardium (a) ready to be cut for samples; (b) showing region used and sample size.

and centrifuged. Absorbance was measured at a wavelength of 656 nm and compared with a standard curve.

2.5 SAXS analysis

In preparation for SAXS analysis, the pericardium was removed from the glutaraldehyde and Tris–HCl, sodium acetate buffer solutions in which they had been stored. After soaking for at least 1 h in buffered saline solution (Lorne Laboratories Ltd), pericardium strips were mounted and diffraction patterns recorded while the pericardium was wet. All diffraction patterns were recorded at room temperature.

Diffraction patterns were recorded on the Australian Synchrotron SAXS/WAXS beamline, utilizing a high-intensity undulator source. Energy resolution of 10^{-4} (*e.g.* 1×10^{-4} Å for 1 Å radiation) was obtained from a cryo-cooled Si(111) double-crystal monochromator and the beam size (FWHM focused at the sample) was 250 × 80 μm, with a total photon flux of about 2×10^{12} ph s^{-1}. All diffraction patterns were recorded with an X-ray energy of 12 keV using a Pilatus 1M detector with an active area of 170 × 170 mm and a sample-to-detector distance of 3371 mm. Exposure time for diffraction patterns was 1 s and data processing was carried out using the software scatterBrainAnalysis V2.30.[42]

The orientation index (OI) is used to give a measure of the spread of fibril orientation (an OI of 1 indicates the fibrils are parallel to each other; an OI of 0 indicates the fibrils are randomly oriented). OI is defined as $(90° - OA)/90°$, where OA is the minimum azimuthal angle range that contains 50% of the fibrils, based on the method of Sacks for light scattering[43] but converted to an index,[27] using the spread in azimuthal angle of one or more *d*-spacing diffraction peaks. The peak area is measured, above a fitted baseline, at each azimuthal angle.

Four samples were prepared of native material, three with treatment by chondroitinase ABC for 24 h and three with treatment by glutaraldehyde. For each sample one diffraction pattern was recorded at each of nine positions.

From each pattern (an example is shown in Fig. 2) the OI was calculated from the azimuthal spread of the 5th collagen diffraction peak (as seen in Fig. 3 at around 0.05 $Å^{-1}$).

2.6 Atomic force microscopy

Small square sections were cut from the native, chondroitinase ABC and glutaraldehyde treated pericardium samples and mounted onto 12 mm diameter magnetic metal discs with double sided tape. The samples were left to air dry for a few h before being imaged. A Nanoscope E (Veeco) atomic force microscope with a JV scanner was used with *x*–*y* calibration to ±3% completed just prior to imaging. CSG01 cantilevers (NT-MDT, Russia) with a force constant of about 0.05 N m^{-1} were used for contact mode imaging.

2.7 Histology

Samples of pericardium were cut and frozen flat in a Leica CM1850 UV cryogenic microtome at −30 °C before being mounted on microtome disks using embedding medium for frozen tissue specimens. 10 μm thick cross-sections were cut and transferred to glass microscope slides. The mounted sections were stained as per the protocols of the Picrosirius Red Stain Kit (Polysciences, Inc.) before being placed in 70% ethanol for 45 s and left to air dry for several h. Optical images were recorded on a Nikon Eclipse TE2000-U microscope fitted with a Nikon Digital Sight DS-Fi2 camera and cross-polarising filters.

2.8 Tensile properties

Three rectangular sections of pericardium with the long axis of the sections equivalent to the long axis of the heart were cut from each of three pericardium sacs and treated with glutaraldehyde or chondroitinase ABC or left as native tissue. From these, samples were cut using a press knife and stress–strain curves were measured by uniaxial strain using an Instron 4467 with the sample mounted vertically at a rate of 100 mm min^{-1}

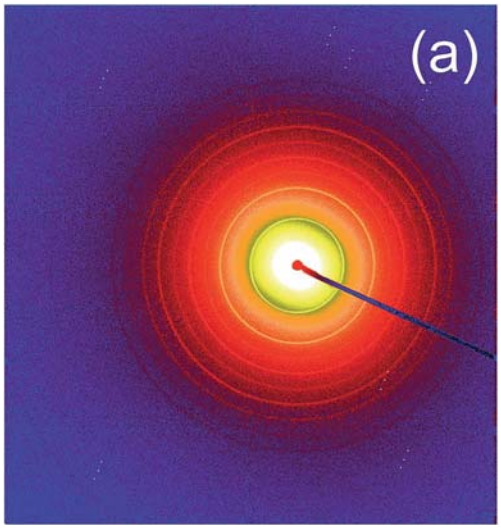

Fig. 2 Representative scattering pattern of pericardium.

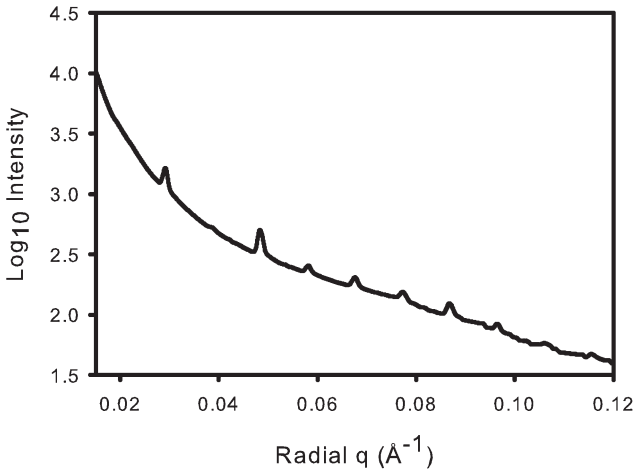

Fig. 3 Representative integrated scattering pattern of pericardium. The sharp peaks are due to diffraction for the *d*-spacing (at different orders).

according to standard ISO 3376:2011. Thickness was measured using method BS EN ISO 2589:2002 but with reduced pressure. Elastic modulus was determined for the linear region of the stress–strain curve.

2.9 Statistical analysis

Statistically significant differences between treatment mean OI values, GAG content and tensile properties were tested for using One Way ANOVA implemented in SigmaPlot 12.0 with a significance level, alpha, of 0.05. If statistical differences were found ($P = <0.001$), pairwise multiple comparisons were performed using the Holm–Sidak method in SigmaPlot 12.0 where the overall significance level used was 0.05. Pairwise comparisons with P-values less than 0.05 were considered to be significantly different.

3. Results

3.1 Chondroitinase ABC GAG removal

The GAG assay found that approximately 81% of GAGs were removed with chondroitinase ABC treatment (Fig. 4) which can be considered a success. As expected, glutaraldehyde treatment did not remove the GAGs, showing similar GAG content to the native material. Therefore the chondroitinase treated samples do represent pericardium with most of the GAGs removed.

3.2 Histology

The picrosirius red stained sections of each of the treated samples show a similar level of crimp in each sample type (Fig. 6). Crimp is the wavy structure of collagen fibrils which is typically seen in tendon and pericardium (with a period of 25–45 μm in pericaridum[23]) but not as prominently in skin. The chondroitinase ABC treated sample and native sample are the most similar. The glutaraldehyde treated pericardium has the appearance of a more open structure (which may be because it did not microtome as well) and it has some variation in colour.

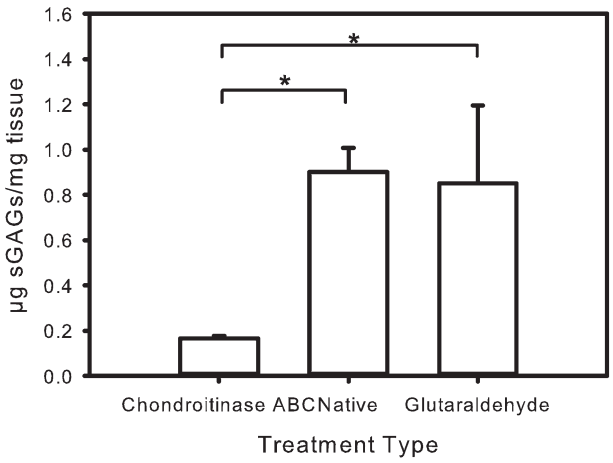

Fig. 4 GAG assay for pericardium for triplicate samples (error bars for 95% confidence intervals). Pairs that are significantly different ($P <$ 0.001 for $\alpha = 0.05$) are shown by a *.

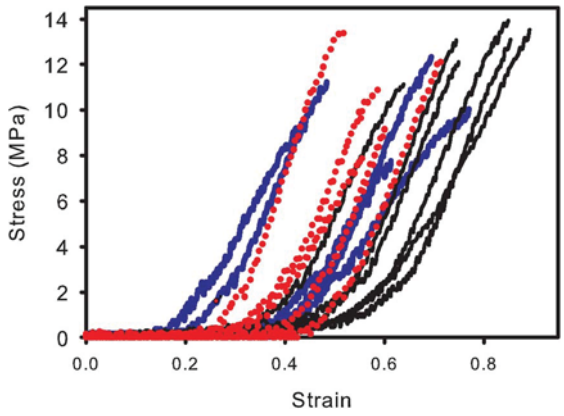

Fig. 5 Stress–strain curves for native pericardium (blue thick lines); chondroitinase ABC treated pericardium (red dotted lines); glutaraldehyde treated pericardium (black thin lines).

While picrosirius red is intended as a specific stain for collagen with type 1 collagen showing as red, other factors can affect birefringence and the resulting colour under cross-polarised filters, such as fibril thickness and the availability of free basic amino acid binding sites. The sulfonic acid groups of the picrosirius red dye molecule bind to the free amino acid residues on collagen, as do the aldehyde groups of glutaraldehyde; therefore binding of glutaraldehyde to these sites will inhibit dye binding and may result in decreased birefringence. The presence of colours other than red in the glutaraldehyde treated samples does not therefore indicate other types of collagen present, but rather, modification to the type I collagen.[44–46]

3.3 Tensile properties

The tensile properties of the pericardia samples had high variability (Fig. 5, Table 1). There is a foot region of variable length followed by an approximately linear region until the material reached its ultimate tensile stress and broke (the failure region is not shown). The chondroitinase treatment perhaps increases the elastic modulus, in agreement with other studies,[17] however with the small sample size this difference cannot be considered statistically significant ($P = 0.043$, $t = -1.9$, for $\alpha = 0.05$). The stress at failure may be higher for glutaraldehyde, also in keeping with other studies,[20,21] but this also cannot be considered statistically significant ($P = 0.012$, $t = -3.1$, for $\alpha = 0.05$). The only statistically significant difference between the mechanical properties of the treatment types is the strain at failure, which is higher for the glutaraldehyde treated material ($P = 0.026$, $t = -2.6$ for $\alpha = 0.05$).

3.4 SAXS

The pericardium gives good scattering patterns with clearly defined diffraction rings due to the d-spacing periodicity (Fig. 2). The integrated intensity plots show well defined peaks corresponding to the collagen D-period (Fig. 3). The odd numbered peaks have a much higher intensity than the even numbered peaks, a characteristic attributed to a fully hydrated sample.[47] This provides some reassurance that the samples are

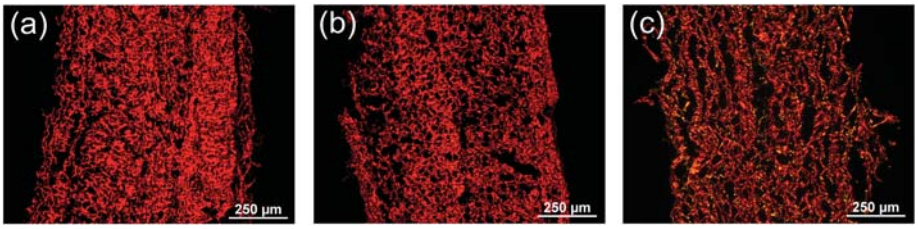

Fig. 6 Picrosirius stained sections of pericardium treated with (a) chondroitinase ABC; (b) native; (c) glutaraldehyde.

maintained in the hydrated state during collection of the diffraction patterns, as intended.

3.5 OI

The distribution of orientation of the fibrils can be seen with a plot of the intensity (we use the peak area) of any of the collagen diffraction peaks (Fig. 7). A narrow peak in this plot is indicative of more highly aligned collagen fibrils, as seen for the native and chondroitinase treated tissue, whereas broader peaks such as that for glutaraldehyde indicate a more isotropic arrangement. This can be quantified as an orientation index, OI. We calculate first an orientation angle (OA) which is defined as the minimum angle which contains 50% of the fibrils.[48] From this the OI is calculated as $(90^\circ - \mathrm{OA})/90^\circ$.

The OI calculated for the three treatments provide different average OI values (Table 2, Fig. 8). There is a statistically significant difference in the OI between the glutaraldehyde treated material and the other two materials but the difference in the OI between the native and chondroitinase treated pericardium does not pass the significance test. Previously we have compared chondroitinase ABC treatment for 48 h and 24 h with diffraction patterns recorded and analysed, however the OI obtained from the 48 h treated samples was not significantly different from that obtained after 24 h, probably indicating that most of the GAGs were removed already by 24 h of treatment (not shown here).

3.6 Atomic force microscopy

Atomic force microscopy provided clear images of collagen fibrils on the fibrous (outer) surface of the pericardium (Fig. 9). AFM provides small area images of a diverse surface so that unbiased selection of images can be difficult. We have selected one image of each material that is generally representative of that sample. The glutaraldehyde treated sample clearly had more of a collagen fibril network with fibrils not so often seen in parallel. In contrast the native material and the pericardium

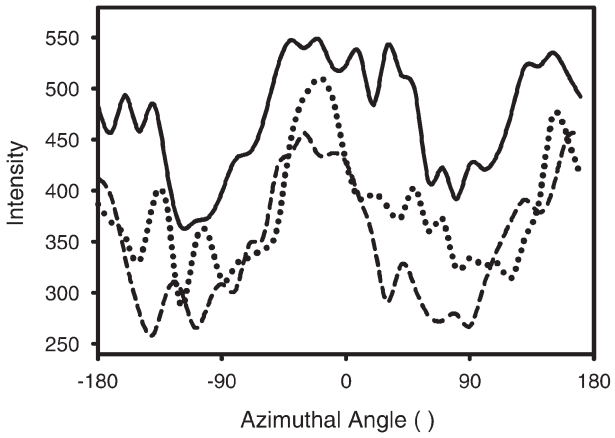

Fig. 7 Representative azimuthal intensity variation plots of the fifth collagen *D*-period diffraction peak for pericardium. The width of the central peak represents the spread in fibril orientation. Solid line, glutaraldehyde; dotted line, native; dashed line, chondroitinase ABC.

treated with chondroitinase ABC contained many aligned collagen fibrils.

4. Discussion

We have found an effect on collagen fibril alignment with cross linking. Native tissue containing GAG cross links has a moderate degree of fibril alignment. When these cross links are removed by treatment with the enzyme chondroitinase ABC the alignment of the fibrils does not show a significant change. When cross links are added, in the form of glutaraldehyde, the alignment of the fibrils decreases, becoming more isotropic with a network like structure forming. These changes do not appear to be associated with a change in crimp. Glutaraldehyde cross links therefore appear to have a direct effect on the arrangement of the collagen fibrils whereas native GAG cross

Table 1 Tensile properties of pericardium (with 95% confidence intervals)

Sample	Elastic modulus in linear region (MPa)	Stress at failure (MPa)	Strain at failure (%)
Native	40 ± 12	10.2 ± 2.2	60 ± 17
Chondroitinase ABC	52 ± 13	10.8 ± 2.7	60 ± 9
Glutaraldehyde	50 ± 6	12.8 ± 1.1	79 ± 10

Table 2 Orientation index obtained for pericardium samples

Sample	Number of diffraction peaks analysed (N)	Mean OI	95% confidence interval
Chondroitinase ABC	27	0.208	0.032
Native	36	0.192	0.021
Glutaraldehyde	27	0.117	0.021

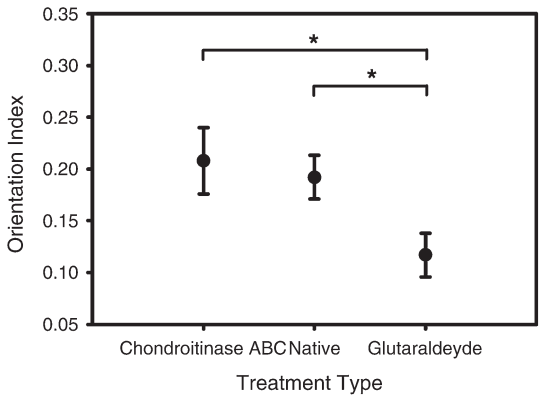

Fig. 8 Orientation index for each of the three levels of cross linking (error bars for 95% confidence intervals). Pairs that are significantly different ($P < 0.001$ for $\alpha = 0.05$) are shown by a *.

links do not have a statistically significant effect on alignment for tissue that is not under any mechanical load.

Glutaraldehyde has long been used as a cross linking agent for collagen, reacting primarily with ε-amino groups of lysine and hydroxylysine located on the outer surface of the triple helix region. Such links have been reported to occur both intramolecularly and intermolecularly depending on the treatment conditions and may involve some polymerisation of the glutaraldehyde to link greater distances.[49–51] Here we have shown that this network structure means not just a cross linked network of collagen but that the collagen fibrils also rearrange into a less aligned, more isotropic network structure under the action of glutaraldehyde cross linking without the application of external force. This chemically induced restructuring results in a decrease in the OI.

We have not specifically investigated the heterogeneity with depth, however the treatment time was ample to enable glutaraldehyde to penetrate the tissue fully.[50] In other work on glutaraldehyde treatment of pericardium, the variation of OI with depth through the glutaraldehyde treated pericardium tissue has been investigated and the OI did not vary greatly throughout the thickness, although a comparison was not been made with untreated pericardium.[52]

In contrast to glutaraldehyde cross links, proteoglycan (containing GAG) cross links are reported to occur solely on the outer surface of collagen fibrils, forming both axially and orthogonally with the majority located orthogonally between adjacent fibrils by the interaction of GAG side chains localised on the surface of collagen fibrils in mature tissues.[53,54] More specifically, it is believed proteoglycan cross links are associated with the gap region of the collagen *d*-spacing, binding to a single tropocollagen molecule.[53,54] We propose that these GAG bridges do not constrain the fibrils in a somewhat unaligned network structure in a higher energy state; these links appear only to form between adjacent fibrils at specific locations. Removal of these links therefore does not result in relaxation of some kind and fibrils do not spontaneously realign into a lower energy state and adopt some sort of preferred alignment. However, we suggest that the removal of the GAG links by chondroitinase ABC may give the potential for fibrils in the treated pericardium to become more easily aligned under tension.

This understanding of structural changes with treatment also has consequences for the preparation of materials for medical applications such as the treatment of bovine pericardium for heart valve repair, or ovine forestomach extracellular matrix material for surgical scaffolds.[55] The modifications imposed on the native tissue due to the processing of the material, sometimes including glutaraldehyde cross linking,

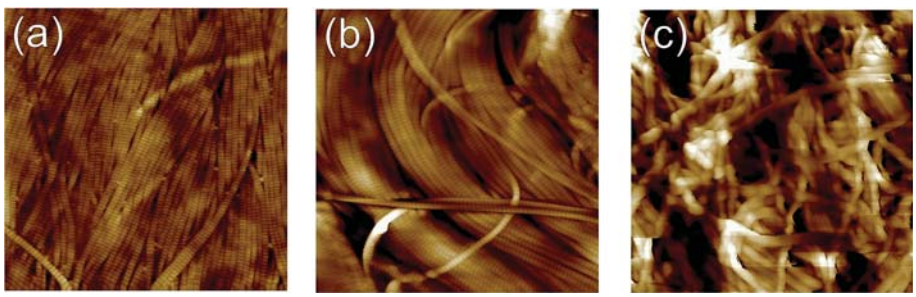

Fig. 9 Atomic force microscopy height images for (a) native bovine pericardium (b) chondroitinase ABC treated pericardium (c) glutaraldehyde treated pericardium. Images are 5 μm square.

may be better understood in terms of the structural changes that lead to altered physical properties. A careful balance of cross linking is then is required to achieve the properties required for in-service applications.

5. Conclusions

We have found that the extent and nature of cross linking present in pericardium has an impact on the collagen fibril orientation. When additional cross links with glutaraldehyde are added the fibrils form more of a network structure. We suggest that formation of cross links *via* glutaraldehyde addition progressively constrains the fibrils into a random network. The relationship between cross linking and fibril alignment provides a perspective on the importance of cross links in determining the structure of tissues. This could have relevance both in the preparation of new biomaterials and in the understanding and treatment of ageing and disorders in human tissues.

Acknowledgements

This research was undertaken on the SAXS/WAXS beamline at the Australian Synchrotron, Victoria, Australia. The NZ Synchrotron Group Ltd is acknowledged for travel funding. John Shannon and Southern Lights Biomaterials supplied the pericardium. Melissa Basil-Jones of Massey University assisted with data collection. Meekyung Ahn assisted with the microtoming and GAG assay, Richard Edmonds assisted with the mechanical tests.

Notes and references

1 D. R. Stamov and T. Pompe, *Soft Matter*, 2012, **8**, 10200–10212.
2 R. C. Picu, *Soft Matter*, 2011, **7**, 6768–6785.
3 J. E. Scott and R. A. Stockwell, *J. Physiol.*, 2006, **574**, 643–650.
4 A. M. Cribb and J. E. Scott, *J. Anat.*, 1995, **187**, 423–428.
5 J. E. Scott, *J. Physiol.*, 2003, **553**, 335–343.
6 R. G. Haverkamp, M. A. K. Williams and J. E. Scott, *Biomacromolecules*, 2005, **6**, 1816–1818.
7 Y. Chan, G. M. Cox, R. G. Haverkamp and J. M. Hill, *Eur. Biophys. J.*, 2009, **38**, 487–493.
8 R. Puxkandl, I. Zizak, O. Paris, J. Keckes, W. Tesch, S. Bernstorff, P. Purslow and P. Fratzl, *Philos. Trans. R. Soc. London*, 2002, **357**, 191–197.
9 S. W. Cranford and M. J. Buehler, *Soft Matter*, 2013, **9**, 1076–1090.
10 G. Fessel and J. G. Snedeker, *J. Theor. Biol.*, 2011, **268**, 77–83.
11 A. Redaelli, S. Vesentini, M. Soncini, P. Vena, S. Mantero and F. M. Montevecchi, *J. Biomech.*, 2003, **36**, 1555–1569.
12 R. G. Haverkamp, A. T. Marshall and M. A. K. Williams, *J. Phys. Chem. B*, 2007, **111**, 13653–13657.
13 S. Rigozzi, A. Stemmer, R. Muller and J. G. Snedeker, *J. Struct. Biol.*, 2011, **176**, 9–15.
14 G. Fessel and J. G. Snedeker, *Matrix Biol.*, 2009, **28**, 503–510.
15 R. B. Svensson, T. Hassenkam, P. Hansen, M. Kjaer and S. P. Magnusson, *Connect. Tissue Res.*, 2011, **52**, 415–421.
16 J. E. Scott, *J. Anat.*, 1995, **187**, 259–269.
17 A. J. Bailey, *Mech. Ageing Dev.*, 2001, **122**, 735–755.
18 M. E. Francis-Sedlak, S. Uriel, J. C. Larson, H. P. Greisler, D. C. Venerus and E. M. Brey, *Biomaterials*, 2009, **30**, 1851–1856.
19 D. J. Leeming, K. Henriksen, I. Byrjalsen, P. Qvist, S. H. Madsen, P. Garnero and M. A. Karsdal, *Osteoporosis Int.*, 2009, **20**, 1461–1470.
20 I. J. Reece, R. Vannoort, T. R. P. Martin and M. M. Black, *Ann. Thorac. Surg.*, 1982, **33**, 480–485.
21 S. E. Langdon, R. Chernecky, C. A. Pereira, D. Abdulla and J. M. Lee, *Biomaterials*, 1999, **20**, 137–153.
22 C. S. Kamma-Lorger, C. Boote, S. Hayes, J. Moger, M. Burghammer, C. Knupp, A. J. Quantock, T. Sorensen, E. Di Cola, N. White, R. D. Young and K. M. Meek, *J. Struct. Biol.*, 2010, **169**, 424–430.
23 T. L. Sellaro, D. Hildebrand, Q. J. Lu, N. Vyavahare, M. Scott and M. S. Sacks, *J. Biomed. Mater. Res., Part A*, 2007, **80A**, 194–205.
24 J. Liao, L. Yang, J. Grashow and M. S. Sacks, *J. Biomech. Eng.*, 2007, **129**, 78–87.
25 T. W. Gilbert, S. Wognum, E. M. Joyce, D. O. Freytes, M. S. Sacks and S. F. Badylak, *Biomaterials*, 2008, **29**, 4775–4782.
26 P. P. Purslow, T. J. Wess and D. W. L. Hukins, *J. Exp. Biol.*, 1998, **201**, 135–142.
27 M. M. Basil-Jones, R. L. Edmonds, S. M. Cooper and R. G. Haverkamp, *J. Agric. Food Chem.*, 2011, **59**, 9972–9979.
28 K. H. Sizeland, R. G. Haverkamp, M. M. Basil-Jones, R. L. Edmonds, S. M. Cooper, N. Kirby and A. Hawley, *J. Agric. Food Chem.*, 2013, **61**, 887–892.
29 M. M. Basil-Jones, R. L. Edmonds, G. E. Norris and R. G. Haverkamp, *J. Agric. Food Chem.*, 2012, **60**, 1201–1208.
30 J. Liao, L. Yang, J. Grashow and M. S. Sacks, *Acta Biomater.*, 2005, **1**, 45–54.
31 K. L. Billiar and M. S. Sacks, *J. Biomech.*, 1997, **30**, 753–756.
32 J. W. Y. Jor, P. M. F. Nielsen, M. P. Nash and P. J. Hunter, *Skin Res. Technol.*, 2011, **17**, 149–159.
33 A. L. Schofield, C. I. Smith, V. R. Kearns, D. S. Martin, T. Farrell, P. Weightman and R. L. Williams, *J. Phys. D: Appl. Phys.*, 2011, **44**, 335302.
34 J. Friedrichs, A. Taubenberger, C. M. Franz and D. J. Muller, *J. Mol. Biol.*, 2007, **372**, 594–607.
35 N. Nwaejike and R. Ascione, *J. Cardiac Surg.*, 2011, **26**, 31–33.
36 J. M. G. Paez, A. C. Sanmartin, E. J. Herrero, I. Millan, A. Cordon, A. Rocha, M. Maestro, R. Burgos, G. Tellez and J. L. Castillo-Olivares, *J. Biomed. Mater. Res., Part A*, 2006, **77**, 839–849.
37 A. Mirnajafi, B. Zubiate and M. S. Sacks, *J. Biomed. Mater. Res., Part A*, 2010, **94**, 205–213.
38 A. Mirnajafi, J. Raymer, M. J. Scott and M. S. Sacks, *Biomaterials*, 2005, **26**, 795–804.
39 M. Yang, C. Z. Chen, X. N. Wang, Y. B. Zhu and Y. J. Gu, *J. Biomed. Mater. Res., Part B*, 2009, **91**, 354–361.

40 P. R. Umashankar, T. Arun and T. V. Kumari, *J. Biomed. Mater. Res., Part A*, 2011, **97**, 311–320.
41 M. B. Schmidt, V. C. Mow, L. E. Chun and D. R. Eyre, *J. Orthop. Res.*, 1990, **8**, 353–363.
42 D. Cookson, N. Kirby, R. Knott, M. Lee and D. Schultz, *J. Synchrotron Radiat.*, 2006, **13**, 440–444.
43 M. S. Sacks, D. B. Smith and E. D. Hiester, *Ann. Biomed. Eng.*, 1997, **25**, 678–689.
44 L. F. Nielsen, D. Moe, S. Kirkeby and C. Garbarsch, *Biotech. Histochem.*, 1998, **73**, 71–77.
45 L. C. U. Junqueira, G. S. Montes and E. M. Sanchez, *Histochemistry*, 1982, **74**, 153–156.
46 D. Dayan, Y. Hiss, A. Hirshberg, J. J. Bubis and M. Wolman, *Histochemistry*, 1989, **93**, 27–29.
47 R. H. Stinson and P. R. Sweeny, *Biochim. Biophys. Acta*, 1980, **621**, 158–161.
48 M. M. Basil-Jones, R. L. Edmonds, T. F. Allsop, S. M. Cooper, G. Holmes, G. E. Norris, D. J. Cookson, N. Kirby and R. G. Haverkamp, *J. Agric. Food Chem.*, 2010, **58**, 5286–5291.
49 L. H. H. O. Damink, P. J. Dijkstra, M. J. A. Van Luyn, P. B. Van Wachem, P. Nieuwenhuis and J. Feijen, *J. Mater. Sci.: Mater. Med.*, 1995, **6**, 460–472.
50 D. T. Cheung, N. Perelman, E. C. Ko and M. E. Nimni, *Connect. Tissue Res.*, 1985, **13**, 109–115.
51 D. T. Cheung and M. E. Nimni, *Connect. Tissue Res.*, 1982, **10**, 201–216.
52 K. H. Sizeland, H. C. Wells, J. J. Higgins, C. M. Cunanan, N. Kirby, A. Hawley and R. G. Haverkamp, *BioMed Res. Int.*, 2014, **2014**, 189197.
53 J. E. Scott and C. R. Orford, *Biochem. J.*, 1981, **197**, 213–216.
54 J. E. Scott, *Biochem. J.*, 1980, **187**, 887–891.
55 E. W. Floden, S. Malak, M. M. Basil-Jones, L. Negron, J. N. Fisher, M. Byrne, S. Lun, S. G. Dempsey, R. G. Haverkamp, I. Anderson, B. R. Ward and B. C. H. May, *J. Biomed. Mater. Res., Part B*, 2010, **96**, 67–75.

RSC Advances

PAPER

Cite this: *RSC Adv.*, 2015, **5**, 103703

Collagen fibril strain, recruitment and orientation for pericardium under tension and the effect of cross links

Hanan R. Kayed,[a] Nigel Kirby,[b] Adrian Hawley,[b] Stephen T. Mudie[b] and Richard G. Haverkamp*[a]

The structural response of collagen fibrils in pericardium and other tissues when subjected to strain and the effect of cross linking on those structural changes are not well understood. Specifically, there is uncertainty about whether natural cross links of glycosaminoglycan (GAG) and synthetic cross links of glutaraldehyde have a mechanical function. Bovine pericardium was treated either with chondroitinase ABC to remove natural cross links or with glutaraldehyde to form synthetic cross links. The collagen fibril orientation index (OI) and *D*-spacing was measured on pericardium subjected to strain using synchrotron-based small angle X-ray scattering (SAXS). Under strain the collagen fibrils become much more oriented in the direction of the strain, with OI increasing from 0.25 to 0.89 in chondroitinase ABC-treated material, 0.22 to 0.93 in native material, and 0.22 to 0.77 in the glutaraldehyde-treated material. The proportion of fibrils that are recruited during stress varies from 36% in chondroitinase ABC-treated material, 12% in native material, to 45% in the glutaraldehyde-treated material. The increase in *D*-spacing shows the individual fibrils are strained in chondroitinase ABC-treated material by 2.4% on average or 4.6% for those in the direction of applied strain, in native material, 2.7% and 4.1%, respectively, and in the glutaraldehyde-treated material, 3.2% and 6.4%, respectively. Glutaraldehyde cross links are, therefore, shown to constrain the collagen fibrils and link them together mechanically. GAGs do not have such a marked mechanical effect; contrarily, the nature of internal structural responses to strain suggests that GAGs may have a lubricating rather than a binding effect.

Received 20th October 2015
Accepted 26th November 2015

DOI: 10.1039/c5ra21870e

www.rsc.org/advances

1. Introduction

The collagen I molecule assembles with a complex hierarchical structure and is a major extracellular matrix component in a multitude of animal structural tissues including pericardium, tendon, cornea, lung and skin. The responses to stresses imposed on collagen materials has been widely studied with the aim of understanding what and how components of collagen play a role in its mechanical properties, both at the macroscopic and microscopic levels.

Collagen materials can be stiff, flexible or extensible, depending on the required function in the body. For example, tendons and ligaments are crucial to joint movement, enabling force transmission and are therefore required to be flexible and have high tensile strength. The mechanical properties of collagen are due in part to its highly fibrillar nature[1,2] and its ability to respond to stresses.[3] However, it has also been suggested that the cross links between collagen fibrils contribute to the mechanical properties of collagen materials.

Proteoglycan bridges are considered to form shapemodules, and are found in the gap regions of collagen fibril *D*-spacing, linking fibrils together in natural tissue.[4–7] These proteoglycan bridges are elastic and predominantly of decoran, containing the glycosaminoglycan (GAG) dermochondan sulfate.[8,9]

The role of GAGs in the mechanical response of collagen tissues to stress is contested. Among those who consider the role of GAGs to be significant, there are divided opinions on how these cross links function under tension. Some believe GAGs act as force-sharing elements, transferring shear forces *via* their connections to the collagen fibrils, allowing fibril stretching and restricting sliding,[10] whilst others propose the hydrophilic nature of GAGs facilitates fibril sliding.[11] How GAGs might transmit forces between fibrils so that the fibrils resist the sliding forces has been modelled.[12–16] The energy absorbed by enthalpic transformations in specific GAGs such as dermochondan sulfate can be significant.[9,17]

Experimental studies of the changes in collagen's mechanical properties resulting from the depletion of the natural GAG content by the application of chondroitinase ABC have highlighted the differences in results and opinions. On one hand the tensile elastic modulus of mouse tendon was found to be reduced over much of the stress–strain curve when GAG content

[a]*School of Engineering and Advanced Technology, Massey University, Private Bag 11222, Palmerston North, New Zealand. E-mail: r.haverkamp@massey.ac.nz*
[b]*Australian Synchrotron, 800 Blackburn Road, Clayton, Melbourne, Australia*

was lowered, while the ultimate tensile force and ultimate stress for the tendon were relatively unchanged.[11,18] However, other work has found no altered mechanical properties in tendon resulting from the removal of GAGs.[15,19,20] Natural cross linking of collagen in connective tissues increases with age due to glycation and older tissues have been shown to have higher stiffness; therefore, a causal link has been proposed between cross links and stiffness.[21]

Synthetic cross links can also be introduced; glutaraldehyde is commonly used as a cross-linking agent, particularly in materials for biological heart valve replacements, forming both inter- and intra-molecular cross links between collagen fibrils.[22–24] As with GAG cross links, there is debate as to the resulting mechanical properties of collagen tissue treated with glutaraldehyde. Such treatment of bovine pericardium has been reported to result in a less extensible and stiffer material which is stronger than the untreated material.[25,26] Contrary to these findings, others have observed an increase in extensibility upon glutaraldehyde treatment,[22,27] reduced ultimate tensile strength,[27] no changes to ultimate tensile strength[22] and increases in elastic modulus.[25,28]

Cross linking of collagen may affect the arrangement of the collagen fibrils. Glutaraldehyde treatment has been shown to result in a less highly oriented material whereas the removal of GAGs does not have a significant modifying effect.[29] The arrangement of collagen fibrils, particularly the extent to which the fibrils are well oriented, is an important determinant of the strength of collagen materials. The structure–function relationship between collagen orientation and its mechanical properties has been determined for a range of tissue types.[30–32] The orientation of collagen measured in-plane has been shown in a range of mammal skins processed to leather to be correlated with strength.[33,34] A useful method of quantitatively measuring this structural arrangement of collagen fibrils is small angle X-ray scattering (SAXS).[30,31,35,36]

Here, we investigate the structural response of collagen cross linked by glutaraldehyde or GAGs to applied strain and stress to add to the understanding of the mechanical function, or lack of mechanical function, of these cross links. Bovine pericardium is used as a suitable model material for this study. Bovine pericardium has an established use for heart valve leaflet replacement[37] and the effect on the mechanical properties of this material by the removal of GAGs has been investigated.[29,38]

2. Methods

2.1 Fresh pericardium samples

Fresh bovine pericardium was obtained from Southern Lights Biomaterials and stored in phosphate-buffered saline (PBS) solution (Lorne Laboratories Ltd). The tissue was rinsed briefly in PBS solution, and then cut into rectangles approximately 45–50 × 15 mm, with the long axis taken from the long axis of the heart. The pericardium was washed for 24 h in a 1% octylphenol ethylene oxide condensate (Triton X-100, Sigma), 0.02% EDTA solution made up in PBS. This washing step was conducted under constant agitation at 4 °C. The samples were then rinsed in PBS buffer and stored in PBS. Samples in this state are referred to as "native". Subsequent processing of this material produced glutaraldehyde-treated or chondroitinase ABC-treated material. All samples were taken from one pericardium and randomly assigned to each treatment method.

2.2 Glutaraldehyde treatment

The native pericardium was incubated in a 0.6% glutaraldehyde solution made up in PBS buffer at 4 °C for 24 h with constant agitation.[39] It was then stored in a sealed container in a solution of the same composition for 12 days, before being rinsed and stored in PBS until SAXS measurements were performed. The total time in storage was approximately 18 days.

2.3 Chondroitinase ABC treatment

Removal of GAG cross links was based on the method described by Schmidt *et al.* (1990). The native pericardium was incubated in 0.125 units of chondroitinase ABC per ml of buffer solution comprising of 0.05 M tris–HCl, 0.06 M sodium acetate and EDTA-free protease inhibitors (complete, EDTA-free protease inhibitor tablets, Roche Diagnostics, Mannheim, Germany) at approximately 27 °C for 24 h before rinsing and storing in 0.05 M tris–HCl and 0.06 M sodium acetate buffer in a sealed container at 4 °C for 12 days. The samples were then rinsed and stored in PBS until SAXS measurements were performed. The total time in storage was approximately 18 days.

Care was taken with all handling, cutting and treatment of the samples not to stretch the material as this might cause fibril alignment to change.

The data here represents a duplication of this experiment (on a different pericardium) with additional care taken in sample selection and handling in the second set of samples and SAXS analysis informed by the experience from the initial experiments. However, one portion of the initial data, that for fibril recruitment, is included (in Section 3.5).

2.4 GAG assay

An assay for sulfated GAGs was performed in triplicate for each of the sample treatments. GAGs were extracted with 1 ml extraction reagent consisting of a 0.2 M sodium phosphate buffer at pH 6.4, containing 8 mg ml^{-1} sodium acetate, 4 mg ml^{-1} EDTA, 0.8 mg ml^{-1} cysteine HCl and 0.1 mg ml^{-1} papain enzyme (*Carica papaya*, Sigma, Biochemika, Enzyme no. 3.4.22.2). Each pericardium sample was incubated at 65 °C for 26 h. These samples were centrifuged and the supernatant containing the extracted GAGs collected. The concentration of GAGs in solution was determined with a Blyscan Sulfated Glycosaminoglycan Assay kit (Bicolor, Carrickfergus, UK). GAGs were precipitated with 1 ml of dye reagent to 20 or 40 μl of supernatant diluted to 100 μl, mechanically inverted for 30 minutes, and then centrifuged. The unbound dye was drained off and 1 ml of Blyscan dissociation reagent was added to the precipitate, left to dissolve for approximately 10 minutes, and centrifuged. Absorbance was measured at a wavelength of 656 nm and compared with a standard curve of chondroitin 4-sulfate GAG reference standard (Biocolor, UK).

2.5 SAXS analysis

The rectangles of pericardium were removed from the PBS solutions in which they were stored, mounted and their diffraction patterns recorded while the pericardium was wet. All diffraction patterns were recorded at room temperature.

Diffraction patterns were recorded on the Australian Synchrotron SAXS/WAXS beamline, utilizing a high-intensity undulator source. Energy resolution of 10^{-4} (*e.g.* 1×10^{-4} Å for 1 Å radiation) was obtained from a cryo-cooled Si(111) double-crystal monochromator and the beam size (FWHM focused at the sample) was 250 × 80 μm, with a total photon flux of about 2×10^{12} ph s^{-1}. All diffraction patterns were recorded with an X-ray energy of 12 keV using a Pilatus 1M detector with an active area of 170 × 170 mm and a sample-to-detector distance of 3371 mm. Exposure time for diffraction patterns was 1 s and data processing was carried out using the software scatterBrainAnalysis V2.71.[40]

Orientation index (OI) is used to give a measure of the uniformity of fibril orientation (an OI of 1 indicates the fibrils are parallel to each other; an OI of 0 indicates the fibrils are randomly oriented). OI is defined as (90° − OA)/90°, where OA is the minimum azimuthal angle range that contains 50% of the fibrils, based on the method of Sacks for light scattering[41] but converted to an index,[33] using the spread in azimuthal angle of one or more *D*-spacing diffraction peaks. The peak area is measured, above a fitted baseline, at each azimuthal angle.

One chondroitinase ABC-treated sample and two of each native and glutaraldehyde-treated samples were tested. Six diffraction patterns were recorded at different positions across the samples following every stretch. From each scattering pattern the OI and *D*-spacing were calculated from the azimuthal spread of the 5th and 9th order collagen diffraction peaks (at around 0.05 $Å^{-1}$ and 0.09 $Å^{-1}$, respectively) and averaged where there were single diffraction peaks. For those diffraction patterns displaying peak splitting and/or double peaks, the 9th order diffraction peak was used to calculate OI and *D*-spacing. For some of the glutaraldehyde-treated samples, the 9th order peak became very complex at higher strains and background intensity could not be identified and subtracted; in such cases, the 5th order diffraction peak was used to determine OI and *D*-spacing. The portion of fibrils experiencing higher stresses (larger *D*-spacing) was determined using the intensities of these split/double diffraction peaks as intensity is proportional to the quantity of collagen fibrils involved in diffraction.

3. Results

3.1 GAG removal by chondroitinase ABC treatment

Chondroitinase ABC treatment removed 81% of GAGs initially present in native pericardium (from 0.90 μg GAGs per mg tissue to 0.17 μg mg^{-1}). Pericardium treated with glutaraldehyde had a similar GAG content to the native material (0.85 μg mg^{-1}). The GAG content of the chondroitinase ABC treated material was statistically significantly lower than the other two materials (Fig. 1).

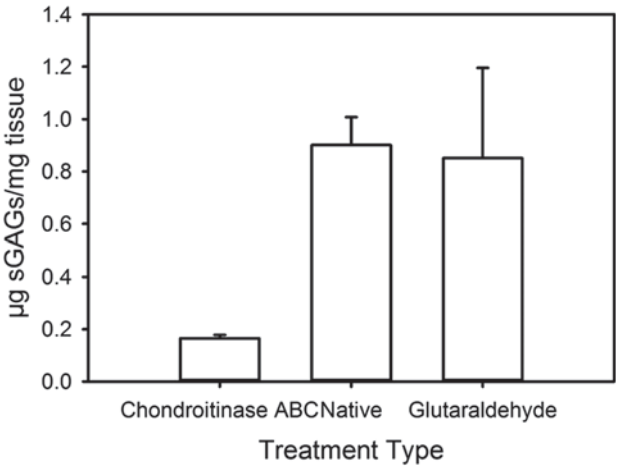

Fig. 1 Assay results for the GAG content of the three materials studied here.

3.2 Tensile properties

Stress–strain curves were recorded on the samples being progressively strained during the SAXS measurements (Fig. 2). The stress–strain curves obtained are typical for collagen, showing a foot region and linear region.[25] While the stress–strain curves are on small samples, and may therefore not give a representative measure of the mechanical properties to be expected of bulk samples of these materials, these curves are important in the context of the structural analysis during strain of these tissues presented in the body of this work. However, in a previous report we found the ultimate tensile stress was highest for glutaraldehyde-treated pericardium.[29] Other studies of glutaraldehyde treatment of bovine pericardium have reported that this material is stronger than the untreated material[25,26] although

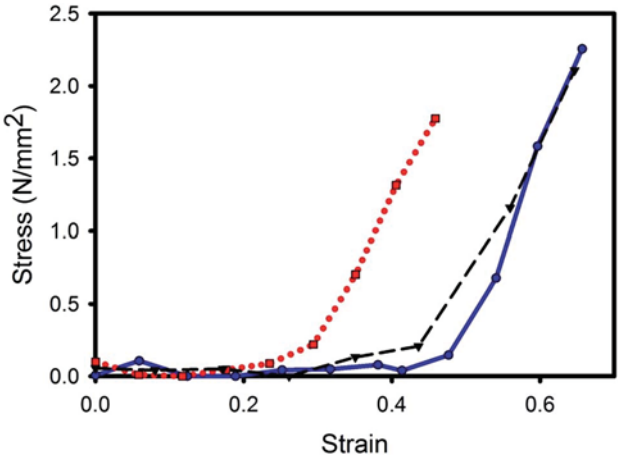

Fig. 2 Stress–strain curves for the pericardium after three different treatments, while under increasing tension during the SAXS measurements: (●, ——, blue) chondroitinase ABC treated; (▼, – – –, black) native; (■, ·····, red) glutaraldehyde treated.

there is a wide variety of opinions regarding changes to other mechanical properties with glutaraldehyde treatment.[22,27,28]

3.3 SAXS

The pericardium scattering patterns had clearly defined diffraction rings due to the *D*-spacing periodicity (Fig. 3). When the tissue was not under strain, these rings were of almost uniform intensity around the circle (Fig. 3a), but as the samples were subjected to more strain, the rings subtended a smaller azimuthal angle (Fig. 3b and c). This was a result of the fibrils aligning in the direction of strain. Also, the central region of the pattern elongated at 90° to the direction of the diffraction rings. (This central region is the low *q* part of the pattern and represents scattering from the collagen fibril diameter, which is at right angles to the *D*-spacing.) Another feature of the scattering patterns of pericardium under strain was the shifting of the *D*-spacing scattering angle, particularly of those fibrils aligned in the direction of the strain. This shift is seen as a protuberance on the inside of the diffraction ring but is more readily seen on the integrated intensity plots (Fig. 4). In these, the splitting of the *D*-spacing into multiple peaks or a broad peak is more apparent at higher diffraction orders. The odd-numbered peaks have a much higher intensity than the even-numbered peaks, a characteristic attributed to a fully hydrated sample.[42]

3.4 OI

The distribution of fibril orientation is measured from a plot of the intensity (we use the peak area) of any of the collagen diffraction peaks (Fig. 5). A narrow peak in this plot is indicative of more highly aligned collagen fibrils whereas a broader peak indicates a more isotropic arrangement. This can be quantified as the orientation index, OI.

Both the OI and the *D*-spacing can be visualized in a three-dimensional plot (Fig. 6), where the *D*-spacing of fibrils in a given direction can be seen more clearly.

3.5 Changes to structure during strain

Initially, the pericardium exhibited little physical resistance to the strain (the stress was low), and there was little change in the

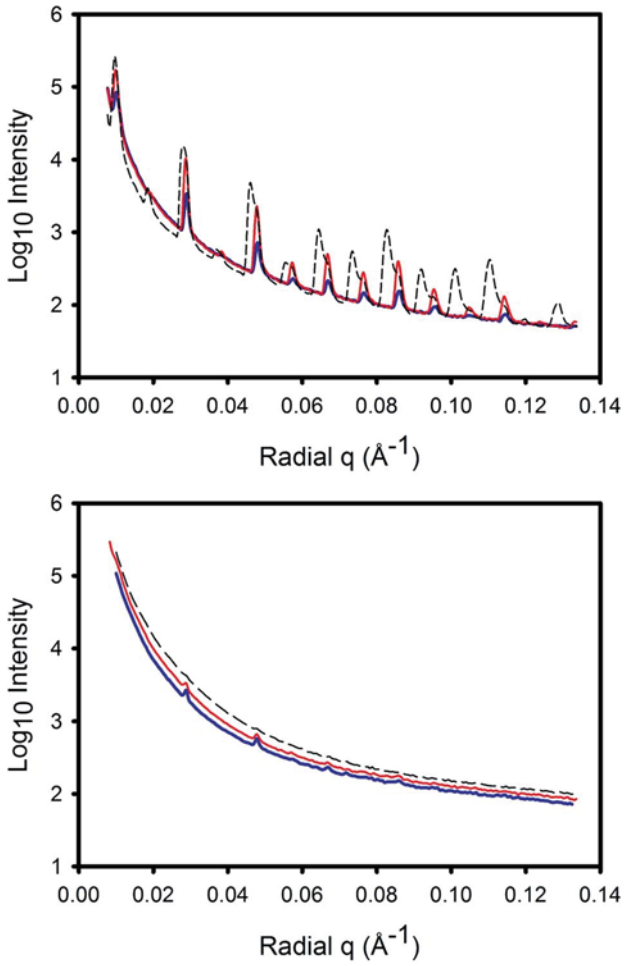

Fig. 4 Representative integrated scattering patterns of pericardium subjected to varying levels of strain: no strain (——, blue); 18% strain (——, red); 45% strain (-----, black). The sharp peaks are due to diffraction of the *D*-spacing (at different orders) and the peaks split at higher strain. The top image is for a 5° azimuthal angle segment in the direction of strain, the bottom image is for a 5° azimuthal angle segment normal to the direction of strain.

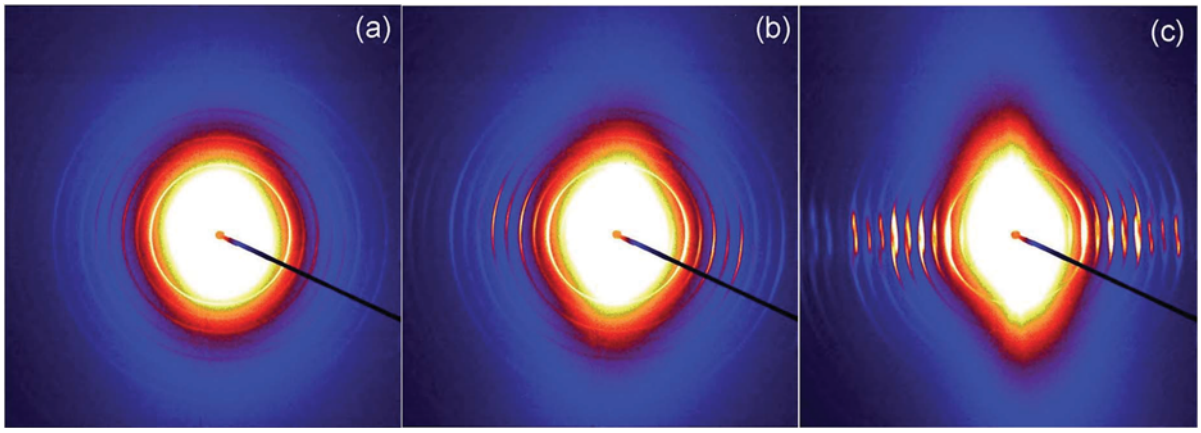

Fig. 3 A series of typical scattering patterns of native pericardium subjected to (a) no strain; (b) strain of 0.18; (c) strain of 0.45.

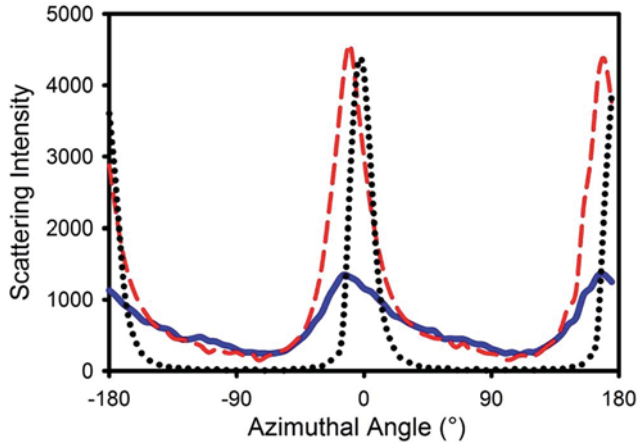

Fig. 5 Representative integrated scattering intensity at the 5th order *D*-spacing diffraction peak verses azimuthal angle for pericardium subjected to: no strain(——, blue); 18% strain (– – –, red); 45% strain (·····, black).

D-spacing (Fig. 7). During this period, however, there was a large change in the OI. The change in OI at this stage of the tensile testing can be attributed to a combination of crimp straightening and re-orientation of the collagen fibrils towards the direction of strain. The *D*-spacing increase represents the stress on individual fibrils and this increased in tandem with the increasing stress on the whole tissue. (Note that the increase in *D*-spacing can arise either from the direct stretching of the collagen molecules in a fibril, so that the relative lengths of the overlap and gap regions remain constant, or from the sliding of the collagen molecules past one another, so that the relative length of the gap and overlap regions change. Or the increase can arise from a combination of the two. The mechanism of *D*-spacing change was not measured here, so *D*-spacing in this work includes the possibilities of both mechanisms.) Not all fibrils experienced the same stress: the fibrils in line with the direction of applied strain experienced greater stress and underwent a greater change in *D*-spacing until there were two distinct diffraction peaks for *D*-spacing at different angles. At the point when these two distinct *D*-spacings could be identified, the split diffraction peaks were fitted individually to obtain both OI and *D*-spacing, and were plotted in Fig. 7 in the high-strain portion of the plot.

While the behaviour for all three samples types was broadly similar there were some differences. All three materials have a portion of fibrils that are highly strained and highly oriented. In the glutaraldehyde-treated material, this portion (which can be called "recruited fibrils", *i.e.* fibrils that participate in absorbing the stresses) was higher (Table 1) and the stress experienced by these fibrils was greater (evidenced in the *D*-spacing in Fig. 7), followed by chondroitinase ABC-treated material and finally native material.

3.6 Comparison of OI between treatments with increasing strain

As the pericardium was strained, the fibrils reoriented to line up in the direction of strain, as reflected in the lowering of the OI.

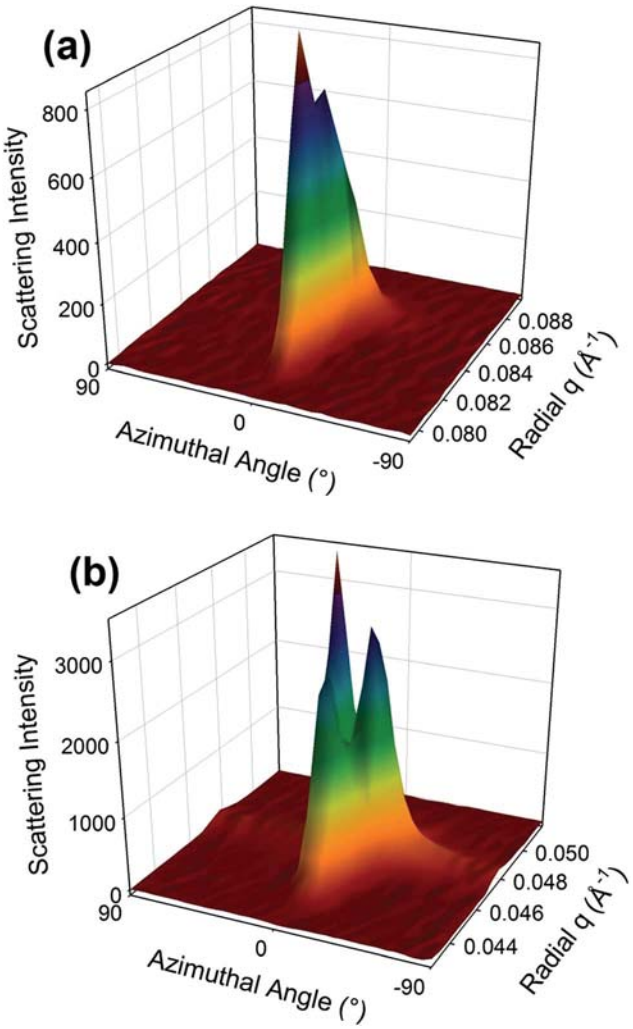

Fig. 6 Three-dimensional representation of an example scattering pattern of (a) native pericardium at a strain of 0.45; (b) chondroitinase ABC-treated pericardium at a strain of 0.69, where both the fibril orientation (from the azimuthal angle axis) and the *D*-spacing shift (from the radial *q* axis) can be visualized. Only the azimuthal range −90° to 90° is represented as the remaining range is a duplication of this information and only a small portion of the radial angle is displayed representing one *D*-spacing diffraction peak.

However, changes in sample OI varied among the treatments (Fig. 8), with the maximum OI achieved being highest for native pericardium, slightly less for the GAG-depleted pericardium and lowest for the glutaraldehyde-cross linked pericardium. The recruited fibrils were all highly oriented as expected[3] whilst the remaining non-recruited fibrils in the collagen matrix were less aligned in the glutaraldehyde-treated pericardium than in the native or chondroitinase ABC-treated tissue (Fig. 8b and c, respectively).

3.7 Comparison of fibril strain with stress

As stress is applied to pericardium, this stress is transmitted to the individual collagen fibrils. This results in an extension of length of the fibrils which can be directly measured by the

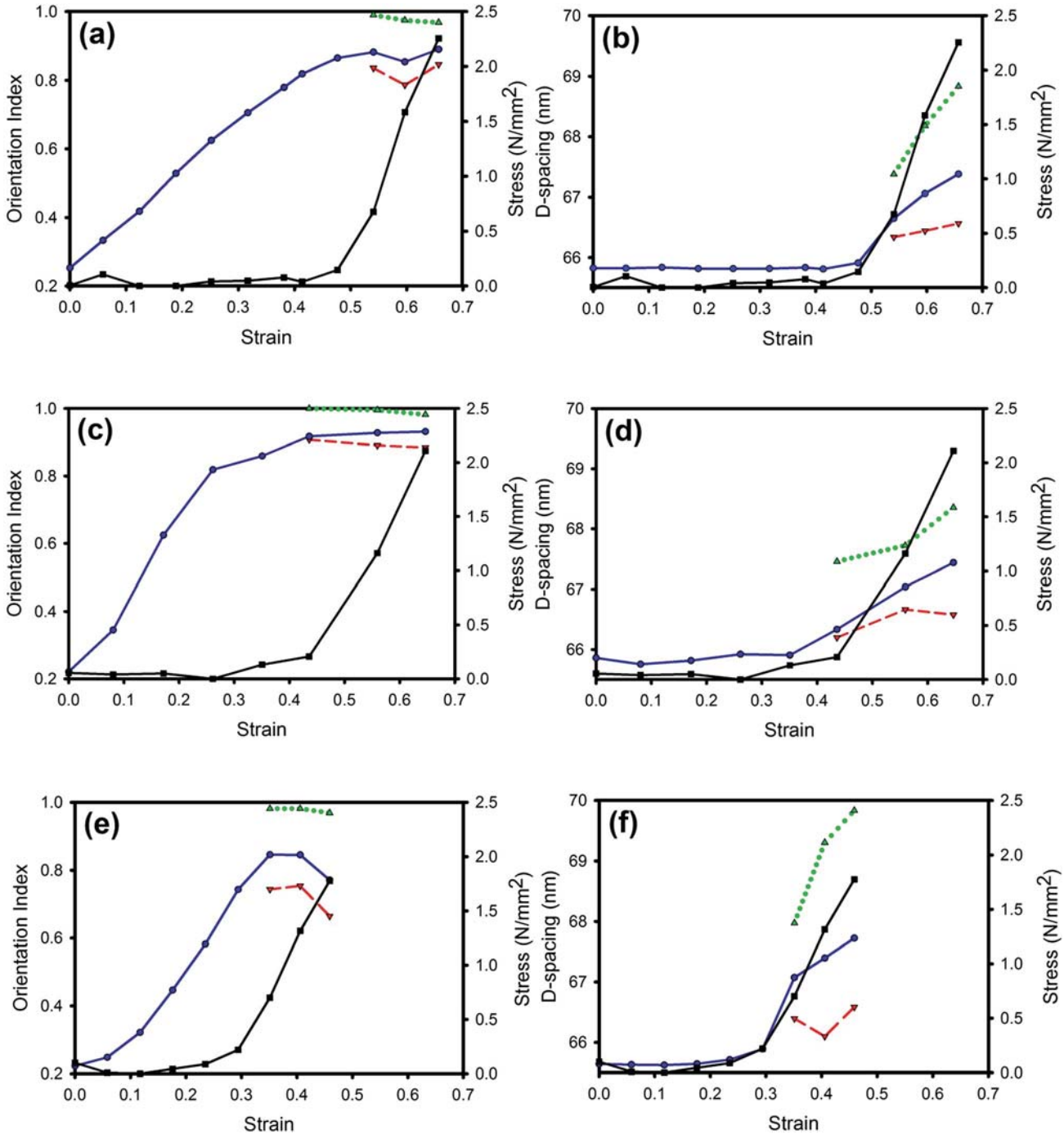

Fig. 7 Changes in OI and *D*-spacing as pericardium was subjected to increasing strain for each of the treatment types: (a and b) chondroitinase ABC treated; (c and d) native; (e and f) glutaraldehyde treated, where stress (■, ——, black); weighted sum OI or *D*-spacing (●, ——, blue); non-recruited fibril OI or *D*-spacing (▼, – – –, red); recruited fibril OI or *D*-spacing (▲, ·····, green).

D-spacing change. The *D*-spacing change, therefore, acts as an internal strain gauge.[2,43] There was a significant variation in the internal strain placed on the collagen fibrils between treatments. Collagen fibrils in the glutaraldehyde-treated materials experienced the greatest strain for a given sample stress, with the chondroitinase ABC-treated material experiencing the least, and native pericardium intermediate between these for the analysis of all the fibrils (Fig. 9). Of those fibrils recruited into stretching, those of native and chondroitinase ABC-treated pericardium experienced similar strains (slightly higher in the latter) whilst those in the glutaraldehyde-treated pericardium experienced significantly higher strains (Fig. 9b).

3.8 Fibril strain and tissue strain

The ratios of fibril strain (measured by *D*-spacing increase) to tissue strain (measured by the extension of the pericardium

Table 1 Recruitment of fibrils during stretching

Pericardium treatment	% Fibrils recruited to stretching (Duplicate pericardium measurements)	(From Fig. 6)	Average
Glutaraldehyde	37.9	52.1	45.0
Native	13.1	10.9	12.0
Chondroitinase ABC	37.4	33.7	35.6

sample; calculated from data in Fig. 7b, d and f) were the following for the overall tissue for each treatment type: chondroitinase ABC-treated samples 0.12; native 0.12; glutaraldehyde-treated samples 0.16. These ratios are similar to that reported elsewhere of 0.18 for a different sample of native pericardium.[2] Of those fibrils taking up the stress, the ratio of fibril strain to tissue strain was 0.24, 0.2 and 0.37 for chondroitinase ABC-treated, native and glutaraldehyde-treated pericardium, respectively.

4. Discussion

The internal structural response and stresses on pericardium collagen fibrils subjected to strain can be interpreted in terms of the contribution that the GAG or glutaraldehyde cross linking has on the rearrangement and stress on the individual collagen fibrils.

We propose that there are three ways in which this tissue can accommodate the strain and the stresses: (1) by removal of crimp and re-orienting of fibrils (manifested as an OI increase);

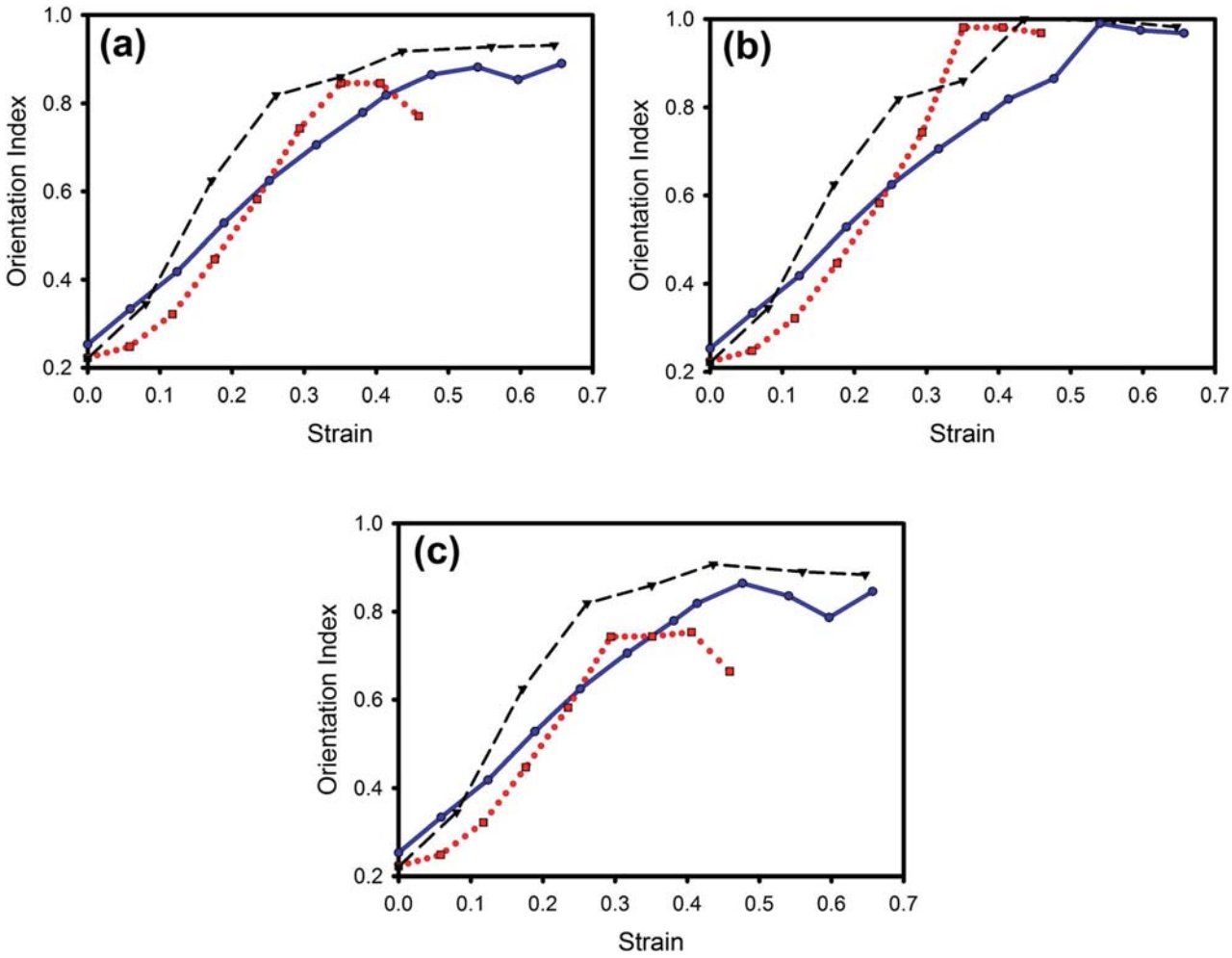

Fig. 8 Comparison of change in OI with increasing strain for the three treatments: (a) average of all fibrils; (b) recruited fibrils; (c) non-recruited fibrils. Chondroitinase ABC-treated pericardium (●, ——, blue); native pericardium (▼, – – –, black); glutaraldehyde-treated pericardium (■, ·····, red).

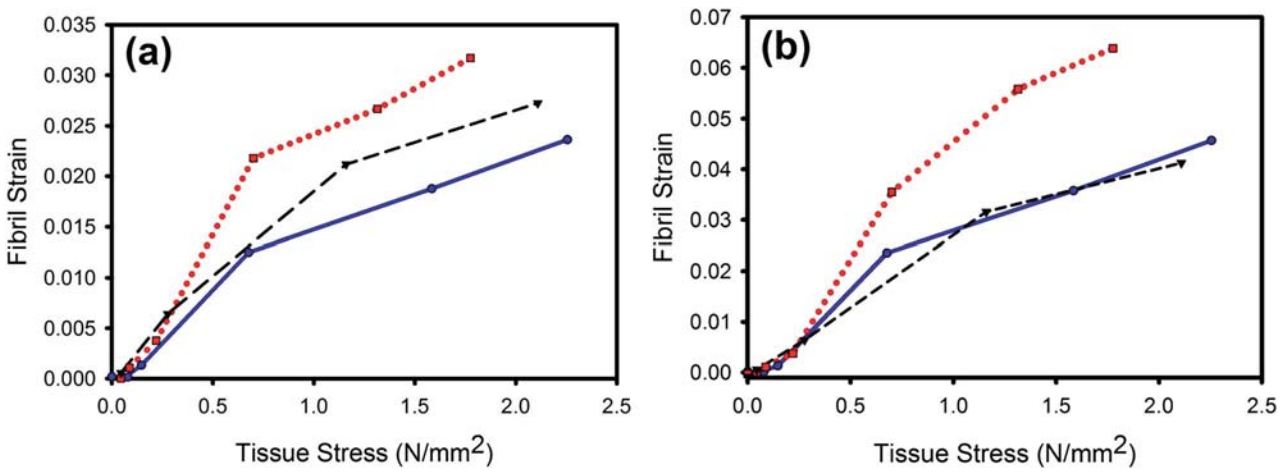

Fig. 9 Comparison of *D*-spacing change (indicating fibril strain) with increasing sample stress for the three treatments: chondroitinase ABC treated (●, ——, blue); native (▼, – – –, black); glutaraldehyde treated (■, ·····, red). (a) Average of all fibrils; (b) recruited fibrils only.

(2) by stretching of fibrils (*D*-spacing increase); (3) by sliding of the fibrils (not directly measured here).

The data, and our analysis of it, yield information about the nanostructural behaviours of pericardium tissue being stretched. In turn, these behaviours – strain-induced recruitment of fibrils; strain-induced changes in OI (from crimp removal and rearrangement); and a *D*-spacing increase from fibril stress – can provide insights into the mechanical structure of the tissue.

4.1 Recruitment

Recruitment is one aspect of re-orientation, and is a measure of the proportion of collagen fibrils that take up the stress that the tissue experiences (Table 1). Fewer fibrils were recruited in the native pericardium (12%) than in the glutaraldehyde-treated (45%) or the chondroitinase ABC-treated pericardium (36%). This suggests that the collagen fibrils in glutaraldehyde treated tissue are mechanically locked together by cross links and, therefore, when collagen fibrils in one direction are subjected to strain, other fibrils also take part in this strain. In native tissue, the minimal recruitment suggests that GAGs do not provide a strong mechanical connection between collagen fibrils. However, if this were so, one would expect the chondroitinase ABC-treated pericardium to behave similarly to the native pericardium, which it does not. So, the evidence from recruitment does not provide evidence for a mechanical cross linking effect of GAGs in tissue.

4.2 Reorientation with strain

The amount of strain that a tissue must undergo before reaching maximum OI was similar for native pericardium (0.35) and glutaraldehyde-treated pericardium (0.35) but higher for chondroitinase ABC-treated (GAG depleted) pericardium (0.5). This suggests that in chondroitinase ABC-treated pericardium, mechanical cross links have been removed, allowing more sliding of the collagen fibrils to occur compared with native and glutaraldehyde-treated pericardium. This is consistent with GAGs having a mechanical cross linking action. However, we note the variability in the length of the toe region of the stress–strain curves within treatment groups[29] could have been influenced by the initial placement of the samples.

4.3 Ratio of fibril strain (stress) to tissue strain

For all three treatment types, the macroscopic tissue strain was larger than the fibril strain, even after the OI reached a plateau, showing that either strain was taken up by other tissue components or that the fibrils had slid axially relative to one another as well as stretching. Therefore, a ratio of fibril strain to tissue strain may indicate the level of fibril sliding.

For overall tissue, that ratio of fibril strain to tissue strain was highest in glutaraldehyde-treated pericardium (0.16), with ratios for native tissue and GAG-depleted tissue being the same (0.12). Of the fibrils experiencing the most stress, glutaraldehyde-treated pericardium again had the highest ratio (0.37), whilst native had the lowest (0.20) and chondroitinase ABC-treated material intermediate (0.24). These findings suggest that in glutaraldehyde-treated pericardium the collagen fibrils are held in place, and less able to slide past each other, by the more highly networked structure resulting from the action of cross links. That the ratio of recruited fibril strain to tissue strain for chondroitinase ABC-treated pericardium was slightly higher than that of native pericardium implies that the presence of GAGs encourages more fibril sliding. This strain ratio data, therefore, does not support the theory of GAGs as mechanical cross linkers.

4.4 Ratio of fibril stress to tissue stress

For a given tissue stress, the individual collagen fibrils in glutaraldehyde-cross linked tissue experienced more stress (reflected by the *D*-spacing increase) than did the native tissue (Fig. 9). The collagen fibrils in GAG-depleted (chondroitinase ABC-treated) tissue experienced less stress than did the native or glutaraldehyde-treated tissue when considering the behaviour of all fibrils. This could be interpreted to mean that in the

glutaraldehyde-treated and native pericardia, there are mechanical cross links that hold the fibrils together so that when the tissue is stressed, this stress is transmitted to a greater proportion of the collagen fibrils in the material. In light of this interpretation, the ratio of fibril stress to tissue stress supports a mechanical action of GAGs. However, for those fibrils aligned in the direction of stress, the fibril strain at a given stress was highest for glutaraldehyde-linked pericardium, but was slightly lower for native than for chondroitinase ABC-treated pericardium. From the behaviour of these fibrils, it appears that GAGs do not transmit stresses to individual fibrils.

4.5 Alternative explanations

The above interpretations of the analyses of fibril stress and orientation change data can be explained by the mechanical action of glutaraldehyde but do not all support GAGs as mechanical cross linking agents. A radically alternative explanation is that GAGs promote fibril sliding perhaps by acting as lubricants to the collagen fibrils. The sliding forces in fibrous protein systems are typically rather large.[44] Lubrication to reduce these forces does not mean weaker material, and it is well known in the leather industry that lubricating processed leather with oil components is necessary to achieve high strength in leather.[45]

Such a role for GAGs acting as lubricants and glutaraldehyde acting as a mechanical cross link are consistent with almost all observations in this work.

The lower fibril recruitment in native material compared to that in chondroitinase ABC-treated material, the ratio of fibril strain to tissue strain (particularly the ratio of the portion of fibrils that take up the most stress), and the ratio of recruited fibril stress to tissue stress are all consistent with GAGs acting as lubricants in the native material, such that the fibrils slide past each other rather than co-opting other fibrils into taking up the applied stress. Unlike glutaraldehyde cross links, which covalently bond to amino acid sidechains on the collagen fibril, GAGs are thought to aggregate through hydrophobic and hydrophilic interactions which can dissociate and reform;[46,47] GAG bridges may, therefore, not be as strong as glutaraldehyde cross links, and rather than pulling fibrils into stretch or directly transferring forces, these GAG bridges may skew, dissociate and possibly re-associate as fibrils slide past one another. There is only one set of observations that is not compatible with GAGs acting as lubricants: the reorientation of fibrils with strain (OI change, maximum) although the differences are small.

5. Conclusions

An investigation into the mechanical nature of glycosaminoglycan present in collagen tissue by comparing native pericardium, GAG-depleted pericardium (using chondroitinase ABC) and robustly cross linked pericardium (using glutaraldehyde) identified significant differences in the nanostructural behaviour of the different tissues during mechanical loading. The evidence suggests both GAG and glutaraldehyde cross links have a role in response to applied tension forces, however, the mechanisms by which they respond vary vastly; glutaraldehyde had a clear role in producing a constrained network structure, involving more fibrils in the mechanical response and experiencing higher fibril strains. In contrast, fewer fibrils in native tissue partake in stretching with the fibrils experiencing lower strains. We propose GAGs may act as a lubricant, resulting in more fibril sliding relative to fibril stretching.

Acknowledgements

This work was supported by the Massey Doctoral Scholarship (HRK). This research was undertaken on the SAXS/WAXS beamline at the Australian Synchrotron, Victoria, Australia. The Australian synchrotron is acknowledged for travel funding. Southern Lights Biomaterials supplied the pericardium. Sue Hallas assisted with editing.

References

1 M. A. Meyers, J. McKittrick and P. Y. Chen, *Science*, 2013, **339**, 773–779.
2 H. C. Wells, K. H. Sizeland, H. R. Kayed, N. Kirby, A. Hawley, S. T. Mudie and R. G. Haverkamp, *J. Appl. Phys.*, 2015, **117**, 044701.
3 W. Yang, V. R. Sherman, B. Gludovatz, E. Schaible, P. Stewart, R. O. Ritchie and M. A. Meyers, *Nat. Commun.*, 2015, **6**, 1–9.
4 J. E. Scott and R. A. Stockwell, *J. Physiol.*, 2006, **574**, 643–650.
5 A. M. Cribb and J. E. Scott, *J. Anat.*, 1995, **187**, 423–428.
6 J. E. Scott and C. R. Orford, *Biochem. J.*, 1981, **197**, 213–216.
7 J. E. Scott, *Biochem. J.*, 1980, **187**, 887–891.
8 J. E. Scott, *J. Physiol.*, 2003, **553**, 335–343.
9 R. G. Haverkamp, M. A. K. Williams and J. E. Scott, *Biomacromolecules*, 2005, **6**, 1816–1818.
10 J. Liao and I. Vesely, *J. Biomech.*, 2007, **40**, 390–398.
11 S. Rigozzi, R. Mueller, A. Stemmer and J. G. Snedeker, *J. Biomech.*, 2013, **46**, 813–818.
12 Y. Chan, G. M. Cox, R. G. Haverkamp and J. M. Hill, *Eur. Biophys. J.*, 2009, **38**, 487–493.
13 R. Puxkandl, I. Zizak, O. Paris, J. Keckes, W. Tesch, S. Bernstorff, P. Purslow and P. Fratzl, *Philos. Trans. R. Soc., B*, 2002, **357**, 191–197.
14 S. W. Cranford and M. J. Buehler, *Soft Matter*, 2013, **9**, 1076–1090.
15 G. Fessel and J. G. Snedeker, *J. Theor. Biol.*, 2011, **268**, 77–83.
16 A. Redaelli, S. Vesentini, M. Soncini, P. Vena, S. Mantero and F. M. Montevecchi, *J. Biomech.*, 2003, **36**, 1555–1569.
17 R. G. Haverkamp, A. T. Marshall and M. A. K. Williams, *J. Phys. Chem. B*, 2007, **111**, 13653–13657.
18 S. Rigozzi, A. Stemmer, R. Muller and J. G. Snedeker, *J. Struct. Biol.*, 2011, **176**, 9–15.
19 G. Fessel and J. G. Snedeker, *Matrix Biol.*, 2009, **28**, 503–510.
20 R. B. Svensson, T. Hassenkam, P. Hansen, M. Kjaer and S. P. Magnusson, *Connect. Tissue Res.*, 2011, **52**, 415–421.
21 A. J. Bailey, *Mech. Ageing Dev.*, 2001, **122**, 735–755.

22 L. Damink, P. J. Dijkstra, M. J. A. Vanluyn, P. B. Vanwachem, P. Nieuwenhuis and J. Feijen, *J. Mater. Sci.: Mater. Med.*, 1995, **6**, 460–472.
23 D. T. Cheung and M. E. Nimni, *Connect. Tissue Res.*, 1982, **10**, 201–216.
24 D. T. Cheung, N. Perelman, E. C. Ko and M. E. Nimni, *Connect. Tissue Res.*, 1985, **13**, 109–115.
25 I. J. Reece, R. Vannoort, T. R. P. Martin and M. M. Black, *Ann. Thorac. Surg.*, 1982, **33**, 480–485.
26 S. E. Langdon, R. Chernecky, C. A. Pereira, D. Abdulla and J. M. Lee, *Biomaterials*, 1999, **20**, 137–153.
27 H. W. Sung, Y. Chang, C. T. Chiu, C. N. Chen and H. C. Liang, *J. Biomed. Mater. Res.*, 1999, **47**, 116–126.
28 A. Mirnajafi, J. Raymer, M. J. Scott and M. S. Sacks, *Biomaterials*, 2005, **26**, 795–804.
29 H. R. Kayed, K. H. Sizeland, N. Kirby, A. Hawley, S. T. Mudie and R. G. Haverkamp, *RSC Adv.*, 2015, **5**, 3611–3618.
30 P. P. Purslow, T. J. Wess and D. W. L. Hukins, *J. Exp. Biol.*, 1998, **201**, 135–142.
31 J. Liao, L. Yang, J. Grashow and M. S. Sacks, *Acta Biomater.*, 2005, **1**, 45–54.
32 T. W. Gilbert, S. Wognum, E. M. Joyce, D. O. Freytes, M. S. Sacks and S. F. Badylak, *Biomaterials*, 2008, **29**, 4775–4782.
33 M. M. Basil-Jones, R. L. Edmonds, S. M. Cooper and R. G. Haverkamp, *J. Agric. Food Chem.*, 2011, **59**, 9972–9979.
34 K. H. Sizeland, M. M. Basil-Jones, R. L. Edmonds, S. M. Cooper, N. Kirby, A. Hawley and R. G. Haverkamp, *J. Agric. Food Chem.*, 2013, **61**, 887–892.
35 M. M. Basil-Jones, R. L. Edmonds, G. E. Norris and R. G. Haverkamp, *J. Agric. Food Chem.*, 2012, **60**, 1201–1208.
36 H. C. Wells, K. H. Sizeland, N. Kirby, A. Hawley and S. Mudie, *ACS Biomater. Sci. Eng.*, 2015, **1**, 1026–1038.
37 N. Nwaejike and R. Ascione, *J. Card. Surg.*, 2011, **26**, 31–33.
38 D. Mavrilas, E. A. Sinouris, D. H. Vynios and N. Papageorgakopoulou, *J. Biomech.*, 2005, **38**, 761–768.
39 P. R. Umashankar, T. Arun and T. V. Kumari, *J. Biomed. Mater. Res., Part A*, 2011, **97**, 311–320.
40 D. Cookson, N. Kirby, R. Knott, M. Lee and D. Schultz, *J. Synchrotron Radiat.*, 2006, **13**, 440–444.
41 M. S. Sacks, D. B. Smith and E. D. Hiester, *Ann. Biomed. Eng.*, 1997, **25**, 678–689.
42 R. H. Stinson and P. R. Sweeny, *Biochim. Biophys. Acta*, 1980, **621**, 158–161.
43 R. G. Haverkamp, *Chem. N. Z.*, 2013, **77**, 12–17.
44 A. Ward, F. Hilitski, W. Schwenger, D. Welch, A. W. C. Lau, V. Vitelli, L. Mahadevan and Z. Dogic, *Nat. Mater.*, 2015, **14**, 583–588.
45 K. H. Sizeland, H. C. Wells, G. E. Norris, R. L. Edmonds, N. Kirby, A. Hawley, S. Mudie and R. G. Haverkamp, *J. Am. Leather Chem. Assoc.*, 2015, **110**, 66–71.
46 J. E. Scott and A. M. Thomlinson, *J. Anat.*, 1998, **192**, 391–405.
47 J. E. Scott, *FASEB J.*, 1992, **6**, 2639–2645.

JOURNAL OF APPLIED PHYSICS **117**, 044701 (2015)

Poisson's ratio of collagen fibrils measured by small angle X-ray scattering of strained bovine pericardium

Hannah C. Wells,[1] Katie H. Sizeland,[1] Hanan R. Kayed,[1] Nigel Kirby,[2] Adrian Hawley,[2] Stephen T. Mudie,[2] and Richard G. Haverkamp[1,a)]
[1]*School of Engineering and Advanced Technology, Massey University, Private Bag 11222, Palmerston North 4442, New Zealand*
[2]*Australian Synchrotron, 800 Blackburn Road, Clayton, Victoria 3168, Australia*

(Received 26 August 2014; accepted 7 December 2014; published online 26 January 2015)

Type I collagen is the main structural component of skin, tendons, and skin products, such as leather. Understanding the mechanical performance of collagen fibrils is important for understanding the mechanical performance of the tissues that they make up, while the mechanical properties of bulk tissue are well characterized, less is known about the mechanical behavior of individual collagen fibrils. In this study, bovine pericardium is subjected to strain while small angle X-ray scattering (SAXS) patterns are recorded using synchrotron radiation. The change in d-spacing, which is a measure of fibril extension, and the change in fibril diameter are determined from SAXS. The tissue is strained 0.25 (25%) with a corresponding strain in the collagen fibrils of 0.045 observed. The ratio of collagen fibril width contraction to length extension, or the Poisson's ratio, is 2.1 ± 0.7 for a tissue strain from 0 to 0.25. This Poisson's ratio indicates that the volume of individual collagen fibrils decreases with increasing strain, which is quite unlike most engineering materials. This high Poisson's ratio of individual fibrils may contribute to high Poisson's ratio observed for tissues, contributing to some of the remarkable properties of collagen-based materials.
[http://dx.doi.org/10.1063/1.4906325]

I. INTRODUCTION

Type I collagen is a key structural material in animals. It is the main structural component of skin and tendons. Type I collagen is also important in products made from animal skin, or related tissues, such as leather and extracellular matrix scaffolds for surgical applications.[1,2] Type II collagen has a fairly similar fibril structure to type I collagen, although with more branching and cross-linking, and is the main structural component of tissues, such as cartilage, therefore parallels may be drawn between type I and type II collagens. The mechanical properties of collagen-based materials are central to the natural and industrial uses of these materials and have been studied in a variety of tissues.

The bulk mechanical properties of tissues have been well characterised, including measurements of Poisson's ratio. Poisson's ratio, ν, is the ratio of transverse strain $\Delta W/W$ (where W is width of a cube or bar) to longitudinal strain $\Delta L/L$ (where L is the length of a cube or bar) in the loading direction

$$= -\frac{(\Delta W/W)}{\Delta L/L}. \quad (1)$$

For isotropic materials, $\nu > 0.5$ is excluded on theoretical grounds, however, fibrillar collagen is anisotropic. When $\nu > 0.5$ for a material under tension, the volume decreases as the tissue is strained. A wide range of values of ν have been measured for type I and II collagen materials in compression and tension, with many of these giving $\nu > 0.5$. These include tendon under compression[3] with $\nu = 0.8$, spinal dura mater under uniaxial tension $\nu = 0.5$–1.6 depending on the direction of the tissue section taken,[4] bovine articular cartilage in compression[5,6] $\nu = 0.15$–0.20 and 0.16 measured by microindentation,[7] and human patellar cartilage measured in tension[8] $\nu = 0.6$–1.9. The Poisson's ratio in tendon fascicles has been shown to increase with stress[9] up to $\nu = 4$ and in articular cartilage up to $\nu = 1.2$ with increasing strain.[10]

While the mechanical properties of tissue have been well characterized, the mechanical properties of individual collagen fibrils that constitute the tissue are less well known. Collagen fibril diameter has been shown to have some influence on tissue strength.[11,12] In addition, proteogylcan connections between collagen fibrils in tendon subjected to tensile stress have been suggested as contributing to the strength of the tissue.[13,14] Examination of individual collagen fibrils in rat tail tendon with atomic force microscopy can yield an estimate of the Poisson's ratio measured in compression in a transverse direction.[15,16]

Modeling of the crimp present in many collagen tissues, such a tendon and ligament or helical structure of the fibrils, has suggested that these features could explain much of the high Poisson's ratio of the tissue composed of collagen.[17] It has also been suggested that in tendon, the strain may be taken up by sliding of fibrils within the tendon rather than by extension of the collagen fibrils.[18] In leather, where there is

a)r.haverkamp@massey.ac.nz

very little crimp, the reorientation of fibrils may be an important mechanism for absorbing strain.[19,20]

Here, the behavior of individual fibrils of collagen I as strain is applied is studied using small angle X-ray scattering (SAXS) to simultaneously measure the fibril length extension and fibril diameter contraction. Bovine pericardium is used as a model material for this work because it is elastic and strong and has application in medical devices.[21]

II. MATERIALS AND METHODS

Fresh bull (Charolais Cross) pericardium samples were obtained from John Shannon, Wairapara, New Zealand, within 2 h of slaughter. The tissue was cut into rectangles ca. 50 mm × 6 mm, with the long axis aligning with the long axis of the heart. The pericardium was washed for 24 h in a 1% octylphenol ethylene oxide condensate (Triton X-100, Sigma), 0.02% EDTA solution made up in phosphate buffered saline (PBS) (Lorne Laboratories Ltd).[22] The samples were stored in PBS. SAXS diffraction patterns were recorded at room temperature while the pericardium was wet.

For transmission electron microscopy (TEM), samples were fixed with 2% formaldehyde and 3% glutaraldehyde in phosphate buffer, post fixed with 1% OsO_4 and dehydrated using an acetone/water series. The sections were stained with uranyl acetate and then with lead citrate and examined with a Philips CM10 TEM (Philips, Eindhoven, The Netherlands). These show the collagen fibrils with the d-banding visible (Fig. 1).

A stretching apparatus was built as described previously.[19] A linear motor, Linmot PS01 48 × 240/30 × 180-C (NTI AG, Switzerland), was mounted on a purpose-built frame. Clamps to hold the pericardium were fitted between the linear motor and a L6D OIML single-point loadcell (Hangzhou Wanto Precision Technology Co., Zhejiang, China). The pericardium was mounted horizontally without tension. The sample (30 mm between jaws) was stretched in 1 mm increments to take up the slack until a force was just registered by the loadcell, then backed off so that it was not under tension. Diffraction patterns were collected in a 0.5 mm grid of eight points. The sample was stretched in 1 mm increments and maintained for 1 min at each extension to stabilize before SAXS patterns, the extension and the force information were recorded. This process was repeated until the sample failed, with the interval between strain increments around 8–13 min.

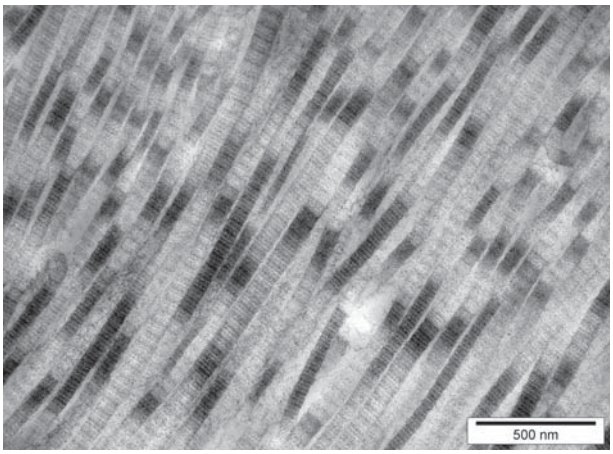

FIG. 1. Transmission electron microscopy of pericardium.

The diffraction patterns were recorded on the Australian Synchrotron SAXS/WAXS beamline which uses a high-intensity undulator source. An X-ray energy of 12 keV was used with energy resolution of 10^{-4} (e.g., 1×10^{-4} for 1 radiation) from a cryo-cooled Si(111) double-crystal monochromator with a beam size (FWHM focused at the sample) of $250 \times 80\ \mu$m, and a total photon flux of about 2×10^{12} ph s^{-1}. A Pilatus 1 M detector with an active area of 170×170 mm and a sample-to-detector distance of 3371 mm was used. Exposure time was 1 s and data processing was carried out using the SAXS15ID software.[23] Each data point presented is the average from of a minimum of eight diffraction patterns recorded on a grid of positions on the sample.

Fibril diameters were calculated from the SAXS data using the Irena software package[24] running within Igor Pro. The data were fitted at the wave vector Q, in the range of 0.01–0.04 $Å^{-1}$ and at an azimuthal angle which was 90° to the long axis of most of the collagen fibrils. This angle was selected by determining the average orientation of the collagen fibrils from the azimuthal angle for the maximum intensity of the d-spacing diffraction peaks. The "cylinder AR" shape model with an arbitrary aspect ratio of 30 was used for all fitting. We did not attempt to individually optimize this aspect ratio and the unbranched length of collagen fibrils may in practice have a length that exceeds an aspect ratio of 30.

The d-spacing was determined from the position of the centre of a Gaussian curve fitted to the 9th order diffraction peak taken from the integrated intensity plots from the azimuthal range from 45° to 135°. The orientation index (OI) is defined by

$$OI = (90^\circ - OA)/90^\circ, \tag{2}$$

where OA (orientation angle) is the minimum azimuthal angle range that contains 50% of the fibrils, based on the method of Sacks for light scattering[25] but converted to an index,[26] using the spread in azimuthal angle of one or more d-spacing diffraction peaks. The OI is used to give a measure of the spread of fibril orientation (an OI of 1 indicates the fibrils are parallel to each other; 0 indicates the fibrils are randomly oriented).

III. RESULTS AND DISCUSSION

The integrated intensity plots show well-defined peaks corresponding to the collagen d-period (Fig. 2). The odd numbered peaks have a much higher intensity than the even numbered peaks, a characteristic attributed to a fully hydrated sample.[27] At right angles to the direction of alignment, the d-peaks are not as apparent, and the scattering results from the fibril diameter distribution. The diffraction that is no longer present at an azimuthal angle rotated by 90° is due to the d-banding, while the broader features that remain or enhanced are due to the fibril diameter or fibrillar spacing.

The stress-strain curve recorded from the *in-situ* stretching is shown in Fig. 3. The maximum strain obtained before

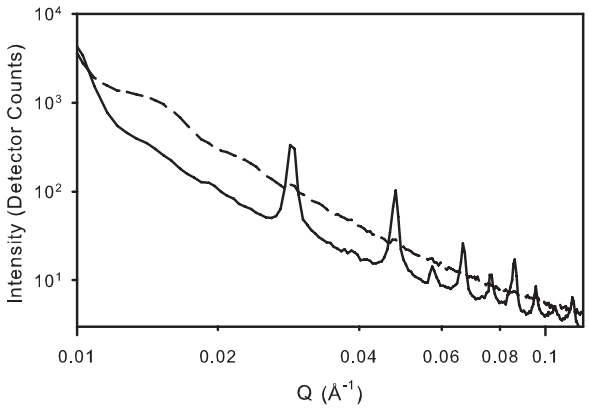

FIG. 2. Representative integrated scattering pattern of pericardium. Solid line—at an azimuthal angle segment centered 90°, which is used for assessing d-spacing; dashed line—at an azimuthal angle segment centered on 0°, which is used for fibril diameter.

rupture was 25%. The time dependency of the stress-strain curve was not considered as it has been found not to affect elastic properties[4] and the time between each data point was approximately constant.

There are two stages in the structural changes at the collagen fibril level we observe. In the first stage (up to a strain, fractional change in length, of about 0.09), we observe is a decrease in collagen fibril diameter with a small increase in d-spacing and a large increase in OI. During this stage, the strain is taken up by reorientation of the fibrils. Pericardium has a marked crimp so that a portion of the observed OI can be due to crimp. It is trivial to show that the shape of the curve from which the OI is derived, if the crimp takes a sinusoidal shape, should have the form

$$I = A\sin(\phi)\cos(\phi), \tag{3}$$

where I is the diffraction peak intensity, ϕ is the azimuthal angle, and A is the magnitude of the crimp. It has been shown elsewhere that, during biaxial strain crimp is maintained,[28] therefore we believe the change in OI is largely due to fibril reorientation rather than straightening of crimp.

During the second stage of strain, there is no significant change in the OI but the d-spacing increases markedly (fibril length) and the fibril diameter decreases (Fig. 4). The

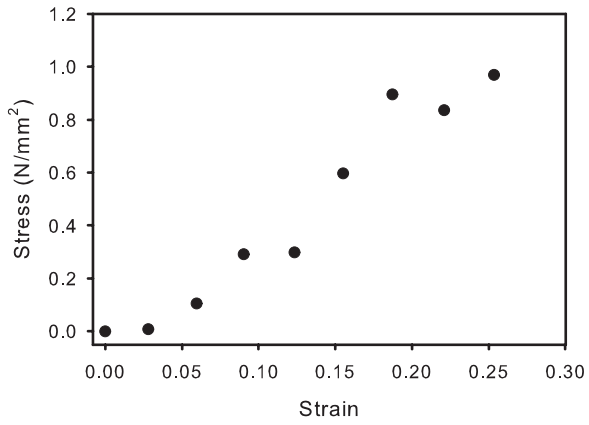

FIG. 3. Stress-strain curve measured on pericardium during *in situ* SAXS measurements.

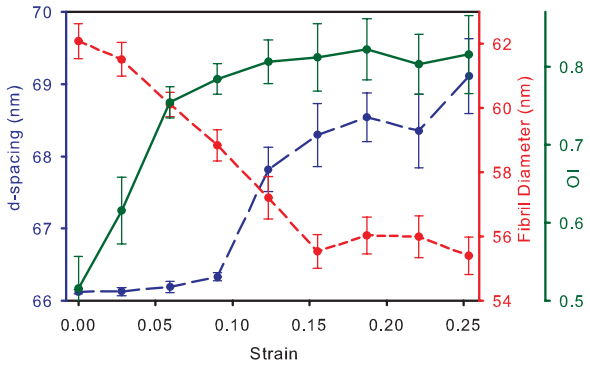

FIG. 4. d-spacing (long dash, blue), fibril diameter (short dash, red), and OI (solid, green) changes with increasing strain. Lines are a guide for the eye only.

d-spacing can be thought of as an internal strain gauge for the collagen fibrils with an increase in d-spacing, indicating an increase in stress on the fibril. At a tissue strain above 0.15, the fibrils continue to stretch but there is a decrease in fibril diameter plateaus. From the unstrained state to the maximum strain state, the d-spacing increases from 66.13 nm to 69.12 nm, a change of 2.99 nm or 4.5%. The OI increases from 0.53 to 0.75 (at a strain of 0.09) and then is stable at around 0.80 at higher strain values (Fig. 4). Fibril diameter decreases from 62.1 nm for the unstretched collagen to 55.4 nm at the maximum strain experienced (Fig. 4), a decrease in 6.7 nm or 10.8%. At first, while the fibril diameter changes, there is little change in d-spacing, then at higher strain, as the fibril diameter decreases, the d-spacing increases.

During this second stage of strain, the change in d-spacing strain (fibril strain) is about 30% of the whole tissue strain. This shows that the strain in the tissue is taken up partly by the strain in the collagen fibrils, as has been observed with light scattering[28] and partly by the tissue strain being transferred to interfibrillar sliding or rearrangement of the fibrils. By contrast, in weak ovine leather (data taken from published work[19]), our calculations of fibril strain versus leather strain give 10% d-spacing strain to whole tissue strain for leather. The collagen fibrils in leather are less aligned than in pericardium, allowing more possibility for realignment. For rat tail tendon, this ratio is 40% for the second (linear) region of the strain curve,[29] perhaps reflecting the high alignment of collagen in tendon.

From the d-spacing change and fibril diameter change, we calculate the Poisson's ratio. Since ν is defined for a cube, we correct the ratio by $\sqrt{\pi}/2$ to account for the approximately cylindrical shape of the collagen fibril (in order to retain the property that a Poisson's ratio of 0.5 represents a material in which the volume does not change with strain). So that the equivalent Poisson's ratio, ν', can be calculated for a rod with diameter D by

$$\nu' = -\frac{\sqrt{\pi}/2(\Delta D/D)}{\Delta L/L}. \tag{4}$$

For collagen in bovine pericardium, at low strain, the Poisson's ratio appears to have a very high value (15–27), but for strain above 0.09, the Poisson's ratio is in the range 2.1–2.8. For the total strain (from 0 to 0.25), the change in

d-spacing and diameter gives $\nu' = 2.1 \pm 0.7$ (these values of ν' can be calculated from Fig. 4). The $\nu' > 0.5$ could be due to tighter packing within the fibril under strain, which may include compression of hydrogen bonding in the fibril, microfibril, or tropocollagen. The extension of the fibrils with increasing strain has previously been ascribed largely to the sliding of the tropocollagen within the fibrils, resulting in an increase in the gap region, rather than to the extension of the tropocollagen molecules that constitute the fibrils.[30] We note that the stress-strain curve does not show a marked foot region, it does not exhibit a low Young's modulus at low strain, which suggests that an entropic straightening of the fibrils may not be a major factor in the strain of the material.

We can know, because of the evidence provided by the OI, that this Poisson's ratio we measure must be due largely to stretching of the fibrils and not to changes in crimp. A straightening of crimp must result in an increase in OI (as can be derived from the relationship represented by (2)), and there was no large increase in OI after the first 0.05 strain and therefore there must be no change in crimp above 0.05 strain.

Using data from a recently published atomic force microscope study on tendon,[31] we calculate $\nu' = 1.9$ (tendon was stretched by 15%), similar to the value we find from our measurements.

IV. CONCLUSIONS

While it has previously been shown that bulk materials based on collagen may have $\nu > 0.5$, we have provided experimental evidence that the collagen fibrils also may have $\nu' > 0.5$. Therefore, this property of collagen fibrils may contribute to the bulk properties of the tissue.

Previously, it has been proposed that much of the high Poisson's ratio of tendon and cartilage is due to the volume loss from fluid exudation[32] although specific attempts to measure this have not always shown water to be exuded.[10,33] We now demonstrate that there is a contribution to the high Poisson's ratio of the tissue from the high Poisson's ratio of the collagen fibrils. This does not exclude the possibility that water is exuded from the fibrils.

ACKNOWLEDGMENTS

This research was undertaken on the SAXS/WAXS beamline at the Australian Synchrotron, Victoria, Australia. The NZ Synchrotron Group Ltd., is acknowledged for travel funding. Melissa Basil-Jones assisted with data collection. John Shannon of Wairarapa supplied the pericardium. Jordan Taylor of the Manawatu Microscopy Centre assisted with TEM. Sue Hallas of Nelson assisted with the editing. The anonymous reviewers are thanked for their input.

[1]E. Floden, S. Malak, M. Basil-Jones, L. Negron, J. Fisher, M. Byrne, S. Lun, S. Dempsey, R. Haverkamp, I. Anderson, B. Ward, and B. May, J. Biomed. Mater. Res. B **96B**, 67–75 (2011).
[2]M. W. Clemens, J. C. Selber, J. Liu, D. M. Adelman, D. P. Baumann, P. B. Garvey, and C. E. Butler, Plastic Reconstr. Surg. **131**, 71–79 (2013).
[3]V. W. T. Cheng and H. R. C. Screen, J. Mater. Sci. **42**, 8957–8965 (2007).
[4]C. Persson, S. Evans, R. Marsh, J. L. Summers, and R. M. Hall, Ann. Biomed. Eng. **38**, 975–983 (2010).
[5]J. S. Jurvelin, M. D. Buschmann, and E. B. Hunziker, J. Biomech. **30**, 235–241 (1997).
[6]P. Kiviranta, J. Rieppo, R. K. Korhonen, P. Julkunen, J. Toyras, and J. S. Jurvelin, J. Orthop. Res. **24**, 690–699 (2006).
[7]G. J. Miller and E. F. Morgan, Osteoarthritis Cartilage **18**, 1051–1057 (2010).
[8]D. M. Elliott, D. A. Narmoneva, and L. A. Setton, J. Biomech. Eng. **124**, 223–228 (2002).
[9]S. P. Reese and J. A. Weiss, J. Biomech. Eng. **135**, 034501 (2013).
[10]L. Edelsten, J. E. Jeffrey, L. V. Burgin, and R. M. Aspden, Soft Matter **6**, 5206–5212 (2010).
[11]D. A. D. Parry, G. R. G. Barnes, and A. S. Craig, Proc. R. Soc. London, Ser. B **203**, 305–321 (1978).
[12]H. C. Wells, R. L. Edmonds, N. Kirby, A. Hawley, S. T. Mudie, and R. G. Haverkamp, J. Agric. Food Chem. **61**, 11524–11531 (2013).
[13]A. M. Cribb and J. E. Scott, J. Anat. **187**, 423–428 (1995).
[14]R. G. Haverkamp, M. A. K. Williams, and J. E. Scott, Biomacromolecules **6**, 1816–1818 (2005).
[15]M. P. E. Wenger and P. Mesquida, Appl. Phys. Lett. **98**, 163707 (2011).
[16]M. Minary-Jolandan and M.-F. Yu, Biomacromolecules **10**, 2565–2570 (2009).
[17]S. P. Reese, S. A. Maas, and J. A. Weiss, J. Biomech. **43**, 1394–1400 (2010).
[18]H. R. C. Screen, D. L. Bader, D. A. Lee, and J. C. Shelton, Strain **40**, 157–163 (2004).
[19]M. M. Basil-Jones, R. L. Edmonds, G. E. Norris, and R. G. Haverkamp, J. Agric. Food Chem. **60**, 1201–1208 (2012).
[20]K. H. Sizeland, M. M. Basil-Jones, R. L. Edmonds, S. M. Cooper, N. Kirby, A. Hawley, and R. G. Haverkamp, J. Agric. Food Chem. **61**, 887–892 (2013).
[21]K. H. Sizeland, H. C. Wells, J. J. Higgins, C. M. Cunanan, N. Kirby, A. Hawley, and R. G. Haverkamp, BioMed Res. Int. **2014**, 189197.
[22]M. Yang, C. Z. Chen, X. N. Wang, Y. B. Zhu, and Y. J. Gu, J. Biomed. Mater. Res. B **91B**, 354–361 (2009).
[23]D. Cookson, N. Kirby, R. Knott, M. Lee, and D. Schultz, J. Synchrotron. Radiat. **13**, 440–444 (2006).
[24]J. Ilavsky and P. R. Jemian, J. Appl. Crystallogr. **42**, 347–353 (2009).
[25]M. S. Sacks, D. B. Smith, and E. D. Hiester, Ann. Biomed. Eng. **25**, 678–689 (1997).
[26]M. M. Basil-Jones, R. L. Edmonds, S. M. Cooper, and R. G. Haverkamp, J. Agric. Food Chem. **59**, 9972–9979 (2011).
[27]R. H. Stinson and P. R. Sweeny, Biochim. Biophys. Acta **621**, 158–161 (1980).
[28]M. S. Sacks, Trans. ASME J. Biomech. Eng. **125**, 280–287 (2003).
[29]P. Fratzl, K. Misof, I. Zizak, G. Rapp, H. Amenitsch, and S. Bernstorff, J. Struct. Biol. **122**, 119–122 (1998).
[30]N. Sasaki and S. Odajima, J. Biomech. **29**, 1131–1136 (1996).
[31]S. Rigozzi, R. Muller, A. Stemmer, and J. G. Snedeker, J. Biomech. **46**, 813–818 (2013).
[32]S. Adeeb, A. Ali, N. Shrive, C. Frank, and D. Smith, Comput. Methods Biomech. **7**, 33–42 (2004).
[33]K. G. Helmer, G. Nair, M. Cannella, and P. Grigg, Trans. ASME J. Biomech. Eng. **128**, 733–741 (2006).

Journal of
Biomaterials and Tissue Engineering
Vol. 6, 1–6, 2016

Age Differences with Glutaraldehyde Treatment in Collagen Fibril Orientation of Bovine Pericardium

Hanan R. Kayed[1], Katie H. Sizeland[2], Hannah C. Wells[1], Nigel Kirby[2], Adrian Hawley[2], Stephen Mudie[2], and Richard G. Haverkamp[1,*]

[1] *School of Engineering and Advanced Technology, Massey University, Palmerston North 4472, New Zealand*
[2] *Australian Synchrotron, 800 Blackburn Road, Clayton, Melbourne, VIC 3168, Australia*

Glutaraldehyde treatment of bovine pericardium produces a more isotropic structure with less oriented collagen fibrils. Skin from old animals has more natural cross linking than skin from young animals and structural differences exist between old and young tissue. However, it was not known whether structural changes resulting from glutaraldehyde treatment (considered to be cross linking) are affected by tissue age. Bovine neonatal and adult pericardia were treated with glutaraldehyde and the collagen fibril orientation measured for both using synchrotron based small angle X-ray scattering (SAXS). Neonatal pericardium is more oriented than adult with a higher orientation index (OI) of 0.40 compared to an OI of 0.19 for adult pericardium (with X-rays normal to the surface). With glutaraldehyde treatment the OI decreased for both tissue types by similar amounts to give an OI of 0.23 for neonatal and 0.12 for adult pericardium, so a 41% and 39% decrease for neonatal and adult pericardium respectively. While there are differences in structure of bovine pericardium with age, the age of the pericardium does not alter relative structural changes that take place on glutaraldehyde treatment. Therefore, the propensity to develop more isotropic structures by glutaraldehyde cross linking is similar for neonatal and adult tissue.

Keywords: Pericardium, Small Angle X-ray Scattering, Collagen Structure, Cross-Linking.

RESEARCH ARTICLE

1. INTRODUCTION

Bovine pericardium is a useful established material for heart valve leaflet replacement.[1–3] This material is normally used after treatment with glutaraldehyde and there are several devices in the market using this material. Although glutaraldehyde treatment is not commonly used for other types of tissue heterografts, in heart valve technology it is believed to stabilize and impart superior mechanical properties on the valve leaflets.[4] Glutaraldehyde was previously in widespread use as a tanning agent although now this is restricted to only very demanding applications of leather such as car dashboards.

It has been shown that glutaraldehyde treated bovine pericardium from neonatal animals has a higher strength than from adult animals and this has been ascribed to the greater degree of orientation of the collagen fibrils in the neonatal material.[5] It has also been shown that glutaraldehyde treatment of pericardium causes a more networked structure to form, thereby reducing the degree of orientation of collagen fibrils.[6] It has not been previously determined whether the young and old native bovine pericardia have the same relationship of more oriented collagen fibrils in the young material than the old as is seen in the glutaraldehyde treated material.

It could be expected that the amount of cross linking that can occur between collagen in young and old pericardium tissue with glutaraldehyde treatment would be different. It has been observed that skin from old animals has more natural cross linking than skin from young animals.[7–9] Ageing of collagen tissues with increased cross linking results in differences in physical properties. The differences in thermal stability of tendon collagen of steers aged 24–30 months and bulls aged 5 years old have been attributed to increased level of maturity and thermally stable cross links.[10] Glycation of collagen increases with age and has been shown to increase stiffness in connective tissues[7] and collagen gels,[11] and increase brittleness in bones.[12] The cross links are in the form of histidinohydroxylysinonorleucine or hexosyl-lysine links in young tissue but then with increasing glycation cross-links as the tissue ages.[7] Glutaraldehyde forms linkages between collagen fibrils by a variety of routes beginning with the reaction of lysine or hydroxylysine amino acid residues of the polypeptide chains to form Schiff base intermediates.[13]

*Author to whom correspondence should be addressed.

Both natural and glutaraldehyde cross links target the lysine or hydroxylysine residues. Therefore if neonatal or adult pericardia have a different propensity to form cross linkages with glutaraldehyde, it might be expected that the amount of structural change in these two tissues upon treatment might be different. To reverse the perspective, a study of the differences in the structural changes in pericardium post glutaraldehyde treatment may be indicative of differences in the cross linking behaviour of pericardium.

Pericardium is a fibrous collagen extracellular matrix material with structural similarities to dermis. Small angle X-ray scattering can be applied to provide quantitative measures of collagen fibril orientation and fibril D-spacing.[14–16] There is a function-structure relationship between collagen alignment and mechanical strength.[17] The orientation of collagen measured edge-on (alignment in-plane) has been shown in skin across a range of mammal species to be correlated with strength.[18–20]

The primary focus of the work presented here is to understand the differences in the effect on the collagen structural arrangement of young and old bovine pericardium tissues when treated with glutaraldehyde for medical applications of these materials. The secondary interest is to learn more about the ability of collagen in pericardium to cross link and the consequences of cross linking with age in general.

RESEARCH ARTICLE

2. METHODS

2.1. Fresh Pericardia Samples

Fresh adult and neonatal bovine pericardia were obtained from Southern Lights Biomaterials and stored in phosphate-buffered saline (PBS) solution (Lorne Laboratories Ltd.). The pericardia were rinsed in PBS solution, and rectangular samples of approximate dimensions $45–50 \times 15$ mm were cut from regions containing both the right and left ventricle and atrium of the ventricular side of the pericardium with the long axis taken from the long axis of the heart (base to apex direction) as shown in Figure 1. The pericardia were then decellularized for 24 h at 4 °C in a 1% octylphenol ethylene oxide condensate (Triton X-100, Sigma), 0.02% EDTA solution made up in PBS. The samples were then rinsed in PBS buffer and stored in PBS. Samples in this state are referred to as "native." It has been suggested the ideal sample selection site is near the left ventricle close to the apex due to higher consistencies in fibril alignment, however the exact location of these so called ideal sites, sizes of these sites and fibril orientations have been stated to vary between different sacs of the same species and age;[21] due to the requirement of multiple samples from one pericardium and regional structural differences, all samples were taken from the same region in the pericardia and randomly assigned to further treatments. All samples were taken from one pericardium (either the adult or neonatal) and randomly assigned to either native treatment or glutaraldehyde treatment with the exception of the adult edge-on samples, originating from a second adult pericardium.

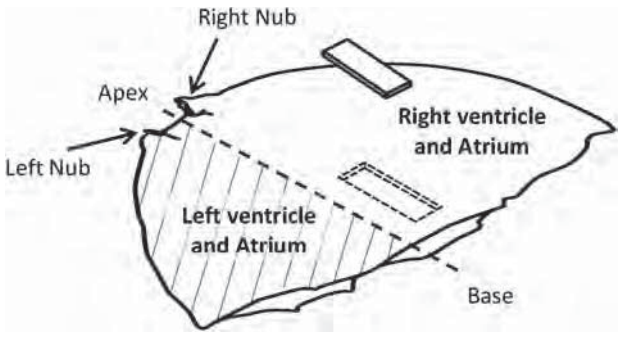

Fig. 1. Ventricular side of pericardium showing sample selection area.

2.2. Glutaraldehyde Treatment

The adult and neonatal native pericardia were incubated in a 0.6% glutaraldehyde solution made up in PBS buffer at 4 °C for 24 h with constant agitation.[22] They were then stored in a sealed container in a solution of the same composition for 12 days, before being rinsed and stored in PBS until SAXS measurements were performed. The total time in storage was approximately 18 days.

2.3. SAXS Analysis

The native and glutaraldehyde adult and neonatal pericardia samples were removed from the PBS solutions, mounted on a metal plate (Fig. 2(a)) and diffraction patterns recorded while the samples were wet. Care was taken to ensure the pericardium stayed wet (free water) throughout the diffraction pattern collection by sealing the samples with Kapton tape (Kapton tape doesn't interfere with the diffraction pattern). The samples were mounted either flat-on (Fig. 2(b)), or edge-on (Fig. 2(c)). Because the pericardium is thin (approximately 0.5 mm), the samples to be measured edge-on were mounted between two rigid polymer strips to ensure the X-ray beam penetrated edge on through the sample parallel to the pericardium surface.

The diffraction patterns were recorded on the Australian Synchrotron SAXS/WAXS beamline, utilizing a high-intensity undulator source. Energy resolution of 10^{-4} (i.e., 1×10^{-4} Å for 1 Å radiation) was obtained from a cryo-cooled Si(111) double-crystal monochromator and the beam size (FWHM focused at the sample) was 250×130 μm, with a total photon flux of about 2×10^{12} ph/s. All diffraction patterns were recorded with an X-ray energy of 12 keV using a Pilatus 1 M detector with an active area of 170×170 mm and a sample-to-detector distance of 3371 mm. Exposure times for diffraction patterns were around 1 s. Diffraction patterns were recorded with the X-rays two different directions relative to the sample—normal to the surface of the pericardium and edge-on to the surface (Fig. 3). A grid of approximately nine points

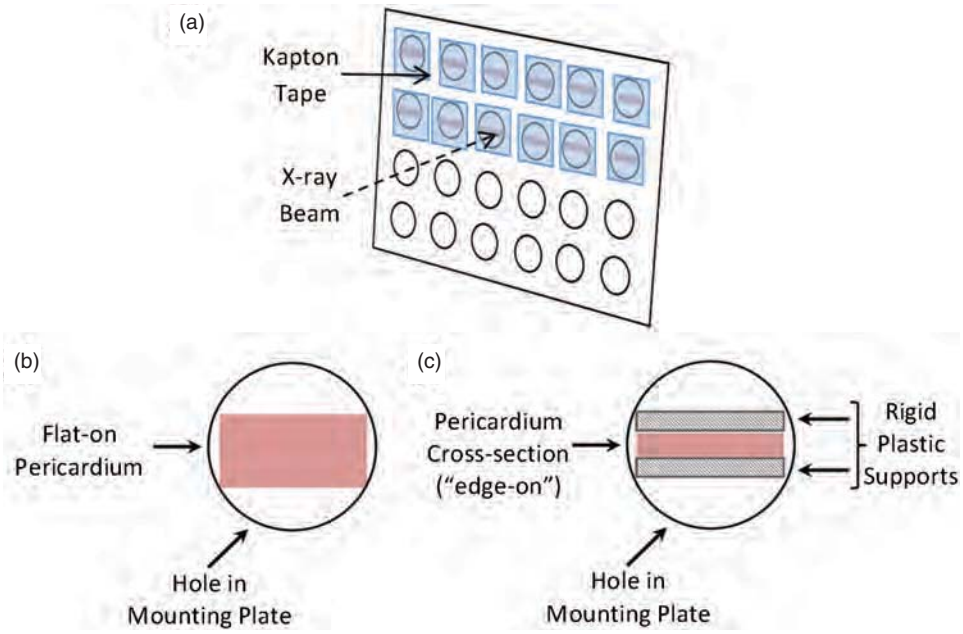

Fig. 2. Mounting of the pericardium samples: (a) metal mounting plate showing holes for the samples and direction of the X-ray beam relative to the mounting plate; (b) mounting of flat-on pericardium samples; (c) mounting of the edge-on pericardium samples between rigid plastic supports in the metal plate.

(nine scattering patterns) were collected for each of the flat-on samples, whilst three lines each consisting of approximately six points (six scattering patterns) were collected along the cross-section for each edge-on sample, so total sample exposure times did not exceed 9 s and 18 s for the flat and edge-on samples respectively. Mapping of the grids was made possible by the use of a camera setup in the control room, allowing accurate selection of data points and maintenance of the beam on the sample, whilst ensuring regions of the pericardium were not re-exposed to the X-ray beams. No beam damage was detected at this exposure time (in separate repeated exposure tests).

Data processing was carried out using the software scatterBrain Analysis V2.71.[23] The fifth order D-period peak was used to calculate orientation index (OI) and D-spacing. Background subtraction for the peak used a logarithmic background over the small q range of the peak at each azimuthal angle. The spread in collagen fibril orientation was quantified using an OI, where an OI of 1 indicates the fibrils are similarly oriented (parallel), and an OI of 0 indicates the fibrils are isotropically orientated. OI is defined as $(90° - OA)/90°$, where OA is the minimum azimuthal angle range that contains 50% of the fibrils, based on the method of Sacks for light scattering[24] but converted to an index,[18] using the spread in azimuthal angle of one or more D-spacing diffraction peaks.

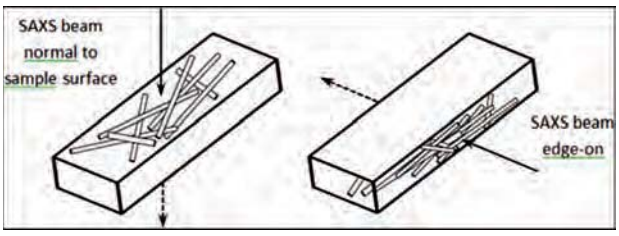

Fig. 3. Experimental setup: (a) measurement with X-rays normal to the surface which provides information on the collagen fibril orientation in the plane of the tissue; (b) measurement with X-rays edge-on to the sample which provides information on the layering of collagen fibrils in the tissue.

From each scattering pattern the OI was calculated from the azimuthal spread of the 5th order collagen diffraction peak at around 0.048 $Å^{-1}$. This provides an OI that represents the spread of collagen fibrils as viewed on a surface (normal X-ray measurement) and an OI that represents the extent to which the fibrils are stacked in layers (the edge-on measurement).

Two native and two glutaraldehyde-treated neonatal samples, and four native and three glutaraldehyde-treated adult samples were analysed normal to the sample surface. For the edge-on OI measurements, one native neonatal and two of each native adult, glutaraldehyde-treated neonatal and glutaraldehyde-treated adult samples were analysed.

3. RESULTS

The pericardium gave clear scattering patterns with well-defined diffraction peaks due to the collagen D-spacing (Figs. 4(a and b)). From the variation of intensity with azimuthal angle (Fig. 4(d)) the orientation index was calculated (Table I).

The adult pericardium in its native state has a lower OI than the neonatal pericardium for both normal to the surface and edge-on measurements, in line with previous

RESEARCH ARTICLE

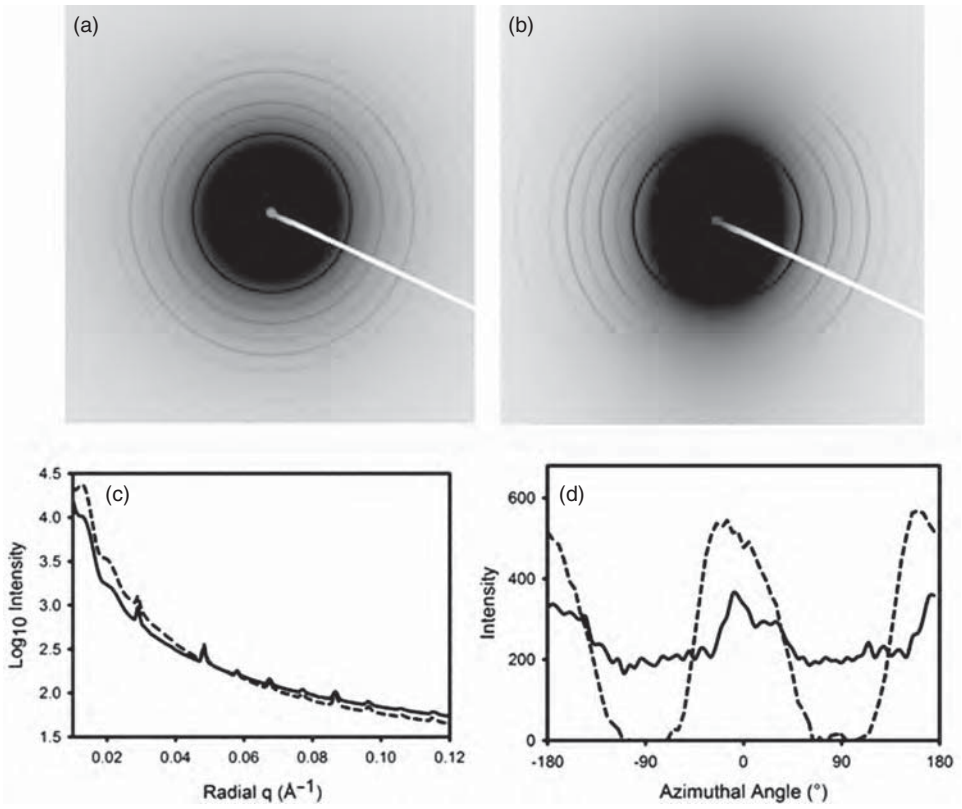

Fig. 4. (a) Representative normal to the sample surface scattering pattern of pericardium; (b) representative edge-on scattering pattern of pericardium; (c) integrated intensity of the scattering pattern: —, normal to the sample surface; - - - -, edge-on; (d) scattering intensity with azimuthal angle for the 5th order collagen diffraction peak at 0.048 A^{-1}: —, normal to the sample surface; - - - -, edge-on.

RESEARCH ARTICLE

Table I. Orientation indices for the native and glutaraldehyde-treated neonatal and adult pericardia samples measured with X-rays both normal to the pericardium face and edge-on. Each diffraction pattern was taken from a separate position.

SAXS measurement type	Sample age and treatment type	No. of pericardia	No. of diffraction patterns analysed (N)	Mean OI	95% confidence interval
Normal to surface	Adult native	1	36	0.19	0.02
	Adult glutaraldehyde-treated	1	27	0.12	0.02
	Neonatal native	1	17	0.40	0.06
	Neonatal glutaraldehyde-treated	1	17	0.24	0.04
Edge-on	Adult native	1	10	0.47	0.04
	Adult glutaraldehyde-treated	1	13	0.33	0.03
	Neonatal native	1	7	0.61	0.07
	Neonatal glutaraldehyde-treated	1	4	0.56	0.04

Table II. *t*-test with $\alpha = 0.05$ for differences in orientation indices between native and glutaraldehyde-treated samples for neonatal and adult tissues, and both normal to the pericardium face and edge-on.

SAXS measurement type	Samples compared	Mean OI	*t*-value	Two tailed *P*-value	Different
Normal to surface	Adult native versus glutaraldehyde-treated	0.19; 0.12	0.19	<0.001	Yes
	Neonatal native versus glutaraldehyde-treated	0.40; 0.24	5.07	<0.001	Yes
Edge-on	Adult native versus glutaraldehyde-treated	0.47; 0.33	5.31	<0.001	Yes
	Neonatal native versus glutaraldehyde-treated	0.61; 0.56	2.03	0.07	No
Normal to surface	Neonatal native versus adult native	0.40; 0.19	8.84	<0.001	Yes
	Neonatal glutaraldehyde-treated versus adult glutaraldehyde-treated	0.24; 0.12	6.03	<0.001	Yes
Edge-on	Neonatal native versus adult native	0.61; 0.47	3.93	=0.001	Yes
	Neonatal glutaraldehyde-treated versus adult glutaraldehyde-treated	0.56; 0.33	10.44	<0.001	Yes

studies[6, 25] (Table I). After glutaraldehyde treatment this relationship is maintained so that the adult pericardium has a lower OI than neonatal pericardium in the cross linked glutaraldehyde treated material. These differences are statistically significant (Table II). There is a change in OI for both adult and neonatal pericardium on glutaraldehyde treatment, with a more isotropic structure developing with treatment (with the exception of the neonatal edge on measurements where the difference is not statistically significant, possibly due to the small sample size for this comparison). This change in OI is a decrease of 39% for the adult pericardium and a decrease of 41% for the neonatal pericardium (with X-rays normal to the surface) or 30% for adult pericardium with X-rays edge-on.

4. DISCUSSION

It is apparent that the young pericardium has a more aligned structure than the older pericardium, as has been seen previously.[5] These differences apply both with the edge-on X-ray measurements and with the measurements taken normal to the surface. The edge-on measurements represent the extent to which the fibrils are stacked in layers, with the neonatal pericardium having a more layer structure with less crossover between the layers. This has been shown to result in greater strength for pericardium[5] but also for a range of leathers made from dermal material[26] and acellular dermal materials for medical scaffolds made from a range of animals including human skin.[27] However, when this structure is too layered with insufficient connection between the layers, in leather this results in a defect known as looseness where failure occurs between the layers.[28, 29] While such an effect has not been reported in other materials than leather it is apparent that some connection is necessary between layers of any tissue in order to maintain structural integrity.

The effect of glutaraldehyde cross linking on the collagen structure in both neonatal and adult bovine pericardia is very similar. In both materials the collagen develops a more isotropic arrangement with glutaraldehyde treatment. We have previously proposed that a decrease in OI from glutaraldehyde cross linking is the result of the formation of more of a networked structure where the formation of cross links via glutaraldehyde addition progressively constrains the fibrils into a random network.[6] However we can now draw two further inferences from the comparison of young and old pericardium, native and cross linked.

It can be inferred that a comparison of the relative OI values in glutaraldehyde treated materials will reflect the relative OI values in the native materials. Previously, a relationship had been established between the OI measured edge-on and the strength of the material for glutaraldehyde treated pericardium[5, 25] and for tanned leather.[18, 20] However, it had not been determined whether this structure-strength relationship also applied to the untreated materials. However, here we have shown that the relative degree of orientation is preserved after cross linking even while there is a significant change in structure. Therefore, it is likely that the relationships between orientation and strength applies to native materials or materials that have not been cross linked, such as many other heterograft materials.[30]

It may also be inferred that the capacity of pericardium to be cross linked by glutaraldehyde may be similar in both neonatal and adult pericardium. We speculate, based on the observation that the amount of structural change is similar, that the number of sites available for glutaraldehyde cross linking may be similar in neonatal and adult pericardium. This may also apply to other tissues. This is despite probable initial differences in the amount of natural cross links present. Although the actual amount of cross linking by glutaraldehyde has not been determined directly here, the consequences of the cross linking on the structure, making it more isotropic, has been determined. This is perhaps more important than a knowledge of the number of cross links as the structure is closely related to the mechanical properties of the materials.[30]

It should be noted that even though the change in OI of the collagen in the pericardium as a result of glutaraldehyde treatment is not dependent on the age of the animal from which the pericardium came, the structural arrangement of collagen fibrils in young and old pericardium is quite different. The young material has a higher OI. As described previously, this difference in the edge-on measured OI is responsible for the higher thickness normalised strength of the neonatal material.[6, 20]

The discovery that the relative structural differences between neonatal and adult pericardium are maintained after glutaraldehyde treatment means that it is possible to assess the differences in structure of native tissues and from these structures to predict the structures of the glutaraldehyde treated processed materials for medical applications.

In conclusion the structural arrangement of collagen in bovine pericardium from neonatal and adult animals was analysed by SAXS before and after treatment with glutaraldehyde. Neonatal pericardium had a more aligned structure than adult pericardium. This relationship was true for both untreated and glutaraldehyde treated material. Glutaraldehyde treatment resulted in a change in the structure to a more isotropic arrangement of the collagen fibrils. The extent of this change is similar in both neonatal and adult pericardium. We speculate that the number of sites available for glutaraldehyde cross linking may be similar in both neonatal and adult pericardium and by implication in other tissues, despite probable initial differences in the amount of natural cross linking present. For the application of pericardium as a medical biomaterial we have shown that both young and old sourced pericardium undergo similar changes on glutaraldehyde treatment, maintaining relative differences between the starting materials.

Declaration of Interest

The authors report no conflicts of interest.

Acknowledgments: This research was undertaken on the SAXS/WAXS beamline at the Australian Synchrotron, Victoria, Australia. Southern Lights Biomaterials supplied the pericardium. The Australian synchrotron is acknowledged for beamtime and travel funding. A Massey University Vice-Chancellor's scholarship supported HRK.

References and Notes

1. N. Nwaejike and R. Ascione, Mitral valve repair for disruptive acute endocarditis: Extensive replacement of posterior leaflet with bovine pericardium. *J. Card. Surg.* 26, 31 **(2011)**.
2. J. M. G. Paez, A. C. Sanmartin, E. J. Herrero, I. Millan, A. Cordon, A. Rocha, et al., Durability of a cardiac valve leaflet made of calf pericardium: Fatigue and energy consumption. *J. Biomed. Mater. Res. Part A* 77A, 839 **(2006)**.
3. A. Cribier, H. Eltchaninoff, C. Tron, A. Bash, N. Borenstein, E. Bauer, et al., Percutaneous artificial cardiac valves: From animal experimentation to the first human implantation in a case of calcified aortic stenosis. *Arch. Mal. Coeur. Vaiss.* 96, 645 **(2003)**.
4. D. T. Cheung and M. E. Nimni, Mechanism of crosslinking of proteins by glutaraldehyde 2. Reaction with monomeric and polymeric collagen. *Connect Tissue Res. 1982* 10, 201 **(1982)**.
5. K. H. Sizeland, H. C. Wells, J. J. Higgins, C. M. Cunanan, N. Kirby, A. Hawley, et al., Age dependant differences in collagen fibril orientation of glutaraldehyde fixed bovine pericardium. *BioMed. Res. Int.* 2014, 189197 **(2014)**.
6. H. R. Kayed, K. H. Sizeland, N. Kirby, A. Hawley, S. T. Mudie, and R. G. Haverkamp, Collagen cross linking and fibril alignment in pericardium. *RSC Adv.* 5, 3611 **(2015)**.
7. A. J. Bailey, Molecular mechanisms of ageing in connective tissues. *Mech. Ageing Devel.* 122, 735 **(2001)**.
8. J. M. Haus, J. A. Carrithers, S. W. Trappe, and T. A. Trappe, Collagen, cross-linking, and advanced glycation end products in aging human skeletal muscle. *J. Appl. Physiol.* 103, 2068 **(2007)**.
9. C. Couppe, P. Hansen, M. Kongsgaard, V. Kovanen, C. Suetta, P. Aagaard, et al., Mechanical properties and collagen cross-linking of the patellar tendon in old and young men. *J. Appl. Physiol.* 107, 880 **(2009)**.
10. T. L. Willett, R. S. Labow, I. G. Aldous, N. C. Avery, and J. M. Lee, Changes in collagen with aging maintain molecular stability after overload: Evidence From an *In Vitro* tendon model. *J. Biomech. Eng-Trans. ASME* 132 **(2010)**.
11. M. E. Francis-Sedlak, S. Uriel, J. C. Larson, H. P. Greisler, D. C. Venerus, and E. M. Brey, Characterization of type I collagen gels modified by glycation. *Biomaterials* 30, 1851 **(2009)**.
12. D. J. Leeming, K. Henriksen, I. Byrjalsen, P. Qvist, S. H. Madsen, P. Garnero, et al., Is bone quality associated with collagen age? *Osteoporosis Int.* 20, 1461 **(2009)**.
13. L. H. H. O. Damink, P. J. Dijkstra, M. J. A. Van Luyn, P. B. Van Wachem, P. Nieuwenhuis, and J. Feijen, Glutaraldehyde as a crosslinking agent for collagen-based biomaterials. *J. Mater. Sci-Mater. M.* 6, 460 **(1995)**.
14. J. Liao, L. Yang, J. Grashow, and M. S. Sacks, Molecular orientation of collagen in intact planar connective tissues under biaxial stretch. *Acta Biomater.* 1, 45 **(2005)**.
15. P. P. Purslow, T. J. Wess, and D. W. L. Hukins, Collagen orientation and molecular spacing during creep and stress-relaxation in soft connective tissues. *J. Exp. Biol.* 201, 135 **(1998)**.
16. M. M. Basil-Jones, R. L. Edmonds, T. F. Allsop, S. M. Cooper, G. Holmes, G. E. Norris, et al., Leather structure determination by small angle X-ray scattering (SAXS): Cross sections of ovine and bovine leather. *J. Agric. Food Chem. 2010* 58, 5286 **(2010)**.
17. P. Fratzl and R. Weinkamer, Nature's hierarchical materials. *Prog. Mater. Sci.* 52, 1263 **(2007)**.
18. M. M. Basil-Jones, R. L. Edmonds, S. M. Cooper, and R. G. Haverkamp, Collagen fibril orientation in ovine and bovine leather affects strength: A small angle X-ray scattering (SAXS) study. *J. Agric. Food Chem.* 59, 9972 **(2011)**.
19. M. M. Basil-Jones, R. L. Edmonds, G. E. Norris, and R. G. Haverkamp, Collagen fibril alignment and deformation during tensile strain of leather: A small-angle X-ray scattering study. *J. Agric. Food Chem.* 60, 1201 **(2012)**.
20. K. H. Sizeland, M. M. Basil-Jones, R. L. Edmonds, S. M. Cooper, N. Kirby, A. Hawley, et al., Collagen alignment and leather strength for selected mammals. *J. Agric. Food Chem.* 61, 887 **(2013)**.
21. E. D. Hiester and M. S. Sacks, Optimal bovine pericardial tissue selection sites. I. Fiber architecture and tissue thickness measurements. *J. Biomed. Mater. Res.* 39, 207 **(1998)**.
22. P. R. Umashankar, T. Arun, and T. V. Kumari, Short duration gluteraldehyde cross linking of decellularized bovine pericardium improves biological response. *J. Biomed. Mat. Res. A* 97A, 311 **(2011)**.
23. D. Cookson, N. Kirby, R. Knott, M. Lee, and D. Schultz, Strategies for data collection and calibration with a pinhole-geometry SAXS instrument on a synchrotron beamline. *J. Synchrotron Radiat.* 13, 440 **(2006)**.
24. M. S. Sacks, D. B. Smith, and E. D. Hiester, A small angle light scattering device for planar connective tissue microstructural analysis. *Ann. Biomed. Eng.* 25, 678 **(1997)**.
25. H. R. Kayed, K. H. Sizeland, N. Kirby, A. Hawley, S. T. Mudie, and R. G. Haverkamp, Collagen fibril strain, recruitment and orientation for pericardium under tension and the effect of cross links. *RSC Adv.* 5, 103703 **(2015)**.
26. K. H. Sizeland, M. M. Basil-Jones, R. L. Edmonds, S. M. Cooper, N. Kirby, A. Hawley, et al., Collagen orientation and leather strength for selected mammals. *J. Agric. Food Chem.* 61, 887 **(2013)**.
27. H. C. Wells, K. H. Sizeland, N. Kirby, A. Hawley, S. Mudie, and R. G. Haverkamp, Collagen fibril structure and strength in acellular dermal matrix materials of bovine, porcine and human origin. *ACS Biomat. Sci. Eng.* 1, 1026 **(2015)**.
28. H. C. Wells, G. Holmes, and R. G. Haverkamp, Looseness in bovine leather: Microstructural characterization. *J. Sci. Food Agric.* 96 **(2015)**.
29. H. C. Wells, G. Holmes, and R. G. Haverkamp, Early detection of looseness in bovine hides using ultrasonic imaging. *J. Am. Leather Chem. As.* 111, 107 **(2015)**.
30. H. C. Wells, K. H. Sizeland, N. Kirby, A. Hawley, S. Mudie, and R. G. Haverkamp, Collagen fibril structure and strength in acellular dermal matrix materials of bovine, porcine and human origin. *ACS Biomat. Sci. Eng.* **(2015)**.

Received: xx Xxxx xxxx. Accepted: xx Xxxx xxxx.

RESEARCH ARTICLE

8.2 Appendix B: Poster Presentations

8.2.1 List of Poster Presentations

1. **Kayed, H. R.,** Sizeland, K. H., Kirby, N., Hawley, A., Mudie, S., & Haverkamp, R. G. "Cross Linking Collagen Affects Fibril Orientation." Poster presented at the Australian Synchrotron Users Meeting, Melbourne, Australia, 21st-22nd November, 2013.

2. Wells, H. C., **Kayed, H.R.**, Sizeland, K. H., Edmonds, R. L., Kirby, N., Hawley, A., Mudie, S., & Haverkamp, R. G. "Poisson Ratio of Collagen Fibrils." Poster presented at the 1st Matrix Biology Europe Conference, Rotterdam, Netherlands, 21st-24th June 2014.

3. Wells, H. C., Sizeland, K. H., **Kayed, H. R**., Kirby, N., Mudie, S., & Haverkamp, R. G. "Poisson Ratio of Collagen Fibrils Measured by SAXS." Poster presented at the Fourth International Conference on Multifunctional, Hybrid, and Nanomaterials, Barcelona, Spain, 9th-13th March, 2015.

4. Sizeland, K. H., Haverkamp, R. G., Wells, H. C., **Kayed, H. R.**, Edmonds, R. L., Kirby, N., Hawley, A., & Mudie, S. "Strength in Collagen Biomaterials." Poster presented at the Fourth International Conference on Multifunctional, Hybrid, and Nanomaterials, Barcelona, Spain, 9th-13th March, 2015.

5. Sizeland, K.H., **Kayed, H.R.**, Wells, H.C., Kirby, N., Hawley, A., Mudie, S., Edmonds, R. L., & R. G. Haverkamp. "Nanostructural Analysis of Bioengineered Tissues for Enhanced Performance." Poster presented at the 9th Annual CIGR Section VI International Technical Symposium, Massey University, Albany Campus, Auckland, New Zealand, 16th – 20th November 2015.

6. **Kayed, H.R.,** Kirby, N., Hawley, A., Mudie, S.T., & Haverkamp, R.G. "The role of cross links on collagen fibril orientation in pericardium." Poster presented at The International Chemical Congress of Pacific Basin Societies, Honolulu, Hawaii, 15-20th December, 2015.[4]

7. Wells, H.C., Sizeland, K.H., **Kayed, H.R.**, Kirby, N., Hawley, A., Mudie, S., & Haverkamp, R.G. "Poisson Ratio of Collagen Fibrils under Tension." Poster presented at The

[4] This poster presentation was awarded a Student Poster Competition Award at the International Chemical Congress of Pacific Basin Societies, Honolulu, Hawaii, 15-20th December, 2015.

International Chemical Congress of Pacific Basin Societies, Honolulu, Hawaii, 15-20th December 2015.

8. Haverkamp, R.G., Sizeland, K.H., Wells, H.C., & **Kayed, H. R.** "Strength in Collagen Materials." Poster presented at the Materials Research Society Spring Meeting, San Francisco, USA, 2015.

8.2.2 Poster Abstracts

1. Cross Linking Collagen Affects Fibril Orientation

Kayed, H. R.,[1] Sizeland, K. H.,[1] Kirby, N.,[2] Hawley, A.,[2] Mudie, S.,[2] & Haverkamp, R. G.[1]

[1]School of Engineering and Advanced Technology, Massey University, Palmerston North, New Zealand;
[2]Australian Synchrotron, Melbourne, Australia

Bovine pericardium is treated with the cross linking agent glutaraldehyde before being used for heart valve repair in cardiovascular surgery. Glycosaminoglycan (GAG) cross links are inherent in pericardium and other collagen tissues. Further cross linking with glutaraldehyde has been reported to increase the mechanical properties of the tissue. Small angle X-ray scattering (SAXS) was used to characterise the nanostructure of a pericardium tissue with different degrees of cross linking to investigate the effect of cross links on pericardium structure. These different tissues were those with removed cross links; pericardium with natural cross links (GAGs); and pericardium with GAGs plus glutaraldehyde cross links. The integrated SAXS patterns of the pericardium under no tension were used to determine the alignment of fibrils within the tissue, reported as an orientation index (OI). Dramatic differences in fibril alignment with the degree of cross linking were found. Decreasing the cross linking increases the OI, and synthetically adding cross links decreases fibril orientation significantly. Pericardium with removed cross links, natural cross links and added glutaraldehyde cross links were found to have OI of 0.25, 0.54 and 0.77 respectively. We suggest progressive addition of cross links constrains the fibrils to form a random and more isotropic network.

2. Poisson Ratio of Collagen Fibrils

Wells, H. C.,[1] Kayed, H.R.,[1] Sizeland, K. H.,[1] Edmonds, R. L.,[2] Kirby, N.,[3] Hawley, A.,[3] Mudie,S.,[3] & Haverkamp, R. G.[1]

[1]School of Engineering and Advanced Technology, Massey University, Palmerston North, New Zealand;
[2]Leather and Shoe Research Association, Palmerston North, New Zealand;
[3]Australian Synchrotron, Melbourne, Australia

The main structural component of skin and tendons is type I collagen. These tissues are elastic and deform reversibly under stress. The mechanical properties of individual collagen fibrils contribute to the mechanical properties of the tissues which they comprise. We have used synchrotron based small angle X-ray scattering to investigate the deformation of collagen fibrils during stress in pericardium. Fibril diameter is calculated from the scattering pattern and fibril elongation is calculated from the diffraction peaks resulting from the d-spacing. As collagen fibrils are stretched their density increases. We are able to determine the Poisson ratio for collagen fibrils. This knowledge may be incorporated into models of the macrolevel behaviour of tissues.

3. Poisson Ratio of Collagen Fibrils Measured by SAXS

Wells, H. C.,[1] Sizeland, K. H.,[1] Kayed, H. R.,[1] Kirby, N.,2 Hawley, A.,[2] Mudie, S.,[2] & Haverkamp, R. G.[1]

[1]School of Engineering and Advanced Technology, Massey University, Palmerston North, New Zealand
[2]Australian Synchrotron, Melbourne, Australia

Tendon, skin and skin products are primarily composed of the fibrous protein, type I collagen. Collagen provides strength and stability in biological tissues and therefore the structure and mechanical properties of collagen are important in understanding the overall behaviour of the tissues. While the bulk tissues themselves have been well characterized in terms of mechanical properties, little is known about the mechanical properties of the individual collagen fibrils. To determine the behaviour of collagen fibrils we have carried out an investigation using synchrotron based small angle X-ray scattering (SAXS) on bovine pericardium under stress. From the SAXS diffraction patterns the fibril diameter is calculated and the fibril elongation is calculated from the diffraction peaks that result from the collagen d-spacing. The tissue is strained 0.25 (25%) with a corresponding strain in the collagen fibrils of 0.045 observed. There are two stages in the collagen fibril structure that we observe while increasing strain. The first stage, at low strain (up to about 0.09) we observe a decrease in fibril diameter, a small increase in d-spacing and a large increase in OI. During this initial stage, the strain is taken up by the reorientation of fibrils and removal of crimp in the fibrils. The second stage involves only a small change in OI but the d-spacing increases significantly and the fibril diameter decreases. This indicates there is an increase in stress on each of the individual fibrils during this stage. At a tissue strain above 0.15 the fibrils continue to be stretched however the fibrils no longer decrease in diameter. We are able to determine the ratio of collagen fibril width contraction to length extension, or Poisson ratio, for collagen fibrils from the changes in fibril diameter and d-spacing observed. The Poisson ratio, corrected for a rod shape, can be calculated using the equation:

$$v' = -\frac{\sqrt{\pi}/2(\frac{\Delta D}{D})}{\Delta L/L}$$

4. Strength in Collagen Biomaterials

Sizeland, K. H.,[1] Wells, H. C.,[1] Kayed, H. R.,[1] Edmonds, R. L.,[2] Kirby, N.,[3]Hawley, A.,[3] Mudie, S.,[3] & Haverkamp, R. G.[1]

[1]School of Engineering and Advanced Technology, Massey University, Palmerston North, New Zealand
[2]Leather and Shoe Research Association, Palmerston North, New Zealand
[3]Australian Synchrotron, Melbourne, Australia

Natural collagen materials are used in industrial and medical applications; for example leather for shoes and garments, and extra cellular matrix materials for surgical scaffolds. For most applications the strength of the material is a critical performance property. Therefore, an improved understanding of how the structure of these natural and processed materials relates to strength is needed. A range of collagen based materials have been characterised using synchrotron based small angle X-ray scattering (SAXS). The distribution of collagen fibril orientation in a material can be determined from this technique. In leather, fibril orientation in the plane of the leather was found to correlate strongly with the tear strength of the leather. Highly aligned collagen fibrils lead to stronger leather. This is explained by a structural model. Mechanisms of nanostructural response to

strain in leather, medical scaffold material and pericardium were also investigated by these techniques. Collagen fibrils rearrange and then stretch but these behaviours are governed by a number of factors and the response can be altered by chemical and physical treatments. A better understanding of the structure and strain characteristics of collagen biomaterials has resulted and this enables the design of stronger materials for industrial and medical applications.

5. Nanostructural Analysis of Bioengineered Tissues for Enhanced Performance

K. H. Sizeland[1], **H. R. Kayed[1]**, H. C. Wells1, , N. Kirby[2], A. Hawley[2], S. Mudie2, R.L. Edmonds[3], R. G. Haverkamp[1]

[1]Massey University, School of Engineering and Advanced Technology, New Zealand.
[2]Australian Synchrotron, 800 Blackburn Road, Clayton, Melbourne, Australia.
[3]Leather and Shoe Research Association, Palmerston North, New Zealand

Collagen is the main structural component of a number of natural and processed biomaterials. The strength of these materials is often of crucial importance to their final applications. The structural foundation of strength in collagen biomaterials is not fully understood. We used synchrotron based small angle X-ray scattering to investigate the fibril structure of collagen in leather, pericardium, and surgical scaffolds. Samples were put under increasing strain so any structure-strength relationships could be investigated. Atomic force microscopy and histology compliment small angle X-ray scattering. Strong correlations between the strength of collagen biomaterials and fibril orientation have been found and are dependent on tissue type, tissue source, tissue age, and the chemical and mechanical processing of the tissue. These findings provide valuable insight into the basis of strength of bioengineered tissues and will inform future tissue selection and processing to maximise the value created from these animal bioresources.

6. The Role of Cross Links on Collagen Fibril Orientation in Pericardium

Kayed, H.R.,[1] Kirby, N.,[2] Hawley, A.,[2] Mudie, S.T.,[2] and Haverkamp, R.G.[1]

[1]School of Engineering and Advanced Technology, Massey University, Palmerston North 4442, New Zealand
[2]Australian Synchrotron, 800 Blackburn Road, Melbourne, Australia

Collagen biomaterials range in end use from commercial leather to biomedical applications with preferred properties to ensure success in the end application. The nanostructure of such materials imparts their mechanical properties and therefore is important to understand. We investigated the role of natural glycosaminoglycan (GAG) cross links and synthetic glutaraldehyde induced cross links on bovine pericardium structure. Synchrotron based small angle X-ray scattering (SAXS) was used quantify collagen fibril alignment in native tissue, chondroitinase ABC treated tissue to remove GAGs, and glutaraldehyde treated tissue. Picrosirius red staining coupled with cross polarised light microscopy and atomic force microscopy (AFM) provided qualitative assessments to accompany the SAXS data. Collagen fibril cross linking was found to be a factor in collagen fibril alignment; native and chondroitinase ABC treated pericardium exhibit similar fibril orientation indices (OI) of 0.19 and 0.21 respectively, whilst glutaraldehyde treated pericardium shows decreased alignment reflected in an OI of 0.12. This difference in alignment is also seen in the AFM images. We therefore suggest that it is not solely the number of cross links present that affects the structure, it is the nature of the cross links present; glutaraldehyde cross links the collagen fibrils into a more isotropic network structure of multiple orientations, whereas natural GAG links do not appear to constrain the fibrils to this extent, hence, their removal does reveals no change in the fibril alignment.

7. Poisson Ratio of Collagen Fibrils under Tension

Wells, H.C.,[1] Sizeland, K.H.,[1] **Kayed, H.R.**,[1] Kirby, N.,[2] Hawley, A.,[2] Mudie, S.,[2] & Haverkamp, R.G.[1]

[1]School of Engineering and Advanced Technology, Massey University, Palmerston North 4442, New Zealand
[2]Australian Synchrotron, 800 Blackburn Road, Melbourne, Australia

Tendon, pericardium, and skin are all primarily composed of type I collagen. Collagen is a fibrous protein that provides strength and stability to biological tissues. Therefore understanding the mechanical properties of collagen based materials is important for their natural and industrial uses. The properties of these bulk tissues have been widely studied, however the behaviour of the individual collagen fibrils that make up these tissues has not yet been studied.

In order to characterise the mechanical properties of individual collagen fibrils, we carried out measurements using small angled X-ray scattering (SAXS) on bovine pericardium tissue while applying stress. From the generated SAXS diffraction patterns we were able to calculate the diameter and elongation of the fibrils, which we could then use to calculate the Poisson ratio of collagen, and the orientation (OI) of the fibrils.

The tissue was strained up to 25% during data collection, which resulted in an observed strain of 4.5% (0.045) in the collagen fibrils. There appeared to be two distinct stages of changes in fibril structure during tissue strain. Initially, the strain was taken up by the reorientation of the collagen fibrils within the tissue. Secondly, above a strain of 0.09, the stress was mostly taken up by the individual fibrils, causing them to elongate.

From the information generated from SAXS, we determined a Poisson ratio of 2.1 ± 0.7 for collagen. The high Poisson's ratio (> 0.5) indicates a decrease in volume during strain. Previous studies on bulk collagen based materials have also shown high Poisson ratios. This study suggests that the unusual property of collagen based materials of a high Poisson ratio during stress may largely be due to the behaviour of the individual fibrils that make up the tissues.

8. Strength in Collagen Materials

Collagen is the main component of many very robust natural materials and some manufactured materials. The strength of the material is normally one of the key properties required in the natural or technological application. The basis for strength in collagen materials is not fully understood. We used small angle X-ray scattering to investigate the collagen fibril structure in leather, pericardium, and surgical scaffold collagen matrix materials and to compare this with tear strength of these materials. This is combined with atomic force microscopy, histology, electron microscopy and other techniques. We discover a complex relationship between strength and a number of structural factors including fibril orientation, fibril diameter and cross linking. These can be related to tissue type, species, and age of the animal. While the picture is far from complete we have made progress on models for structure and strength in collagen materials that can assist in the preparation of synthetic analogues of natural tissue.

8.2.3 Posters

1. Cross Linking Collagen Affects Fibril Orientation

Australian Synchrotron Users Meeting, Melbourne, Australia
21-22 November 2012

MASSEY UNIVERSITY
TE KUNENGA KI PŪREHUROA

Cross Linking Collagen Affects Fibril Orientation

Hanan R. Kayed†, Katie H. Sizeland†, Nigel Kirby‡, Adrian Hawley‡, Stephen Mudie†, Richard G. Haverkamp†

†School of Engineering and Advanced Technology, Massey University, Palmerston North, New Zealand
‡Australian Synchrotron, Victoria, Australia

1.0 Introduction

Bovine pericardium (BP) is a collagen rich fibrous tissue cross linked with glycosaminoglycans (GAGs). BP is treated with glutaraldehyde prior to use as heart valve replacements in cardiovascular surgeries to stabilise the tissue and reduce its immunogenicity. It is widely believed that glutaraldehyde further cross links collagen and is reported to increase its strength. Understanding the effects of cross links on BP tissue structure is vital in explaining their role on tissue properties which in turn influences their functionality. Small angle X-ray scattering (SAXS) was used to characterise the nanostructure of BP tissue with different degrees of cross linking to investigate the effect of these links on pericardium structure. This study uses SAXS to investigate specifically the alignment of collagen fibrils within BP, reported as an orientation index (OI).

2.0 Experimental Methods

2.1 Materials and processing

This study considered fresh bull (Charolais Cross) pericardium in three different states:

1. Pericardium with removed cross links (chondroitinase ABC treated)
2. Pericardium with natural cross links (GAGs)
3. Pericardium with synthetically added cross links (glutaraldehyde treated)

Samples were processed as depicted in Figure 1.

2.2 SAXS

Hydrated samples were mounted between clamps with the sample flat aligned perpendicular to the X-ray beam (Figure 2 and 3). SAXS scattering patterns were recorded with an X-ray energy of 12 keV using a Pilatus 1 M detector with an active area of 170 × 170 mm and sample-to-detector distance of 2271 mm at the Australian Synchrotron SAXS/WAXS beamline. An X-ray beam size of 250 x 80 µm and total flux of 2 x 10^{11} ph.s^{-1} was used.

3.0 Results and Discussions

Representative X-ray scattering patterns are provided in Figure 3. Examination of these patterns alone reveals significant differences between the differently cross linked tissues; the glutaraldehyde treated pericardium shows even scattering around the diffraction ring (Figure 3a), as scattering is occurring from many directions, suggesting the fibrils are randomly aligned. The chondroitinase treated pericardium shows the other extreme where the Bragg diffraction bands only partially extend a full circle. This results from scattering in a limited angle range, implying higher fibril alignment.

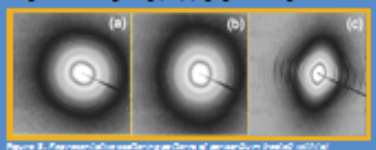

Plotting the variation of intensity with azimuthal angle (Figure 4) is another way of demonstrating the fibril orientation distribution. The width of the peaks in Figure 4 equate to the widths of the diffraction bands in the X-ray scattering pattern so the broader the peak the more isotropic the tissue. From this plot the OI was calculated and falls within the range 0 ≤ OI ≤ 1, where 1 corresponds to highly aligned fibrils and 0 indicates an isotropic material.

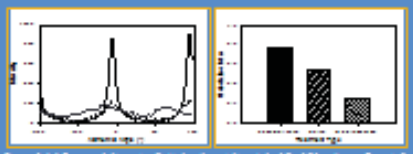

It was found that the OI of the glutaraldehyde, natural and chondroitinase treated pericardium are statistically significantly different at 0.225, 0.528 and 0.770 respectively. Therefore the degree of cross linking in collagenous tissues has a large role in fibril orientation and so nanostructure. Removal of natural GAG links (e.g. via enzyme digestion) causes higher fibril alignment and cross link addition (e.g. via glutaraldehyde treatment) results in a network structure.

We suggest that the natural tendency of fibrils is to align, as did the 'free' fibrils consequent to GAG removal, whilst the addition of synthetic cross links progressively constrains the collagen fibrils into a random network structure.

4.0 Conclusion

Our SAXS experiment on pericardium tissues has highlighted the importance of the role of cross links, both natural and synthetic, in determining tissue nanostructure, specifically in terms of collagen fibril orientation. This cross linking-fibril alignment relationship is likely to have implications on the mechanical properties of pericardium and this knowledge could potentially be useful in the biomedical industry for the preparation and development of new biomaterials.

5.0 Acknowledgements

This research was undertaken on the SAXS/WAXS beamline at the Australian Synchrotron, Victoria, Australia. The NZ Synchrotron Group Ltd is acknowledged for travel funding. Melissa Reid-Jones of Massey University assisted with data collection. John Shannon supplied the pericardium.

2. Poisson Ratio of Collagen FIbrils

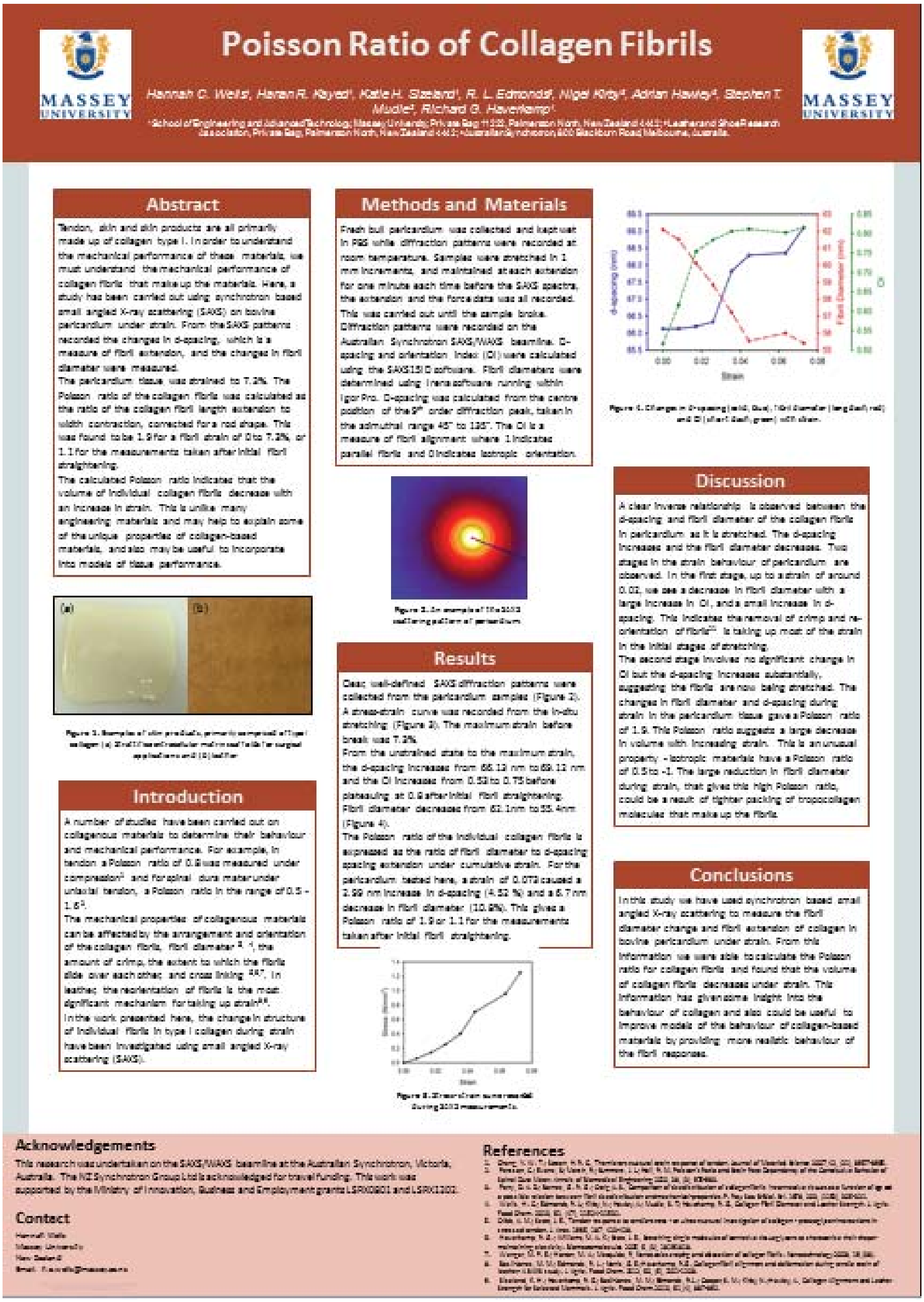

3. Poisson Ratio of Collagen Fibrils Measured by SAXS

Poisson Ratio of Collagen Fibrils Measured by SAXS

Hannah C. Wells[1], Katie H. Sizeland[1], Hanan R. Kayed[1], Nigel Kirby[2], Adrian Hawley[2], Stephen T. Mudie[2], Richard G. Haverkamp[1].

[1]School of Engineering and Advanced Technology, Massey University, Private Bag 11222, Palmerston North, New Zealand 4442; [2]Australian Synchrotron, 800 Blackburn Road, Melbourne, Australia.

Fourth International Conference on Multifunctional, Hybrid and Nanomaterials
9-13th March 2015, Sitges, Spain

Introduction

Type I collagen is the main structural protein of tendon, skin and skin products, providing strength and stability in these biological tissues. The mechanical properties of collagen-based tissues are fundamental to their natural and industrial uses. While the bulk materials have been widely studied, the mechanical properties of the individual collagen fibers that make up these materials have not.

Here we look at the Poisson ratio (ν) of collagen fibrils to characterize the collagen fibril structure and performance in tissue during tension. Previous studies on the bulk tissues have given Poisson ratio values greater than 0.5, indicating the volume of the tissue decreases as it is strained.

We have determined the behavior of collagen fibrils when stress is applied using synchrotron based small angle X-ray scattering (SAXS). Bovine pericardium was used as a collagen source, which was strained up to 25% during data collection.

Methods

SAXS Analysis

Bull pericardium was used as the collagen source for analysis using SAXS. The pericardium was kept fresh in PBS buffer while diffraction patterns were recorded on the SAXS/WAXS beam line at the Australian Synchrotron. The samples were stretched in 1 mm increments and were maintained at each position for one minute before SAXS spectra, the extension and the force were recorded. This was repeated for each sample, until the sample broke.

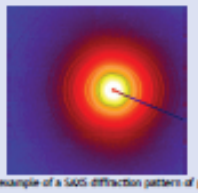

Figure 1. An example of a SAXS diffraction pattern of pericardium

From the recorded diffraction patterns, the d-spacing and orientation index (OI) were determined using saxs1SID software, and the fibril diameters were determined using Irena software running with Igor Pro. The d-spacing is a measure of fibril extension, the OI is a measure of fibril alignment in the bulk material.

Calculating Poisson's Ratio

The Poisson's ratio, ν, is the ratio of transverse strain to longitudinal strain in the loading direction and is calculated from the equation:

$$\nu = \frac{\frac{\Delta W}{W}}{\frac{\Delta L}{L}}$$

Where W is the width of a cube or bar, and L is the length of a cube or bar.

The Poisson ratio for collagen fibrils can be expressed as the ratio of fibril diameter to d-spacing extension under cumulative strain. Since ν is defined for a cube, we corrected the ratio by $\sqrt{\pi}/2$. Therefore, the equation for the Poisson ratio of collagen fibrils becomes:

$$\nu' = \frac{\sqrt{\pi}/2\left(\frac{\Delta D}{D}\right)}{\frac{\Delta L}{L}}$$

Where D is the fibril diameter and L is the d-spacing or fibril extension.

Collagen Structure During Tension

The tissue was strained up to 25%. We observed two stages in the structural changes at the collagen fibril level during strain.

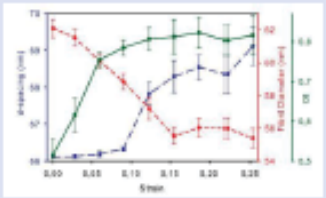

Figure 2. Changes in d-spacing (blue), fibril diameter (red), and orientation index (OI) of the collagen fibrils in pericardium as strain is increased. Figure from Wells et al. (2015) J. Appl. Phys. 117, 044701.

In the first stage (up to strain of 0.09), we notice a decrease in the collagen fibril diameter with a small increase in d-spacing and a large increase in OI. During this phase of strain, most of the strain is taken up by the reorientation of the individual fibrils within the tissue.

The second stage of strain (above 0.09) there is little change in OI, however the d-spacing begins to increase and the fibril diameter decreases. This indicates the stress is now mostly on the individual collagen fibrils. At a strain above 0.15, the fibrils continue to stretch however the change in fibril diameter plateaus.

Poisson's Ratio

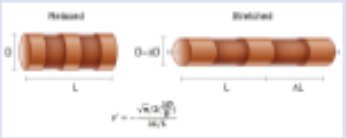

From an unstrained state to maximum strain before rupture, the d-spacing with the fibrils increased 4.5%. The fibril diameter decreased 10.8%. From the changes in d-spacing and fibril diameter, the Poisson's ratio was calculated to be 2.1±0.7 when the tissue is strained up to 25%.

The high Poisson's ratio (>0.5) indicates a volume decrease in the fibrils as the tissue is strained. This could help to explain some of the unique properties of collagen based materials. The high Poisson ration could be explained by tighter packing within the fibril under strain, where there could be compression of hydrogen bonding within the fibril, micro fibril or tropocollagen.

Conclusion

Synchrotron based SAXS has been a useful tool for characterizing the structure of individual collagen fibrils within pericardium tissue, as strain is applied to the tissue. From the SAXS diffraction patterns, the collagen d-spacing (or fibril extension), fibril diameter and orientation of the fibrils were determined and used to calculate the Poisson's ratio of collagen of 2.1 ± 0.7.

Previous studies on collagen based bulk materials have given ν > 0.5 and here we have provided experimental evidence that the individual collagen fibrils may also have ν' > 0.5. This suggests that this property of collagen fibrils may contribute to the bulk properties of tissues.

Acknowledgements

This research was carried out on the SAXS/WAXS beamline at the Australian Synchrotron, Victoria, Australia. The HZ Synchrotron Group Ltd is acknowledged for travel funding. This work was supported by the Ministry of Innovation, Business and Employment.

4. Strength in Collagen Biomaterials

Strength in Collagen Biomaterials

Katie H. Sizeland[1], Hannah Wells[1], Hanan Kayed[1], Richard L. Edmonds[2], Nigel Kirby[3], Adrian Hawley[3], Stephen Mudie[3], and Richard G. Haverkamp[1].

[1]School of Engineering and Advanced Technology, Massey University, Palmerston North, New Zealand 4442, Massey University, Private Bag 11222, Palmerston North 4442, New Zealand. [2]Leather and Shoe Research Association, Palmerston North, New Zealand 4442, [3]Australian Synchrotron, Clayton, Vic 3168, Australia.

Introduction

Collagen I assembles with a complex hierarchical structure and forms the basis of many structural components in animals such as skin, pericardium, and other tissues. The network of collagen fibrils plays a definitive role in the overall physical properties of these biomaterials. By characterising some of the structural features of collagen we can gain a better understanding of how collagen reacts to different chemical and mechanical processes. This knowledge would inform future developments and may enable us to manipulate processes to maximise a material's final physical properties. This has formed the basis of our research where we have utilised small angle X-ray scattering (SAXS) to characterise the collagen structures in pericardium, leather and surgical scaffold materials.

SAXS Analysis

SAXS provides a wealth of useful information that may be used to characterise and compare leathers, skin, and connective tissue. Samples were analysed either statically or under strain. SAXS produces diffraction patterns (Fig. 1a) and the collagen fibril structure is represented by the rings in these patterns. The intensity of the whole pattern is integrated (Fig. 1b) allowing clear identification of each peak's position. From these the d spacing is determined. The orientation index (OI) is calculated from the spread in azimuthal angle around a d-spacing peak, generally we used the sixth order peak at approximately 0.055-0.060 Å^{-1}. The peak area is measured, above a fitted baseline, at each azimuthal angle. These results were analysed and in some experiments were compared with strain, stress and tensile strength results.

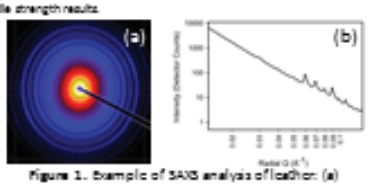

Figure 1. Example of SAXS analysis of leather: (a) raw SAXS pattern; (b) integrated intensity profile.

Pericardium

Heart valve leaflets can be replaced percutaneously with bovine pericardium using adult or neonatal pericardium. The mechanical strength and performance of the material are important properties for a long life in service. Pericardium is a fibrous collagen extracellular matrix similar to skin and other tissues. Neonatal pericardium was found to have a higher modulus of elasticity (82.7 MPa) to adult pericardium (32.5 MPa), a higher tensile strength (22.9 MPa) to adult pericardium (19.1 MPa). The collagen fibrils were found to be far more aligned in neonatal pericardium (OI ~ 0.78) than in adult pericardium (OI ~ 0.62) (Fig. 2).

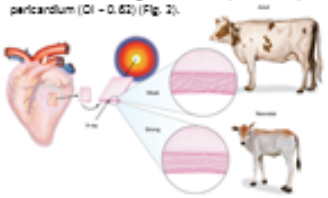

Figure 2. Pericardium, the outside sac of the heart; a weaker material with less aligned fibrils for adult tissue and a stronger material with more aligned fibrils for neonatal tissue.

To achieve high strength, it is thought that the structure of collagen materials requires cross linking of the fibrils to restrict them from sliding past one another. We analysed the structural effects of natural cross linking by glycosaminoglycan (GAG), synthetic cross linking by glutaraldehyde, and the removal of all cross links by chondroitinase ABC. Alignment of the fibrils was found to be affected with the OI of native pericardium (0.19) and the chondroitinase ABC treated pericardium (0.21) being higher than the glutaraldehyde treated pericardium (0.12) (Fig. 3).

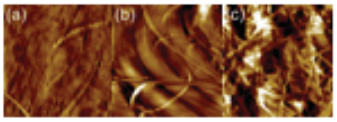

Figure 3. Atomic force microscopy images for (a) native pericardium; (b) chondroitinase ABC treated pericardium; (c) glutaraldehyde treated pericardium.

Leather

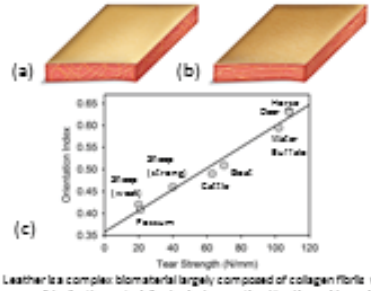

Figure 4. OI of collagen fibrils in edge on ovine leather: (a) low OI, weaker material; (b) high OI, stronger material; (c) Collagen fibril orientation and tear strength for leather from different animals.

Leather is a complex biomaterial largely composed of collagen fibrils which are partly responsible for the material's physical properties. Used in a wide variety of applications, the physical properties exhibited are of importance for both strength and aesthetic reasons. Using SAXS, it has been shown that the fibril orientation strongly correlates with strength in ovine leather; stronger leather has a high OI and weaker leather has a low OI (Fig. 4a and 4b). This correlation was shown to exist across a range of different animals (Fig. 4c). When subjected to strain it has been shown that initially fibres reorient to become more aligned (as seen by an increase in OI) (Fig. 5). Then as the strain increases it is taken up by the individual fibrils (as seen by the d-spacing increase).

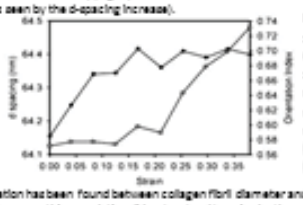

Figure 5. d spacing and OI versus strain measured edge-on for ovine leather. (○) d spacing (●) OI.

A correlation has been found between collagen fibril diameter and tear strength in bovine leather, however this correlation did not extend to ovine leather or across a selection of other animal leathers. Samples were analysed throughout the processing of skin to leather and it was found that the changes in OI are not a fundamental redistribution of fibrils, but rather are due to thickness differences and hydration with a wet sample having a higher OI than a dry sample. A correlation was also found between the amount of fat liquor used in the production of leather and the d spacing such that as the amount of fat liquor increases, the d-spacing of the collagen fibrils also increases.

Surgical Scaffolds

Biomaterials are an implantable mesh that stimulates, supports, and hosts cell colonization of a tissue leading to regeneration. The surgical scaffold must be engineered with suitable biophysical properties to allow for clinical use. An ovine forestomach matrix (Fig. 6) was analysed and determined to retain the native collagen architecture which in turn imparted excellent biophysical properties to this surgical scaffold.

Figure 6. Example of an OFM scaffold material.

Conclusions

We have found SAXS to be a particularly suitable method for the structural analysis of collagen I in a number of biomaterials. We have successfully determined the OI and d spacing of collagen in a number of different experiments and have been able to link these structural features to the strength of the materials too. We hope these findings will lead to the development of processes to maximise the final strength of the material. We plan to continue with our SAXS-based collagen research in the future.

Acknowledgements

This research was supported by grants from the Ministry of Business Innovation and Employment. This research was undertaken on the SAXS/WAXS beamline at the Australian Synchrotron, Victoria, Australia.

MASSEY UNIVERSITY TE KUNENGA KI PŪREHUROA

Ministry of Business, Innovation & Employment

Poster presented at the Fourth International Conference on Multifunctional, Hybrid and Nanomaterials, Barcelona, 9th-13th March 2015.

LASRA®

5. Nanostructural Analysis of Bioengineered Tissues for Enhanced Performance

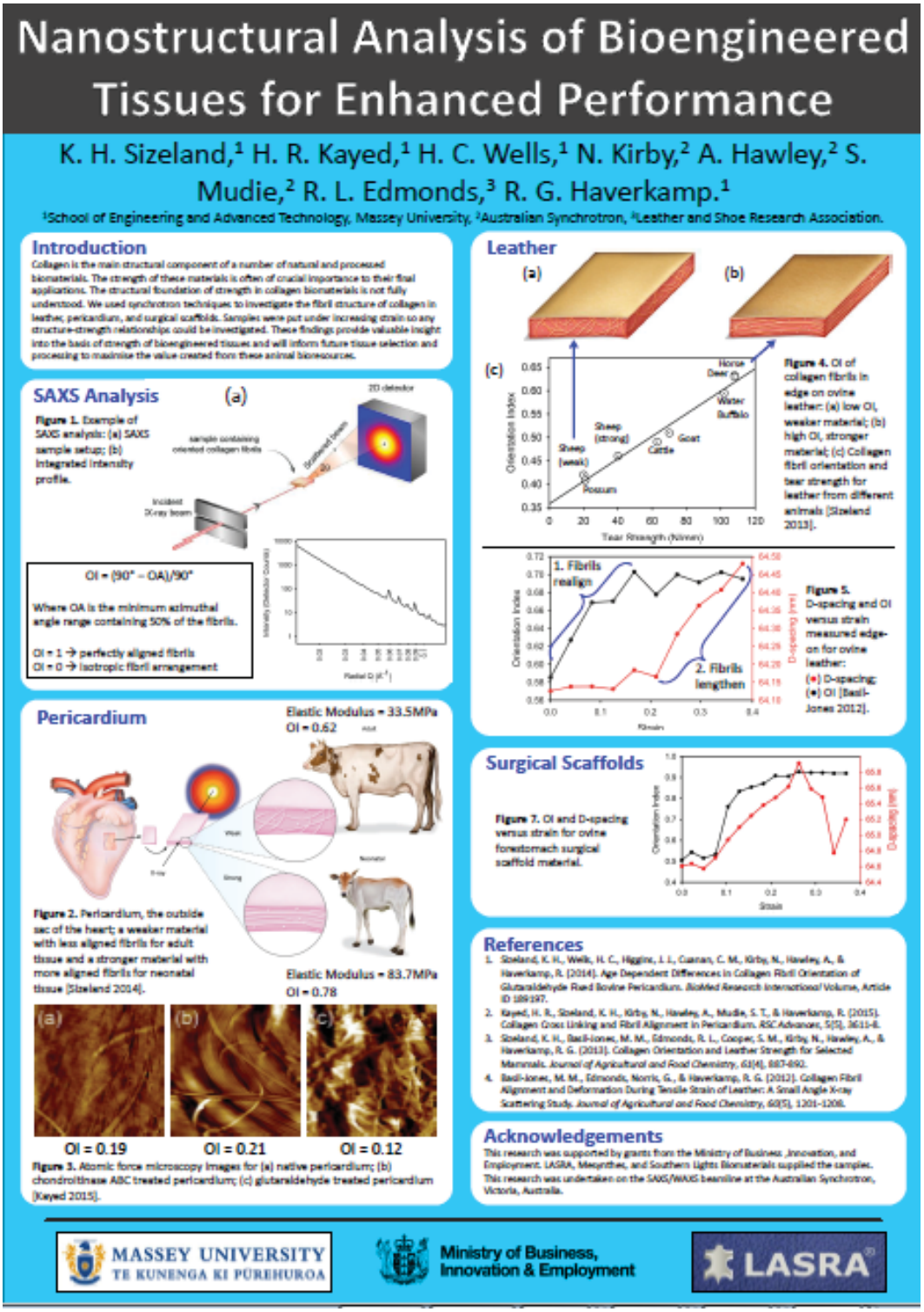

6. The Role of Cross Links on Collagen Fibril Orientation in Pericardium

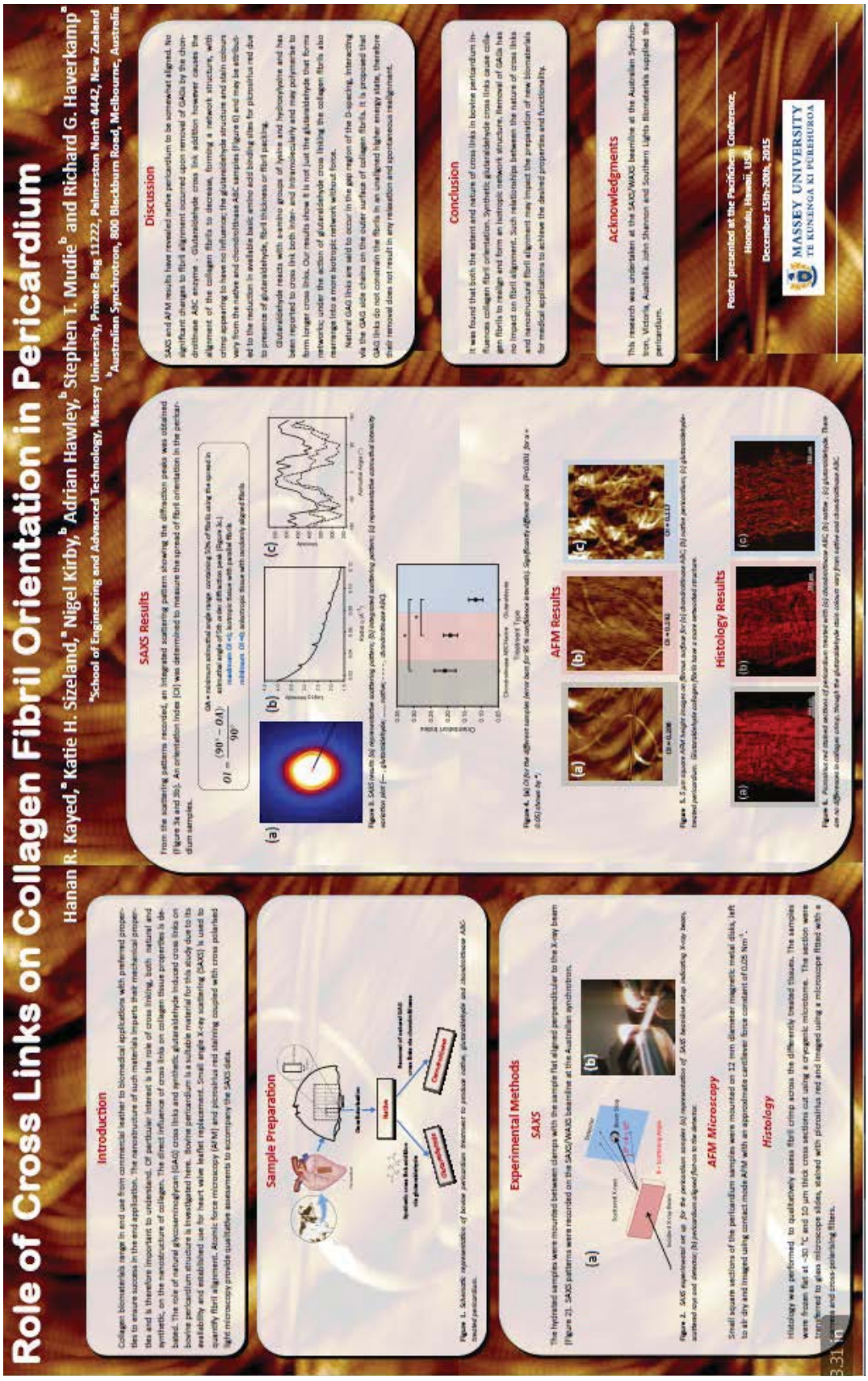

7. Poisson Ratio of Collagen Fibrils under Tension

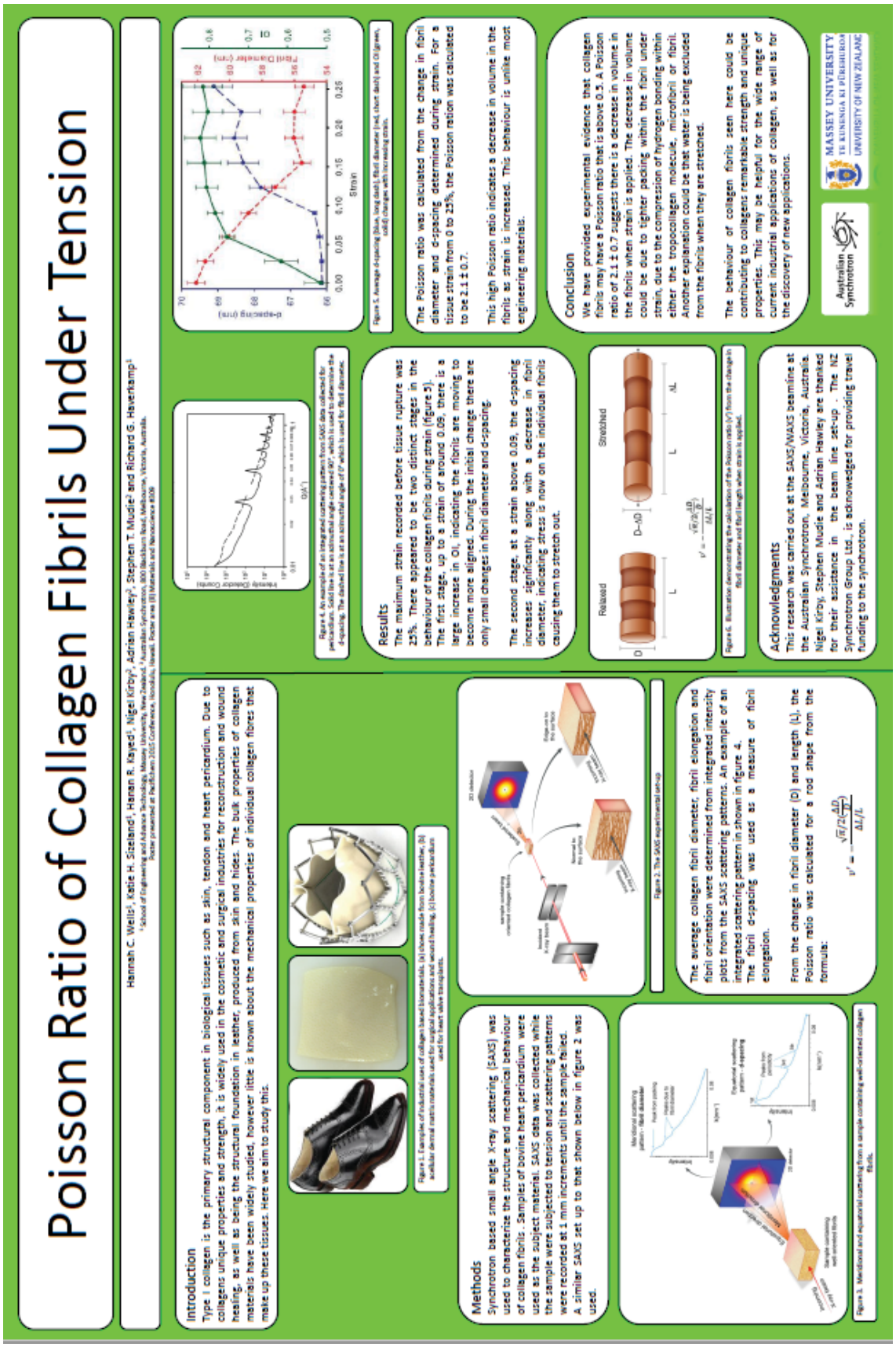

8. Strength in Collagen Materials

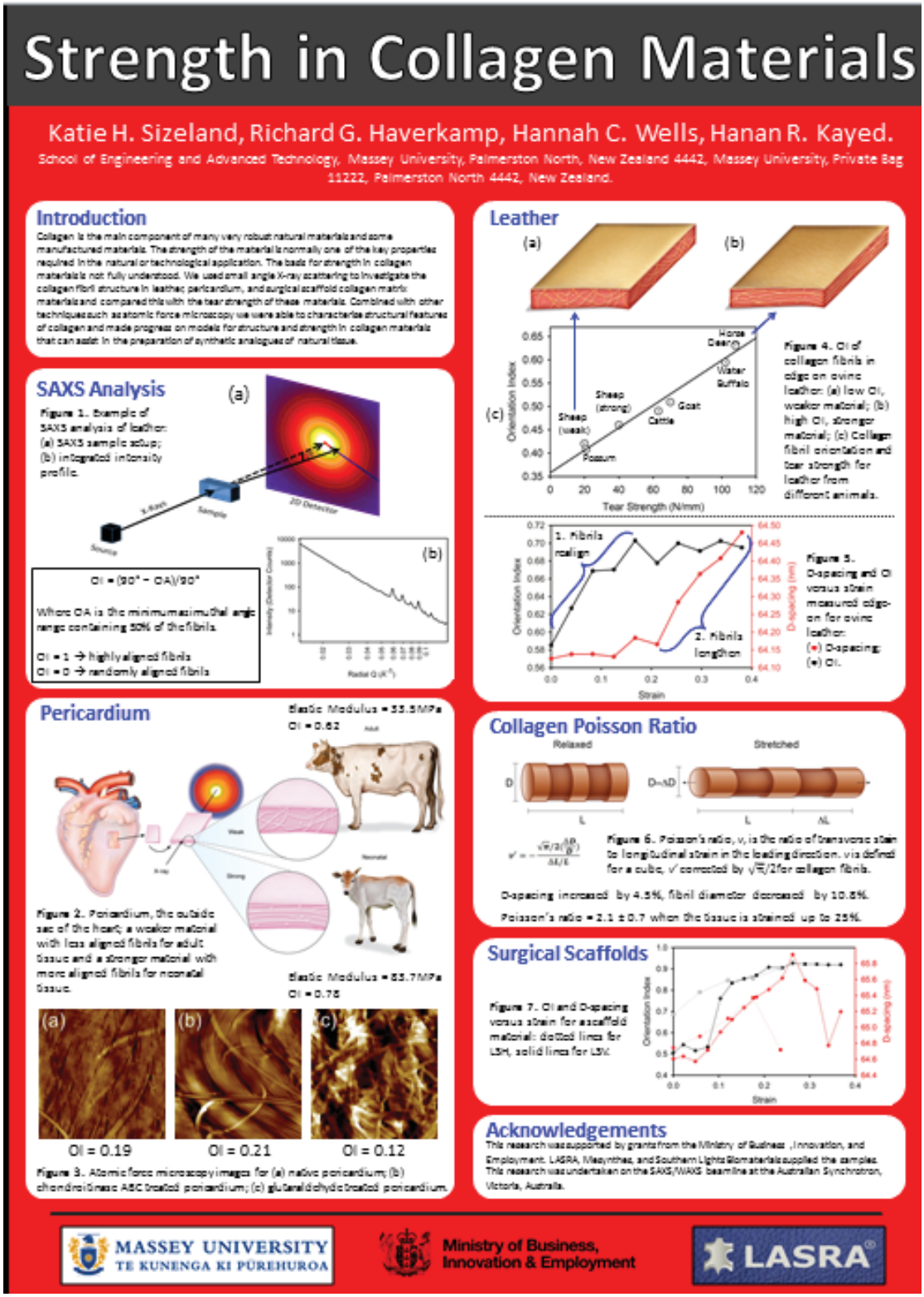

8.3 Appendix C: Conference Presentations

8.3.1 List of Conference Presentations

1. Haverkamp, R.G., Sizeland, K.H., Wells, H.C., **Kayed, H.R.**, Basil-Jones, M.M., Edmonds, R.L., Kirby, N., Hawley, A., & Mudie, S. "Collagen Structure in Useful Biomaterials." Symposium presented at 12th International Conference on Frontiers of Polymers and Advanced Materials Auckland, 8th-13th December, 2013.

2. Haverkamp, R. G., Sizeland, K. H., Wells, H. C., **Kayed, H. R.**, Edmonds, R. L., Kirby, N., Hawley, A., & Mudie, S. "Orientation of Collagen Fibrils in Tissue." Symposium presented at the 1st Matrix Biology Europe Conference, Rotterdam, Netherlands, 21st-24th June, 2015.

3. Haverkamp, R.G., Sizeland, K.H., **Kayed, H.R.**, Wells, H.C., Edmonds, R.L., Kirby, N., Hawley, A., & Mudie, S. "Structure and strength in collagen materials". Symposium presented at The International Chemical Congress of Pacific Basin Societies, 15th-20th December **2015,** Honolulu, Hawaii.

4. Haverkamp, R.G., Sizeland, K.H., Wells, H.C., & **Kayed, H.R.** Collagen structure and strength in leather and other biomaterials. Symposium presented at the FILK Conference, Freiberg, Germany, 16th March, 2015

8.3.2 Conference Presentation Abstracts

1. Collagen Structure in Useful Biomaterials

Haverkamp, R.G.,[1] Sizeland, K.H., Wells, H.C.,[1] **Kayed, H.R.**,[1] Basil-Jones, M.M.,[1] Edmonds, R.L.,[2] Kirby, N.,[3] Hawley, A.,[3] & Mudie, S.[3]

[1]School of Engineering and Advanced Technology, Massey University, Palmerston North 4442, New Zealand;
[2]Leather and Shoe Research Association, PO Box 8094, Palmerston North 4446, New Zealand;
[3]*Australian Synchrotron, 800 Blackburn Road, Clayton, VIC 3168, Australia*

Collagen (Type I) forms the main structure of skin and other animal tissues. These tissues can be processed to make useful biomaterials. We have investigated leather and pericardium for use in heart valves using synchrotron based small angle X-ray scattering both in a relaxed state and under tension. It is possible to obtain quantitative measurements of fibril orientation, fibril size, and details of the structure (D-spacing) of individual fibrils. Under tension, the extension of fibrils can also be quantified. We found that strength (for leather and pericardium) is a function of collagen fibril alignment. When fibrils are aligned in the plane of the tissue the material is stronger. When tissues are stretched the fibrils first align in the direction of stress and then individual fibrils begin to stretch. Cross linking of the collagen, both naturally occurring links and synthetically formed links, affect the structure and performance of collagen materials. Processing treatments alter the collagen structure in ways that can be explained chemically. These studies provide an insight into the structural basis of strength in fibrous collagen materials and the behaviour of these materials under stress.

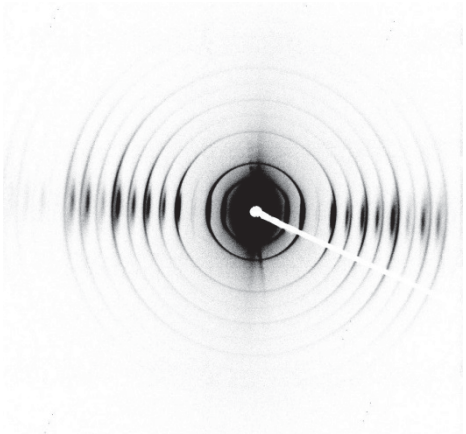

Figure 1. SAXS pattern of pericardium under tension

2. Orientation of Collagen Fibrils in Tissue

Haverkamp, R. G.,[1] Sizeland, K. H., Wells,[1] H. C., **Kayed, H. R.**,[1] Edmonds, R. L.,[2] Kirby, N.,[3] Hawley, A.,[3] & Mudie, S.[3]

[1]School of Engineering and Advanced Technology, Massey University, Palmerston North 4442, New Zealand;
[2]Leather and Shoe Research Association, PO Box 8094, Palmerston North 4446, New Zealand;
[3]*Australian Synchrotron, 800 Blackburn Road, Clayton, VIC 3168, Australia*

Collagen (Type I) is the main structural component of skin and other animal tissues. There is a large variation observed in the strength of tissues even with similar amounts of collagen. We have investigated aspects of the structure of leather and pericardium using synchrotron based small angle X-ray scattering, particularly with a view to understanding strength. We obtained quantitative measurements of fibril orientation, fibril size, and d-spacing of individual fibrils. We measured tissues both in a relaxed state and under tension. When tissues are stretched the fibrils first align in the direction of stress and then individual fibrils begin to stretch. We found that strength for leather and pericardium is a function of collagen fibril alignment. When fibrils are aligned in the plane of the tissue the material is stronger. These studies provide an insight into the structural basis of strength in tissues and the behaviour of these materials under stress.

3. Structure and Strength in Collagen Materials

Haverkamp, R.G.[1], Sizeland, K.H.,[1] **Kayed, H.R.,**[1] Wells, H.C.,[1] Edmonds, R.L.,[2] Kirby, N.,[3] Hawley, A.,[3] & Mudie, S.[3]

[1]School of Engineering and Advanced Technology, Massey University, Palmerston North 4442, New Zealand;
[2]Leather and Shoe Research Association, PO Box 8094, Palmerston North 4446, New Zealand;
[3]*Australian Synchrotron, 800 Blackburn Road, Clayton, VIC 3168, Australia*

Collagen is a principal component of many strong and elastic natural materials and manufactured materials derived from these. One of the key functions of these materials is mechanical strength. The basis for strength in collagen materials is still not fully understood. We have investigating the collagen fibril structure in leather, pericardium, and surgical scaffold collagen matrix materials using small angle X-ray scattering and compared this with tear strength of these materials. Combined with atomic force microscopy, histology, electron microscopy and other techniques we propose a complex relationship between strength and a number of structural factors including fibril orientation, fibril diameter and cross linking. There is a relationship with tissue type, species, and age of the animal. While there is much still to be learned we have made progress on models for structure and strength in collagen materials to assist in the understanding of natural tissues and preparation of manufactured materials.

The Physical Structure, Function of Biological and Bioinspired Soft Matter (#347)4

4. Collagen Structure and Strength in Leather and other Biomaterials

Haverkamp, R.G.,[1] Sizeland, K.H.,[1] Wells, H.C.,[1] & **Kayed, H.R.**.[1]

[1]School of Engineering and Advanced Technology, Massey University, Palmerston North 4442, New Zealand

Strength is an important property of leather, medical scaffold materials and replacement heart valve leaflets. However, it is not well understood what factors give strength to these materials. We have used synchrotron based small angle X-ray scattering combined with atomic force microscopy, ultrasonic imaging and other techniques to learn about the structure and strength of collagen materials. We have investigated collagen fibril alignment, collagen fibril diameter, collagen fibril strain, cross linking both natural and synthetic, and addition of fats and other components. Some of these factors are important to strength and mechanical behaviour of leather and collagen materials. This talk will describe some of our recent discoveries in this area.

Chapter 9

8. List of References

AL JAMAL, R., ROUGHLEY, P. J. & LUDWIG, M. S. 2001. Effect of glycosaminoglycan degradation on lung tissue viscoelasticity. *American Physiological Society,* 280**,** L306-L315.

ALTURKISTANI, H. A., TASHKANDI, F. M. & MOHAMMEDSALEH, Z. M. 2015. Histological stains: A literature review and case study. *Global Journal of Health Science,* 8**,** 72-79.

ASLAM, A. K., ASLAM, A. F., VASAVADA, B. C. & KHAN, I. A. 2007. Prosthetic heart valves: Types and echocardiographic evaluation. *International Journal of Cardiology,* 122**,** 99-110.

ATHAR, Y., ZAINUDDIN, S. L. A., BERAHIM, Z., HASSAN, A., SAGHEER, A. & ALAM, M. K. 2014. Bovine pericardium: A highly versatile graft material. *International Medical Journal,* 21**,** 321-324.

BADER, A., SCHILLING, T., TEEBKEN, O. E., BRANDES, G., HERDEN, T., STEINHOFF, G. & HAVERICH, A. 1998. Tissue engineering of heart valves: Human endothelial cell seeding of detergent acellularized porcine valves. *European Journal of Cardio-Thoracic Surgery,* 14**,** 279-284.

BAILEY, A. J. 2001. Molecular mechanisms of ageing in connective tissues. *Mechanisms of Ageing and Development,* 122**,** 735-755.

BAILEY, A. J., PAUL, R. G. & KNOTT, L. 1998. Mechanisms of maturation and ageing of collagen. *Mechanisms of Ageing and Development,* 106**,** 1-56.

BASIL-JONES, M. M., EDMONDS, R. L., ALLSOP, T. F., COOPER, S. M., HOLMES, G., NORRIS, G. E., COOKSON, D. J., KIRBY, N. & HAVERKAMP, R. G. 2010. Leather structure determination by small angle X-ray scattering (SAXS): Cross sections of ovine and bovine leather. *Journal of Agricultural and Food Chemistry,* 58**,** 5286-5291.

BASIL-JONES, M. M., EDMONDS, R. L., COOPER, S. M. & HAVERKAMP, R. G. 2011. Collagen fibril orientation in ovine and bovine leather affects strength: A small angle X-ray scattering (SAXS) study. *Journal of Agricultural and Food Chemistry,* 59**,** 9972-9979.

BASIL-JONES, M. M., EDMONDS, R. L., NORRIS, G. E. & HAVERKAMP, R. G. 2012. Collagen fibril alignment and deformation during tensile strain of leather: A SAXS study. *Journal of Agricultural and Food Chemistry,* 60**,** 1201-1208.

BAYNES, J. W. 2003. Chemical modification of proteins by lipids in diabetes. *Clinical Chemistry and Laboratory Medicine,* 41**,** 1159-1165.

BELLA, J., EATON, M., BRODSKY, B. & BERMAN, H. M. 1994. Crystal and molecular structure of a collagen-like peptide at 1.9 Å resolution. *Science,* 266**,** 75-81.

BHATTACHARJEE, A. & BANSAL, M. 2005. Collagen structure: The Madras triple helix and the current scenario. *IUBMB Life,* 57**,** 161-172.

BILLIAR, K. L. & SACKS, M. S. 1997. A method to quantify the fiber kinematics of planar tissues under biaxial stretch. *Journal of Biomechanics,* 30**,** 753-756.

BLANCHET, C. E. & SVERGUN, D. I. 2013. Small-angle X-ray scattering on biological macromolecules and nanocomposites in solution. *Annual Review of Physical Chemistry,* 64**,** 37-54.

BOLDON, L., LALIBERTE, F. & LIU, L. 2015. Review of the fundamental theories behind small angle X-ray scattering, molecular dynamics simulations, and relevant integrated application. *Nano Reviews,* 6**,** 25661.

BRODSKY, B. & RAMSHAW, J. A. M. 1997. The collagen triple-helix structure. *Matrix Biology,* 15**,** 545-554.

BUEHLER, M. J. 2008. Nanomechanics of collagen fibrils under varying cross-link densities: Atomistic and continuum studies. *Journal of the Mechanical Behavior of Biomedical Materials,* 1**,** 59-67.

BUEHLER, M. J. & WONG, S. Y. 2007. Entropic elasticity controls nanomechanics of single tropocollagen molecules. *Biophysical Journal,* 93**,** 37-43.

CHACHRA, D., GRATZER, P. F., PEREIRA, C. A. & LEE, J. M. 1996. Effect of applied uniaxial stress on rate and mechanical effects of cross-linking in tissue-derived biomaterials. *Biomaterials,* 17**,** 1865-1875.

CHAN, Y., COX, G. M., HAVERKAMP, R. G. & HILL, J. M. 2009. Mechanical model for a collagen fibril pair in extracellular matrix. *European Biophysics Journal,* 38**,** 487-493.

CHEN, R. N., HO, H. O. & SHEU, M. T. 2005. Charaterization of collagen matrices crosslinked using microbial transglutaminase. *Biomaterials,* 26**,** 4229-4235.

CHENG, V. W. T. & SCREEN, H. R. C. 2007. The micro-structural strain response of tendon. *Journal of Materials Science,* 42**,** 8957-8965.

CHEUNG, D. T. & NIMNI, M. E. 1982. Mechanism of crosslinking of proteins by glutaraldehyde II. Reaction with monomeric and ploymeric collagen. *Connective Tissue Research,* 10**,** 201-216.

CHEUNG, D. T., PERELMAN, N., KO, E. C. & NIMNI, M. E. 1985. Mechanism of crosslinking of proteins by glutaraldehyde III. Reaction with collagen in tissues. *Connective Tissue Research,* 13**,** 109-115.

CHOI, J. B., YOUN, I. & KIM, J. K. 2006. Zonal differences in the deformation characteristics of the cartilage chondron. *Biomaterials Research,* 10**,** 61-66.

CHU, B. & HSIAO, B. S. 2001. Small-angle X-ray scattering of polymers. *Chemical Reviews,* 101**,** 1727-1761.

CONSTANTINE, V. S. & MOWRY, R. W. 1968. The selective staining of human dermal collagen II. The use of picrosirius red F3BA with polarization microscopy. *The Journal of Investigative Dermatology,* 50**,** 419-423.

COOKSON, D., KIRBY, N., KNOTT, R., LEE, M. & SCHULTZ, D. 2006. Strategies for data collection and calibration with a pinhole-geometry SAXS instrument on a synchrotron beamline. *Journal of Synchrotron Radiation,* 13**,** 440-444.

COUPPE, C., HANSEN, P., KONGSGAARD, M., KOVANEN, V., SUETTA, C., AAGAARD, P., KJAER, M. & MAGNUSSON, S. P. 2009. Mechanical properties and collagen cross-linking of the patellar tendon in old and young men. *Journal of Applied Physiology,* 107**,** 880-886.

COURTMAN, D. W., PEREIRA, C. A., KASHEF , V., MCCOMB, D., LEE, J. M. & WILSON, G. J. 1994. Development of a pericardial acellular matrix biomaterial: Biochemical and mechanical effects of cell extraction. *Journal of Biomedical Materials Research,* 28**,** 655-666.

CRANFORD, S. W. & BUEHLER, M. J. 2013. Critical cross-linking to mechanically couple polyelectrolytes and flexible molecules. *Soft Matter,* 9**,** 1076-1090.

CRIBB, A. M. & SCOTT, J. E. 1995. Tendon response to tensile-stress - an ultrastructural investigation of collagen - proteoglycan interactions in stressed tendon. *Journal of Anatomy,* 187**,** 423-428.

CRIBIER, A., ELTCHANINOFF, H., TRON, C., BASH, A., BORENSTEIN, N., BAUER, E., DERUMEAUX, G., PONTIER, G., LABORDE, F. & LEON, M. B. 2003. Percutaneous artificial cardiac valves: from animal experimentation to the first human implantation in a case of calcified aortic stenosis. *Archives de Maladies du Coeur et des Vaisseaux,* 96**,** 645-652.

DAHL, S. L., KOH, J., PRABHAKAR, V. & NIKLASON, L. E. 2003. Decellularized native and engineered arterial scaffolds for transplantation. *Cell Transplantation* 12**,** 659-666.

DAYAN, D., HISS, Y., HIRSHBERG, A., BUBIS, J. J. & WOLMAN, M. 1989. Are the Polarization Colors of Picrosirius Red-stained Collagen Determined Only by the Diameter of the Fibers? *Histochemistry,* 93**,** 27-29.

ELLIOT, D. M., KYDD, S. R., PERRY, C. H. & SETTON, L. A. Year. Direct measurement of the Possion's Ratio of human articular cartilage in tension. *In:* 45th Annual Meeting, Orthopaedic Reseach Society February 1st-4th 1999 Anaheim, California. 649.

EXPOSITO, J. Y., CLUZEL, C., GARRONE, R. & LETHIAS, C. 2002. Evolutions of collagens. *The Anotomical Record,* 268**,** 302-316.

EYRE, D. R., PAZ, M. A. & GALLOP, P. M. 1984. Cross-linking in collagen and elastin. *Annual Review of Biochemistry,* 53**,** 717-748.

FEIGIN, L. A. & SVERGUN, D. I. 1987. *Structure analysis by Small-Angle X-ray and Neutron Scattering,* New York, Springer Science+Business Media.

FESSEL, G. & SNEDEKER, J. G. 2009. Evidence against proteoglycan mediated collagen fibril load transmission and dynamic viscoelasticity in tendon. *Matrix Biology,* 28**,** 503-510.

FESSEL, G. & SNEDEKER, J. G. 2011. Equivalent stiffness after glycosaminoglycan depletion in tendon - an ultra-structural finite element model and corresponding experiments. *Journal of Theoretical Biology,* 268**,** 77-83.

FLODEN, E. W., MALAK, S., BASIL-JONES, M. M., NEGRON, L., FISHER, J. N., BYRNE, M., LUN, S., DEMPSEY, S. G., HAVERKAMP, R. G., ANDERSON, I., WARD, B. R. & MAY, B. C. H. 2010. Biophysical characterization of ovine forestomach extracellular matrix biomaterials. *Journal of Biomedical Materials Research Part B: Applied Biomaterials,* 96B**,** 67-75.

FOLKHARD, W., GEERCKEN, W., KNORZER, E., NEMETSCHEK-GANSLER, H., NEMETSCHEK, T. & KOCH, M. H. J. 1987. Quantitative analysis of the molecular sliding mechanism in native tendon collagen - time-resolved dynamic studies using synchrotron radiation. *International Journal of Biological Macromolecules,* 9**,** 169-175.

FRANCIS-SEDLAK, M. E., URIEL, S., LARSON, J. C., GREISLER, H. P., VENERUS, D. C. & BREY, E. M. 2009. Characterization of type I collagen gels modified by glycation. *Biomaterials,* 30**,** 1851-1856.

FRASER, R. D. B., MACRAE, T. P., MILLER, A. & SUZUKI, E. 1983. Molecular conformation and packing in collagen fibrils. *Journal of Molecular Biology,* 167**,** 497-521.

FRASER, R. D. B., MACRAE, T. P. & SUZUKI, E. 1979. Chain conformation in the collagen molecule. *Journal of Molecular Biology,* 129**,** 463-481.

FRATZL, P. (ed.) 2008. *Collagen: Structure and mechanics,* New York: SpringerScience+Business Media.

FRATZL, P., MISOF, K., ZIZAK, I., RAPP, G., AMENITSCH, H. & BERNSTORFF, S. 1997. Fibrillar structure and mechanical properties of collagen. *Journal of Structural Biology,* 122**,** 119-122.

FRATZL, P. & WEINKAMER, R. 2007. Nature's hierarchical materials. *Progress in Materials Science,* 52**,** 1263-1334.

FREYTES, D. O., BADYLAK, S. F., WEBSTER, T. J., GEDDES, L. A. & RUNDELL, A. E. 2004. Biaxial strength of multilaminated extracellular matrix scaffolds. *Biomaterials,* 25**,** 2353-2361.

FRIEDRICHS, J., TAUBENBERGER, A., FRANZ, C. M. & MULLER, D. J. 2007. Cellular remodelling of individual collagen fibrils visualized by time-lapse AFM. *Journal of Molecular Biology,* 372**,** 594-607.

FRIESS, W. 1998. Collagen-Biomaterial for drug delivery. *European Journal of Pharmaceutics and Biopharmaceutics,* 45**,** 113-136.

GAMBA, P. G., CONCONI, M. T., LO PICCOLO, R., ZARA, G., SPINAZZI, R. & PARNIGOTTO, P. P. 2002. Experimental abdominal wall defect repaired with acellular matrix. *Pediatric Surgery International,* 18**,** 327-331.

GARCÍA PÁEZ, J. M., JORGE-HERRERO, E., CARRERA SAN MARTÍN, A., GARCÍA SESTAFE, J. V., TÉLLEZ, G., MILLÁN, I., SALVADOR, J., COŕDÓN, A. & CASTILLO-OLIVARÉS, J. L. 2000. The influence of chemical treatment and suture on the elastic behavior of calf pericardium utilized in the construction of cardiac bioprostheses. *Journal of Materials Science: Materials in Medicine,* 11**,** 459-464.

GELSE, K., PÖSCHL, E. & AIGNER, T. 2003. Collagens-structure, function, and biosynthesis. *Advanced Drug Delivery Reviews,* 55**,** 1531-1546.

GILBERT, T. W., SELLARO, T. L. & BADYLAK, S. F. 2006. Decellularization of tissues and organs. *Biomaterials,* 27**,** 3675-3683.

GILBERT, T. W., WOGNUM, S., JOYCE, E. M., FREYTES, D. O., SACKS, M. S. & BADYLAK, S. F. 2008. Collagen fiber alignment and biaxial mechanical behavior of porcine urinary bladder derived extracellular matrix. *Biomaterials,* 29**,** 4775-4782.

GRAUSS, R. W., HAZEKAMP, M. G., VAN VLIET, S., GITTENBERGER-DE GROOT, A. C. & DERUITER, M. C. 2003. Decellularization of rat aortic valve allografts reduces leaflet destruction and extracellular matrix remodeling. *Journal of Thoracic and Cardiovascular Surgery,* 126**,** 2003-2010.

GUSTAVSON, K. H. 1956. *The Chemistry and Reactivity of Collagen,* New York, USA, Academic Press Inc.

HAMAI, A., HASHIMOTO, N., MOCHIZUKI, H., KATO, F., MAKIGUCHI, Y., HORIE, K. & SUZUKI, S. 1997. Two distinct chondroitin sulfate ABC lyases. An endoeliminase yielding tetrasaccharides and an exoeliminase preferentially acting on oligosaccharides. *The Journal of Biological Chemistry,* 272**,** 9123-9130.

HANSEN, P., HASSENKAM, T., SVENSSON, R. B., AAGAARD, P., TRAPPE, T., HARALDSSON, B. T., KJAER, M. & MAGNUSSON, P. 2009. Glutaraldehyde cross-linking of tendon-mechanical effects at the level of the tendon fascicle and fibril. *Connective Tissue Research,* 50**,** 211-222.

HARDINGHAM, T. E. & FOSANG, A. J. 1992. Proteoglycans: many forms and many functions. *FASEB Journal,* 6**,** 861-870.

HAUS, J. M., CARRITHERS, J. A., TRAPPE, S. W. & TRAPPE, T. A. 2007. Collagen, cross-linking, and advanced glycation end products in aging human skeletal muscle. *Journal of Applied Physiology,* 103**,** 2068-2076.

HAVERKAMP, R. G. 2013. The Australian Synchrotron-a powerful tool for chemical research available to New Zealand scientists. *Chemistry in New Zealand,* 77**,** 12-17.

HAVERKAMP, R. G., MARSHALL, A. T. & WILLIAMS, M. A. K. 2007. Entropic and enthalpic contributions to the chair-boat conformational transformation in dextran under single molecule stretching. *The Journal of Physical Chemisrty B,* 111**,** 13653-13657.

HAVERKAMP, R. G., WILLIAMS, M. A. K. & SCOTT, J. E. 2005. Stretching single molecules of connetive tissue glycans to characterize their shape-maintaining elasticity. *Biomacromolecules,* 6**,** 1816-1818.

HIESTER, E. D. & SACKS, M. S. 1998a. Optimal bovine pericardial tissue selection sites. I. Fiber architecture and tissue thickness measurements. *Journal of Biomedical Materials Research,* 39**,** 207-214.

HIESTER, E. D. & SACKS, M. S. 1998b. Optimal bovine pericardial tissue selection sites. II. Cartographic analysis. *Journal of Biomedical Materials Research,* 39**,** 215-221.

HIRSHBERG, A., SHERMAN, S., BUCHNER, A. & DAYAN, D. 1999. Collagen fibres in the wall of odontogenic keratocysts: a study with pircrosirius red and polarizing microscopy. *Journal of Oral Pathology and Medicine,* 28**,** 410-412.

HODGE, A. J. & SCHMITT, F. O. 1960. The charge profile of the tropocollagen macromolecule and the packing arrangement in native-type collagen fibrils. *Proceedings of the National Academy of Sciences of the United States of America,* 46**,** 186-197.

ILAVSKY, J. & JEMIAN, P. R. 2009. Irena: tool suite for modeling and analysis of small-angle scattering. *Journal of Applied Crystallography,* 42**,** 347-353.

ISHIHARA, T., FERRANS, V. J., JONES, M., BOYCE, S. W. & ROBERTS, W. C. 1981. Structure of bovine parietal pericardium and of unimplanted Ionescu-Shiley pericardial valvular bioprostheses. *Journal of Thoracic and Cardiovascular Surgery,* 81**,** 747-757.

IVANOVA, V. P. & KRIVCHENKO, A. I. 2012. A current viewpoint on structure and evolution of collagens. I. Fibrillar collagens. *Journal of Evolutionary Biochemistry and Physiology,* 48**,** 127-139.

JACKSON, D. W., GROOD, E. S. & WILCOX, P. 1988. The effects of processing techniques on the mechanical properties of bone-anterior cruciate ligament-bone allografts. An experimental study in goats. *American Journal of Sports Medicine,* 16**,** 101-105.

JACQUES, D. A. & TREWHELLA, J. 2010. Small-angle scattering for structural biology-Expanding the frontier while avoiding the pitfalls. *Protein Science,* 19**,** 642-657.

JANG, W., CHOI, S., KIM, S. H., YOON, E., LIM, H.-G. & KIM, Y. J. 2012. A comparative study on mechanical and biochemical properties of bovine pericardium after single or double crosslinking treatment. *Korean circulation journal,* 42**,** 154-63.

JASTRZEBSKA, M., WRZALIK, R., KOCOT, A., ZALEWSKA-REJDAK, J. & CWALINA, B. 2003. Raman spectroscopic study of glutaraldehyde-stabilized collagen and pericardium tissue. *Journal of Biomaterials Science, Polymer Edition,* 14**,** 185-197.

JAYAKRISHNAN, A. & JAMEELA, S. R. 1996. Glutaraldehyde as a fixative in bioprostheses and drug delivery matrices. *Biomaterials,* 17**,** 471-484.

JOR, J. W. Y., NIELSEN, P. M. F., NASH, M. P. & HUNTER, P. J. 2011. Modelling collagen fibre orientation in porcine skin based upon confocal laser scanning microscopy. *Skin Research and Technology,* 17**,** 149-159.

JUNQUEIRA, L. C. U., BIGNOLAS, G. & BRENTANI, R. R. 1979. Picrosirius Staining Plus Polarization Microscopy, A Specific Method for Collagen Detection in Tissue-sections. *Histochemical Journal,* 11**,** 447-455.

JUNQUEIRA, L. C. U., BIGNOLAS, G., MOURÃO, P. A. S. & BONETTI, S. S. 1980. Quantitiation of collagen-proteoglycan interaction in tissue sections. *Connective Tissue Research,* 7**,** 91-96.

JUNQUEIRA, L. C. U., COSSERMELLI, W. & BRENTANI, R. 1978. Differential staining of collagens type-I, type-II and type-III by sirius red and polarization microscopy. *Archivum Histologicum Japonicum,* 41**,** 267-274.

JUNQUEIRA, L. C. U., MONTES, G. S. & SANCHEZ, E. M. 1982. The Influence of Tissue Section Thickness on the Study of Collagen by the Picrosirius-Polarization Method. *Histochemistry,* 74**,** 153-156.

KADLER, K. E., BALDOCK, C., BELLA, J. & BOOT-HANDFORD, R. P. 2007. Collagens at a glance. *Cell Science at a Glance,* 120**,** 1955-1958.

KAMMA-LORGER, C. S., BOOTE, C., HAYES, S., MOGER, J., BURGHAMMER, M., KNUPP, C., QUANTOCK, A. J., SORENSEN, T., DI COLA, E., WHITE, N., YOUNG, R. D. & MEEK, K. M. 2010. Collagen and mature elastic fibre organisation as a function of depth in the human cornea and limbus. *Journal of Strucural Biology,* 169**,** 424-430.

KATO, Y., NISHIKAWA, T. & KAWAKISHI, S. 1995. Formation of protein-bound 3,4-dihydroxyphenylalanine in collagen type I and type IV exposed to ultraviolet light. *Photochemistry and Photobiology,* 61**,** 367-372.

KAYED, H. R., KIRBY, N., HAWELY, A., MUDIE, S. T. & HAVERKAMP, R. G. 2015a. Collagen fibril strain, recruitment and orientation for pericardium under tension and the effect of cross links. *RSC Advances,* 5**,** 103703-103712.

KAYED, H. R., SIZELAND, K. H., KIRBY, N., HAWLEY, A., MUDIE, S. T. & HAVERKAMP, R. G. 2015b. Collagen cross linking and fibril alignment in pericardium. *RSC Advances,* 5**,** 3611-3618

KAYED, H. R., SIZELAND, K. H., WELLS, H. C., KIRBY, N., HAWLEY, A., MUDIE, S. T. & HAVERKAMP, R. G. 2016. Age differences with glutaraldehyde treatment in collagen fibril orientation of bovine pericardium. *Journal of Biomaterials and Tissue Engineering,* 6**,** 992-997.

KIERNAN, J. A. 2010. Carbohydrate histochemistry. *Connection (Dako Inc. Scientific Magazine),* 14**,** 68-78.

KIVIRANTA, P., RIEPPO, J., KORHONEN, R. K., JULKUNEN, P., TOYRAS, J. & JURVELIN, J. S. 2006. Collagen network primarily controls Poisson's ratio of bovine articular cartilage in compression. *Journal of Orthopaedic Research,* 24**,** 690-699.

KIVIRIKKO, K. I. & MYLLYLÄ, R. 1985. Post-translational processing of procollagens. *Annals New York Academy of Sciences,* 460**,** 187-201.

KJELLEN, L. & LINDAHL, U. 1991. Proteoglycans: structures and interactions. *Annual Review of Biochemistry,* 60**,** 443-475.

LANGDON, S. E., CHERNECKY, R., PEREIRA, C. A., ABDULLA, D. & LEE, J. M. 1999. Biaxial mechanical/structural effects of equibiaxial strain during crosslinking of bovine pericardial xenograft materials. *Biomaterials,* 20**,** 137-153.

LEEMING, D. J., HENRIKSEN, K., BYRJALSEN, I., QVIST, P., MADSEN, S. H., GARNERO, P. & KARSDAL, M. A. 2009. Is bone quality associated with collagen age? *Osteoporosis International,* 20**,** 1461-1470.

LI, X., GUO, Y., ZIEGLER, K., MODEL, L., EGHBALIEH, S. D. D., BRENES, R., KIM, S., SHU, C. & DARDIK, A. 2011. Current usage and future directions for the bovine pericardial patch. *Annals of Vascular Surgery,* 25**,** 561-568.

LIAO, J., JOYCE, E. M. & SACKS, M. S. 2008. Effects of decellularization on the mechanical and structural properties of the porcine aortic valve leaflet. *Biomaterials,* 29**,** 1065-1074.

LIAO, J. & VESELY, I. 2007. Skewness angle of interfibrillar proteoglycans increases with applied load on mitral valve chordae tendineae. *Journal of Biomechanics,* 40**,** 390-398.

LIAO, J., YANG, L., GRASHOW, J. & SACKS, M. S. 2005. Molecular orientation of collagen in intact planar connective tissues under biaxial stretch. *Acta Biomaterialia,* 1**,** 45-54.

LIAO, J., YANG, L., GRASHOW, J. & SACKS, M. S. 2007. The relation between collagen fibril kinematics and mechanical properties in the mitral valve anterior leaflet. *Journal of Biomechanical Engineering,* 129**,** 78-87.

LOVEKAMP, J. J., SIMIONESCU, D. T., MERCURI, J. J., ZUBIATE, B., SACKS, M. S. & VYAVAHARE, N. R. 2006. Stability and Function of Glycosaminoglycans in Porcine Bioprosthetic Heart Valves. *Biomaterials,* 27**,** 1507-1518.

LUJAN, T. J., UNDERWOOD, C. J., HENNINGER, H. B., THOMPSON, B. M. & WEISS, J. A. 2007. Effect of dermatan sulfate glycosaminoglycans on the quasi-static material properties of the human medial collateral ligament. *Journal of Orthopaedic Research,* 25**,** 894-903.

LUJAN, T. J., UNDERWOOD, C. J., JACOBS, N. T. & WEISS, J. A. 2009. Contribution of glycosaminoglycans to viscoelastic tensile behavior of human ligament. *American Physiological Society* 106**,** 423-431.

MAVRILAS, D., SINOURIS, E. A., VYNIOS, D. H. & PAPAGEORGAKOPOULOU, N. 2005. Dynamic mechanical characteristics of intact and structurally modified bovine pericardial tissues. *Journal of Biomechanics,* 38**,** 761-768.

MAYNE, R. & BURGESSON, R. E. (eds.) 1987. *Structure and function of collagen types,* Orlando: Academic Press Inc (London) Ltd.

MCFETRIDGE, P. S., DANIEL, J. W., BODAMYALI, T., HORROCKS, M. & CHAUDHURI, J. B. 2004. Preparation of porcine carotid arteries for vascular tissue engineering applications. *Journal of Biomedical Materials Research Part A,* 70A**,** 224-234.

MEEK, K. M. 1981. The use of glutaraldehyde and tannic acid to preserve reconstituted collagen for electron microscopy. *Histochemistry,* 73**,** 115-120.

MENDOZA-NOVELO, B., AVILA, E. E., CAUICH-RODRÍGUEZ, J. V., JORGE-HERRERO, E., ROJO, F. J., GUINEA, G. V. & MATA-MATA, J. L. 2011. Decellularization of Pericardial Tissue and its Impact on Tensile Viscoelasticity and Glycosaminoglycan Content. *Acta Biomaterialia,* 7**,** 1241-1248.

MEYERS, M. A., MCKITTRICK, J. & CHEN, P. Y. 2013. Structural biological materials: Critical mechanics-materials connections. *Science,* 339**,** 773-779.

MIRNAJAFI, A., RAYMER, J., SCOTT, M. J. & SACKS, M. S. 2005. The effects of collagen fiber orientation on the flexural properties of pericardial heterograft biomaterials. *Biomaterials,* 26**,** 795-804.

MIRNAJAFI, A., ZUBIATE, B. & SACKS, M. S. 2010. Effects of cyclic flexural fatigue on porcine bioprosthetic heart valve heterograft biomaterials. *Journal of Biomedical Materials Research Part A,* 94A**,** 205-213.

MOSLER, E., FOLKHARD, W., KNORZER, E., NEMETSCHEK-GANSLER, H., NEMETSCHEK, T. & KOCH, M. H. J. 1985. Stress-induced molecular rearrangement in tendon collagen. *Journal of Molecular Biology,* 182**,** 589-596.

MURPHY, D. B., SALMON, E. D., SPRING, K. R., ABRAMOWITZ, M., PLUTA, M., PARRY-HILL, M., SUTTER, R. T. & DAVIDSON, M. W. 2012. *Polarized light microscopy*. Olympus America Inc. Available: http://olympus.magnet.fsu.edu/primer/techniques/polarized/polarizedhome.html.

NÉMETHY, G. & SCHERAGA, H. A. 1986. Stabilisation of collagen fibrils by hydroxyproline. *Biochemistry,* 25**,** 3184-3188.

NIELSON, L. F., MOE, D., KIRKEBY, S. & GARBARSCH, C. 1998. Sirius red and acid fuchsin staining mechanism. *Biotechnic and Histochemistry,* 73**,** 71-77.

NWAEJIKE, N. & ASCIONE, R. 2011. Mitral valve repair for disruptive acute endocarditis: Extensive replacement of posterior leaflet with bovine pericardium. *Journal of Cardiac Surgery,* 26**,** 31-33.

OLDE DAMINK, L. H. H. O., DIJKSTRA, P. J. & VAN LUYN, M. J. A. 1996. Cross-linking of dermal sheep collagen using a water-soluble carbodiimide. *Biomaterials,* 17**,** 765-773.

OLDE DAMINK, L. H. H. O., DIJKSTRA, P. J., VAN LUYN, M. J. A., VAN WACHEM, P. B., NIEUWENHUIS, P. & FEIJEN, J. 1995. Glutaraldehyde as a crosslinking agent for collagen-based biomaterials. *Journal of Materials Science: Materials in Medicine,* 6**,** 460-472.

ORGEL, J., IRVING, T. C., MILLER, A. & WESS, T. J. 2006. Microfibrillar structure of type I collagen in situ. *Proceedings of the National Academy of Sciences of the United States of America,* 103**,** 9001-9005.

ORGEL, J. P. R. O., EID, A., ANTIPOVA, O., BELLA, J. & SCOTT, J. E. 2009. Decorin core protein (Decoron) shape complements collagen fibril surface structure and mediates its binding *PloS One,* 4**,** e7028.

OTTANI, V., MARTINI, D., FRANCHI, M., RUGGERI, A. & RASPANTI, M. 2002. Hierachical structures in fibrillar collagens. *Micron,* 33**,** 587-596.

PAEZ, J. M. G., SANMARTIN, A. C., HERRERO, E. J., MILLAN, I., CORDON, A., ROCHA, A., MAESTRO, M., BURGOS, R., TELLEZ, G. & CASTILLO-OLIVARES, J. L. 2006. Durability of a cardiac valve leaflet made of calf pericardium: Fatigue and energy consumption. *Journal of Biomedical Materials Research Part A,* 77A**,** 839-849.

PARRY, D. A. D., BARNES, G. R. G. & CRAIG, A. S. 1978. Comparison of size distribution of collagen fibrils in connective tissues as a function of age and a possible relation between fibril size distribution and mechanical-properties. *Proceedings of the Royal Society B: Biological Sciences,* 203**,** 305-321.

PAUW, B. R. 2013. Everything SAXS: Small-angle scattering pattern. *Journal of Physics-Condensed Matter*, 25**,** 383201.

PERSSON, C., EVANS, S., MARSH, R., SUMMERS, J. L. & HALL, R. M. 2010. Poisson's ratio and strain rate dependency of the constitutive behavior of spinal dura mater. *Annals of Biomedical Engineering,* 38**,** 975-983.

PETERKOFSKY, B. & UDENFRIEND, S. 1963. Conversion of proline to collagen hydroxyproline in a cell-free system from chick embryo. *The Journal of Biological Chemistry,* 238**,** 3966-3977.

PETRUSKA, J. A. & HODGE, A. J. 1964. Subunit model for tropocollagen macromolecule. *Proceedings of the National Academy of Sciences of the United States of America,* 51**,** 871-876.

PICU, R. C. 2011. Mechanics of random fiber networks-a review. *Soft Matter,* 7**,** 6768-6785.

PIEZ, K. A., EIGNER, E. A. & LEWIS, M. S. 1963. The chromatographic separation and amino acid composition of the subunits of several collagens. *Biochemistry,* 2**,** 58-66.

PRAWOTO, Y. 2012. Seeing auxetic materials from the mechanics point of view: A structural review on the negative Poisson'e ratio. *Computational Materials Science,* 58**,** 140-153.

PURSLOW, P. P., WESS, T. J. & HUKINS, D. W. L. 1998. Collagen orientation and molecular spacing during creep and stress-relaxation in soft connective tissues. *Journal of Experimental Biology,* 201**,** 135-142.

PUXKANDL, R., ZIZAK, I., PARIS, O., KECKES, J., TESCH, W., BERNSTORFF, S., PURSLOW, P. & FRATZL, P. 2002. Viscoelastic properties of collagen: synchrotron radiation investigations and structural model. *Philosophical Transactions of the Royal Society,* 357**,** 191-197.

REDAELLI, A., VESENTINI, S., SONCINI, M., VENA, P., MANTERO, S. & MONTEVECCHI, F. M. 2003. Possible role of decorin glycosaminoglycans in fibril to fibril force transfer in relative mature tendons - a computational study from molecular to microstructural level. *Journal of Biomechanics,* 36**,** 1555-1569.

REDDY, N., REDDY, R. & JIANG, Q. 2015. Crosslinking bioploymers for biomedical applications. *Trends in Biotechnology,* 33**,** 362-369.

REECE, I. J., VAN NOORT, R., MARTIN, T. R. P. & BLACK, M. M. 1982. The physical properties of bovine pericardium: a study of the effects of stretching during chemical treatment in glutaraldehyde. *Annals of Thoracic Surgery,* 33**,** 480-485.

RICE, R. V., CASASSA, E. F., KERWIN, R. E. & MASER, W. D. 1964. On the length and molecular weight of tropocollagen from calf skin. *Archives of Biochemistry and Biophysics,* 105**,** 409-423.

RICH, A. & CRICK, F. H. C. 1961. The molecular structure of collagen. *Journal of Molecular Biology,* 3**,** 483-506.

RICH, L. & WHITTAKER, P. 2005. Collagen and picrosirius red staining: A polarized light assessment of fibrillar hue and spatial distribution. *Brazilian Journal of Morphological Sciences,* 22**,** 97-104.

RIEDER, E., KASIMIR, M. T., SILBERHUMER, G., SEEBACHER, G., WOLNER, E., SIMON, P. & WEIGEL, G. 2004. Decellularization protocols of porcine heart valves differ importantly in efficiency of cell removal and susceptibility of the matrix of recellularization. *Journal of Thoracic and Cardiovascular Surgery,* 127**,** 399-405.

RIGOZZI, S., MUELLER, R. & SNEDEKER, J. G. 2009. Local strain measurement reveals a varied regional dependence of tensile tendon mechanics on glycosaminoglycan content. *Journal of Biomechanics,* 42**,** 1547-1552.

RIGOZZI, S., MUELLER, R., STEMMER, A. & SNEDEKER, J. G. 2013. Tendon glycosaminoglycan proteoglycan sidechains promote collagen fibril sliding-AFM observations at the nanoscale. *Journal of Biomechanics,* 46**,** 813-818.

RIGOZZI, S., STEMMER, A., MULLER, R. & SNEDEKER, J. G. 2011. Mechanical response of individual collagen fibrils in loaded tendon as measured by atomic force microscopy. *Journal of Structural Biology,* 176**,** 9-15.

ROBERTS, T. S., DREZ, D. & MCCARTHY, W. 1991. Anterior cruciate ligament reconstruction using freeze-dried, ethylene oxide-sterilized, bone-patellar tendon-bone allografts. Two year results in thirty-six patients. *American Journal of Sports Medicine,* 19**,** 35-41.

ROBINS, S. P. & BAILEY, A. J. 1972. Age-related changes in collagen: the identification of reducible lysine-carbohydrate condensation products. *Biochemical and Biophysical Research Communications,* 48**,** 76-84.

ROBINSON, P. C. & DAVIDSON, M. W. 2000. *Introduction to Polarized Light Microscopy*. Available: http://www.microscopyu.com/articles/polarized/polarizedintro.html.

SACKS, M. S., CHUONG, C. J. & MORE, R. 1994. Collagen fiber architecture of bovine pericardium. *American Society for Artificial Internal Organs,* 40**,** M632-M637.

SACKS, M. S., SMITH, D. B. & HIESTER, E. D. 1997. A small angle light scattering device for planar connective tissue microstructural analysis. *Annals of Biomedical Engineering,* 25**,** 678-689.

SAITO, H., YAMAGATA, T. & SUZUKI, S. 1968. Enzymatic methods for the determination of small quantities of isomeric chondroitin sulfates. *The Journal of Biological Chemistry,* 243**,** 1536-1542.

SCHENKE-LAYLAND, K., VASILEVSKI, O., F, O., KONIG, K., RIEMANN, I., HALBHUBER, K. J., WAHLERS, T. & STOCK, U. A. 2003. Impact of decellularization of xenogeneic tissue on extracellular matrix integrity for tissue engineering of heart valves. *Journal of Structural Biology* 143**,** 201-208.

SCHMIDT, C. E. & BAIER, J. M. 2000. Acellular vascular tissues: natural biomaterials for tissue repair and tissue engineering. *Biomaterials,* 21**,** 2215-2231.

SCHMIDT, M. B., MOW, V. C., CHUN, L. E. & EYRE, D. R. 1990. Effects of proteoglycan extraction on the tensile behavior of articular-cartilage. *Journal of Orthopaedic Research,* 8**,** 353-363.

SCHMITT, F. 1956. Molecular interaction patterns in biological systems. *Proceedings of the American Philosophical Society,* 100**,** 476-486.

SCHOEN, F. J. & LEVY, R. J. 1999. Tissue heart valves: Current challenges and future research perspectives. *Journal of Biomedical Materials Research,* 47**,** 439-465.

SCHOEN, F. J., TSAO, J. W. & LEVY, R. J. 1986. Calcification of bovine pericardium used in cardiac valve bioprostheses: Implications for the mechanisms of bioprosthetic tissue mineralzation. *American Journal of Pathology,* 123**,** 134-145.

SCHOFIELD, A. L., SMITH, C. I., KEARNS, V. R., MARTIN, D. S., FARRELL, T., WEIGHTMAN, P. & WILLIAMS, R. L. 2011. The use of reflection anisotropy spectroscopy to assess the alignment of collagen. *Journal of Physics D: Applied Physics*, 44**,** 335302.

SCOTT, J. E. 1980. Collagen-proteoglycan interactions. Localization of proteoglycans in tendon by electron microscopy. *Biochemical Journal,* 187**,** 887-891.

SCOTT, J. E. 1988. Proteoglycan-fibrillar collagen interactions. *Biochemical Journal,* 252**,** 313-323.

SCOTT, J. E. 1992. Supramolecular organization of extracellular matrix glycosaminoglycans, in vitro and in the tissues. *FASEB Journal,* 6**,** 2639-2645.

SCOTT, J. E. 1995. Extracellular-Matrix, Supramolecular Organization and Shape. *Journal of Anatomy,* 187**,** 259-269.

SCOTT, J. E. 1996. Proteodermatan and proteokeratan sulfate (decorin, lumican/fibromodulin) proteins are horseshoe shaped. Implications for their interactions with collagen. *Biochemistry,* 35**,** 8795-8799.

SCOTT, J. E. 2003. Elasticity in extracellular matrix 'shape modules' of tendon, cartilage, etc. A sliding proteoglycan-filament model. *Journal of Physiology,* 553**,** 335-343.

SCOTT, J. E. & ORFORD, C. R. 1981. Dermatan sulfate-rich proteoglycan associates with rat tail-tendon collagen at the d band in the gap region. *Biochemical Journal,* 197**,** 213-216.

SCOTT, J. E. & STOCKWELL, R. A. 2006. Cartilage elasticity resides in shape module decoran and aggrecan sumps of damping fluid: implications in osteoarthrosis. *Journal of Physiology-London,* 574**,** 643-650.

SCOTT, J. E. & THOMLINSON, A. M. 1998. The structure of interfibrillar proteoglycan bridges ('shape modules') in extracellular matrix of fibrous connective tissues and their stability in various chemical environments. *Journal of Anatomy,* 192**,** 391-405.

SELLARO, T. L., HILDEBRAND, D., LU, Q. J., VYAVAHARE, N., SCOTT, M. & SACKS, M. S. 2007. Effects of collagen fiber orientation on the response of biologically derived soft tissue biomaterials to cyclic loading. *Journal of Biomedical Materials Research Part B: Applied Biomaterials,* 80A**,** 194-205.

SHI, D. (ed.) 2006. *Introduction to biomaterials,* China: Tsinghua University Press and World Scientific Publishing Co. Pte. Ltd.

SIMIONESCU, D., IOZZO, R. V. & KEFALIDES, N. A. 1989. Bovine pericardial proteoglycan: Biochemical, immunochemical and ultrastructural studies. *Matrix,* 9**,** 301-310.

SIMIONESCU, D., SIMIONESCU, A. & DEAC, R. 1993. Mapping of glutaraldehyde-treated bovine pericardium and tissue selection for bioprosthetic heart valves. *Journal of Biomedical Materials Research,* 27**,** 697-704.

SINGHAL, P., LUK, A. & BUTANY, J. 2013. Bioprosthetic heart valves: Impact of implantation on Biomaterials. *ISRN Biomaterials***,** 728791.

SIZELAND, K. H., BASIL-JONES, M. M., EDMONDS, R. L., COOPER, S. M., KIRBY, N., HAWLEY, A. & HAVERKAMP, R. G. 2013. Collagen orientation and leather strength for selected mammals. *Journal of Agricultural and Food Chemistry,* 61**,** 887-892.

SIZELAND, K. H., WELLS, H. C., HIGGINS, J. J., CUNANAN, C. M., KIRBY, N., HAWLEY, A. & HAVERKAMP, R. G. 2014. Age dependant differences in collagen fibril orientation of glutaraldehyde fixed bovine pericardium. *BioMed Research International,* 2014**,** 189197.

SIZELAND, K. H., WELLS, H. C., NORRIS, G. E., EDMONDS, R. L., KIRBY, N., HAWLEY, A., MUDIE, S. & HAVERKAMP, R. G. 2015. Collagen D-spacing and the effect of fat liquor addition. *Journal of the American Leather Chemists Association* 110**,** 66-71.

STAMOV, D. R. & POMPE, T. 2012. Structure and function of ECM-inspired composite collagen type I scaffolds. *Soft Matter,* 8**,** 10200-10212.

STINSON, R. H. & SWEENY, P. R. 1980. Skin collagen has an unusual D-spacing. *Biochimica et Biophysica Acta,* 621**,** 158-161.

SUH, H., LEE, W. K. & PARK, J. C. 1999. Evaluation of the degree of cross-linking in UV irradiated porcine valves. *Yonsei Medical Journal,* 40**,** 159-165.

SUNG, H. W., CHANG, Y., CHIU, C. T., CHEN, C. N. & LIANG, H. C. 1999. Crosslinking characteristics and mechanical properties of a bovine pericardium fixed with a naturally occurring crosslinking agent. *Journal of Biomedical Materials Research,* 47**,** 116-126.

SVENSSON, R. B., HASSENKAM, T., HANSEN, P., KJAER, M. & MAGNUSSON, S. P. 2011. Tensile force transmission in human patellar tendon fascicles is not mediated by glycosaminoglycans. *Connective Tissue Research,* 52**,** 415-421.

TANG, Y., BALLARINI, R., BUEHLER, M. J. & EPPELL, S. J. 2010. Deformation micromechanics of collagen fibrils under uniaxial tension *Journal of The Royal Society Interface,* 7**,** 839-850.

TEEBKEN, O. E., BADER, A., STEINHOFF, G. & HAVERICH, A. 2000. Tissue engineering of vascular grafts: Human cell seeding of decellularised porcine matrix. *European Journal of Vascular and Endovascular Surgery,* 19**,** 381-386.

UMASHANKAR, P. R., ARUN, T. & KUMARI, T. V. 2011. Short duration gluteraldehyde cross linking of decellularized bovine pericardium improves biological response. *Journal Biomedical Materials Research Part A,* 97A**,** 311-320.

VADER, D., KABLA, A., WEITZ, D. & MAHADEVAN, L. 2009. Strain-induced alignment in collagen gels. *PLOS ONE*, 4**,** e5902.

VAN DER REST, M. & GARRONE, R. 1991. Collagen family of proteins. *FASEB Journal,* 5**,** 2814-2823.

VESELY, I. 2005. Heart valve tissue engineering. *Circulation Research,* 97**,** 743-755.

VINCENT, J. 2012. *Structural Biomaterials,* Princeton, New Jersey, USA, Princeton University Press.

WÅGSÄTER, D., PALOSCHI, V., HANEMAAIJER, R., HULTENBY, K., BANK, R. A., FRANCO-CERECEDA, A., LINDEMAN, J. H. N. & ERIKSSON, P. 2013. Impaired collagen biosynthesis and cross-linking in aorta of patients with bicuspid aortic valve. *Journal of the American Heart Association*, 2**,** UNSPe000034.

WARD, A., HILITSKI, F., SCHWENGER, W., WELCH, D., LAU, A. W. C., VITELLI, V., MAHADEVAN, L. & DOGIC, Z. 2015. Solid friction between soft filaments. *Nature Materials,* 14**,** 583-588.

WEADOCK, K. S., MILLER, E. J., KEUFFEL, E. L. & DUNN, M. G. 1996. Effect of physical crosslinking methods on collagen-fiber durability in proteolytic solutions. *Journal of Biomedical Materials Research,* 32**,** 221-226.

WELLS, C. H., SIZELAND, K. H., KIRBY, N., HAWELY, A., MUDIE, S. T. & HAVERKAMP, R. G. 2015a. Collagen fibril structure and strength in acellular dermal matrix materials of bovine, porcine and human origin. *ACS Biomaterials Science & Engineering,* 1**,** 1026-1038.

WELLS, H. C., EDMONDS, R. L., KIRBY, N., HAWLEY, A., MUDIE, S. T. & HAVERKAMP, R. G. 2013. Collagen fibril diameter and leather strength. *Journal of Agricultural and Food Chemistry,* 61**,** 11524-11531.

WELLS, H. C., HOLMES, G. & HAVERKAMP, R. G. 2015b. Looseness in bovine leather: microstructural characterization. *Journal of the Science of Food and Agriculture,* 96**,** 2731-2736.

WELLS, H. C., SIZELAND, K. H., KAYED, H. R., KIRBY, N., HAWLEY, A., MUDIE, S. T. & HAVERKAMP, R. G. 2015c. Poisson's ratio of collagen fibrils measured by SAXS of strained bovine pericardium. *Journal of Applied Physics,* 117**,** 044701.

WILLETT, T. L., LABOW, R. S., ALDOUS, I. G., AVERY, N. C. & LEE, J. M. 2010. Changes in collagen with aging maintain molecular stability after overload: Evidence from an in vitro tendon model. *Journal of Biomechanical Engineering,* 132**,** 1-8.

YAMADA, Y., KÜHN, K. & DE CROMBRUGGHE, B. 1983. A conserved nucleotide sequence, coding for a segment of the C-propeptide, is found at the same location in different collagen genes. *Nucleic Acids Research,* 11**,** 2733-2744.

YANG, M., CHEN, C. Z., WANG, X. N., ZHU, Y. B. & GU, Y. J. 2009. Favorable effects of the detergent and enzyme extraction method for preparing decellularized bovine pericardium scaffold for tissue engineered heart valves. *Journal of Biomedical Material Research Part B: Applied Biomaterials,* 91B**,** 354-361.

YANG, W., SHERMAN, V. R., GLUDOVATZ, B., SCHAIBLE, E., STEWART, P., RITCHIE, R. O. & MEYERS, M. A. 2015. On the tear resistance of skin. *Nature Communications*, 6**,** 6649.